Synthesis reactivity and mechanistic studies on 0X0, alkoxo and tertiary phosphine derivatives of niobium and tantalum

Terence Phillip Kee

SYNTHESIS, REACTIVITY AND MECHANISTIC STUDIES ON OXO, ALKOXO AND TERTIARY PHOSPHINE DERIVATIVES OF NIOBIUM AND TANTALUM.

by

Terence Phillip Kee, B.Sc.(Dunelm)

University of Durham

A Thesis submitted in part fulfillment of the requirements for the degree of Doctor of Philosophy at the University of Durham.

January 1989

Dedicated with all my heart
to my Mother and Father.

"A man would do nothing
if he waited until he could
do it so well that no-one
would find fault with what
he had done" **Cardinal Newman.**

ACKNOWLEDGEMENTS

I would like primarily to express my sincere gratitude to my supervisor, Dr. Vernon Gibson, for availing himself selflessly throughout my period of research at Durham. His ability to inspire and to stimulate the study of Chemistry in a wide variety of areas has made it a great pleasure to work in his laboratory.

To my colleagues, past and present, go my heartfelt thanks especially the current encumbents of CG101 and CG106; Alan, Dave, Pete and Jon for providing an outstanding atmosphere in which to work. My thanks go also to Drs. Bob Sorrell, Rab Mulvey and Ezat Khosravi-Babadi for many stimulating discussions over the past three years.

I am especially indebted to Drs. W. Clegg (University of Newcastle-Upon-Tyne), M. McPartlin and A.P. Bashall (Polytechnic of North London) for solving the crystal structures described herein and Dr. D. Reed (University of Edinburgh) for helping to solve several complicated NMR spectra. Furthermore, without the help and co-operation of the Senior Experimental and Technical Staff at the Chemistry Department at Durham, the work described in this thesis would not have been possible.

I am most grateful to Dr. Nigel Smith for typing this thesis. His expertise, patience and constructive comments have smoothed the transition from handwritten manuscript to the final, typewritten product. Many thanks also to Mrs. E. Wood and Mr. C. Greenhalgh for invaluable help during the latter stages.

Finally, the award of an S.E.R.C. studentship is gratefully acknowledged.

STATEMENT OF COPYRIGHT.

DECLARATION

The work described in this thesis was carried out in the Department of Chemistry at the University of Durham between September 1985 and July 1988. All the work is my own, unless stated to the contrary, and it has not been submitted previously for a degree at this or any other University.

ABSTRACT

SYNTHESIS, REACTIVITY AND MECHANISTIC STUDIES ON OXO, ALKOXO AND TERTIARY PHOSPHINE DERIVATIVES OF NIOBIUM AND TANTALUM.

The research described in this thesis is directed towards the development of the organometallic and coordination chemistry of niobium and tantalum with tertiary phosphine and oxygen containing ligands.

Chapter 1 highlights the influence of tertiary phosphine ligands on various areas of organometallic and coordination chemistry.

Chapter 2 describes syntheses and reactivity studies on several half-sandwich, tertiary phosphine complexes including $(\eta^5\text{-}C_5H_5)TaCl_2(PMe_3)_3$, $(\eta^5\text{-}C_5Me_5)TaCl_2(PMe_3)(CO)_2$ and the paramagnetic, d^2-complex, $(\eta^5\text{-}C_5Me_5)TaCl_2(PMe_3)_2$.

Chapter 3 describes the synthesis and characterisation of ring and phosphine metallated isomers of $(\eta^5\text{-}C_5Me_5)Ta(PMe_3)_2$, *viz.* $(\eta^7\text{-}C_5Me_3(CH_2)_2)Ta(H)_2(PMe_3)_2$ and $(\eta^5\text{-}C_5Me_5)Ta(PMe_3)(H)_2(\eta^2\text{-}CHPMe_2)$ respectively.

Subsequently, Chapter 4 describes aspects of the reactivity and derivative chemistry of $(\eta^5\text{-}C_5Me_5)Ta(PMe_3)(H)_2(\eta^2\text{-}CHPMe_2)$. The exploitation of reversible hydrogen migrations has facilitated the preparation of a number of complexes including, $(\eta^5\text{-}C_5Me_5)Ta(dmpe)(H)(\eta^2\text{-}CH_2PMe_2)$ and $(\eta^5\text{-}C_5Me_5)Ta(CO)_2(PMe_3)_2$, whilst reactions with alkyl halides or olefins result in the retention of the $Ta(\eta^2\text{-}CHPMe_2)$ moiety, *eg.* $(\eta^5\text{-}C_5Me_5)Ta(PMe_3)HX(\eta^2\text{-}CHPMe_2)$; $(\eta^5\text{-}C_5Me_5)TaX_2(\eta^2\text{-}CHPMe_2)$ (X = Cl, Br, I) and $(\eta^5\text{-}C_5Me_5)Ta(CH_2CH_2CMe_3)_2(\eta^2\text{-}CHPMe_2)$.

Chapters 5 and 6 develop the use of Me_3SiOR (R = Me, Et, $SiMe_3$) reagents as sources of the oxygen ligands 'O' and 'OR' for the mild, controllable synthesis of transition metal oxyhalides and alkoxyhalides. Chapter 5 describes various niobium compounds including $Nb(O)Cl_3$ and $Nb(O)Cl_3L_2$ (L = CH_3CN, THF) and a number of aryloxide and tertiary phosphine derivatives of $Nb(O)Cl_3$. Chapter 6 describes several half-sandwich tantalum systems including $(\eta^5\text{-}C_5Me_5)TaCl_3.OR$ (R = Me, Et, C_3H_5, ReO_3), $[(\eta^5\text{-}C_5Me_5)TaCl_3]_2(\mu\text{-}O)$ and $(\eta^5\text{-}C_5Me_5)Ta(O)Cl_2$.

Chapter 7 gives experimental details for Chapters 2-6.

Terence Phillip Kee (January 1989)

ABBREVIATIONS

NMR	Nuclear Magnetic Resonance
L	General 2-electron donor ligand
X	General 1-electron donor ligand
Cp	Cyclopentadienyl (C_5H_5)
Cp^*	Pentamethylcyclopentadienyl (C_5Me_5)
Cp'	Generalised (C_5R_5) ligand
dppe	1,2-bis(diphenylphosphino)ethane
dmpe	1,2-bis(dimethylphosphino)ethane
THF	Tetrahydrofuran
PCy_3	Tricyclohexylphosphine
ESR	Electron Spin Resonance
Np*H*	Naphthalene
δ(oop)	Out of plane bending vibration
IR	Infrared
$t_{\frac{1}{2}}$	Half-life
HOMO	Highest Occupied Molecular Orbital
LUMO	Lowest Unoccupied Molecular Orbital
NOE	Nuclear Overhauser Effect
DMSO	Dimethylsulphoxide
HMPA	Hexamethylphosphoramide
bipy	Bipyridine
TPPO	Triphenylphosphine oxide

CONTENTS PAGE

CHAPTER ONE

THE INFLUENCE OF TERTIARY PHOSPHINE LIGANDS ON THE CHEMISTRY OF TRANSITION METAL COMPOUNDS.

1.1 INTRODUCTION

The work described in this thesis is directed towards the development of the organometallic and coordination chemistry of the heavier Group 5 elements, niobium and tantalum. These studies have concerned the following areas.

(I) The synthesis and reactivity of mononuclear, half-sandwich compounds of tantalum, containing the small, highly basic ligand trimethylphosphine (PMe_3), including the use of trimethylphosphine as a reactive solvent medium.

(II) The activation of small molecules of relevance to industrial catalysis, *e.g* CO, CO_2 and olefins.

(III) Oxidative cleavage of main group-hydrogen bonds including the intramolecular activation of C-H bonds and the intermolecular cleavage of O-H bonds.

(IV) The development of convenient synthetic routes to oxo and alkoxo compounds, with a view to assessing the role of transition metal bound oxygen atoms in oxidation catalysis.

Since much of the work described herein has involved the use of tertiary phosphine ligands, and particularly trimethylphosphine, the remainder of Chapter 1 will be concerned with an overview of the influences of tertiary phosphine ligands on various aspects of the chemistry of transition metals. The review is not intended to be comprehensive, but highlights areas of chemistry of relevance to the theme of this thesis.

Tertiary phosphine ligands have played a central role in the development of transition metal chemistry, from classical coordination

compounds to organometallic complexes, for several reasons:

a) They are known to bind to elements throughout the transition series.

b) A large variety of such ligands are known, allowing control over the steric and electronic environment surrounding the metal.

c) They are generally involatile liquids or crystalline solids, permitting ease of manipulation.

d) The ^{31}P-nucleus has nuclear spin=$\frac{1}{2}$, 100% natural abundance and a good receptivity, facilitating study by NMR spectroscopy.

The coordination of tertiary phosphine ligands to transition metals permits structural and electronic modifications to the metal environment, thus influencing the reactivity at metal centres. Three general facets of tertiary phosphine ligands are fundamental in their ability to influence reactivity:

a) The coordinative stabilisation and solubilisation of low nuclearity, transition metal fragments.

b) The generation of a labile coordination sphere, either through association/dissociation of the phosphine ligands themselves, or through their influence on the coordinating ability of attendant ligands.

c) The steric and electronic properties of tertiary phosphine ligands may be exploited to influence the structural geometry and hence reactivity of compounds.

The importance of these properties will be demonstrated in the following sections.

1.2 ELECTRONIC AND STERIC PROPERTIES OF TERTIARY PHOSPHINES

These have been previously discussed in some detail[1,2] and this section gives only a brief outline of the models used to define electronic and steric parameters for tertiary phosphines. These parameters have been widely used to correlate structure and reactivity in transition metal-phosphine compounds.

1.2.1 The Electronic Parameter[3], ν

Mixing $Ni(CO)_4$ and L (phosphorus ligand) in a 1:1 ratio in dichloromethane solvent results in the rapid formation of $Ni(CO)_3L$. The fully symmetric, A_1, carbonyl stretching frequencies (ν) for these compounds are strong, can be accurately measured (± 0.3 cm^{-1}) and are dependent upon the electronic nature of the ligand, L (steric effects have been shown to be small)[3].

L	ν (cm^{-1})	Θ (^{0})
$P(OPh)_3$	2085.3	128
$P(OMe)_3$	2079.5	107
PMe_3	2064.1	118
PEt_3	2061.7	132
$P(i\text{-}Pr)_3$	2059.2	160
$P(t\text{-}Bu)_3$	2056.1	182

Table 1.1 *ν and Θ values for selected Phosphines*

For phosphorus ligands, $PX_1X_2X_3$ it is possible to define substituent contributions χ_i. The additivity of these contributions allows the calculation of ν for ligands for which it has not been measured[3], according to Equation 1.1.

$$\nu = 2056.1 + \sum_{i=1}^{3} \chi_i \qquad (1.1)$$

Generally, it is observed that those PX_3 ligands with bulky, electron releasing substituents have lower ν values as a result of their ability to transfer more electron density to the metal and thence to the carbonyl ligands. Some representative values are given in Table 1.1.

1.2.2 The Steric Parameter[4], Θ

This measurement was introduced by Tolman[4] to explain the ability of phosphorus ligands to compete for coordination positions on Ni(0), which did not correlate well with the electronic factors, ν, but did correlate with the relative size of the ligands. Similarly, it was found that in the substitution reactions of $Ni(CO)_4$ (Equation 1.2) with L, the degree of substitution was greater for the smaller ligands and *vice versa*.

$$Ni(CO)_4 \underset{\longleftarrow}{\xrightarrow{xs\ L}} Ni(CO)_3L \underset{\longleftarrow}{\xrightarrow{L}} Ni(CO)_2L_2 \underset{\longleftarrow}{\xrightarrow{L}} Ni(CO)L_3 \qquad (1.2)$$

Tolman defined the steric parameter, Θ, as the apex angle of a cylindrical cone, centred 2.28Å from the centre of the phosphorus atom, which just touches the Van der Waals radii of the outermost atoms of the molecule (Figure 1.1). Some Θ values are given in Table 1.1.

Although cone angles have been widely used as a measure of steric effects in phosphorus ligand chemistry[1], the model is limited in that PX_3 ligands do not have true cylindrical symmetry and can specifically orientate themselves with respect to attendant ligands. Furthermore, the angles between substituents on phosphorus ligands are generally less than the tetrahedral angles assumed in the model, and the M-P bond

length used (2.28Å) is not necessarily valid for each metal [M-P can range from *ca.* 2.12Å in $[Ni(PF_3)_4]$[1] to *ca.* 2.71Å in $Cp^*TaCl_2(PMe_3)(CO)_2$][5]. Consequently, most reliability in the application of cone angles should be achieved when other variables are restricted.

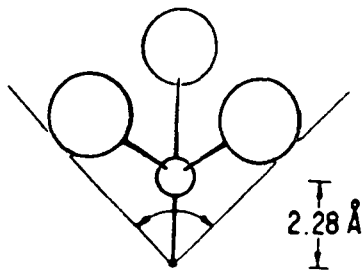

Figure 1.1 *Representation of the Ligand Cone Angle*

1.2.3 Polydentate Tertiary Phosphine Ligands

Stereochemical control can often be facilitated by the use of chelating, polydentate ligands wherein variations in the nature of the hydrocarbon backbone between phosphorus donor atoms can dictate whether the ligand spans *cis* positions in a complex[6] [Figure 1.2(a)], *trans* positions[7] [Figure 1.2(b)] or preferentially bridges two metal centres[8] [Figure 1.2(c)].

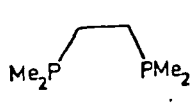

(a)

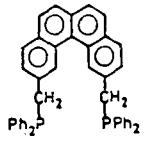

(b)

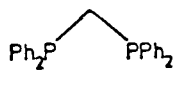

(c)

Figure 1.2

The coordination may be anchored in an electronically unfavourable geometry by the use of phosphine ligands of higher denticity[9]. For example, the tridentate ligand $CH_3C(CH_2PPh_2)_3$ enforces a distorted tetrahedral geometry upon the d^8, Ni(II) cation (Figure 1.3), instead of the normal square plane[10].

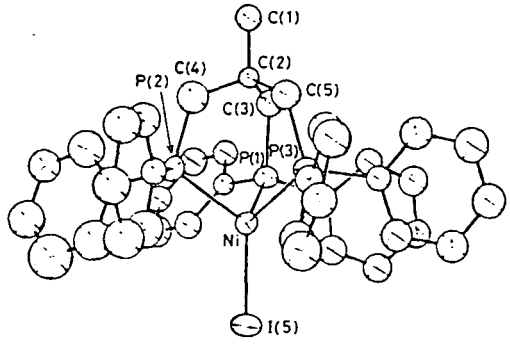

Figure 1.3

1.3 THE STABILISATION OF LOW NUCLEARITY FRAGMENTS IN COORDINATION AND ORGANOMETALLIC CHEMISTRY

1.3.1 Halide Compounds

Tertiary phosphine ligands are capable of stabilising mononuclear complexes of metal halides *via* the cleavage of bridging halogen ligands. In certain cases, reduction of the metal has been observed. Some examples are given in Table 1.2.

The structure of $NbCl_5(PPh_3)_2$ has not been elucidated but it may be either a seven-coordinate monomer or a chloride-bridged, eight-coordinate dimer. Both coordination numbers are known for niobium compounds[22,23]. Of the compounds of the form $MCl_2(PR_3)_2$ (Table 1.2),

the iron and cobalt derivatives are tetrahedral and paramagnetic, whereas the nickel compounds can exist in both paramagnetic tetrahedral and diamagnetic *trans*-square planar forms depending upon the halide and and phosphine ligands used.

METAL HALIDE	REACTION CONDITIONS	PRODUCT	REF
$NbCl_5$	PPh_3/C_6H_6, RT	$NbCl_5(PPh_3)_2$	11
β-$ReCl_4$	xs PPh_3/CH_3CN, RT	*trans*-$ReCl_4(PPh_3)_2$	12
$TcCl_4$	xs PPh_3, EtOH/Reflux	$TcCl_4(PPh_3)_2$	13
$FeCl_2$	xs PR_3, C_6H_6/Reflux (R_3=Ph_3,Ph_2Et,$PhEt_2$,Et_3)	$FeCl_2(PR_3)_2$	14,15
$RuCl_3$	xs PPh_3, MeOH/Reflux	$RuCl_2(PPh_3)_3$	16
$CoCl_2$	xs PEt_3 reagent	$CoCl_2(PEt_3)_2$	17
$RhCl_3$	xs PPh_3, EtOH/Reflux	$RhCl(PPh_3)_3$	18
$NiCl_2$	PR_3, Alcohol (R_3=Alkyl, aryl)	$NiCl_2(PR_3)_2$	19-21

Table 1.2 *Some Tertiary Phosphine Metal Halide Compounds*

In particular, for a given phosphine ligand the stability of the tetrahedral form increases Cl < Br < I presumably for steric reasons. For a given halide it was observed that the tetrahedral isomer is favoured as aryl substituents replace alkyl substituents in $R_xAr_{3-x}P$[21]. This has been explained in terms of increasing ligand field stabilisation energy for the tetrahedral isomer in this order[20].

In organometallic chemistry also, tertiary phosphines can cleave bridge bonds. Although the detailed structures of $Cp'MCl_4$ (Cp'=Cp,Cp^*; M=Nb,Ta) are not known, they are believed to be at least dimeric containing halogen bridges[24] (Chapter 2, section 2.1.2). They have, however, been shown to form complexes with tertiary phosphines as illustrated in Equation 1.3.

$$[Cp'MCl_4]_n + L \longrightarrow Cp'MCl_4.L \qquad (1.3)$$

M=Ta; Cp'=Cp; L=PMe_3, PCy_3[25]
M=Ta; Cp'=Cp*; L=PMe_3, dppe[26]
M=Nb; Cp'=C_5H_4Me; L=dppe[24]

Again, although structural data is lacking for these compounds, they are presumed to be essentially isostructural to $Cp^*ReCl_4.PMe_3$ which has been studied crystallographically[27], and is illustrated in Figure 1.4.

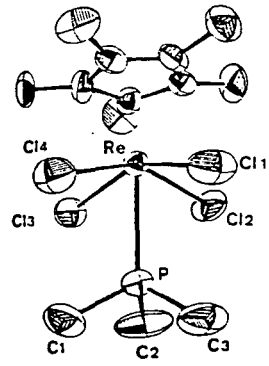

Figure 1.4 *X-Ray Structure of $Cp^*ReCl_4.PMe_3$*

The reduction of metal halides in a suitable solvent in the presence of tertiary phosphines has led to the isolation of lower oxidation state complexes. Such compounds are often very reactive towards oxidising substrates and the phosphine coordination sphere is often labile (Equations 1.4 and 1.5).

$$TaCl_5 \xrightarrow{\text{xs } PMe_3/2Na(Hg)/Et_2O} TaCl_3(PMe_3)_3^{28} \qquad (1.4)$$

$$TaCl_5 \xrightarrow{\text{xs } PMe_3/3Na(Hg)/Et_2O} TaCl_2(PMe_3)_4^{29} \qquad (1.5)$$

The molecular structure of $TaCl_2(PMe_3)_4$ (Figure 1.5) showed a distorted, *trans* octahedron[29].

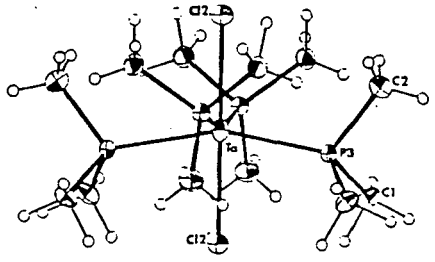

Figure 1.5 *X-Ray Structure of* $TaCl_2(PMe_3)_4$

The PMe_3 ligands of $TaCl_3(PMe_3)_3$ were found to be very labile and the compound decomposed readily in solution to form the dimer $[TaCl_3(PMe_3)_2]_2$ which has been studied crystallographically and shown to possess an edge-shared, bioctahedral geometry with two PMe_3 ligands occupying axial sites on one tantalum atom and equatorial sites on the other[30].

Cotton and co-workers have studied the structural chemistry of the d^1-compounds, $MCl_4(PR_3)_n$ where M = Nb, Ta and PR_3 is a tertiary phosphine ligand. The value of n and the molecular structure of these complexes is dependent upon the phosphine ligand and preparative procedure used. With PEt_3, $PEtPh_2$ and larger ligands, *trans*-octahedral monomers were obtained, $MCl_4(PR_3)_2$ for both niobium[23] and tantalum[31] [Figure 1.6(a)]. However, with the sterically less demanding tertiary phosphine, PMe_3 a seven-coordinate monomer[31,32] and a quadruply bridged, eight-coordinate dimer[23,32] were found [Figures 1.6(b) and 1.6(c)] for both metals, the mononuclear derivatives being favoured by higher PMe_3 concentrations in the preparative procedure. Interestingly, with the phosphine, PMe_2Ph, niobium formed a dimer, $[NbCl_4(PMe_2Ph)_2]_2$

structurally analogous to the PMe_3 complex[22], whereas tantalum crystallised as a six-coordinate monomer $TaCl_4(PMe_2Ph)_2$ in which the two phosphorus ligands were disposed *cis* to each other[31] [Figure 1.6(d)]. This geometry is presumably electronically more favourable on the basis of *trans* influence arguments. These data indicated that for PMe_2Ph, steric considerations were not predominant and that the *cis*-geometry of $TaCl_4(PMe_2Ph)_2$ was a result of electronic factors.

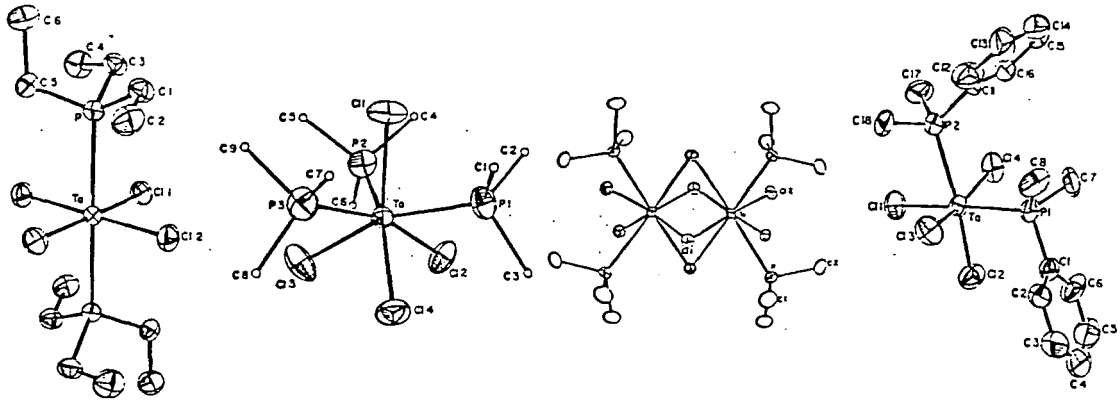

(a) (b) (c) (d)

Figure 1.6 *Crystal Structures of* $MCl_4(PR_3)_n$

1.3.2 Homoleptic Tertiary Phosphine Complexes

Complexes of the form $M(PR_3)_n$ are known for a number of metals and in general they conform to the 18-electron rule. Nickel forms several $Ni(PR_3)_4$ complexes, (*eg.* R_3 = Et_3, Ph_3, Me_3) for which various synthetic procedures have been employed (Equations 1.6-1.8).

$$Ni(\eta^3\text{-}C_3H_5)_2 + 4PPh_3 \longrightarrow \text{Diallyl} + Ni(PPh_3)_4 \quad [33] \qquad (1.6)$$

$$K_4[Ni(CN)_4] + 2dppe \xrightarrow[\text{liq.}NH_3]{-33^oC} 4\ KCN + Ni(dppe)_2^{34} \qquad (1.7)$$

$$Ni(vapour) + PMe_3\ (xs) \longrightarrow Ni(PMe_3)_4^{35} \qquad (1.8)$$

Both the cobalt and palladium derivatives, $M(PMe_3)_4$ have been prepared by metal atom vapour techniques[35] (*cf.* Equation 1.8) and they are presumed to have a tetrahedral structure.

The co-condensation of iron vapour with excess PMe_3 led to the isolation of $Fe(PMe_3)_5$ as a very reactive, yellow-red solid[35]. Reduction of $MCl_2(PMe_3)_n$ (M = Fe[36], n=2; M = Ru[37], Os[38], n=4) using either sodium amalgam or sodium naphthalinide in the presence of PMe_3 produced $M(PMe_3)_4$. However, the structure of these complexes is not as trivial as the stoichiometry suggests and is discussed in more detail in Section 1.5.

As the transition metal series is traversed from Group 10 to Group 5, so the homoleptic tertiary phosphine complexes, $M(PR_3)_n$, especially with PMe_3, become very reactive towards ligand displacement and oxidation reactions mirroring the concomitant increase in valence d-electron energy from right to left across a particular transition metal series. For Groups 6 and 5, metal vapour-ligand condensation techniques have proved particularly fruitful in the synthesis of the homoleptic tertiary phosphine complexes, $Mo(PMe_3)_6$[39], $Mo(dmpe)_3$[40], $Cr(dmpe)_3$[40], $W(dmpe)_3$[40] and $M(dmpe)_3$[40] (M = V, Nb, Ta). The niobium and tantalum compounds are rare examples of M(0), d^5 complexes. All the dmpe derivatives are essentially isostructural, Figure 1.7(a) illustrates the geometry for the chromium compound.

$Mo(PMe_3)_6$ has an octahedral structure as illustrated in Figure 1.7(b)[39]. The larger steric requirements of six PMe_3 ligands results in a considerably longer molybdenum-phosphorus distance of 2.467(2)Å over the chelating analogue $Mo(dmpe)_3$ [Mo-P = 2.421(3)Å][39], and consequently

a more labile coordination sphere. Indeed, $Mo(PMe_3)_6$ is a very reactive molecule, some aspects of its chemistry are discussed in Section 1.4.

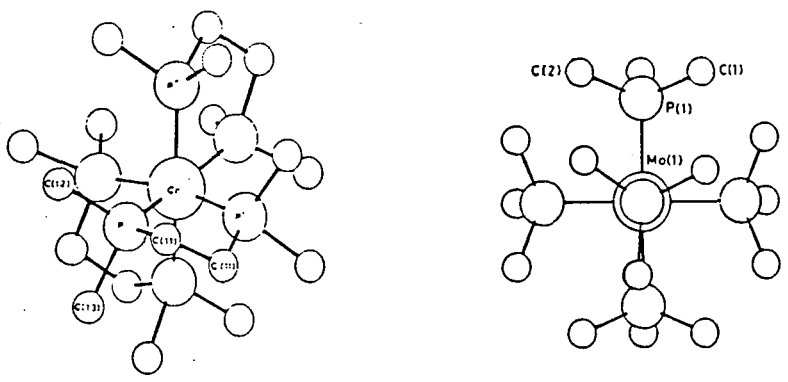

(a) (b)

Figure 1.7 *Crystal Structures of $Cr(dmpe)_3$ and $Mo(PMe_3)_6$*

Interestingly, $W(PMe_3)_6$ could not be obtained by metal vapour synthesis, instead a complex with the stoichiometry $W(PMe_3)_5$ was produced in *ca.* 20% yield[41]. This compound is discussed in Section 1.5.

1.3.3 Polyhydrido Complexes

As with the metal halides, tertiary phosphine ligands are capable of stabilising mononuclear hydrido complexes[42]. Considerable recent interest in polyhydrido complexes has been directed to their use in C-H bond activation[43], carbon monoxide reduction[44] and olefin insertion reactions[45], and in many cases tertiary phosphines have been favoured co-ligands, as illustrated in Equations (1.9) to (1.12).

$$H_7Re(PPh_3)_2 \xrightarrow[THF,CpH]{25^oC} (\eta^4\text{-}C_5H_6)ReH_3(PPh_3)_2 \xrightarrow[5^oC]{h\nu} (\eta^5\text{-}C_5H_5)ReH_4(PPh_3)^{43} \quad (1.9)$$

$$(\eta^5\text{-}C_5H_4R)MoCl_2(PMe_3)_2 \xrightarrow[Toluene]{LiAlH_4} (\eta^5\text{-}C_5H_4R)MoH_3(PMe_3)_2{}^{46} \quad (R={}^iPr) \quad (1.10)$$

$$Cp^*WCl_4.PMe_3 \xrightarrow[b)\ MeOH/Et_2O]{a)\ LiAlH_4/Et_2O} Cp^*WH_5.PMe_3{}^{47} \quad (1.11)$$

$$Cp^*TaMe_4 \xrightarrow[PMe_3\ (xs)]{H_2\ (100\ atm.)} Cp^*TaH_4(PMe_3)_2{}^{48} \quad (1.12)$$

The molybdenum complex shown in Equation 1.10 was anticipated to display similar chemistry to the compound Cp_2WH_2 on the basis of the steric and electronic analogy between a $(\eta^5\text{-}C_5H_5)$ ligand and the "$(PMe_3)_2H$" ligand set (Figure 1.8). Indeed, the complex did catalyse H/D exchange between D_2 and various organic substrates[46].

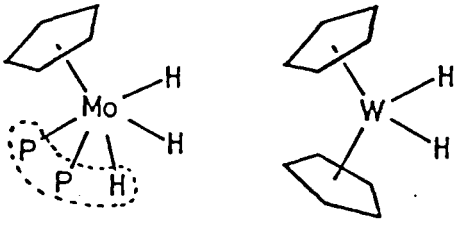

Figure 1.8

The thermal and photochemical reactions of polyhydrido-phosphine complexes often involve either dihydrogen or phosphine elimination as an initial step. The lability of the phosphine ligand is therefore an important consideration which is discussed further in Section 1.4.

1.3.4 Compounds Containing M-C σ-Bonds

These include metal alkyls, aryls, vinyls and acyls. Most homoleptic alkyls [*eg.* $TaMe_5$[49] and $Ta(CH_2Ph)_5$[49]] do not possess β-hydrogens since such alkyls are generally susceptible to decomposition *via* β-hydrogen elimination reactions[50]. The presence of tertiary phosphine ligands in electronically saturated complexes can reduce the tendency for this decomposition reaction, since ligand dissociation is then required to generate the vacant coordination site necessary for β-elimination. Thus, compounds such as $CpFe(CH_2CHMe_2)(CO)(PPh_3)$[51] and $CpRe(CH_2CH_2CH_3)(NO)(PPh_3)$[52] are stable under ambient conditions. Furthermore, homoleptic alkyls frequently undergo facile fluxional rearrangement in solution which may be retarded when tertiary phosphine ligands (particularly chelating ligands) are present. For example, $TaMe_5$ is an unstable fluxional molecule at 25°C, whereas the chemically distinct methyls of the stable adduct $TaMe_5(dmpe)$ are resolved at -18°C (^1H NMR) and are consistent with this complex possessing a pentagonal bipyramidal geometry with axial methyl ligands[53]. Lower valent metal alkyls generally conform to the 18-electron rule such as, $Co(CH_3)(CO)(PMe_3)_3$[54], $Ta(CH_3)(CO)_2(dmpe)_2$[55] and $CpMo(CH_3)(CO)_2(PPh_3)$[56]. For the latter complex, the *trans* isomer is more stable than the *cis* (K_{eq} [*cis*]/[*trans*] = 0.08 in toluene solution) presumably for steric reasons. Similarly, vinyl and acyl complexes may be stabilised towards decomposition by phosphine coordination as in the 18-electron compounds, $CpFe(CH{=}CMe_2)(dppe)$[57] and $CpFe(COMe)(CO)(PR_3)$[58]. The "Fe(dppe)" five-membered chelate ring in the former renders ligand displacement unfavourable. Sterically undemanding chelating phosphines such as dmpe have been used in the structural study of agostic C-H··M interactions[59]. The phosphine ligand prevents dimerisation, confers crystallinity,

stability and does not hinder the interactions of the alkyl ligands with the metal (Figure 1.9).

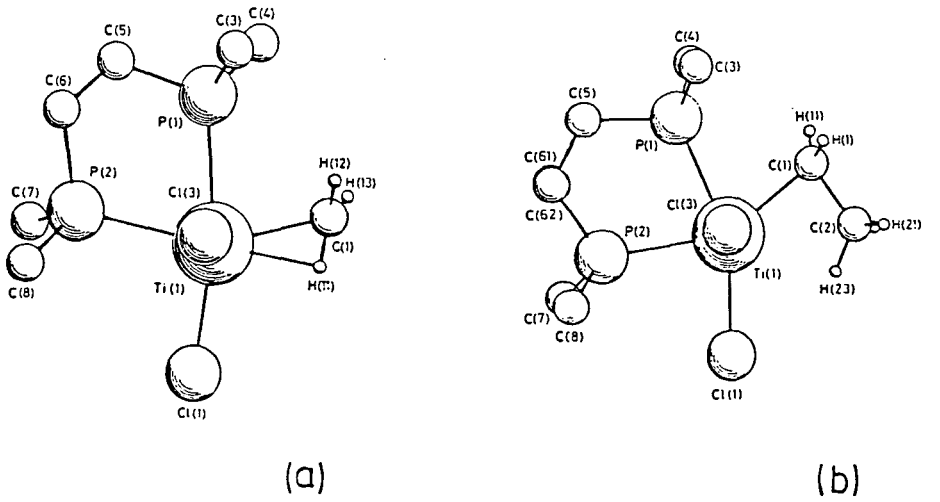

Figure 1.9 *Agostic C-H→M Interactions in $TiRCl_3(dmpe)$ (R=Me(a), Et(b))*

1.4 REACTIONS OF TERTIARY PHOSPHINE COMPLEXES WITH SMALL CATALYTICALLY IMPORTANT MOLECULES

1.4.1 Dihydrogen

The oxidative addition of dihydrogen to a transition metal complex is an important step in catalytic cycles such as olefin hydrogenation, hydroformylation and in the conversion of synthesis gas (CO/H_2) to higher hydrocarbons[50]. The oxidative addition process is favoured by a low valent metal with a strongly basic ligand field and by the availability of vacant metal orbitals of appropriate energy. Early transition metal tertiary phosphine complexes satisfy these criteria, representative examples are shown in Equations 1.13 and 1.14.

$$TaCl_2(PMe_3)_4 \xrightarrow[25^oC/Et_2O]{H_2\ (1\ atm.)} TaCl_2H_2(PMe_3)_4 \quad ^{29} \qquad (1.13)$$

$$Ta_2Cl_6(PMe_3)_4 \xrightarrow[25^oC/toluene]{H_2\ (1\ atm.)} Ta_2Cl_6H_2(PMe_3)_4 \quad ^{30} \qquad (1.14)$$

Rates of reaction are correspondingly slower where ligand dissociation is required to generate a vacant coordination site (Equation 1.15).

$$Os(CO)_4(PPh_3) \xrightarrow[130^oC]{H_2\ (120\ atm.)} H_2Os(CO)_3(PPh_3) \quad ^{60} \qquad (1.15)$$

As indicated in Equation 1.15, selective displacement of carbon monoxide has occurred, under thermal conditions. Similar selectivity can be observed under photolytic conditions, thus flash photolysis of $RhCl(CO)(PPh_3)_2$ generates the reactive 14-electron intermediate $[RhCl(PPh_3)_2]$ (a presumed intermediate in catalytic hydrogenations involving Wilkinson's catalyst) by selective CO dissociation. This intermediate rapidly adds dihydrogen to form $RhH_2Cl(PPh_3)_2$[61] with a rate constant of *ca.* $1 \times 10^5\ M^{-1}\ sec^{-1}$ at 25^oC. Presumably of the two possible intermediates generated by photolysis, $[RhCl(PPh_3)_2]$ and $[RhCl(CO)(PPh_3)]$, the former, containing the more basic ligand set, reacts faster with dihydrogen than the latter.

The addition of dihydrogen to a transition metal centre has been postulated to be most favourable with side-on approach of H_2 rather than end-on[50], in which the transition state for oxidative addition retains considerable H-H bonding. These postulates have been recently vindicated by the isolation of η^2-molecular dihydrogen complexes, an example of which is illustrated in Figure 1.10[62]. A number of derivatives have been prepared, in which both the steric and electronic properties of the phosphine ligands used were found to be important in stabilising the product[63]. Such compounds are presumably formed, albeit

transiently, in the oxidative addition of H_2 to unsaturated metal centres.

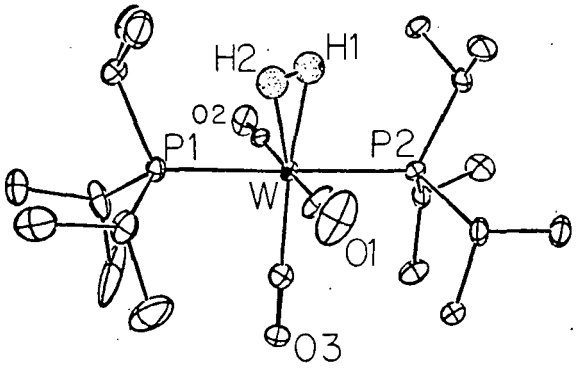

Figure 1.10 *X-Ray of* $W(\eta^2\text{-}H_2)(CO)_3(Pcy_3)_2$

1.4.2 Dinitrogen

Stimulated by the catalytic reduction of N_2 to NH_3 under ambient conditions by the nitrogenase metalloenzymes, the study of transition metal dinitrogen complexes has been widely pursued. Dinitrogen is both a weaker σ-donor and π-acceptor than CO, with which it is isoelectronic and $d\pi$-$p\pi$ back-bonding is essential in stabilising dinitrogen compounds. Thus, low valent, electron-rich, early transition metals form the most stable N_2 complexes, particularly the 4d and 5d congeners. Consequently, the basic tertiary phosphine ligands have been found to be ideal co-ligands (Equations 1.16-1.18).

$$WCl_4(PMe_2Ph)_2 + N_2 \xrightarrow[PMe_2Ph\ (xs)]{Na(Hg)} W(N_2)_2(PMe_2Ph)_4{}^{64} \qquad (1.16)$$

$$Mo(PMe_3)_6 \xrightarrow{N_2\ (15\ atm.)} Mo(N_2)(PMe_3)_5{}^{39} \qquad (1.17)$$

$$ReCl_2(PPh_3)_2(N_2COPh)L \xrightarrow[\text{boiling MeOH}]{PMe_2Ph\ (xs)} Re(N_2)Cl(PMe_2Ph)_4{}^{65} \qquad (1.18)$$

(L = PMe_2Ph)

Linear dinitrogen bridged complexes, particularly of electronically unsaturated metal centres have been studied since they are chemically more reactive than the saturated derivatives. This results from the μ_2-N_2 ligand being best represented as a linked diimido ligand with a formal N-N single bond (Equation 1.19).

$$Ta(CHCMe_3)(PMe_3)_4Cl \xrightarrow[1\ atm.]{N_2} [Ta(CHCMe_3)(PMe_3)_2Cl]_2(\mu\text{-}N_2){}^{28} \qquad (1.19)$$

In this compound, N_2 has displaced two PMe_3 ligands per tantalum, the electronic deficiency presumably being compensated for by $p\pi \rightarrow d\pi$ interactions between nitrogen and tantalum. The molecular structure of the derivative in which chloride is replaced by neopentyl is shown in Figure 1.11[66].

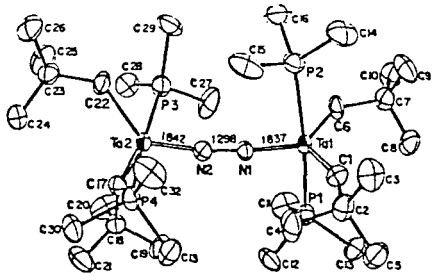

Figure 1.11 *X-Ray of* $[Ta(CHCMe_3)(PMe_3)_2(CH_2CMe_3)]_2(\mu\text{-}N_2)$

The Ta-N distance of 1.84Å is comparable to Ta(V) imido complexes [*cf.* 1.765Å in $Ta(NPh)(THF)(PEt_3)Cl_3$][67] and the N-N bond is *ca.* 0.2Å longer that that in free nitrogen [1.0976Å][28] consistent with a predominant structural form of [Ta=N-N=Ta].

The protonation of dinitrogen compounds can yield different products (Equations 1.20-1.22).

$$[Ta]{=}N\text{-}N{=}[Ta] \xrightarrow{HCl} NH_2NH_2.2HCl^{28} \qquad (1.20)$$

$$M(N_2)_2(dppe)_2 \xrightarrow[THF]{H_2SO_4} [M(dppe)_2(HSO_4)(NNH_2)]^+ + N_2^{68} \qquad (1.21)$$
(M=Mo,W)

$$M(N_2)_2(PMePh_2)_4 \xrightarrow[MeOH]{H_2SO_4} NH_3 \begin{matrix}(1.9\ NH_3/W\ atom)\\(0.7\ NH_3/Mo\ atom)\end{matrix}^{68} \qquad (1.22)$$
(M=Mo,W)

Reactions 1.21 and 1.22 illustrate the effect that different tertiary phosphine ligands have on the products of protonation. Phosphine labilisation is required in this system, allowing PR_3 to be replaced by the sulphate or hydrogen sulphate ligands. The chelate derivatives do not react to give NH_3 in other than boiling acid media[68].

1.4.3 Dioxygen

Extensive research has been conducted on transition metal dioxygen compounds, motivated by the chemistry of oxygen transport and hydrocarbon oxygenations in biological systems[69].

Tertiary phosphine complexes of d^n ($n \geq 2$) metals can react with dioxygen in a formal 2-electron transfer reaction to form a η^2-O_2^{2-}, peroxide ligand (Equations 1.23 and 1.24). In these reactions, the importance of the tertiary phosphine ligands in stabilising the products lies in their providing a strongly basic, substitutionally inert ligand set[69].

$$[Co(diphos)_2]^+BF_4^- \xrightarrow[C_6H_6]{O_2} [(\eta^2\text{-}O_2)Co(diphos)_2]^+BF_4^-{}^{70} \qquad (1.23)$$
(diphos = $Ph_2PCH{=}CHPPh_2$)

$$(Ph_3P)_2Pt(\eta^2\text{-}C_2H_4) \xrightarrow[C_7H_8]{O_2} (Ph_3P)_2Pt(\eta^2\text{-}O_2)\ ^{71} \qquad (1.24)$$

Reversible O_2 binding has been observed in the series of manganese compounds $MnX_2(PR_3)$ (X = Cl, Br, I; R_3 = $^nBu_3$, $^nBu_2Ph$, $^nBuPh_2$)[72,73]. Significantly, the stability of the 1:1 complexes formed, $[MnX_2(PR_3)(O_2)]$ was dependent upon the nature of the phosphine ligand used, such that stability increased in the order PR_3 > $PPhR_2$ > PPh_2R > PPh_3, although the reasons for this trend have not been fully elucidated[73].

1.4.4 Carbon Dioxide

Carbon dioxide is an important industrial feedstock, as a source of chemical carbon[74]. Transition metal complexes can interact with CO_2 in a variety of ways depending upon the nature of the metal and the attendant ligands (Scheme 1.1).

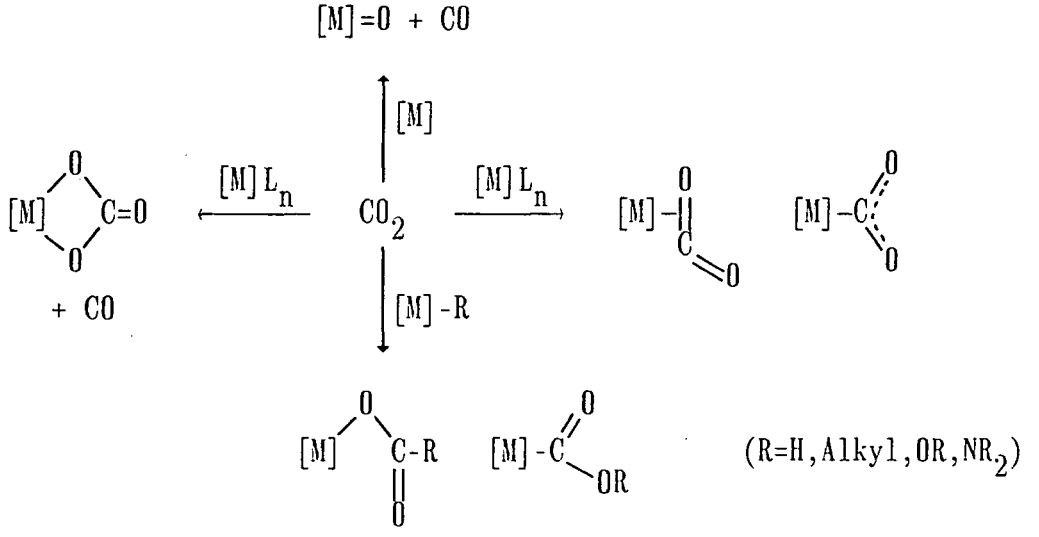

Scheme 1.1 *Some Metal Mediated Transformations of CO_2*

Tertiary phosphine metal complexes permit many of these transformations. For example, low-valent, electron rich complexes may coordinate CO_2 as either η^2-CO_2 or C-bonded η^1-CO_2 (Figure 1.12) depending upon the ligand environment, and the basicity of the metal (Equations 1.25 and 1.26).

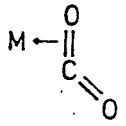

(A) η^2-CO_2

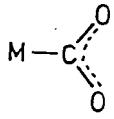

(B) C-bonded η^1-CO_2

Figure 1.12

$$[Ir(dmpe)_2]^+Cl^- \xrightarrow[1\ atm.]{CO_2} [Ir(\eta^1\text{-}CO_2)(dmpe)_2]^+Cl^- \quad [\nu(CO_2)=1550,1230\ cm^{-1}] \quad ^{75} \qquad (1.25)$$

$$Ni(PCy_3)_3 \xrightarrow[1\ atm.]{CO_2} Ni(\eta^2\text{-}CO_2)(PCy_3)_2 \quad [\nu(CO_2)=1740,1150\ cm^{-1}] \quad ^{76} \qquad (1.26)$$

The nickel complex above has been shown by X-ray crystallography to possess a bent η^2-CO_2 ligand, but the iridium complex was proposed to be bonded as in Figure 1.12(B) on the basis of infrared data. It was argued that this mode of coordination was favoured because of the high basicity of the iridium centre[75]. A further effect of the high metal basicity in phosphine rich compounds is in the formation of metallacycles. Equation 1.27 illustrates one such reaction wherein it was proposed that initial nucleophilic attack of the electron-rich metal centre on CO_2 was followed by nucleophilic attack of the oxygen atom (of the intermediate oxycarbonyl unit) upon a second molecule of CO_2 to give the final product[77].

$$IrCl(C_8H_{14})(PMe_3)_3 \xrightarrow[C_6H_6]{CO_2} \text{(1.27)}$$

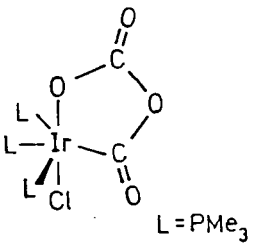

For low-valent, electron-rich complexes of the more oxophilic early transition metals, deoxygenation (Equation 1.28) and disproportionation (Equation 1.29) of CO_2 are common reactions.

$$(\eta^2\text{-}C_2H_4)Mo(dppe)_2 \xrightarrow[\text{Reflux}]{CO_2/\text{Toluene}} cis\text{-}Mo(CO)_2(dppe)_2 + Ph_2(O)PCH_2CH_2P(O)Ph_2 \quad ^{78} \quad (1.28)$$

$$cis\text{-}(N_2)_2Mo(PMe_2Ph)_4 \xrightarrow[THF]{CO_2} Mo(CO_2)_2(PMe_2Ph)_4 \xrightarrow{THF} (CO)(PMe_2Ph)_3Mo(OCO)_2Mo(PMe_2Ph)_3(CO) \quad ^{79} \quad (1.29)$$

As indicated in Scheme 1.1, CO_2 can formally insert into a number of metal bound substituents such as H, alkyl, alkoxide and amide. Of particular relevance is the reaction of CO_2 with $Fe(PMe_3)_4$. This complex undergoes rapid, reversible, intramolecular oxidative addition of a PMe_3, C-H bond in solution (see Section 1.5). Both tautomers react with CO_2 in solution according to Scheme 1.2[80].

Tautomer (I) has effected both coordination and disproportionation of CO_2 whereas tautomer (II) reacts initially *via* CO_2 insertion into the Fe-CH_2 bond producing a five-membered metallaheterocycle, followed by CO_2 insertion into the metal hydride ligand to afford a chelating formato ligand[80].

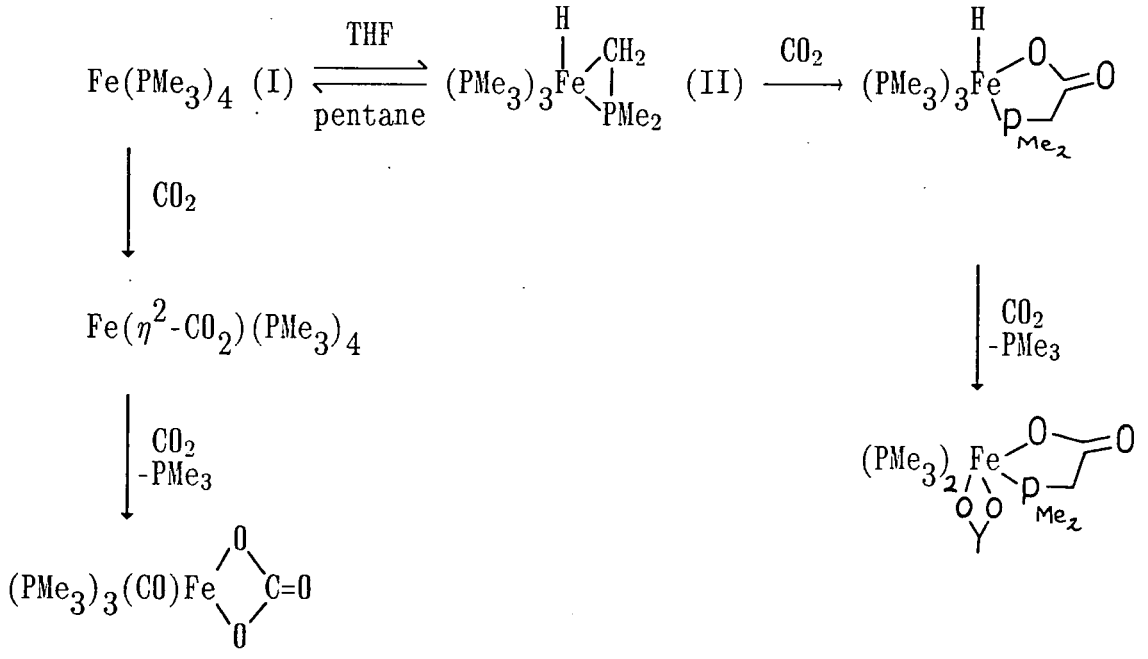

Scheme 1.2

1.4.5 Carbon Monoxide

The use of carbon monoxide in the production of commodity chemicals is well known, for example, Monsanto's acetic acid process, the oxo process for aldehyde and alcohol production and the Fischer-Tropsch reaction for the conversion of synthesis gas (CO/H_2) into hydrocarbons. All of these processes are transition metal catalysed and involve metal coordinated carbon monoxide.

The treatment of low-valent, tertiary phosphine rich complexes with CO generally results in phosphine displacement, but complete replacement is rarely achieved. The product of Equation 1.30[39b], contains three carbonyl ligands *trans* to three PMe_3 ligands. Since PMe_3 is a weaker *trans* influencing ligand than CO, further phosphine substitution would result in the relatively less favourable *trans* di-carbonyl arrangement, and consequently does not occur under these reaction conditions[39b].

$$Mo(PMe_3)_6 \xrightarrow[25^0C]{CO\ (2\ atm.)} \textit{fac}\text{-}Mo(CO)_3(PMe_3)_3 \qquad (1.30)$$

Carbon monoxide can displace other molecules such as dihydrogen from polyhydrido compounds, thus resulting in reduction of the metal centre (Equation 1.31)[48].

$$Cp^*Ta(PMe_3)_2H_4 \xrightarrow[25^oC]{CO} \underset{+\ H_2}{Cp^*Ta(PMe_3)_2H_2(CO)} \xrightarrow[80^oC]{CO} \underset{+\ H_2}{Cp^*Ta(PMe_3)_2(CO)_2} \quad (1.31)$$

However, the rate limiting step of the above reaction was shown to involve PMe_3 displacement and the formation of a transient intermediate, $[Cp^*Ta(PMe_3)H_4(CO)]$ prior to H_2 elimination[48].

The use of ligated tertiary phosphines in the synthesis of otherwise poorly accessible carbonyl complexes has been reported. The reaction presented in Equation 1.32 is particularly interesting[81].

$$CpVCl_2(PEt_3)_2 \xrightarrow[THF,\ 20^oC]{Zn(xs),CO(1\ atm)} \underset{70\%}{CpV(CO)_3(PEt_3)} \quad (1.32)$$

The starting V(III) complex does not react with CO at 20°C, thus the initial step involves reduction to V(II). The V(II) intermediate has been isolated[81] and shown to react with CO, in the absence of a reducing agent, *via* a disproportionation reaction to afford $CpV(CO)_3(PEt_3)$ and $CpVCl_2(PEt_3)$ which subsequently re-enters the reaction cycle. The proposed mechanism is shown in Scheme 1.3[81].

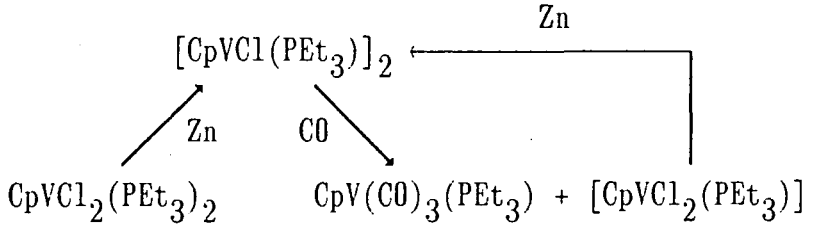

Scheme 1.3

Tertiary phosphine complexes have been widely used in the catalytic reactions of CO. Reversible CO binding to a transition metal is often

important and McAuliffe has shown that the compounds, $MnX_2(PR_3)$ (X = Cl, Br, I; PR_3 = PMe_2Ph, PEt_2Ph, PPr^n_3) reversibly bind CO[82] (reversible O_2 binding in these complexes was mentioned in Section 1.4.3). ESR measurements in frozen THF solutions[82] indicated the CO complexes to have the axially symmetrical geometry shown in Figure 1.13.

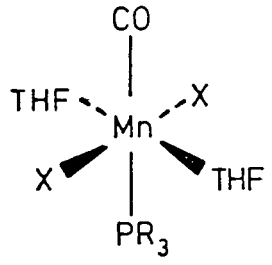

Figure 1.13

For X = Cl, the rate of CO uptake increases in the order PPr^n_3 > $PPhEt_2$ ≈ $PPhMe_2$, presumably as a result of the strong *trans* effect of PPr^n_3 upon the precursor molecule in which THF replaces CO in Figure 1.13.

The platinum complex, $Pt(P^iPr_3)_3$ has been shown to be an active catalyst for the water-gas shift reaction[83] (Equation 1.33).

$$CO + H_2O \rightleftharpoons CO_2 + H_2 \qquad (1.33)$$

The relatively bulky, strongly basic phosphine ligand, P^iPr_3, promotes the oxidative addition of H_2O to platinum. Reaction with solvent molecules generates an hydroxide salt[83] from which the solvent molecule is displaced by CO (Scheme 1.4). Nucleophilic attack of OH^- on coordinated CO affords an hydroxycarbonyl which can decarboxylate to produce $Pt^{II}H_2(P^iPr_3)_2$ from which dihydrogen may be obtained by reductive elimination (Scheme 1.4)[83].

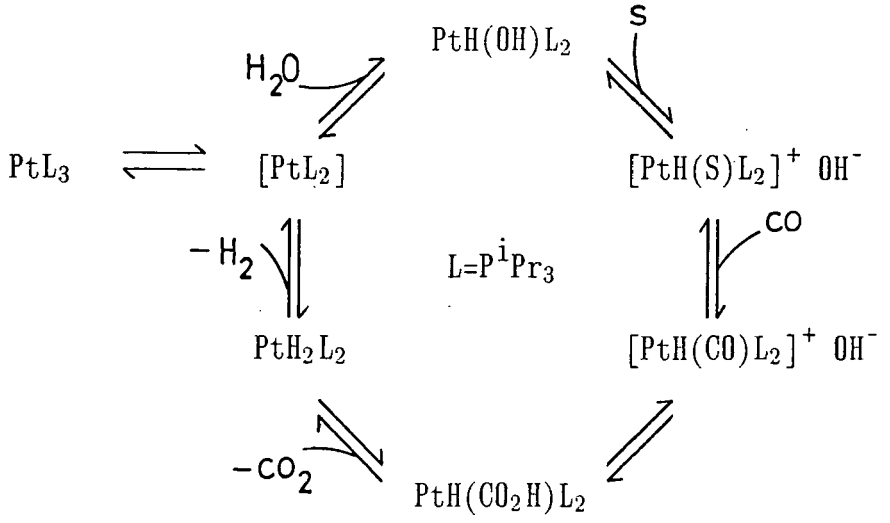

Scheme 1.4 *Proposed Catalytic Cycle for PtL_3 Catalysed Water Gas Shift Reaction*

The use of a less bulky tertiary phosphine such as PEt_3 retards the reaction due to the low ability of CO to displace PEt_3 from $[PtH(PEt_3)_3]^+ OH^-$ formed in the catalytic cycle[83].

Tertiary phosphine modified cobalt and rhodium catalysts have been used in the selective synthesis of linear aldehydes and alcohols *via* the oxo reaction (hydroformylation)[84]. One particular example involves $HRh(CO)_4$. In the absence of tertiary phosphines, competing equilibria result in the formation of catalytically inactive clusters such as $Rh_4(CO)_{12}$ and $Rh_6(CO)_{16}$.

With a $Rh:PR_3$ ratio of 1:2, the catalytic cycle illustrated in Scheme 1.5 is plausible. The tertiary phosphine inhibits rhodium-carbonyl cluster formation, prevents excessive olefin hydrogenation and isomerisation and generally promotes high selectivity for producing linear aldehydes. The latter is connected with the olefin insertion step in Scheme 1.5, where it has been shown that bulky phosphines, L, favour anti-Markovnikov addition, presumably for steric reasons[84].

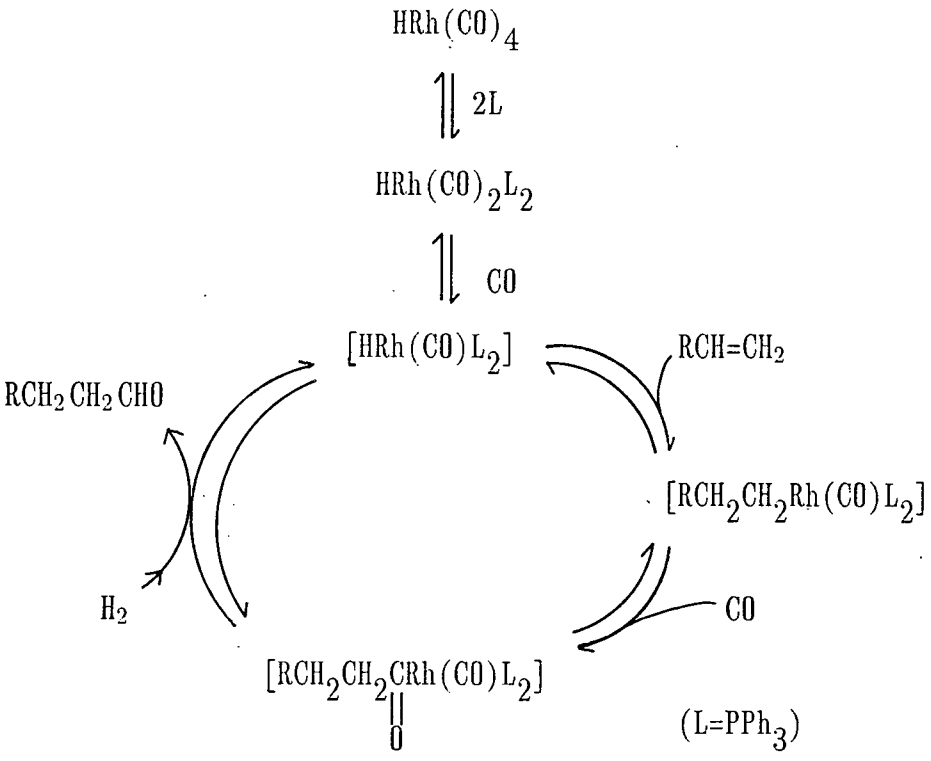

Scheme 1.5 *Plausible Mechanism for Rhodium Catalysed, Phosphine Assisted Oxo Process.*

1.4.6 Olefins and Acetylenes

The interaction of an olefin or acetylene molecule with a transition metal centre consists of both σ and π components and bears similarity to carbon monoxide coordination. The electronic environment of the metal dictates both the structure and reactivity of the resulting complexes.

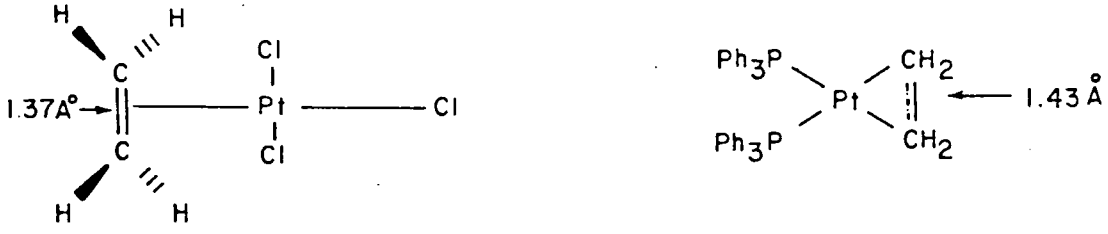

(a) (b)

Figure 1.14

Thus, the more electron rich, formally Pt(0) complex [Figure 1.14(b)] has a longer C=C bond to that of Zeise's salt [Figure 1.14(a)], and the olefin is orientated in the molecular plane. The ethylene ligand in Zeise's salt is perpendicular to the $[PtCl_3]$ plane[50].

The subsequent chemistry of metal coordinated olefins and acetylenes is strongly affected, therefore, by the nature of the metal and its ligand field. Olefins can displace the more basic PMe_3 ligands in $Mo(PMe_3)_6$ according to Equation 1.34[39b].

$$Mo(PMe_3)_6 \xrightarrow{C_2H_4\ (3\ atm.)} \textit{trans}\text{-}Mo(C_2H_4)_2(PMe_3)_4 \qquad (1.34)$$

The stronger *trans* effect of C_2H_4 over PMe_3 results in the preferential displacement of the second PMe_3 ligand, *trans* to coordinated C_2H_4. The molecular structure[85] revealed the coordinated ethylene to possess relatively long C=C bonds of 1.40(1)Å. The electron rich nature of this complex was further illustrated by the lability of the PMe_3 ligands, dissociating readily in solution[85].

Certain strained cycloalkynes that are unstable in the free state have been stabilised by complexation in tertiary phosphine containing metal compounds. For example, cyclohexyne and cycloheptyne have been "trapped" in the complexes (A)[86] and (B)[87] shown in Figure 1.15.

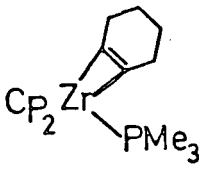

(A)

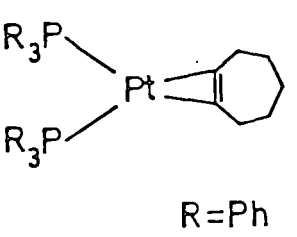

(B)

Figure 1.15

In both cases the coordinated alkyne is best viewed as a metallacyclopropene complex. The zirconium complex (A), undergoes a number of insertion reactions with unsaturated organic substrates *via* initial PMe_3 displacement (Scheme 1.6)[86].

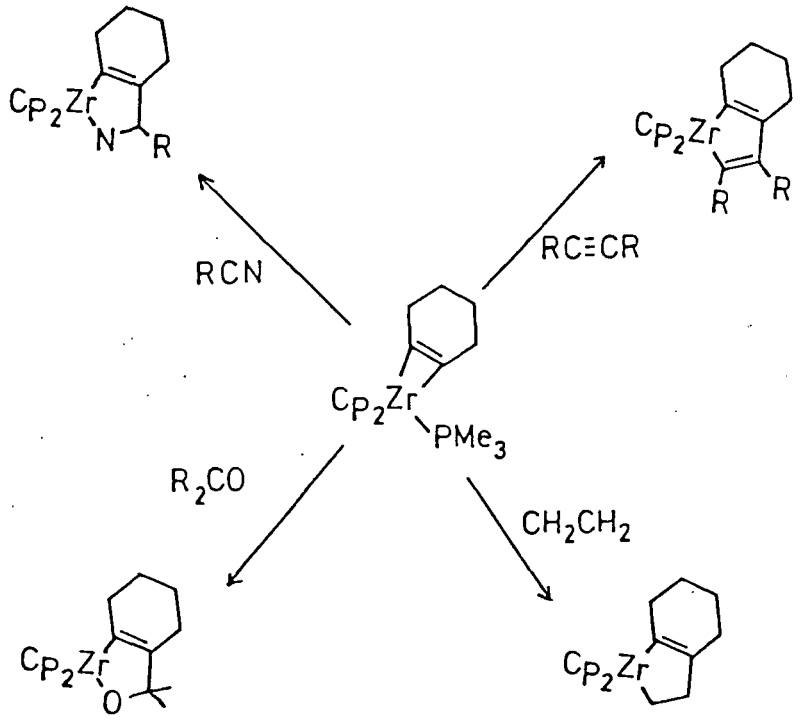

Scheme 1.6

Both nucleophilic and electrophilic reagents can attack coordinated olefins. Normally, free olefins are not susceptible to nucleophilic attack, but when complexed to metals in a relatively high oxidation state (II to IV) in cationic systems, nucleophilic addition is possible. The ligand field requirements include substitutionally inert, electron withdrawing ligands, and the tertiary phosphine, PPh_3 or its phosphite analogue, $P(OPh)_3$, have been employed successfully (Equation 1.35)[88].

$$[CpPd(PPh_3)(CH_2{=}CH_2)]^+ + [CH(OMe)_2]^- \xrightarrow[-19^0]{THF} CpPd(PPh_3)(CH_2CH_2CH(COMe)_2) \quad (1.35)$$

Similar reactivity is displayed by cationic alkyne complexes resulting in the formation of σ-vinyl ligands.

Among the most widely studied transformations of olefins has been their insertion into metal coordinated hydrido and alkyl ligands, forming the basis of olefin hydrogenation, hydroformylation (Section 1.4.5) and model systems for the polymerisation of olefins[50]. In the stoichiometric hydrogenation of substituted styrenes (Equation 1.36), Halpern[89] has demonstrated a number of competing factors in the rate of reaction.

$$RhH_2Cl(PR_3)_3 + CH_2{=}CHPh' \longrightarrow RhCl(PR_3)_3 + CH_3CH_2Ph' \qquad (1.36)$$

$PR_3 = PPh_3$, $P(p\text{-}X\text{-}C_6H_4)_3$; X = Cl, F, Me, OMe
Ph' = Ph, p-X-Ph; X = Cl, F, Me, OMe

The reaction involves initial phosphine displacement, subsequent olefin coordination followed by olefin insertion into a metal hydride ligand, and finally, reductive elimination of alkane. Although no clear trend was found between the equilibrium constants of olefin coordination and the substituted phosphine used, the rate of the insertion step was observed to be increased by the more electron donating para-substituents, X, of the phosphine ligand[89]. It was proposed that the more electron releasing tertiary phosphines were better able to stabilise the electronically unsaturated transition state for olefin insertion[89].

The complex $WH(\eta^2\text{-}CH_2PMe_2)(PMe_3)_4$ (see Section 1.5) has been reported to facilitate the oxidative dimerisation of ethylene to butadiene[90], *via* the complex $W(\eta^2\text{-}C_2H_4)_2(PMe_3)_4$ (Equation 1.37).

$$WH(\eta^2\text{-}CH_2PMe_2)(PMe_3)_4 \xrightarrow[25^oC]{C_2H_4\ (1\ atm)} W(\eta^2\text{-}C_2H_4)_2(PMe_3)_4$$

$$\xrightarrow[60^oC]{C_2H_4\ (2\ atm)} W(\eta^4\text{-}C_4H_6)_2(PMe_3)_2 \qquad (1.37)$$

It was considered that this dimerisation reaction was associated with the electron rich nature of the tungsten precursor[90].

1.5 INTRAMOLECULAR C-H BOND ACTIVATION IN TERTIARY PHOSPHINE COMPLEXES

Transition metal centres have been shown to insert into C-H bonds *via* a formal intramolecular oxidative addition reaction, represented schematically below.

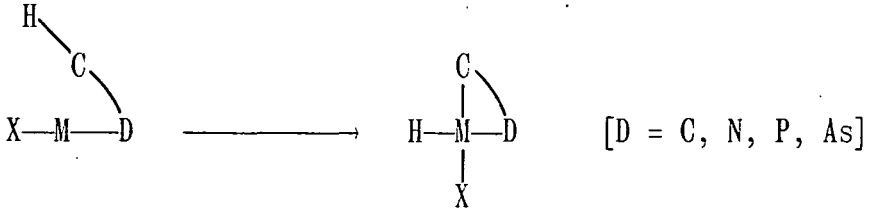

Scheme 1.7

The resulting metallacycles may contain 3, 4, 5 or 6 atoms with 4- and 5-membered rings being most common[91].

Both low valent, electron rich and formally electron deficient, higher valent metal complexes have been reported to undergo such cyclometallation reactions although, for the higher valent derivatives the reaction is often driven to completion by condensation of a stable molecule, HX, such as HCl or CH_4 (Scheme 1.7; X = Cl or CH_3) as illustrated in Equation 1.38[92].

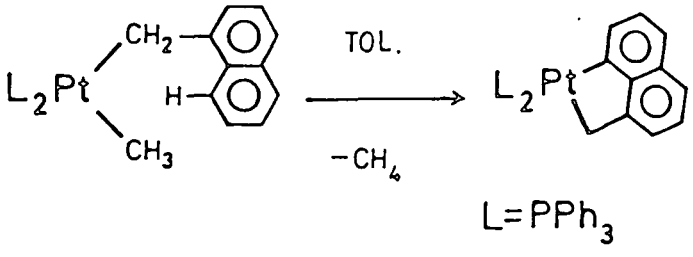

(1.38)

In the more electron rich, lower valent complexes, HX elimination is not generally required and the hydrogen atom may remain bound to the metal[50] (Equation 1.39).

$$(Me_3P)_4IrCl \xrightarrow[-PMe_3]{LiCH_2CMe_3} (Me_3P)_3(H)Ir\langle C(Me)(Me) \rangle \qquad (1.39)$$

Many examples of C-H bond activation in aryl phosphine ligands are known (*ie.* Scheme 1.7; D=P) and this subject has been reviewed[91]. Recently, however, intramolecular C-H bond cleavage reactions of trialkyl-phosphines have been demonstrated to produce 3-membered metallacycles as in Scheme 1.8. Furthermore, in many cases the process is reversible.

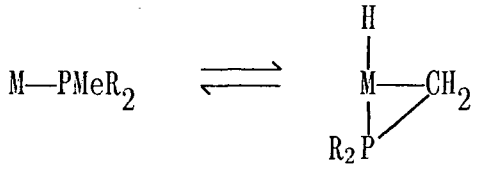

Scheme 1.8

The formation of these 3-membered, metallaheterocycles has generally been achieved by reduction of a metal tertiary phosphine complex in the presence of an excess of the phosphine, as illustrated in Equation 1.40.

$$MCl_2(PMe_3)_n \xrightarrow{(x)} MH(\eta^2\text{-}CH_2PMe_2)(PMe_3)_3 \rightleftharpoons [M(PMe_3)_4] \qquad (1.40)$$

M=Fe[36]; n=2; (x)=Na(Hg), THF, PMe_3 (xs)
M=Ru[37]; n=4; (x)=Na(Hg), C_6H_6
M=Os[38]; n=4; (x)=NaNp, THF, (Np=naphthalene)

Werner and co-workers have shown that the equilibrium in Scheme 1.8 lies almost completely to the hydrido side for M = Ru and Os (Equation 1.40) and consequently the compounds do not readily react with nucleophiles such as CO[38]. The iron analogue, however, is fluxional in solution and reacts readily with CO to form $Fe(PMe_3)_3(CO)_2$[93]. This contrasting

reactivity has been attributed to the stability of the higher oxidation state for ruthenium and osmium[37], resulting in a negligible concentration of $M(PMe_3)_4$ in the equilibrium mixture.

Trimethylphosphine has also been used as a reactive solvent medium to prepare such compounds *via* the dehalogenation of metal halides by dispersed sodium metal in the neat phosphine (Scheme 1.9)[41].

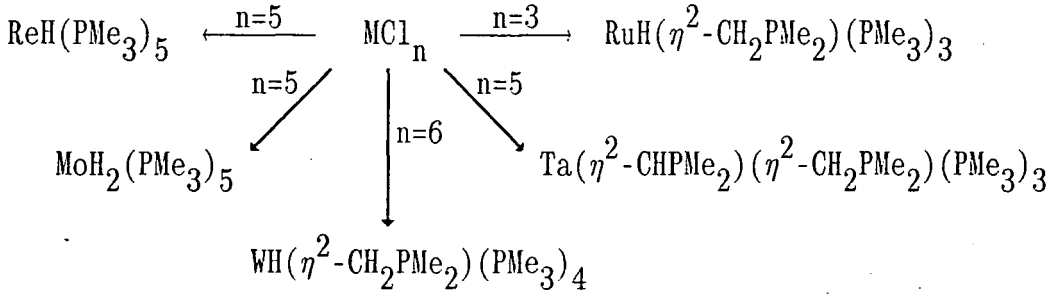

Scheme 1.9

The molecular structures of the tungsten and tantalum compounds have been elucidated by X-ray diffraction[41] [Figures 1.16(a) and 1.16(b)] and clearly show the pseudo-pentagonal bipyramidal geometry of each.

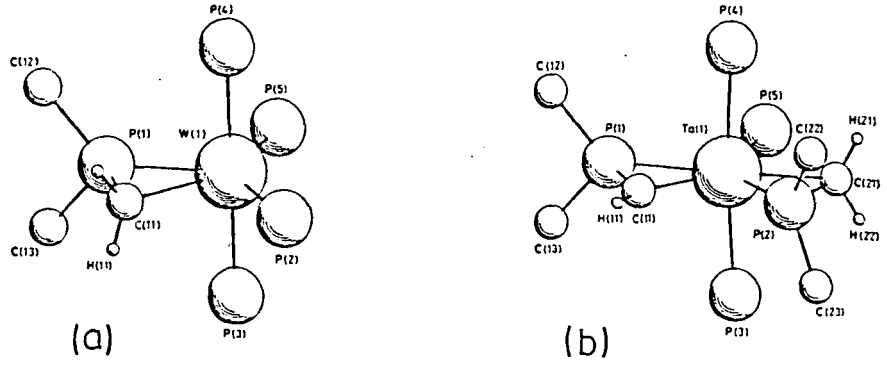

Figure 1.16 *X-ray structures of (a) $WH(\eta^2\text{-}CH_2PMe_2)(PMe_3)_4$ and (b) $Ta(\eta^2\text{-}CHPMe_2)(\eta^2\text{-}CH_2PMe_2)(PMe_3)_3$*

Both contain the $(\eta^2\text{-}CH_2PMe_2)$ moiety with M-C distances of 2.307(5)Å (W)

and 2.324(4)Å (Ta) consistent with single bonds. Although the hydrido ligand was not located in the tungsten compound it was proposed to occupy an equitorial site between P(2) and P(5) [Figure 1.16(a)]. The tantalum complex in Figure 1.16(b) is unusual in that it has not retained the metal hydride ligand. Moreover, it was found to contain the unusual metallacycle, (η^2-$CHPMe_2$). Formally, this moiety may be considered to arise from a C-H bond cleavage reaction of the (η^2-CH_2PMe_2) unit (Scheme 1.10). Consequently, the Ta-C(11) distance of 2.105(4)Å is *ca.* 0.22Å shorter than the single bond in the (η^2-CH_2PMe_2) moiety and is more consistent with a double bond (see Chapter 3).

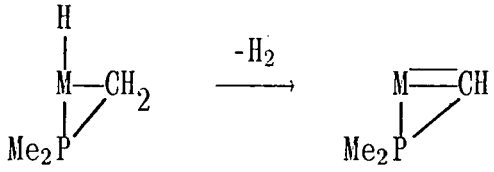

Scheme 1.10

The complex, $WH(\eta^2\text{-}CH_2PMe_2)(PMe_3)_4$ has been shown to display a wide range of reactions involving oxidation of the tungsten centre which serve to highlight the electron rich nature of this complex (Scheme 1.11[90], see also Section 1.4.6). The reactions with dinitrogen and carbon monoxide are analogous to the corresponding reactions of $Mo(PMe_3)_6$ described in Sections 1.4.2 and 1.4.5 respectively. The reaction with methanol is unusual as it involves both O-H and C-H bond cleavage, resulting in the formation of a η^2-formaldehyde ligand[95]. Significantly, this complex was reported to evolve methanol when treated with dihydrogen (15 atms., 63°C) thus modelling the latter stages of the catalytic conversion of synthesis gas (CO/H_2) to methanol[95].

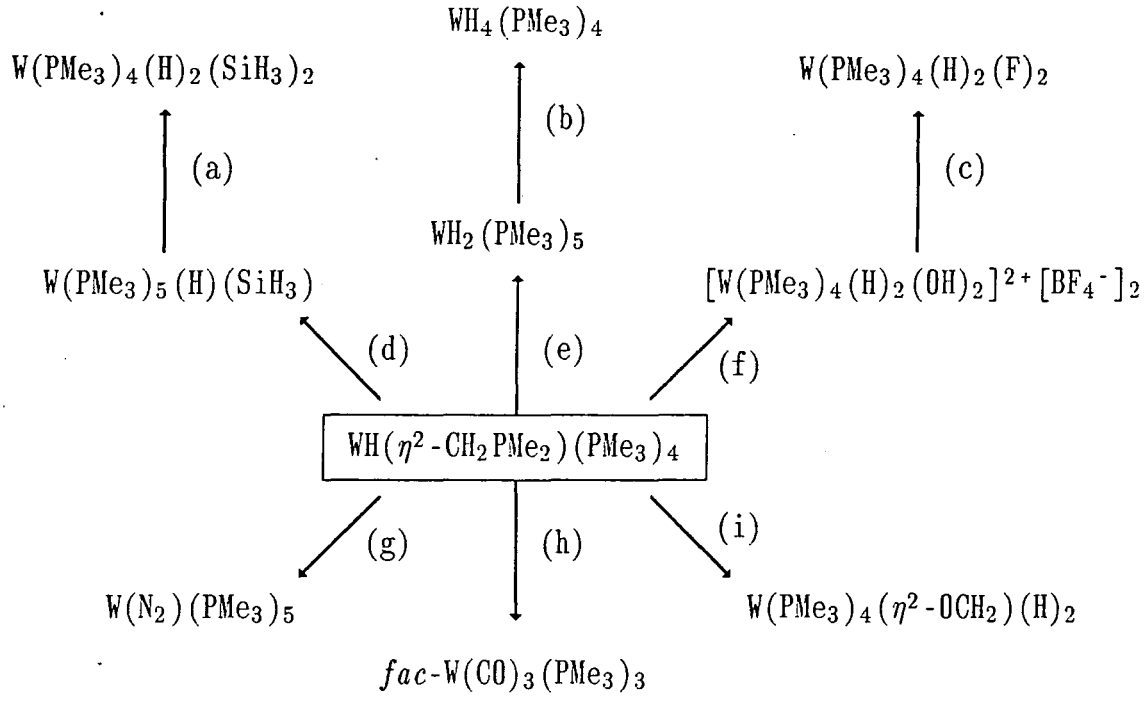

(a) 45°C/SiH_4 (b) H_2(2.5 atm.)/60°C (c) KH/THF
(d) 45°C/SiH_4 (e) H_2(2 atm.)/60°C (f) HBF_4/aq
(g) N_2(1 atm.)/60°C (h) CO(2 atm.)/60°C (i) MeOH/25°C

Scheme 1.11 *Some Reactions of* $WH(\eta^2\text{-}CH_2PMe_2)(PMe_3)_4$

1.6 INTERMOLECULAR C-H BOND ACTIVATION IN TERTIARY PHOSPHINE COMPLEXES

The direct conversion of hydrocarbon petroleum feedstocks to commodity chemicals has initiated extensive research into the activation of hydrocarbons *via* C-H bond cleavage reactions on a metal centre under mild conditions. Both electron rich, low valent complexes and higher valent, electrophilic systems have been shown to activate C-H bonds[96]. Tertiary phosphines have become a favoured ligand in low valent metal systems as a result of their wide ranging electronic and steric properties, examples of which are discussed below.

Chatt and Davidson demonstrated in 1965, that incipient $[Ru(dmpe)_2]$ would insert into various aryl C-H bonds[97] (Equation 1.41).

$$trans\text{-}RuCl_2(dmpe)_2 \xrightarrow[THF]{NaNpH} [Ru(dmpe)_2] \xrightarrow[THF]{NpH} (dmpe)_2Ru\begin{matrix}H\\Np\end{matrix} \qquad (1.41)$$

(NpH= naphthalene)

The product of this reaction eliminated naphthalene when heated to 150°C, generating $[Ru(dmpe)_2]$ which subsequently inserted into the methyl C-H bonds of a coordinated dmpe ligand[98].

Recently, the research of Bergman[99] and Graham[100] has been directed towards the thermal or photolytic generation of low valent, low coordinate intermediates of the form $Cp'ML_n$ (Cp' = Cp, Cp^*; M = Rh, Ir, Re; n = 1,2) which are capable of inserting into aliphatic C-H bonds (Equation 1.42). Trimethylphosphine was considered an ideal co-ligand due to its lability, low steric requirements and relatively basic nature[99].

$$Cp^*Ir(PR_3)H_2 \xrightarrow[-H_2]{h\nu \geq 275nm} [Cp^*Ir(PR_3)] \xrightarrow{R'H} Cp^*Ir(H)(R')(PR_3) \qquad (1.42)$$

$$R_3 = Me_3,\ Ph_3;\quad R' = Ph,\ Me,\ {}^tBuCH_2,\ C_6H_{11}$$

Moreover, it was observed that whilst the PPh_3 derivative was prone to competitive cyclometallation, the PMe_3 analogue was far less so[99]. Detailed selectivity studies established that the 16-electron intermediate $[Cp^*Ir(PR_3)]$ inserted into C-H bonds in the following relative order: C-H (aryl) > C-H (primary) > C-H (secondary) > C-H (tertiary). This order is the reverse of that expected from a radical mechanism (providing further support for the reductive elimination / oxidative addition mechanism of Equation 1.42) and was considered to reflect the relative steric environments of the C-H bonds[101]. Jones and co-workers have reported similar results for the rhodium analogue, $Cp^*Rh(PMe_3)H_2$[102].

More recently, Bergman has extended the above synthetic strategy to

the rhenium complex, $CpRe(PR_3)_3$[103], which was postulated to react with hydrocarbons as illustrated in Equation 1.43[103b].

$$CpRe(PMe_3)_3 \xrightarrow[-PMe_3]{h\nu} [CpRe(PMe_3)_2] \xrightarrow{RH} CpRe(PMe_3)_2(H)(R) \qquad (1.43)$$

The absolute stabilities of the rhenium products were lower than those of the iridium analogues[103b], possibly resulting, in part, from the sterically more encumbered rhenium coordination sphere. Moreover, the higher coordination number in the postulated rhenium intermediate resulted in increased selectivity such that only primary C-H bonds were attacked upon photolysis under ambient conditions[103b].

Similar conclusions have been drawn from the reactivity of the 16-electron fragments $[(NP_3)M]^+$ [M = Co, Rh, Ir; $NP_3 = N(CH_2CH_2PPh_2)_3$] where it was also found that the ability to insert into C-H bonds increased in the order: Co < Rh < Ir and that competing cyclometallation decreased in the order: Rh > Ir due to the sterically less encumbered coordination sphere for the iridium analogue[104].

1.7 SUMMARY

This chapter has attempted to highlight the important role of tertiary phosphine ligands in the development of the organometallic and coordination chemistry of the transition metals. Their ability to influence both structure and reactivity through steric and electronic modifications has been, and will continue to be, exploited constructively.

In this thesis, studies will be described which take advantage of the many facets of tertiary phosphine ligands to induce novel

reactivity, stabilise unusual bonding modes and facilitate the synthesis of otherwise inaccessible complexes.

1.8 REFERENCES

1. C.A. Tolman, *Chem.Rev.*, 1977, 77, 313.
2. A. Pidcock in "*Transition Metal Complexes of Phosphorus, Arsenic and Antimony Ligands*", Edited by C.A. McAuliffe, Macmillan, London (1973).
3. C.A. Tolman, *J.Am.Chem.Soc.*, 1970, 92, 2953.
4. C.A. Tolman, *J.Am.Chem.Soc.*, 1970, 92, 2956.
5. V.C. Gibson, T.P. Kee and W. Clegg, *J.Organometallic Chem.*, 1988, 353, C23.
6. W. Levason and C.A. McAuliffe, *Adv.Inorg.Chem.Radiochem.*, 1972, 14, 173 and references therein.
7. A. Gillie and J.K. Stille, *J.Am.Chem.Soc.*, 1980, 102, 4933.
8. See for example: F.A. Cotton, L.W. Shive and B.R. Stults, *Inorg. Chem.*, 1976, 15, 2239.
9. D.W. Meek and T.J. Mazanec, *Acc.Chem.Res.*, 1981, 14, 266.
10. C.A. Ghilardi, S. Midollini, S. Moneti and A. Orlandini, *J.C.S. Chem Commun.*, 1988, 1241.
11. J. Desnoyers and R. Rivest, *Can.J.Chem.*, 1965, 43, 1879.
12. M.G.B. Drew, D.G. Tisley and R.A. Walton, *J.C.S. Chem Commun.*, 1970, 600.
13. J.E. Fergusson and J.H. Hickford, *J.Inorg.Nucl.Chem.*, 1966, 28, 2293.
14. G. Booth and J. Chatt, *J.Chem.Soc.*, 1962, 2099.
15. L.H. Pignolet, D. Forster and W. De W. Horrocks, Jr., *Inorg.Chem.*, 1968, 7, 828.
16. T.A. Stephenson and G. Wilkinson, *J.Inorg.Nucl.Chem.*, 1966, 28, 945.
17. W.E. Hatfield and J.T. Yoke (III), *Inorg.Chem.*, 1962, 1, 475.
18. J.A. Osborn, F.H. Jardine, J.F. Young and G. Wilkinson, *J.Chem.Soc (A).*, 1966, 1711.

19. K.A. Jensen, P.H. Nielsen and C.T. Pedersen, *Acta.Chem.Scand.*, 1963, 17, 1115.

20. L.H. Pignolet, W. De W. Horrocks, Jr. and R.H. Holm, *J.Am.Chem. Soc.*, 1970, 92, 1855.

21. P.J. Stone and Z. Dori, *Inorg.Chim.Acta.*, 1971, 5, 434.

22. F.A. Cotton and W.J. Roth, *Inorg.Chem.*, 1984, 23, 945.

23. F.A. Cotton, S.A. Duraj and W.J. Roth, *Inorg.Chem.*, 1984, 23, 3592.

24. M.J. Bunker, A. De Cian, M.L.H. Green, J.J.E. Moreau and N. Siganporia, *J.Chem.Soc.Dalton Trans.*, 1980, 2155.

25. R.J. Burt, G.J. Leigh and D.L. Hughes, *J.Chem.Soc.Dalton Trans.*, 1981, 793.

26. R.D. Sanner, S.T. Carter and W.J. Bruton, Jr., *J.Organometallic Chem.*, 1982, 240, 157.

27. W.A. Herrmann, U. Küsthardt and E. Herdtweck, *J.Organometallic Chem.*, 1985, 294, C37.

28. S.M. Rocklage, H.W. Turner, J.D. Fellmann and R.R. Schrock, *Organometallics*, 1982, 1, 703.

29. M.L. Leutkens, Jr., J.C. Huffman and A.P. Sattelberger, *J.Am.Chem. Soc.*, 1983, 105, 4474.

30. A.P. Sattelberger, R.B. Wilson, Jr. and J.C. Huffman, *J.Am.Chem. Soc.*, 1980, 102, 7111.

31. F.A. Cotton, S.A. Duraj and W.J. Roth, *Inorg.Chem.*, 1984, 23, 4046.

32. F.A. Cotton, M.P. Diebold and W.J. Roth, *Polyhedron*, 1985, 4, 1103.

33. G. Wilke, *Angew.Chem.Int.Ed.Engl.*, 1963, 2, 105.

34. H. Behrens and A. Müller, *Z.Anorg.Allg.Chem.*, 1965, 341, 124.

35. P.L. Timms, *Angew.Chem.Int.Ed.Engl.*, 1975, 14, 273.

36. a) J.W. Rathke and E.L. Meutterties, *J.Am.Chem.Soc.*, 1975, 97, 3272.

    b) H.H. Karsch, H.-F. Klein and H. Schmidbauer, *Angew.Chem.Int.Ed. Engl.*, 1975, 14, 637.

37. H. Werner and R. Werner, *J.Organometallic Chem.*, 1981, 209, C60.

38. H. Werner and J. Gotzig, *Organometallics*, 1983, 2, 547.

39. a) F.G.N. Cloke, K.P. Cox, M.L.H. Green, J. Bashkin and K. Prout, *J.C.S. Chem Commun.*, 1982, 393.

b) M. Brookhart, K.P. Cox, F.G.N. Cloke, J.C. Green, M.L.H. Green, P.M. Hare, J. Bashkin, A.F. Derome and P.D. Grebenik, *J.Chem.Soc. Dalton Trans.*, 1985, 423.

40. F.G.N. Cloke, P.J. Fyne, M.L.H. Green, M.J. Ledoux, A. Gourdon and K. Prout, *J.Organometallic Chem.*, 1980, 198, C69.

41. V.C. Gibson, C.E. Graimann, P.M. Hare, M.L.H. Green, J.A. Bandy, P.D. Grebenik and K. Prout, *J.Chem.Soc.Dalton Trans.*, 1985, 2025.

42. J.P. Jesson in "*Transition Metal Hydrides*", Edited by E.L. Meutterties, Dekker, New York (1971).

43. W.D. Jones and J.A. Maguire, *Organometallics*, 1987, 6, 1301.

44. a) P.A. Belmonte, R.R. Schrock, M.R. Churchill and W.J. Youngs, *J.Am.Chem.Soc.*, 1980, 102, 2858.

b) P.T. Wolczanski and J.E. Bercaw, *Acc.Chem.Res.*, 1980, 13, 121.

45. N.M. Doherty and J.E. Bercaw, *J.Am.Chem.Soc.*, 1985, 107, 2670.

46. P.D. Grebenik, M.L.H. Green, A. Izquierdo, V.S.B. Mtetwa and K. Prout, *J.Chem.Soc.Dalton Trans.*, 1987, 9.

47. J. Okuda, R.C. Murray, J.C. Dewan and R.R. Schrock, *Organometallics*, 1986, 5, 1681.

48. J.M. Mayer and J.E. Bercaw, *J.Am.Chem.Soc.*, 1982, 104, 2157.

49. R.R. Schrock, *J.Organometallic Chem.*, 1976, 122, 209.

50. J.P. Collman, L.S. Hegedus, J.R. Norton and R.G. Finke, "*Principles and Applications of Organotransition Metal Chemistry*", University Science Books, California (1987).

51. D.L. Reger and E.C. Culbertson, *J.Am.Chem.Soc.*, 1976, 98, 2789.

52. W.A. Kiel, G.-Y. Lin, G.S. Bodner and J.A. Gladysz, *J.Am.Chem. Soc.*, 1983, 105, 4958.

53. R.R. Schrock and P. Meakin, *J.Am.Chem.Soc.*, 1974, 96, 5288.

54. H.-F. Klein and H.H. Karsch, *Chem.Ber.*, 1975, 108, 944.

55. S. Datta and S.S. Wreford, *Inorg.Chem.*, 1977, 16, 1134.

56. J.W. Faller and A.S. Anderson, *J.Am.Chem.Soc.*, 1970, 92, 5852.

57. A. Davison and J.P. Selegue, *J.Am.Chem.Soc.*, 1980, 102, 2455.

58. M.J. Wax and R.G. Bergman, *J.Am.Chem.Soc.*, 1981, 103, 7028.

59. Z. Dawoodi, M.L.H. Green, V.S.B. Mtetwa and K. Prout, *J.C.S. Chem Commun.*, 1982, 802; 1410.

60. F. L'Eplattenier and F. Calderazzo, *Inorg.Chem.*, 1968, 7, 1290.

61. D. Wink and P.C. Ford, *J.Am.Chem.Soc.*, 1985, 107, 1794.

62. G.J. Kubas, R.R. Ryan, B.I. Swanson, P.J. Vergamini and H.J. Wasserman, *J.Am.Chem.Soc.*, 1984, 106, 451.

63. G.J. Kubas, *J.C.S. Chem Commun.*, 1980, 61.

64. B. Bell, J. Chatt and G.J. Leigh, *J.Chem.Soc.Dalton Trans.*, 1972, 2492.

65. J. Chatt, J.R. Dilworth and G.J. Leigh, *J.Chem.Soc.Dalton Trans.*, 1973, 612.

66. M.R. Churchill and H.J. Wasserman, *Inorg.Chem.*, 1981, 20, 2899.

67. M.R. Churchill and H.J. Wasserman, *Inorg.Chem.*, 1982, 21, 223.

68. J. Chatt, A.J. Pearman and R.L. Richards, *J.Chem.Soc.Dalton Trans.*, 1977, 16, 1852; 2139.

69. E.C. Niederhoffer, J.H. Timmons and A.E. Martell, *Chem.Rev.*, 1984, 84, 137.

70. N.W. Terry (III), E.L. Amma and L. Vaska, *J.Am.Chem.Soc.*, 1972, 94, 653.

71. C.D. Cook, P.-T. Cheng and S.C. Nyburg, *J.Am.Chem.Soc.*, 1969, 91, 2123.

72. C.A. McAuliffe, M.G. Little and J.B. Raynor, *J.C.S. Chem Commun.*, 1982, 68.

73. C.A. McAuliffe, H.F. Al-Khateeb, D.S. Barratt, J.C. Briggs, A. Challita, A. Hosseiny, M.G. Little, A.G. Mackie and K. Minten, *J.Chem.Soc.Dalton Trans.*, 1983, 2147.

74. R.P.A. Sneeden in "*Comprehensive Organometallic Chemistry*", Edited by G. Wilkinson, F.G.A. Stone and E.W. Abel, Pergamon, Oxford (1982), Chapter 50.4.

75. T. Herskovitz, *J.Am.Chem.Soc.*, 1977, 99, 2391.

76. M. Aresta, C.F. Nobile, V.G. Albano, E. Forni and M. Manassero, *J.C.S. Chem Commun.*, 1975, 636.

77. T. Herskovitz and L.J. Guggenberger, *J.Am.Chem.Soc.*, 1976, 98, 1615.

78. T. Ito and A. Yamamoto, *J.Chem.Soc.Dalton Trans.*, 1975, 1398.

79. J. Chatt, M. Kubota, G.J. Leigh, F.C. March, R. Mason and D.J. Yarrow, *J.C.S. Chem Commun.*, 1974, 1033.

80. H.H. Karsch, *Chem.Ber.*, 1977, 110, 2213.

81. J. Nieman and J.H. Teuben, *Organometallics*, 1986, 5, 1149.

82. C.A. McAuliffe, D.S. Barratt, C.G. Benson, A. Hosseiny, M.G. Little and K. Minton, *J.Organometallic Chem.*, 1983, 258, 35.

83. T. Yoshida, Y. Ueda and S. Otsuka, *J.Am.Chem.Soc.*, 1978, 100, 3941.

84. C.A. Tolman and J.W. Faller, "*Homogeneous Catalysis with Metal Phosphine Complexes*", Edited by L.H. Pignolet, Plenum, New York (1983).

85. E. Carmona, J.M. Marin, M.L. Poveda, R.D. Rogers and J.L. Atwood, *J.Am.Chem.Soc.*, 1983, 105, 3014.

86. S.L. Buchwald, R.T. Lum and J.C. Dewan, *J.Am.Chem.Soc.*, 1986, 108, 7441.

87. M.A. Bennett and T. Yoshida, *J.Am.Chem.Soc.*, 1978, 100, 1750.

88. H. Kurosawa and N. Asaka, *Tetrahedron Lett.*, 1979, 255.

89. J. Halpern and T. Okamoto, *Inorg.Chim.Acta.*, 1984, 89, L53.

90. M.L.H. Green, G. Parkin, M. Chen and K. Prout, *J.Chem.Soc.Dalton Trans.*, 1986, 2227.

91. M.I. Bruce, *Angew.Chem.Int.Ed.Engl.*, 1977, 16, 73.

92. J.A. Duff. B.L. Shaw and B.A. Turtle, *J.Organometallic Chem.*, 1974, 66, C18.

93. H.H. Karsch, H.-F. Klein and H. Schmidbauer, *Chem.Ber.*, 1977, 110, 2200.

94. J.A. Labinger in "*Comprehensive Organometallic Chemistry*", Edited by G. Wilkinson, F.G.A. Stone and E.W. Abel, Pergamon, Oxford (1982), Chapter 25, page 725.

95. M.L.H. Green, G.Parkin, K.J. Moynihan and K. Prout, *J.C.S. Chem Commun.*, 1984, 1540.

96. See for example:

    a) J. Halpern, *Inorg.Chim.Acta.*, 1985, 100, 41.
    b) R.H. Crabtree, *Chem.Rev.*, 1985, 85, 245.
    c) I.P. Rothwell, *Polyhedron*, 1985, 4, 177.

97. J. Chatt and J.M. Davidson, *J.Chem.Soc.*, 1965, 843.

98. F.A. Cotton, B.A. Frenz and D.L. Hunter, *J.C.S. Chem Commun.*, 1974, 755.

99. A.H. Janowicz and R.G. Bergman, *J.Am.Chem.Soc.*, 1982, 104, 352.

100. J.K. Hoyano and W.A.G. Graham, *J.Am.Chem.Soc.*, 1982, 104, 3723.

101. A.H. Janowicz and R.G. Bergman, *J.Am.Chem.Soc.*, 1983, 105, 3929.

102. W.D. Jones and F.J. Feher, *J.Am.Chem.Soc.*, 1984, 106, 1650.

103.a) R.G. Bergman, P.F. Seidler and T.T. Wenzel, *J.Am.Chem.Soc.*, 1985, 107, 4358.

b) T.T. Wenzel and R.G. Bergman, *J.Am.Chem.Soc.*, 1986, 108, 4856.

104.C. Bianchini, D. Masi, A. Meli, M. Peruzzini and F. Zanobini, *J.Am.Chem.Soc.*, 1988, 110, 6411.

CHAPTER TWO

SYNTHESIS AND REACTIVITY OF TERTIARY PHOSPHINE DERIVATIVES OF HALF SANDWICH TANTALUM HALIDES.

2.1 INTRODUCTION

2.1.1 General

Half-sandwich metal halides are known for many of the transition elements encompassing a variety of metal oxidation states. Representative examples are given in Table 2.1 from which it can be seen that derivatives of the early transition metals predominate.

GP.4	GP.5	GP.6	GP.7	GP.9	GP.10
$CpTiX_3$[1] *X=Cl,Br,I*	$CpVCl_3$[3,4]	$CpCrX_2$[8] *X=Cl,I*			
	$CpVI_2$[4]				
Cp^*ZrCl_3[2]	$CpNbX_4$[5] *X=Cl,Br*	$CpMoCl_4$[9]		Cp^*RhCl_2[12,13]	
	$CpNbBr_3$[6]				
Cp^*HfCl_3[2]	$CpTaX_4$[5] *X=Cl,Br*	Cp^*WCl_4[10]	Cp^*ReCl_4[11]	Cp^*IrCl_2[12,13]	Cp^*PtBr_3[14]
	Cp^*TaCl_3[7]				

Table 2.1 *Half-Sandwich Transition Metal Halides.*

Many of these compounds have been shown to provide a useful synthetic entry into the chemistry of half-sandwich derivatives, particularly low-valent complexes, for example by reductive dehalogenation in the presence of suitable donor molecules (Equation 2.1, [RED] = reductant).

$$CpM^{X}Cl_{X-1} + [RED] \xrightarrow{L} CpM^{X-1}Cl_{X-2}.L_y + [RED]Cl \quad (2.1)$$

However, the chemistry of half-sandwich tantalum complexes has remained largely undeveloped. In this chapter we describe the synthesis

and characterisation of a number of tertiary phosphine complexes with metal oxidation states ranging from (V) to (I) and some aspects of their derivative chemistry.

2.1.2 Complexes Of The Form $Cp'MCl_4$ (M = Nb, Ta; Cp'=Cp, Cp^*)

A systematic study of the chemistry of half-sandwich tantalum complexes has recently been made possible by the development of convenient syntheses of $Cp'TaCl_4$ employing either tin[5] or silicon[1] compounds as Cp' transfer reagents. The action of more conventional cyclopentadienylating agents (such as sodium cyclopentadienide) on tantalum pentachloride, leads to both reduction of the metal and the incorporation of more than one Cp ring (Equation 2.2)[15].

$$NaCp + TaCl_5 \longrightarrow (\eta^5\text{-}C_5H_5)_2Ta(\sigma\text{-}C_5H_5)_2 \qquad (2.2)$$

The silicon and tin reagents however, have been found to provide more controllable sources of Cp' ligands and their reactions are generally free of complicating side reactions. A representative synthesis of $Cp'TaCl_4$ is outlined in Equations 2.3 and 2.4.

$$NaCp' + {}^nBu_3SnCl \xrightarrow{\text{Toluene}} {}^nBu_3SnCp' + NaCl \qquad (2.3)$$

$$^nBu_3SnCp' + TaCl_5 \xrightarrow{\text{Toluene}} Cp'TaCl_4 + {}^nBu_3SnCl \qquad (2.4)$$

$$[Cp' = C_5H_5,\ C_5H_4Me,\ C_5Me_5]$$

The byproduct in Equation 2.4, $^nBu_3SnCl$, is a hydrocarbon soluble liquid which may be readily separated from the sparingly soluble $Cp'TaCl_4$.

The most notable omission from the list of known $Cp'MCl_4$ compounds is Cp^*NbCl_4. This compound has now been synthesised in this laboratory (see Chapter 7, section 7.2.6) and characterisation is given in

Appendix 5.

The solid state structures of $Cp'MCl_4$ (M = Nb, Ta) have not been unambiguously defined. They contain, formally, 14-electron metal centres and are thus highly unsaturated and capable of acting as Lewis acids. For this reason they were postulated to be at least dimeric and possibly of a form reminiscent of $[TaCl_5]_2$ (Figure 2.1)[16,18].

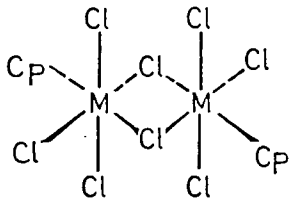

Figure 2.1 *Possible Geometry of $CpMCl_4$ Dimer.*

This pseudo-octahedral, six-coordinate geometry in which a formal 2 electron donating atom is *trans* to the Cp ligand is not unusual (*vide infra*). No evidence for a dimeric structure was obtained from mass spectral studies and low solubility in common organic solvents precluded molecular weight measurements. However, $(\eta^5\text{-}C_5Et_4{}^tBu)WCl_4$ has been shown to be dimeric in solution by molecular weight determination[17].

2.2 SYNTHESIS OF COMPLEXES OF THE FORM $Cp'TaCl_xL_y$ [L = TERTIARY PHOSPHINE, (x+y) = 4 or 5]

2.2.1 Preparation Of $CpTaCl_4.PMe_3$ (1)

The compounds, $Cp'TaCl_4.L$ are potentially the simplest half-sandwich chloro-phosphine derivatives to prepare, by direct interaction

of $Cp'TaCl_4$ and the donor compound L. However, although Cp^*TaCl_4 reacts with donor molecules in solution, relatively few simple adducts have been isolated in pure form[19]. Therefore, as a prelude to further studies, we have re-examined an earlier report of the preparation of $CpTaCl_4.PMe_3$ for which characterising data was not provided[19], and a full description of this complex is presented here.

$CpTaCl_4$ reacted over the course of 16h., at room temperature, with PMe_3 in either toluene or dichloromethane solvent to produce yellow crystalline $CpTaCl_4.PMe_3$ in *ca.* 30% yield. Elemental analysis was consistent with the above formulation and infrared data support the presence of coordinated (η^5-C_5H_5) and PMe_3 ligands, displaying characteristic bands for (η^5-C_5H_5) at 3120, 3100 cm^{-1} [ν(CH)] and 855 cm^{-1} [δ_{oop}(C-H)] and PMe_3 absorptions at 1285 cm^{-1} [$\delta_s(CH_3)$], 960 cm^{-1} [$\rho(CH_3)$] and 740 cm^{-1} [ν_{as}(P-C)][20].

The 250 MHz ^1H NMR (d^6-benzene) spectrum shows a singlet resonance for the (η^5-C_5H_5) hydrogens at 6.16 ppm and a doublet signal for coordinated PMe_3 at 1.50 ppm, $^2J(PH)$ = 10.9 Hz, considerably shifted from the resonance of free PMe_3 (0.79 ppm, $^2J(PH)$ = 2.1 Hz). The ^{31}P resonance in (1) was found at considerably higher frequency (11.83 ppm) than that of free PMe_3 (-63 ppm), indicative of the high Lewis acidity of the Ta(V), d^0 metal centre in $CpTaCl_4$[21]. The $^{13}C\{^1H\}$-NMR spectrum is entirely consistent with the ^1H and ^{31}P NMR spectra of (1) displaying a singlet absorption at 124.20 ppm for the equivalent, olefinic (η^5-C_5H_5) carbons and a doublet signal for the PMe_3 carbons at 14.13 ppm for which the $^1J(PC)$ coupling constant of 29.4 Hz is larger than that of free PMe_3 (13 Hz) as expected upon coordination to a metal[21].

Unfortunately, the low solubility of (1) in common organic solvents precluded molecular weight measurements, and mass spectrometry did not reveal a parent ion. The highest mass fragment at m/e (CI^+,^{35}Cl) 427

corresponds to $[M\text{-}Cl]^+$. Thus, in the absence of further data it is probable that (1) is essentially isostructural to the crystallographically characterised rhenium analogue, $Cp^*ReCl_4.PMe_3$ (see Chapter 1, section 1.3.1)[22].

2.2.2 Preparation Of $CpTaCl_3.PMe_3$ (2)

Purple crystals of (2) were isolated in 68% yield from the stoichiometric reduction of $CpTaCl_4$ with magnesium turnings in THF solvent, in the presence of excess PMe_3 (typically 2 equivalents), by a procedure analogous to that described for $Cp^*TaCl_3.PMe_3$[23]. The phosphine ligand of (2) was found to be very labile. Inert atmosphere toluene solutions decomposed in the absence of excess free PMe_3 to deposit a pale solid which was not examined. The lability of the phosphine is likely to be the cause of the variable elemental analyses obtained for (2). Similar problems have been noted for other PMe_3 complexes[24]. However the presence of absorptions at 3090 cm^{-1} and 955 cm^{-1} in the infrared spectrum clearly indicate the presence of coordinated (η^5-C_5H_5) and PMe_3 ligands respectively, and the ^1H and ^{31}P NMR spectra show no signals at ambient temperature, consistent with the paramagnetic Ta(IV), d^1 metal centre in (2). Mass spectrometry did not reveal a parent ion. The most prominent peaks, occurring at m/e 351 and 316, correspond to $[M\text{-}PMe_3]^+$ and $[M\text{-}PMe_3\text{-}Cl]^+$ (^{35}Cl) respectively.

There was no evidence for the formation of isolable $CpTaCl_3(PMe_3)_2$ in the synthesis of (2) using excess PMe_3 in contrast to observations on the niobium analogue[25]. This may be due in part to the lower Lewis acidity of Ta over Nb. The solution instability of (2) precluded further studies, but it is presumed to be monomeric and isostructural with $Cp^*TaCl_3.PMe_3$ whose molecular structure is described later in this

chapter (section 2.3).

2.2.3 Preparation of $Cp^*TaCl_3(dmpe)$ (3)

Using an analogous preparative procedure to that described for (2), complex (3) was isolated in 60% yield as a purple crystalline solid. It was envisaged that the presence of a chelating phosphine ligand would provide a less labile coordination sphere, and indeed this proved to be the case. Accurate, and reproducible elemental analyses were obtained for (3) (Chapter 7, section 7.2), and inert atmosphere toluene solutions of the complex showed no signs of decomposition over *ca.* 48 hours at room temperature. Further, solid samples of (3) showed no evidence (IR) of hydrolysis upon 3-4 minutes exposure to moist air, whereas (2) had completely decomposed within the same time period.

Complex (3) did not show ^1H or ^{31}P NMR signals at room temperature, consistent with the presence of a paramagnetic metal centre. Magnetic susceptibility measurements in d^6-benzene, following a modification of the method described by Evans[26] gave an effective magnetic moment, μ_{eff} of 1.5 BM, supportive of a Ta(IV) d^1 metal (theoretical spin-only value = 1.73 BM), and within the range found (1.41-1.69 BM) for several Nb(IV) analogues of (3)[25].

Like (1) and (2), (3) did not give a parent ion in the mass spectrum, the highest mass fragment corresponding to phosphine loss at m/e 420 $[M\text{-dmpe-H}]^+$ (^{35}Cl). Complex (3) is presumed to be isostructural to $CpNbCl_3(dppe)$[27] which possesses a pseudo-octahedral geometry with a meridional arrangement of halogen atoms.

2.2.4 Preparation of $CpTaCl_2(PMe_3)_3$ (4)

The reduction of $CpTaCl_4$ with one equivalent of magnesium turnings in THF in the presence of four equivalents of PMe_3 proceeded smoothly over 12h. at room temperature to afford a red solution. Removal of the volatiles under reduced pressure and crystallisation of the residue from toluene produced $CpTaCl_2(PMe_3)_3$ (4) in 30% yield. Although derivatives of the form $CpTaCl_2L_3$ are known *eg.* $CpTaCl_2(PMe_2Ph)_2(CO)$[19] and $CpTaCl_2(CO)_3$[28], (4) is the first example containing three phosphine ligands.

Elemental analysis and infrared spectroscopy (Chapter 7, section 7.2.4) are consistent with the composition of (4), in particular, infrared absorptions at 3090 cm^{-1} and 945 cm^{-1} are indicative of (η^5-C_5H_5) and PMe_3 ligands respectively. The 250 MHz ^1H NMR spectrum of (4) reveals the Cp hydrogens as a partially resolved multiplet, with couplings to two sets of chemically inequivalent PMe_3 phosphorus nuclei. Two resonances in the ratio 2:1 are observed at 1.20 and 1.11 ppm respectively, assignable to PMe_3 hydrogens in two different PMe_3 environments. The unique PMe_3 hydrogens are observed as a doublet with $^2J(PH)$ = 6.7 Hz, whereas the hydrogens of the two remaining equivalent PMe_3 ligands display virtual coupling appearing as an apparent triplet. Such an effect is often observed with *trans* orientated phosphines and results from coupling of the PMe_3 hydrogens of one ligand to the phosphorus nucleus of the other[29].

The consistent presence of free trimethylphosphine in the ^1H NMR spectrum suggests that the phosphine ligands are quite labile. This is further supported by the reactivity of (4) (section 2.4).

The ^{31}P and ^{13}C NMR data for (4) are consistent with the ^1H NMR spectrum. In particular, two broadened signals ($\Delta\frac{1}{2}$ ~ 16 Hz) in a 2:1

ratio, at -29.79 and -26.46 ppm respectively are observed in the $^{31}P\{^{1}H\}$ NMR spectrum, in which the expected $^{2}J(PP)$ coupling is not resolved at room temperature, presumably the result of phosphine exchange processes. The ^{13}C NMR spectrum reveals a doublet at 24.01 ppm [$^{1}J(PC)$ = 21.9 Hz] for the carbon atoms of the unique phosphine and an apparent triplet due to virtual coupling[29] for the remaining chemically equivalent phosphines at 16.83 ppm [J(PC) = 10.3 Hz].

The spectroscopic data described above are insufficient to define, without ambiguity, the coordination geometry of (4). Formally, the tantalum atom has achieved an 18-electron valence configuration and thus (4) is presumably monomeric with a pseudo octahedral ligand geometry, assuming the Cp ligand to occupy a single coordination site. There are three possible geometrical isomers for this geometry, illustrated in Figure 2.2.

The virtual coupling effects in the ^{1}H NMR support the presence of *trans* orientated PMe_3 ligands, thus indicating either the *cis*-meridional (II) or *trans*-meridional (III) isomers.

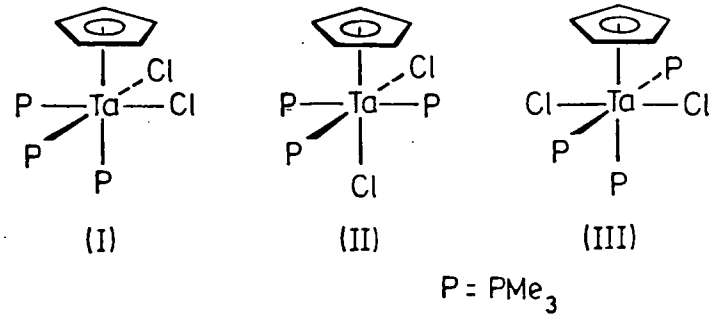

Figure 2.2 *Geometrical isomers of* $CpTaCl_2(PMe_3)_3$

However, the NMR data does not distinguish between the two. It is possible that, in solution, both forms are present and are inter-convertable *via* phosphine exchange. However, the infrared spectrum of

(4) displays ν(Ta-Cl) bands at 352 cm^{-1} and 260 cm^{-1}; similar in position and relative intensity to those found in $CpTaCl_2(PMe_3)_2(CO)$ (356 cm^{-1} and 273 cm^{-1}). The latter is presumed to be isostructural to the crystallographically defined PMe_2Ph derivative[19] which has the geometry illustrated in Figure 2.3.

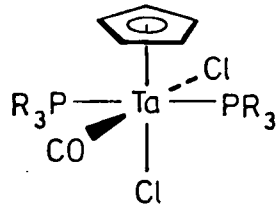

Figure 2.3 *Molecular Geometry of $CpTaCl_2(PR_3)_2(CO)$ [R_3=Me_3, Me_2Ph].*

Thus the solid state geometry of (4) is indicated by infrared to be similar, *i.e cis*-meridional isomer (II). Analogous infrared analyses have been used to distinguish *cis* and *trans* dichloride geometries in quadruply bonded dimolybdenum complexes[30].

2.2.5 Preparation and Solution Behaviour of $Cp^*TaCl_2(PMe_3)_2$ (5)

In view of the improved solubility and crystallinity of (η^5-C_5Me_5) derivatives over their (η^5-C_5H_5) counterparts[31], an attempt was made to prepare the pentamethylcyclopentadienyl analogue of (4).

The reduction of Cp^*TaCl_4 with one equivalent of magnesium in THF, in the presence of 3.5 equivalents of PMe_3, proceeded smoothly over the course of 10 h. at room temperature. Removal of the volatile components under reduced pressure and extraction of the residue into light

petroleum ether produced a deep red solution, from which deep-red crystals [compound (5)] were obtained upon concentration and cooling to $-78^{o}C$.

An infrared spectrum (Nujol mull) of the crystals revealed the presence of (η^5-C_5Me_5) and PMe_3 ligands; absorptions at 1028 cm^{-1} and 951 cm^{-1} being indicative of Cp^* (ring breathing) and PMe_3 [$\rho(CH_3)$] respectively.

The 250 MHz ^1H NMR (d^6-benzene) spectrum, however, was completely different to that of (4); no signals at all were observed in the usual region (12 to 0 ppm) at room temperature, indicating the complex to be paramagnetic. Indeed, expansion of the spectral range to +200 ppm, located contact-shifted signals due to the (η^5-C_5Me_5) and PMe_3 ligands at 91.45 ppm and 20.56 ppm respectively (0.037M solution) in a ratio consistent with the presence of two PMe_3 ligands per (η^5-C_5Me_5) ligand (Figure 2.4). No signals were observed in the $^{31}P\{^1H\}$ spectrum at room temperature.

A solution magnetic moment of 2.1 BM (d^6-benzene) supported the presence of a d^2, Ta(III) metal centre. The observed effective magnetic moment is somewhat lower than those reported for the half-sandwich vanadium(III) complexes, $CpVCl_2(PR_3)_2$ which have μ_{eff} values of *ca.* 2.8 BM[20] (theoretical spin only value = 2.83 BM). Possible reasons for this discrepancy include partial solution decomposition (*vide infra*) and partial occupancy of the singlet (S=0) state. Similar suggestions have been offered to explain the complex solution behaviour of $TaBr_3(PMe_2Ph)_2$[32] which has μ_{eff} = 0.37 BM at 298K in CD_2Cl_2 (0.035M).

These data suggested the complex to have the empirical formula, $Cp^*TaCl_2(PMe_3)_2$ (5). Elemental analyses, although hampered by the lability of the PMe_3 ligands, were also consistent with this formulation:

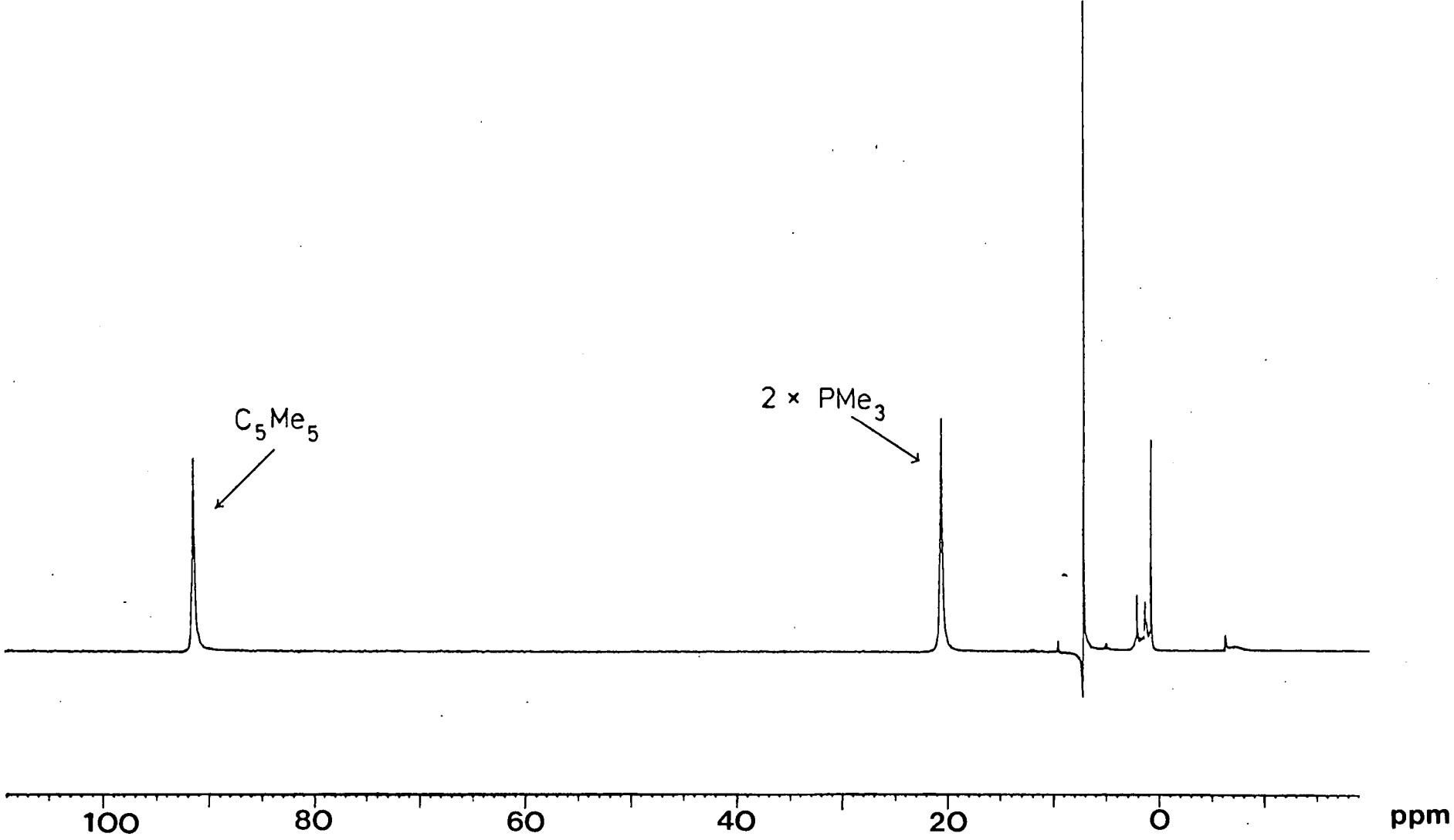

Figure 2.4 *^1H NMR Spectrum of (5) (250 MHz, d^6-benzene).*

Elemental Analysis for $C_{16}H_{33}Cl_2P_2Ta$:
Found (Required): %C, 35.00 (35.63); %H, 6.04 (6.18)

Mass spectrometry did not show any ion fragments assignable to an organometallic species. However, the above stoichiometry has been confirmed from the derivative chemistry of (5) (section 2.4).

The paramagnetism of (5) argues against a dimeric structure in solution. Such a structure would presumably contain bridging chlorine ligands allowing tantalum to achieve an 18-electron valence configuration, and in the absence of a readily accessible LUMO would be expected to be diamagnetic. Complex (5) is therefore most probably monomeric in solution possessing a four-legged "piano-stool" arrangement of ligands. A *trans* displacement of the PMe_3 ligands is anticipated to be favoured on steric grounds (similar to *trans*-$CpVCl_2(PMe_3)_2$ which has been crystallographically characterised)[20].

Attempts to grow crystals of (5) suitable for an X-ray structure determination, from either light petroleum ether or toluene, resulted in decomposition and the preferential crystallisation of $Cp^*TaCl_3.PMe_3$ which was subsequently studied crystallographically (section 2.3). The formation of this complex from (5) probably results from a disproportionation reaction, proceeding *via* an intermediate Ta(III) dimer (*vide infra*).

Solutions of (5) in d^6-benzene invariably contain a significant quantity of free PMe_3 (*ca.* 0.5 equiv.) along with a small amount of a diamagnetic complex. These solutions are stable at room temperature over many weeks in sealed tubes. However, removal of the solvent and consequently the liberated PMe_3, results in decomposition to $Cp^*TaCl_3.PMe_3$ as noted above and presumably a Ta(II) species.

These observations indicate a solution equilibrium involving PMe_3 displacement from (5) as in Equation 2.5.

$$\underset{(5)}{Cp^*TaCl_2(PMe_3)_2} \rightleftharpoons \underset{(5a)}{[Cp^*TaCl_2(PMe_3)]} + PMe_3 \qquad (2.5)$$

Complex (5a) is unlikely to exist as a monomer and presumably engages in a monomer-dimer equilibrium (Equation 2.6).

$$2\ Cp^*TaCl_2(PMe_3) \rightleftharpoons \underset{(5b)}{[Cp^*TaCl_2(PMe_3)]_2} \qquad (2.6)$$

Complex (5b) appears to be stable towards decomposition in the presence of excess PMe_3 but upon its removal, disproportionates to $Cp^*TaCl_3.PMe_3$ and a Ta(II), d^3 complex. The latter compound is presumably paramagnetic and has not been investigated further. Interestingly, the reaction between $[Cp^*TaCl_2]_2$ and PMe_3 has been reported to give a mixture of products of which only $Cp^*TaCl_3.PMe_3$ was identified. This compound may have resulted from the decomposition of intermediate $[Cp^*TaCl_2(PMe_3)]_2$[33a]. Moreover, further support for the intermediacy of (5b) is provided by the recent isolation of a stable analogue, $[CpTaCl_2(PMe_2Ph)]_2$[33b].

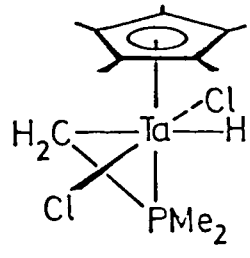

Figure 2.5 *Proposed Structure of (5c)*

No direct evidence for the presence of (5b) could be obtained from the ^1H NMR spectrum of (5). Signals assignable to a diamagnetic species were present but were not consistent with a complex of the form (5b).

In particular, a singlet resonance at 2.11 ppm is assignable to the equivalent hydrogens of a (η^5-C_5Me_5) ligand, whilst a doublet at 1.43 ppm, [^{2}J(PH) = 9.1 Hz] may be attributable to the six equivalent hydrogens of a -PMe_2 moiety. Furthermore, a doublet resonance at 11.97 ppm, [^{2}J(PH) = 49.7 Hz] is supportive of a single hydride ligand, coordinated to a Ta(V), d^0 metal centre.

These data may be interpreted in terms of the structure (5c) illustrated in Figure 2.5 in which tantalum has inserted into the C-H bond of a phosphine methyl group (Equation 2.7).

$$\underset{(5)}{Cp^*TaCl_2(PMe_3)_2} \rightleftharpoons \underset{(5c)}{Cp^*TaCl_2H(\eta^2\text{-}CH_2PMe_2)} + PMe_3 \qquad (2.7)$$

Cyclometallation reactions of this type have been observed in a number of cases and are discussed in more detail in Chapters 1 and 3. It appears that (5c) is in equilibrium with (5) (Equation 2.7) since deuteriobenzene solutions of (5) sealed in 5 mm NMR tubes in the presence of 3.3-dimethylbut-1-ene (neohexene), dihydrogen or THF respectively show an increase in the intensity of the signals due to (5c), with respect to those of (5).

Thus, Scheme 2.1 summarises the solution behaviour of (5) consistent with the available data.

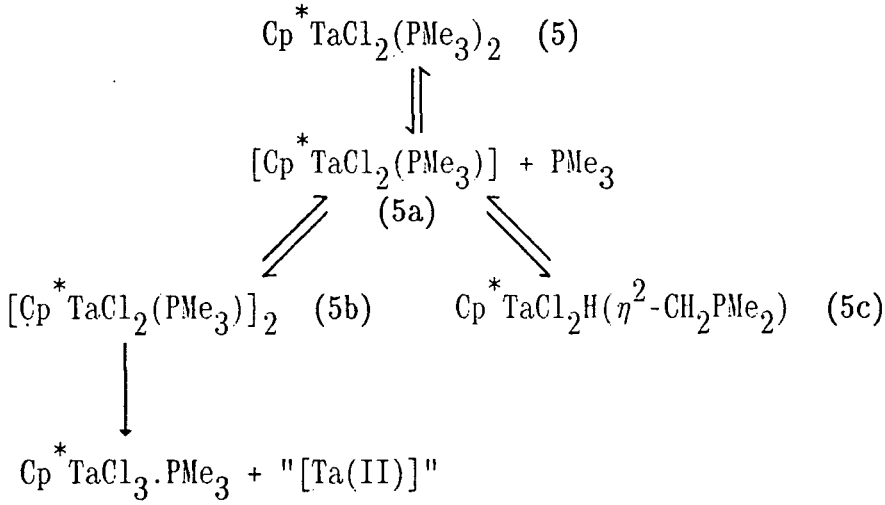

Scheme 2.1 *Proposed Solution Behaviour of (5)*

Finally, a solution of (5) in deuteriobenzene containing excess PMe_3 showed no evidence (^1H NMR) for the formation of diamagnetic $Cp^*TaCl_2(PMe_3)_3$.

2.3 THE MOLECULAR STRUCTURE OF $Cp^*TaCl_3.PMe_3$

Red prisms of $Cp^*TaCl_3.PMe_3$ were obtained from a saturated toluene solution of $Cp^*TaCl_2(PMe_3)_2$ (5), cooled to -35°C for 24h. (see section 2.2.5). The X-Ray diffraction study was performed by Dr. W.Clegg at the University of Newcastle-Upon-Tyne.

Ta-Cl(1)	2.400(3)	Cl(1)-Ta-Cl(2)	131.8(1)
Ta-Cl(2)	2.395(3)	Cl(1)-Ta-Cl(3)	83.8(1)
Ta-Cl(3)	2.416(3)	Cl(2)-Ta-Cl(3)	83.1(1)
Ta-P	2.608(3)	Cl(1)-Ta-P	79.2(1)
		Cl(2)-Ta-P	78.7(1)
Ta-C(4)	2.325(9)	Cl(3)-Ta-P	135.8(1)
Ta-C(5)	2.319(10)		
Ta-C(6)	2.424(9)	Ta-P-C(1)	104.0(4)
Ta-C(7)	2.448(9)	Ta-P-C(2)	119.3(4)
Ta-C(8)	2.390(10)	Ta-P-C(3)	119.4(4)
P-C(1)	1.843(13)	C(1)-P-C(2)	103.6(6)
P-C(2)	1.827(11)	C(1)-P-C(3)	103.8(6)
P-C(3)	1.846(11)	C(2)-P-C(3)	104.6(6)
C(4)-C(5)	1.474(14)	X-Ta-Cl(1)	104.6
C(4)-C(8)	1.423(14)	X-Ta-Cl(2)	113.1
C(4)-C(9)	1.517(15)	X-Ta-Cl(3)	114.3
C(5)-C(6)	1.383(14)	X-Ta-P	109.9
C(5)-C(10)	1.548(15)		
C(6)-C(7)	1.397(13)	Z-C(4)-C(9)	5.8
C(6)-C(11)	1.487(16)	Z-C(5)-C(10)	4.7
C(7)-C(8)	1.418(14)	Z-C(6)-C(11)	2.5
C(7)-C(12)	1.526(16)	Z-C(7)-C(12)	11.0
C(8)-C(13)	1.521(16)	Z-C(8)-C(13)	7.3
X-Ta	2.053		

Table 2.2 *Bond Lengths (Å) and Angles (°) for $Cp^*TaCl_3.PMe_3$; X=Centre of Ring; Z=Best plane through atoms C(4)-C(8).*

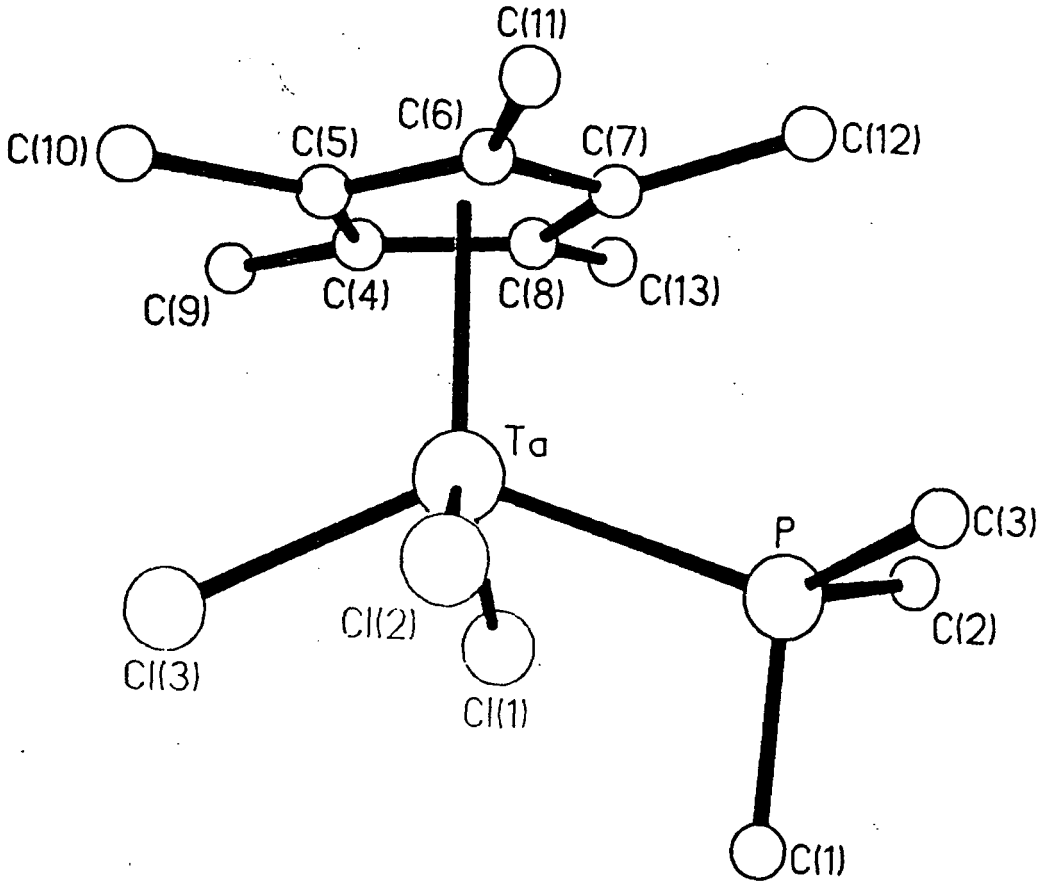

Figure 2.6 *The Molecular Structure of $Cp^*TaCl_3.PMe_3$.*

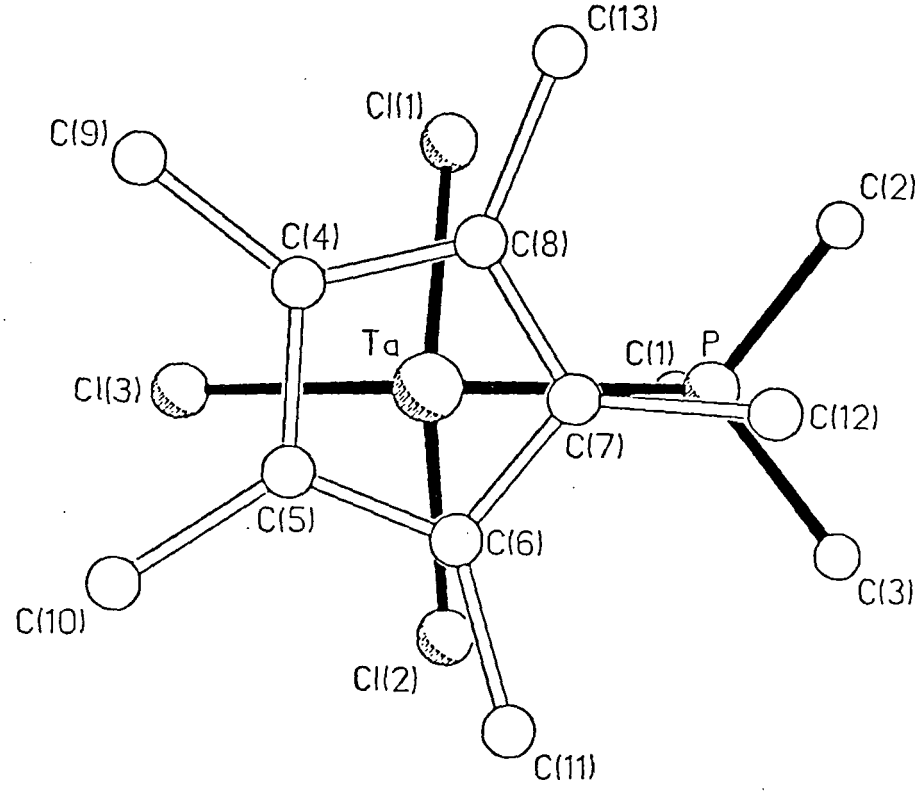

Figure 2.7 *View of $Cp^*TaCl_3.PMe_3$ along the Ring Centroid-Tantalum Vector.*

The crystal data for this complex are reproduced in Appendix 1A and the molecular structure is illustrated in Figures 2.6 and 2.7. Selected bond distances and angles are given in Table 2.2.

The complex is monomeric, possessing a distorted, four-legged "piano stool" geometry typical of $(\eta^5\text{-}C_5R_5)ML_3L'$ compounds[35]. As in other $CpML_3L'$ compounds, $Cp^*TaCl_3.PMe_3$ contains a pseudo mirror plane passing through P, Ta and Cl(3) (Figure 2.7) and is geometrically similar to the 18-electron $CpM(CO)_3X$ complexes[35] (M = Mo,W; X = halide, alkyl) in which the unique ligand X lies beneath a ring carbon atom and the carbonyl ligand *trans* to X lies beneath a C-C bond of the Cp ring (Figure 2.7).

As in other $(\eta^5\text{-}C_5Me_5)$ complexes[36], all of the ring methyl carbon atoms are bent away from the mean C(4)-C(8) ring plane and the tantalum atom in this case by an average of *ca.* 6^o (Table 2.2). However, the C(7)-C(12) bond is displaced considerably further from the ring plane (11^o), presumably as a result of unfavourable steric interactions with the PMe_3 ligand. Significantly, the PMe_3 ligand is orientated with one methyl substituent *exo* and two methyls *endo* to the pentamethyl-cyclopentadienyl ring (Figure 2.6), thus avoiding close contacts between PMe_3 and $(\eta^5\text{-}C_5Me_5)$ methyl substituents. Indeed, rotation about the Ta-P bond brings C(1) to within 2.1 Å of C(12) (carbon-carbon Van der Waals separation is *ca.* 3.3Å)[37].

The average tantalum-ring carbon distance of 2.381(26)Å is somewhat shorter than is usually found in Cp^*Ta complexes[38] (*ca.* 2.42Å) and there is a significant range of individual distances from 2.319(10)Å [Ta-C(5)] to 2.448(9)Å [Ta-C(9)] with ΔM = 0.129Å (ΔM = difference between longest and shortest distances). Comparative values of ΔM and ΔR (corresponding difference for inter-ring carbon-carbon distances) are reproduced in Table 2.3. The range of tantalum-carbon distances appears to be caused

by a tilting of the (η^5-C_5Me_5) ring, bringing atoms C(4) and C(5) closer to the metal (2.325(9)Å and 2.319(10)Å respectively). This type of behaviour has also been observed in the 18-electron complexes $CpM(CO)_3X$ (M = Mo,W; X = halide, alkyl)[35d] and explained on the basis of maximising overlap between the metal d_{xy} orbital and the unoccupied Cp π-orbital of suitable symmetry[39].

The vector from tantalum, normal to the ring is displaced from the ring centroid by 0.159Å in a direction towards the C(4)-C(5) edge. Significantly the C(4)-C(5) distance is the longest inter-ring distance [1.474(16)Å]. Thus the ring distortions found in $Cp^*TaCl_3.PMe_3$ probably arise due to a combination of electronic factors and the steric influence of the relatively bulky PMe_3 ligand.

COMPLEX	ΔR(Å)	ΔM(Å)	REF
$Cp^*Ta(CHPh)(CH_2Ph)_2$	0.05	0.08	40
$Cp^*Ta(CPh)(PMe_3)_2Cl$	0.03	0.12	41
$Cp^*Ta(CHCMe_3)(\eta^2\text{-}C_2H_4)(PMe_3)$	0.01	0.04	36
$Cp^*TaCl_2.(\eta^2\text{-}PhC{\equiv}CPh)$	0.03	0.03	42
$Cp^*TaH_4(PMe_3)_2$	0.05	0.07	38
$Cp^*TaCl_3.PMe_3$	0.09 ±0.02	0.13	‡‡

Table 2.3 *ΔR and ΔM Values for Some [Cp*Ta] Complexes.* ‡‡ = *this work.*

The tantalum-chlorine distances of 2.400(3)Å [Cl(1)], 2.395(3)Å [Cl(2)] and 2.416(3)Å [Cl(3)] are within the range found for other Ta(IV)-Cl distances and correlate well with the formal valence electron count of the metal, such that those complexes with lower formal electron counts have the shorter tantalum-chlorine distances (Table 2.4), presumably as a result of increased L → M, pπ-dπ interactions. Significantly, it is the chlorine atom [Cl(3)] lying opposite to the phosphine (angle Cl-Ta-P = 135.8°) that gives the longest Ta-Cl bond,

presumably the result of the *trans* influence of the PMe_3 ligand[43].

The phosphorus-carbon bond lengths within the PMe_3 ligand are normal, 1.827(11)-1.846(11)Å[38]. The C-P-C angles of 104.0(3)° (average) are all less than the tetrahedral value of 109.5°, as expected upon coordination of PMe_3 to a metal centre[21]. Finally, the tantalum-phosphorus bond length of 2.608(3)Å is within the range usually found for Ta(IV)-PMe_3 complexes, *e.g* $TaCl_4(PMe_3)_3$[44] [d(Ta-P) = 2.640Å] and $TaCl_2H_2(PMe_3)_4$[45] [d(Ta-P) = 2.597Å].

COMPLEX	FEC	d(Ta-Cl)	REF
$TaCl_4(dmpe)_2$	17	2.505	46
$TaCl_2H_2(dmpe)_2$	17	2.552	47
$Ta_2Cl_8(PMe_3)_4$	17	2.497	48
$Ta_2Cl_6H_2(PMe_3)_4$	15	2.478	49
$TaCl_4(PMe_3)_3$	15	2.447	44
		2.417	
$TaCl_4(PMe_2Ph)_2$	13	2.342	44
$TaCl_4(PEt_3)_2$	13	2.347	44
		2.373	

Table 2.4 *Representative (Ta-Cl) distances (Å) for Ta(IV) complexes; FEC=Formal Electron Count.*

2.4 SOME ASPECTS OF THE DERIVATIVE CHEMISTRY OF THE COMPLEXES $Cp'TaCl_x(PMe_3)_y$ [(x+y) = 4 or 5]

2.4.1 Reactions With Chlorocarbons

The complexes, $Cp'TaCl_3.PMe_3$, $Cp^*TaCl_2(PMe_3)_2$ and $CpTaCl_2(PMe_3)_3$ were found to react with chlorocarbon solvent at room temperature to form, ultimately, the corresponding tetrachloride adducts, $Cp'TaCl_4.PMe_3$ which were identified by comparison of their ^1H NMR spectra with those of authentic samples[50].

The reactions were monitored by ^1H NMR spectroscopy in d-chloroform

solvent and revealed relative rates of formation of $Cp'TaCl_4.PMe_3$ according to the following sequence (approximate times for completion of reaction are given in parentheses):

$$Cp^*TaCl_3.PMe_3 \approx Cp^*TaCl_2(PMe_3)_2 > CpTaCl_3.PMe_3 > CpTaCl_2(PMe_3)_3$$
$$[ca.\ 20\ min.] \qquad [<24h.] \qquad [>24h.]$$

Only $CpTaCl_2(PMe_3)_3$ gave rise to intermediates detectable by ^1H NMR spectroscopy. These possess signals attributable to (η^5-C_5H_5) at 6.18 ppm and 6.08 ppm and several broadened resonances between 1.5 and 1.8 ppm corresponding to coordinated PMe_3 ligands. As it did not prove possible to isolate these intermediates from the reaction mixture they were not investigated further.

Nevertheless, the above results suggest that the Cp^* derivatives are more reactive towards chlorocarbons than their Cp analogues. A possible explanation for this may lie in the greater electron releasing properties of Cp^* over that of Cp[34], which would be expected to lead to destabilisation of the lower oxidation state, half-sandwich halides. Moreover, as coordination of $CDCl_3$ to tantalum is probably required prior to halogen atom transfer, the slowest rate would be expected for electronically saturated $CpTaCl_2(PMe_3)_3$. This is indeed the case and reflects the necessity for PMe_3 dissociation to generate a vacant coordination site. The other complexes, however, are coordinatively unsaturated and ligand loss is thus not a prerequisite.

2.4.2 Reaction of $Cp^*TaCl_2(PMe_3)_2$ (5) With Substituted Alkynes, PhC≡CR (R = Ph, H)

The reaction between $Cp^*TaCl_2(PMe_3)_2$ (5) and diphenylacetylene (1 equivalent) in toluene solvent proceeded slowly at room temperature to afford an orange solution from which orange crystals were obtained upon

concentration and cooling to -78°C. The crystals were isolated and characterised (Chapter 7, section 7.2.7) as the compound, $Cp^*TaCl_2(\eta^2$-PhC≡CPh) which has been prepared previously by the reaction of $Cp^*TaCl_2(\eta^2$-olefin) with PhC≡CPh[42].

When the reaction was followed by ^{1}H NMR spectroscopy in d^6-benzene solvent, no intermediates or organometallic byproducts were observed, and the integrated spectrum showed that two equivalents of PMe_3 had been displaced (Equation 2.8).

$$Cp^*TaCl_2(PMe_3)_2 + PhC_2Ph \xrightarrow{\text{Toluene}} Cp^*TaCl_2(\eta^2\text{-}PhC_2Ph) + 2PMe_3 \quad (2.8)$$

A similar, although considerably faster reaction was observed between (5) and phenylacetylene. The product, $Cp^*TaCl_2(\eta^2$-PhC≡CH)[42], was characterised by ^{1}H NMR spectroscopy (Table 2.5).

SHIFT (ppm)	REL.INT	MULT.	J (Hz)	ASSIGNMENT
11.89	1	s	---	PhC≡C<u>H</u>
7.77	2	d	$^3J(H_oH_m)$=7.4	Ph-H_o
7.25	2	dd	$^3J(H_pH_m)$=7.3 $^3J(H_oH_m)$=7.4	Ph-H_m
7.08	1	t	$^3J(H_pH_m)$=7.3	Ph-H_p
1.80	15	s	---	C_5Me_5

Table 2.5 *250 MHz ^{1}H NMR Spectral Data for $Cp^*TaCl_2(\eta^2$-PhC≡CH) (d^6-benzene).*

Monitoring of the reaction by ^{1}H NMR spectroscopy revealed the displacement of two equivalents of PMe_3, and again, no intermediates or byproducts were observed.

The complex, $Cp^*TaCl_2(\eta^2$-PhC≡CH) had been reported previously[42] but the acetylenic proton was not found in the ^{1}H NMR spectrum. We find this signal at 11.89 ppm, at a considerably higher frequency than for uncomplexed, terminal alkynes (1.7-1.9 ppm)[51], or electronically

saturated alkyne complexes [*e.g* $Cp_2NbCl(\underline{H}C{\equiv}CMe)$, 7.98 ppm)[52]. This may reflect the mode of alkyne coordination in these electronically unsaturated complexes, in which the alkyne has been proposed to act as a 4-electron donating ligand[42].

2.4.3 Reaction of $Cp^*TaCl_2(PMe_3)_2$ (5) With 1,3-Butadiene

The reaction between (5) and 1,3-butadiene (1 equivalent) was monitored by ^1H NMR spectroscopy and found to proceed smoothly over 12h. at room temperature to produce a single product in high yield.

SHIFT (ppm)	REL.INT	MULT.	ASSIGNMENT
7.06	2	m	H_2, H_2'
1.85	15	s	$C_5\underline{Me}_5$
0.81	2	m	H_1, H_1'
-0.13	2	m	H_3, H_3'

Table 2.6 *250 MHz ^1H NMR Data for $Cp^*TaCl_2(\eta\text{-}C_4H_6)$ (d^6-benzene).*

It has been characterised, by comparison of ^1H NMR data (Table 2.6) with those of an authentic sample, as the previously reported complex, $Cp^*TaCl_2(\eta\text{-}C_4H_6)$[53].

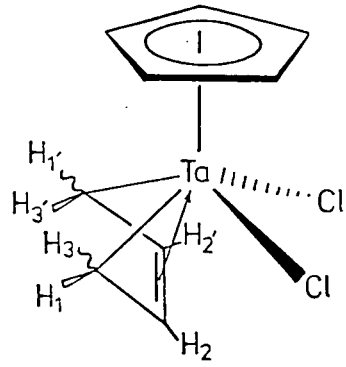

Figure 2.8 *Molecular Structure of $CpTaCl_2(\eta\text{-}C_4H_6)$.*

This complex is presumably isostructural with the crystallographically characterised Cp analogue[53] (Figure 2.8), in which the butadiene coordination is best described as a metallacyclopentene.

No intermediates in this reaction were detected by ^{1}H NMR spectroscopy.

2.4.4 Reaction of $CpTaCl_2(PMe_3)_3$ (4) With 1,3-Butadiene

The reaction of (4) with 1,3-butadiene proceeded rapidly to equilibrium within *ca.* 15 min. at room temperature. Heating the mixture at 70°C for 20h. did not alter the composition, confirming that equilibrium had been reached.

In contrast to the reaction of (5) with butadiene, complex (4) was shown to be in equilibrium with a single product (6) by ^{1}H NMR spectroscopy (d^6-benzene solvent), displaying an apparent triplet resonance at 4.61 ppm with J(PH) = 2.1 Hz, due to five equivalent Cp hydrogens coupled to the phosphorus nuclei of two PMe_3 ligands. The two PMe_3 groups however, are not equivalent giving signals at 1.26 ppm, ^{2}J(PH) = 7.5 Hz and 1.17 ppm, ^{2}J(PH) = 7.6 Hz respectively. Free PMe_3 is observed in the ^{1}H NMR spectrum, along with multiplets assignable to olefinic protons.

It is apparent that (4) has undergone a substitution reaction in which one PMe_3 ligand has been displaced by 1,3-butadiene which, presumably, coordinates to tantalum *via* only one olefinic linkage (Equation 2.9).

$$\underset{(4)}{CpTaCl_2(PMe_3)_3} \overset{\text{=}\!\!\diagup\!\!\text{=}}{\underset{C_6D_6}{\rightleftharpoons}} \underset{(6)}{CpTaCl_2(PMe_3)_2(\eta^2\text{-}C_4H_6)} + PMe_3 \quad (2.9)$$

By analogy to the reaction of (4) with carbon monoxide (*vide infra*) it

is reasonable to propose that (6) possesses a structure close to that illustrated in Figure 2.9.

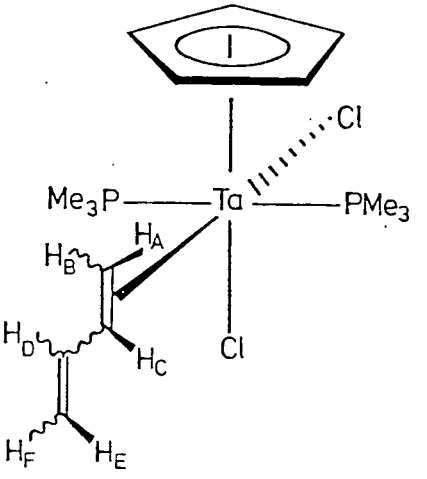

Figure 2.9 *Proposed Structure of (6).*

The butadiene coordination prevents mirror symmetry such that the two PMe_3 ligands are chemically inequivalent. The ^1H NMR resonances for the butadiene hydrogens in (6) are significantly different to those of the (η^4-C_4H_6) ligand in $Cp'TaCl_2(\eta^4$-$C_4H_6)$ complexes[53]. The lower symmetry of η^2-coordination in (6) requires all six hydrogens to be inequivalent. The available 250 MHz ^1H NMR data for (6) are displayed in Table 2.7. Signals due to H_D, H_E and H_F are found in the usual olefinic region[51]. Small (<2 Hz) couplings are observable but unresolved for H_F and H_E presumably due to *gem* $^2J(H_EH_F)$, and also at H_D due to *vic* $^3J(H_CH_D)$. This latter coupling is usually *ca.* 10 Hz[51] but coordination to the metal may result in a dihedral angle between H_C and H_D approaching *ca.* 90^o, and consequently reducing $^3J(H_CH_D)$[51]. Only two of the remaining three butadiene hydrogen resonances are observed, the other signal presumably being obscured by absorptions in the region 1.4-1.0 ppm.

The ^{1}H NMR data for (6) is similar to that observed for the complex, $Cp^*_2TaH(\eta^2\text{-}C_4H_6)$ which has been shown[54] to possess an η^2-*trans*-C_4H_6 geometry.

SHIFT (ppm)	REL.INT.	MULT.	J (Hz)	ASSIGNMENT
5.79	1	m	$J(H_DH_E)$=16.4	H_D
			$J(H_DH_F)$=8.5	
4.66	1	m	$J(H_DH_E)$=16.4	H_E
4.61	5	t	J(PH)=2.1	$C_5\underline{H}_5$
4.53	1	m	$J(H_DH_F)$=8.5	H_F
3.20	1	m	J(PH)=18.2	H_C
			$J(H_CH_B)$=10.0	
			$J(H_CH_A)$=10.0	
1.90	1	m	J(PH)=11.0	H_A
			$J(H_CH_A)$=11.0	
			$J(H_AH_B)$=4.6	
1.26	9	d	^{2}J(PH)=7.5	PMe_3
1.17	9	d	^{2}J(PH)=7.6	PMe_3

Table 2.7 *250 MHz ^{1}H NMR Spectral Data for (6) (d^6-benzene); (Signal for H_B not observed).*

Attempts to isolate (6) proved unsuccessful, the more volatile butadiene being more readily removed and consequently displacing equilibrium 2.9 to the left-hand side.

Interestingly, (6) can be heated for several hours at 70°C without decomposition to the known complex, $CpTaCl_2(\eta^4\text{-}C_4H_6)$[53]. These observations again highlight the steric and electronic differences between Cp^* and Cp ligands, leading to the reduced stability of lower oxidation states and lower Lewis acidity for the Cp^* derivatives.

2.4.5 Reaction of $CpTaCl_2(PMe_3)_3$ (4) With Carbon Monoxide

$CpTaCl_2(PMe_3)_3$ (4) reacted cleanly with carbon monoxide (*ca.* 1 atm.) in toluene solvent over the course of 1h. at room temperature to afford the previously reported complex, $CpTaCl_2(PMe_3)_2(CO)$ (7) in 87% yield (Equation 2.10).

$$\underset{(4)}{CpTaCl_2(PMe_3)_3} + CO \xrightarrow{\text{Toluene}} \underset{(7)}{CpTaCl_2(PMe_3)_2(CO)} + PMe_3 \qquad (2.10)$$

The preparative procedure described by Leigh *et al.*[19] involved the reduction of $CpTaCl_4$ by magnesium turnings in THF solvent in the presence of PMe_3 and carbon monoxide. This led to the isolation of (7) as a THF solvate and full characterising data were not provided.

Here complex (7) is characterised by elemental analysis, infrared and ^1H, ^{31}P and ^{13}C NMR spectroscopies (Chapter 7, section 7.2.8). In particular, a single strong carbonyl absorption is found at 1890 cm^{-1} in the infrared spectrum. The $^{31}P\{^1H\}$ NMR spectrum consists of a single resonance at -28.10 ppm indicating the two PMe_3 ligands to occupy equivalent solution environments. This is supported by the 250 MHz ^1H NMR spectrum in which the PMe_3 hydrogens display a virtual coupling pattern of three lines, at 1.19 ppm [J(PH) = 8.2 Hz]. Further, a triplet at 4.44 ppm [J(PH) = 2.5 Hz] may be assigned to the Cp hydrogens coupled to the two equivalent phosphorus nuclei. The $^{13}C\{^1H\}$-NMR spectrum (d^6-benzene) shows the PMe_3 carbons as a virtual coupled triplet at 16.41 ppm [J(PC) = 10.1 Hz] and the carbonyl carbon is found to resonate at 247.76 ppm in a similar region to other tantalum carbonyl complexes[56]. $^2J(PC)$ coupling to the carbonyl carbon was not resolved.

The above data suggest that (7) is isostructural with the crystallographically characterised derivative, $CpTaCl_2(PMe_2Ph)_2(CO)$

(Figure 2.3)[19].

In the presence of excess carbon monoxide, (7) is reluctant to undergo further phosphine substitution: no reaction is observed after 24h. at 70°C, by ^1H NMR spectroscopy.

2.4.6 Reaction of $Cp^*TaCl_2(PMe_3)_2$ (5) With Carbon Monoxide

$Cp^*TaCl_2(PMe_3)_2$ (5) reacted smoothly with carbon monoxide (*ca.* 1 atm.) in toluene solvent at room temperature (Equation 2.11). Within 3h. the red colouration of (5) had been replaced by a purple coloured toluene solution. Filtration of this solution, followed by concentration and cooling to -78°C afforded purple crystals, which were collected, washed with light petroleum ether and dried *in vacuo*. The product was characterised as $Cp^*TaCl_2(PMe_3)(CO)_2$ (8) by elemental analysis, infrared, ^1H, ^{31}P and ^{13}C NMR spectroscopies (Chapter 7, section 7.2.9).

$$\underset{(5)}{Cp^*TaCl_2(PMe_3)_2} + CO \xrightarrow{\text{Toluene}} \underset{(8)}{Cp^*TaCl_2(PMe_3)(CO)_2} + PMe_3 \qquad (2.11)$$

The infrared spectrum confirms the presence of ligated carbon monoxide (1988, 1900 and 1880 cm^{-1}) and PMe_3 ligands (975, 960 and 745 cm^{-1}), and the 250 MHz ^1H NMR spectrum (d^6-benzene) confirms the presence of one PMe_3 ligand per molecule, with a doublet signal at 1.26 ppm [$^2J(PH)$ = 9.8 Hz]. The phosphorus nucleus resonates at -26.60 ppm in the $^{31}P\{^1H\}$ NMR spectrum.

Assuming the Cp^* ligand to occupy a single coordination site, (8) may be described as an electronically saturated, six-coordinate complex possessing a pseudo-octahedral geometry. Several geometrical isomers are possible as illustrated in Figure 2.10. Although the above NMR data indicate only one isomer to be present in solution, they do not

distinguish between the possibilities.

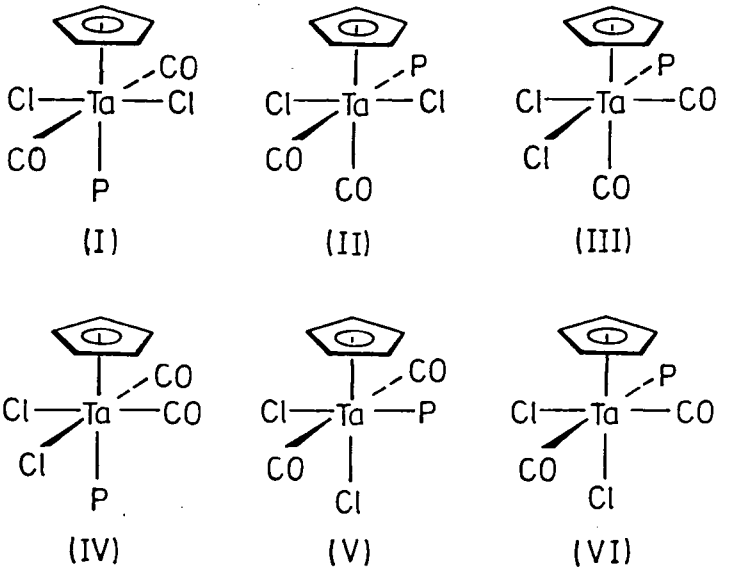

Figure 2.10 *Possible Geometrical Isomers for $Cp^*TaCl_2(PMe_3)(CO)_2$ (8).*

However, $^{13}C\{^1H\}$ NMR spectroscopy reveals a single carbonyl resonance at 238.10 ppm [$^2J(PC)$ = 25.2 Hz] indicating that the carbon monoxide ligands possess equivalent solution environments. Fluxionality, involving the rapid interconversion of two or more isomers, is unlikely since similar pseudo-octahedral complexes, $Cp'MCl_2L_3$, have been generally shown to retain their solid state structures in solution[19,25]. Thus, the ^{13}C NMR data permits the elimination of isomers (II), (III) and (VI).

Furthermore, a semi-quantitative analysis of the infrared bands attributable to the symmetric and antisymmetric carbonyl stretching modes at 1990 cm^{-1} and 1890 cm^{-1} respectively (CH_2Cl_2 solution), following the method of Cotton[55], indicates a OC-M-CO bond angle of 101° suggesting a *cis* displacement of the carbonyl ligands.

Only isomer (IV) in Figure 2.10 is consistent with all of the above

observations. This assignment was corroborated by an X-ray diffraction study on a single crystal of (8) grown from a saturated toluene solution. The details of this study are discussed in section 2.5.

A comparison of the reactions of $CpTaCl_2(PMe_3)_3$ (4) and $Cp^*TaCl_2(PMe_3)_2$ (5) with carbon monoxide is interesting. Presumably (5) reacts to give initially $Cp^*TaCl_2(PMe_3)_2(CO)$, which then rapidly reacts further to produce (8) (Scheme 2.2).

$$Cp^*TaCl_2(PMe_3)_2 \quad (5)$$
$$\downarrow \text{ CO}$$
$$[Cp^*TaCl_2(PMe_3)_2(CO)]$$
$$\text{Fast} \downarrow \text{ CO; } -PMe_3$$
$$Cp^*TaCl_2(PMe_3)(CO)_2 \quad (8)$$

Scheme 2.2 *Potential Pathway for the Reaction of (5) with CO.*

No intermediates were observed, however, when the reaction was monitored by ^1H NMR spectroscopy, suggesting that they are too short-lived under the reaction conditions. This is consistent with the observations of Mayer and Bercaw[56] who reported that $Cp^*TaH_2(PMe_3)_2(CO)$ is stable in solution whereas $Cp^*TaHCl(PMe_3)_2(CO)$ exists in equilibrium with $Cp^*TaHCl(PMe_3)(CO)_2$. It was proposed that this resulted from replacing hydrogen with the more sterically demanding and π-basic chloride ligand[56]. Complex (8), containing two chloride ligands, accentuates this trend such that $Cp^*TaCl_2(PMe_3)_2(CO)$ is not observable.

However in the (η^5-C_5H_5) system, $CpTaCl_2(PMe_3)_2(CO)$ is the only product obtained from the reaction of (4) with CO, and shows no tendency to react further with CO under mild conditions to form $CpTaCl_2(PMe_3)(CO)_2$.

The steric and electronic differences between Cp^* and Cp ligands provide an attractive rationale for these observations. The lower Lewis acidity and more sterically constrained environment of $[Cp^*TaCl_2]$ over $[CpTaCl_2]$ results in firstly, the inability of $[Cp^*TaCl_2]$ to accommodate more than two PMe_3 ligands, whereas $[CpTaCl_2]$ is able to coordinate three, and secondly, the instability of $[Cp^*TaCl_2(PMe_3)_2(CO)]$ towards further PMe_3 displacement, whereas the Cp analogue is quite stable.

2.4.7 Other Reactions of $Cp^*TaCl_2(PMe_3)_2$ (5)

Several further reactions were performed with (5) and monitored by ^1H NMR spectroscopy, the results of which are briefly described below.

Reaction with dppe

Complex (5) showed no indications of reaction with dppe after 30h. at 70°C. Higher temperatures led to decomposition.

Reaction with lithium methoxide

Complex (5) was reacted with lithium methoxide in toluene solvent at 70°C for 7h., in the presence of a small amount of PMe_3. Upon work up, starting material only was recovered.

Reaction with ethylene

Complex (5) was reacted with ethylene (2 equiv.) at room temperature and followed by ^1H NMR spectroscopy. After 16h. no starting complex remained and two new Cp^* signals at 1.95 ppm and 1.93 ppm were observed which did not appear to be associated with coordinated PMe_3. Considerable amounts of free PMe_3 were observed. After 3 days, signals assignable to new olefins were observed, indicating that olefin

oligomerisation had occurred, presumably in a similar manner to that described for $Cp'TaCl_2(\eta^2\text{-}CH_2CH_2)$[7]. Due to the complex nature of the reaction however, the system was not studied further.

Reaction with cycloheptene

No reaction was observed between (5) and cycloheptene (1 equiv.) after 6 days at 70°C.

Reaction with 1,5-cyclooctadiene

No reaction was observed between (5) and 1,5-cyclooctadiene (1 equiv.) after 6 days at 70°C.

2.4.8 Preparation of *cis*-$Cp^*Ta(CO)_2(PMe_3)_2$ (9)

The reaction of $Cp^*TaCl_2(PMe_3)(CO)_2$ (8) with sodium amalgam (2 equivalents) in THF solvent, in the presence of PMe_3 proceeded smoothly over 24h. at room temperature. Removal of the volatile components and extraction of the dried residue with toluene afforded an orange-red solution. Filtration followed by concentration and cooling to -78°C gave orange crystals.

Elemental analysis of the crystals supported the formula $Cp^*Ta(CO)_2(PMe_3)_2$ (9):

Elemental analysis for $C_{18}H_{33}O_2P_2Ta$:
Found (Required): %C, 41.00 (41.22); %H, 6.78 (6.36).

Furthermore, the mass spectrum (CI^+, isobutane) revealed a parent ion at m/e 525 $[M+H]^+$ and fragments formed by sequential loss of two carbonyl and two PMe_3 ligands.

Trans-$Cp^*Ta(CO)_2(PMe_3)_2$ has been previously reported by Bercaw and co-workers[56]. However, a comparison of infrared and ^1H NMR data

revealed that (9) was not identical to this compound (Table 2.8).

	Trans-$Cp^*Ta(CO)_2(PMe_3)_2$[56]	(9)
IR (Nujol) (cm^{-1})	1842, ν_s(CO) 1750, ν_a(CO)	1822, ν_s(CO) 1732, ν_a(CO)
^1H NMR, C_6D_6 (ppm)	1.90, s, C_5Me_5 1.35, m, $2PMe_3$ [J(PH)=6.4 Hz]	1.93, s, C_5Me_5 1.13, m, $2PMe_3$ [J(PH)=6.4 Hz]

Table 2.8 *Selected Spectroscopic Data for (9) and trans-Cp*Ta(CO)$_2$(PMe$_3$)$_2$.*

The spectroscopic data in Table 2.8 differ only slightly indicating (9) to be an isomer of *trans*-$Cp^*Ta(CO)_2(PMe_3)_2$, the most reasonable possibility being the *cis* form. Further support for this assignment is provided by $^{13}C\{^1H\}$ NMR spectroscopy. The equivalent carbonyl ligands of *trans*-$Cp^*Ta(CO)_2(PMe_3)_2$ display a triplet signal at 278.11 ppm [$^2J(PC)$ = 19.5 Hz][56] due to coupling to two equivalent PMe_3 phosphorus nuclei. The equivalent carbonyls of (9), however, are found at 278.11 ppm as a doublet resonance [$^2J(PC)$ = 22.9 Hz] indicating each carbonyl carbon to be strongly coupled to only one phosphorus nucleus. This is similar to the ^{13}C NMR data for *cis*-$Cp^*Ta(CO)_2(dmpe)$[56] in which the carbonyl carbons couple strongly to one phosphorus nucleus [J(PC) = 17 Hz] but only weakly to the other [J(PC) = 4 Hz]. For (9) this smaller coupling was not resolved.

The ν(CO) absorptions in the infrared spectrum of (9) are lower than those for *trans*-$Cp^*Ta(CO)_2(PMe_3)_2$, consistent with the greater $M \rightarrow CO$, $d\pi$-π^* back donation expected for a *cis* geometry. Moreover, a semi-quantitative analysis[55] of the symmetric and anti-symmetric ν(CO) absorptions in the infrared spectrum (Nujol) of (9) indicated a OC-M-CO

bond angle of 97°, supportive of a *cis*-dicarbonyl geometry.

It is of interest to compare the syntheses of the *cis* and *trans* isomers of $Cp^*Ta(CO)_2(PMe_3)_2$ since they appear to be highly selective (Equations 2.12 and 2.13).

$$\underset{(8)}{Cp^*TaCl_2(PMe_3)(CO)_2} \xrightarrow[THF,PMe_3]{2Na/Hg} \underset{(9)}{cis\text{-}Cp^*Ta(CO)_2(PMe_3)_2} \qquad (2.12)$$

$$Cp^*Ta(PMe_3)_2H_4 \xrightarrow{CO} Cp^*Ta(PMe_3)_2H_2(CO) \xrightarrow{CO} trans\text{-}Cp^*Ta(PMe_3)_2(CO)_2 \qquad (2.13)$$

Equation 2.12 involves a heterogeneous reaction and thus postulations on the mechanism are tenuous but overall the reaction has proceeded with retention of the *cis*-dicarbonyl geometry in going from (8) to (9). Furthermore, analysis of the crude product revealed no trace of the *trans*-isomer, indicating the reaction to be 100% selective.

Equation 2.13 illustrates the synthesis of the *trans*-isomer[56]. Again the reaction proceeds with overall retention of geometry as the PMe_3 ligands are orientated *trans* in $Cp^*Ta(PMe_3)_2H_4$[38].

The above observations indicate that the two isomers are not readily interconvertible under the reaction conditions employed nor do they interconvert at room temperature in solution over many months in sealed tubes. However, the isomers do interconvert at temperatures > 70°C in deuteriobenzene solvent, and the isomerisation process has been examined more closely.

2.4.9 *Cis-trans* isomerism of $Cp^*Ta(CO)_2(PMe_3)_2$

Upon thermolysis in d^6-benzene solvent at 100°C the *cis* form of $Cp^*Ta(CO)_2(PMe_3)_2$ is converted to the *trans* isomer with a first half-

life of 84 min. The equilibrium between the two lies to the side of the *trans* isomer indicating the latter to be the thermodynamically more stable (Equation 2.14).

$$cis \underset{K > 1}{\overset{K}{\rightleftharpoons}} trans \qquad (2.14)$$

This observation may be rationalised on both steric and electronic grounds. The relatively bulky PMe_3 ligands will prefer to occupy *trans*-orientated positions, as observed for $CpMX_2(PMe_3)_2$ compounds[20]. Moreover, extended Hückel calculations on $CpMo(CO)_2(PH_3)X$ [X = H, Cl] also show the *trans* isomer to be more stable than the *cis* by *ca.* 3-4 kcal/mol[39]. Electronically, M → CO $d\pi$-π^* interactions are less effective in the *trans* geometry (re: the carbonyl stretching frequencies of Table 2.8), but the M-PMe_3 σ-bonds are expected to be stronger in the *trans* arrangement. Presumably a balance of factors is involved but steric factors most probably exert a dominating influence[59].

Mechanism

Two general types of mechanism have been postulated to account for the isomerisation of $CpM(CO)_2LX$ compounds[59], an intramolecular rearrangement or a dissociative process. The experimental observations provide strong evidence for ligand dissociation rather than intramolecular pseudo-rotation processes.[57]

Of the two possibilities, PMe_3 dissociation or CO dissociation, PMe_3 dissociation may be rejected as the rate of conversion, [*cis*] → [*trans*] was found to be independent of added PMe_3. Had phosphine displacement been important, then a significant rate reduction would have been anticipated under these conditions. Unfortunately it was not possible to confirm CO dissociation by performing the reaction in the presence of excess CO, as $Cp^*Ta(CO)_2(PMe_3)_2$ reacts with CO (1 atm.)

according to Equation 2.15.

$$Cp^*Ta(CO)_2(PMe_3)_2 + CO \rightleftharpoons Cp^*Ta(CO)_3(PMe_3) + PMe_3 \qquad (2.15)$$

[$T_{\frac{1}{2}}$ *ca.* 7 days at 25°C]

Although slow at ambient temperature, the reaction rate is appreciable at 100°C. Consistently during thermolyses of *cis*-$Cp^*Ta(CO)_2(PMe_3)_2$, small quantities of $Cp^*Ta(CO)_3(PMe_3)$ are produced, presumably the result of CO dissociation and subsequent reaction with $Cp^*Ta(CO)_2(PMe_3)_2$ according to Equation 2.15. Thus a mechanism involving CO dissociation appears likely under these conditions.

It is possible to construct a mechanistic pathway for the isomerisation process and a subsequent rate equation that is consistent with the observations (Equations 2.16-2.19).

$$\underset{(A)}{cis\text{-}Cp^*Ta(CO)_2(PMe_3)_2} \underset{k_{-1}}{\overset{k_1}{\rightleftharpoons}} \underset{(B)}{[Cp^*Ta(CO)(PMe_3)_2]} + CO \qquad (2.16)$$

$$[Cp^*Ta(CO)(PMe_3)_2] + CO \underset{k_{-2}}{\overset{k_2}{\rightleftharpoons}} \underset{(C)}{trans\text{-}Cp^*Ta(CO)_2(PMe_3)_2} \qquad (2.17)$$

$$cis\text{-}Cp^*Ta(CO)_2(PMe_3)_2 + CO \underset{k_{-3}}{\overset{k_3}{\rightleftharpoons}} \underset{(D)}{Cp^*Ta(CO)_3(PMe_3)} + PMe_3 \qquad (2.18)$$

$$trans\text{-}Cp^*Ta(CO)_2(PMe_3)_2 + CO \underset{k_{-4}}{\overset{k_4}{\rightleftharpoons}} \underset{(D)}{Cp^*Ta(CO)_3(PMe_3)} + PMe_3 \qquad (2.19)$$

Assuming that $[Cp^*Ta(CO)(PMe_3)_2]$, (B), is in a steady state throughout most of the reaction, the expression for the rate of loss of [*cis*-$Cp^*Ta(CO)_2(PMe_3)_2$] can be obtained[58] (Equation 2.20). This assumption seems reasonable as such an electronically unsaturated molecule as B would be expected to be short-lived in the presence of donor molecules, and indeed, no indications of its presence could be detected by ^1H NMR spectroscopy.

$$-\frac{d[A]}{dt} = \left(C_1 + k_3[CO]\right).[A] - C_2[C] - k_{-3}[D][PMe_3] \qquad (2.20)$$

$$\text{where } C_1 = \left(k_1 - \frac{k_1 k_{-1}}{k_{-1}+k_2}\right) \text{ and } C_2 = \left(\frac{k_{-1}k_{-2}}{k_{-1}+k_2}\right)$$

and A = *cis*-$Cp^*Ta(CO)_2(PMe_3)_2$

C = *trans*-$Cp^*Ta(CO)_2(PMe_3)_2$

D = $Cp^*Ta(CO)_3(PMe_3)$

As expected, this is essentially the rate equation for the simple equilibrium:

$$cis \underset{k_{-1}}{\overset{k_1}{\rightleftharpoons}} trans$$

$$-\frac{d[A]}{dt} = k_1[A] - k_{-1}[C]$$

modified to account for side reactions. It is found that the reaction in Equation 2.19 does not affect the rate of loss of A, but will affect the rate of formation of C.

The thermolysis of *cis*-$Cp^*Ta(CO)_2(PMe_3)_2$ in d^6-benzene at 100°C was monitored by ^1H NMR spectroscopy, the concentrations of each component being approximated to their percentage contribution(%) to the total product mixture. The composition of the reaction mixture as a function of time is displayed in Table 2.9 and in graphical form in Figure 2.11.

TIME (MIN.)	%CIS	%TRANS	%D	ln[%CIS]
15	82.8	12.6	2.3	4.42
40	71.5	22.6	3.0	4.27
75	57.9	35.4	3.4	4.06
105	47.5	45.8	3.4	3.86
120	33.7	45.9	10.2	3.52
180	27.2	56.6	8.1	3.30
250	26.8	59.2	7.0	3.29
330	23.3	60.4	8.2	3.15
410	18.6	64.7	8.3	2.92

Table 2.9 *Composition of cis-trans $Cp^*Ta(CO)_2(PMe_3)_2$ reaction Mixture as a function of time (d^6-benzene, 100°C).*

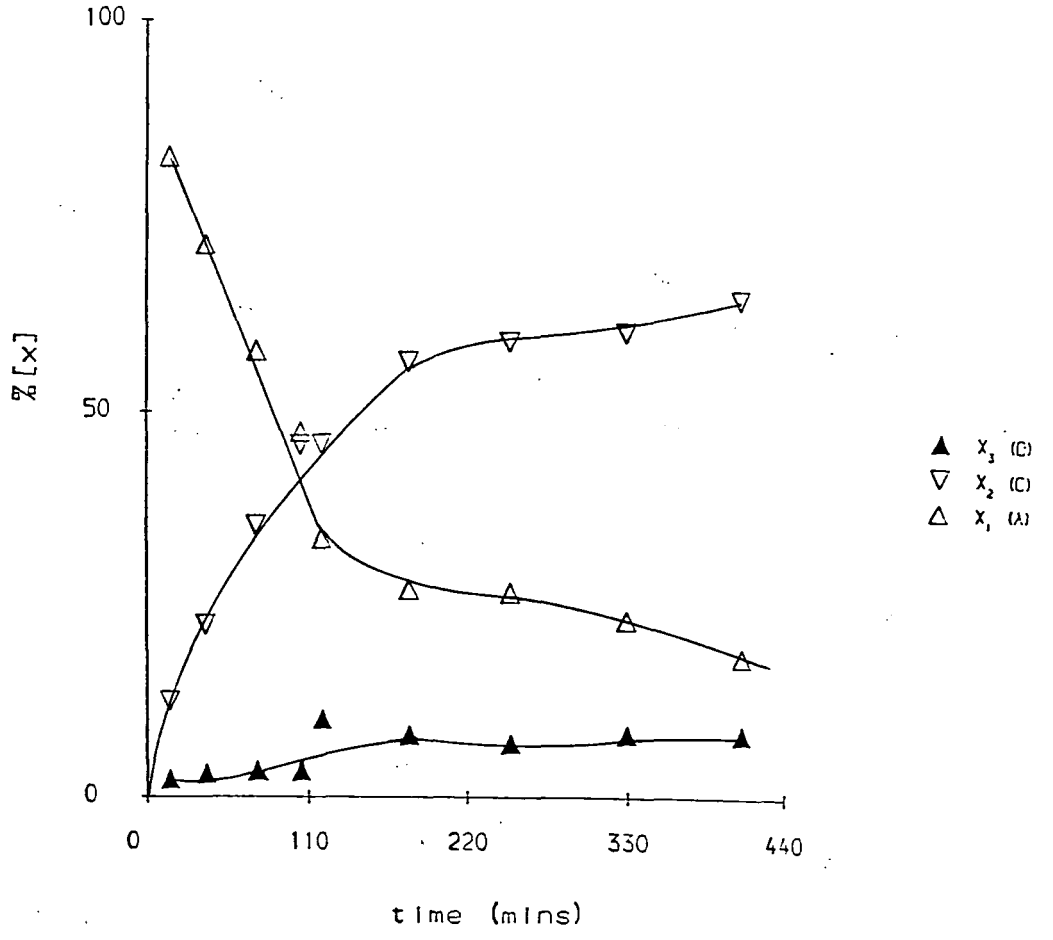

Figure 2.11 *Composition of the cis-trans $Cp^*Ta(CO)_2(PMe_3)_2$ Reaction Mixture as a Function of Time (d^6-benzene, 100°C).*

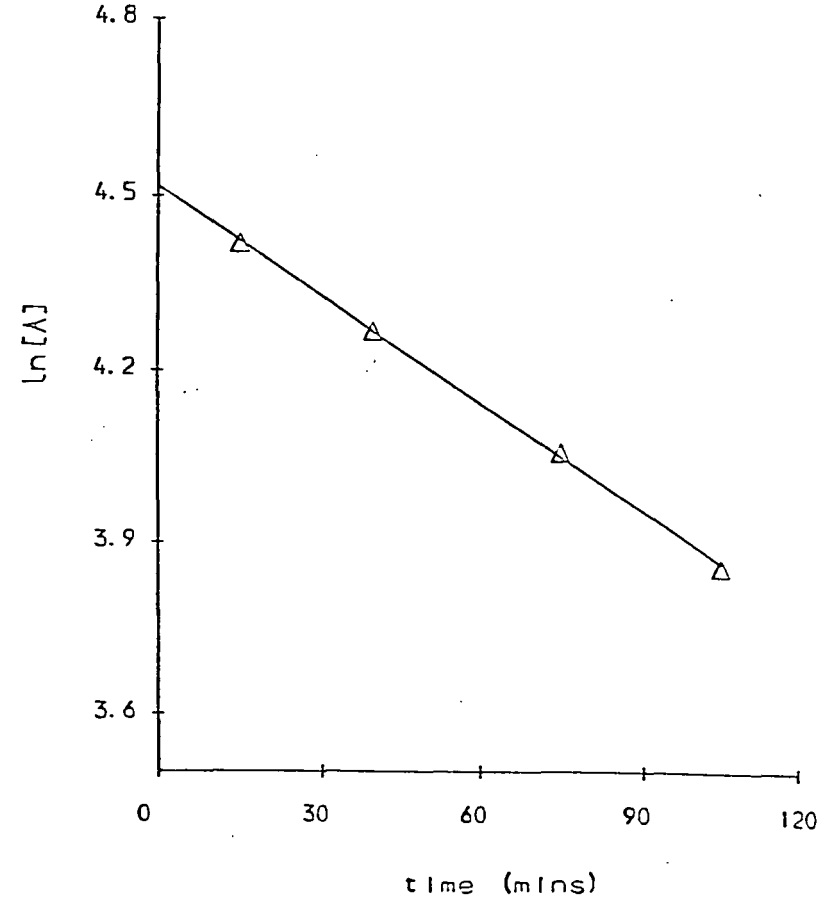

Figure 2.12 *Plot of Ln [% cis] versus Time (100°C)*

It can be seen from Figure 2.11 that $Cp^*Ta(CO)_3(PMe_3)$ remains at relatively low concentrations throughout the reaction. During the first half-life, first order kinetics are obeyed quite well (Figure 2.12). Examination of Equation 2.20 supports this, since in the early stages of reaction the concentrations of [C], [D] and [PMe_3] are low and, under these conditions:

$$-\frac{d[A]}{dt} \approx \left(C_1 + k_3[CO]\right).[A]$$

Since [CO] will be very low initially and it is reasonable to expect $k_{-1} \approx k_2 >> k_1$ or k_3, the observed pseudo first order rate constant (k_{obs}) may be approximated to k_1 which, from Figure 2.12 is 9.9 x 10^{-5} s^{-1}. This is significantly smaller than $k_{cis \rightarrow trans}$ for $CpMo(CO)_2LR$ complexes which can range from *ca.* 0.2 s^{-1} (-56°C) for R=H, L=$P(OPh)_3$, to *ca.* 0.4 s^{-1} (123°C) for R=Cl, L=$P(OMe)_3$[59] and which have been shown to isomerise *via* non-dissociative mechanisms.

As the reaction proceeds, so [C], [D] and [PMe_3] increase and the rate of loss of [A] decreases. In the absence of any side reactions, at equilibrium d[A]/dt should be zero. However in this system, this is not the case, presumably due to the involvement of the reaction in Equation 2.15. Thus, in Equation 2.20 the $k_3[CO]$ term causes a steady loss of [A] throughout the course of the reaction and, under these conditions, prevents the attainment of a simple [*cis*] ⇌ [*trans*] equilibrium.

Therefore, although an intramolecular rearrangement mechanism for isomerisation cannot be unambiguously disproved, the experimental observations suggest that CO dissociation is important and a dissociative mechanism provides an adequate qualitative explanation of the experimental data. Since intramolecular rearrangements have been invoked for a number of $CpM(CO)_2LX$ compounds[59] for which there was no evidence of ligand dissociation, it appears that for $Cp^*Ta(CO)_2(PMe_3)_2$

the activation barrier for intramolecular rearrangement must be comparable, at least, to the tantalum-carbonyl bond dissociation energy.

2.4.10 Preparation of $Cp^*Ta(CO)_4$ (10)

Half-sandwich carbonyl complexes of the general type $Cp'M(CO)_4$ (Cp' = Cp, Cp^*; M = V, Nb, Ta) are potentially valuable precursors to low oxidation state half-sandwich complexes of these elements[60] and have found use as reagents in organic synthesis[61]. However, forcing conditions are generally found to be necessary for their preparation, typically requiring CO pressures of *ca.* 330 bar and temperatures in excess of 100^oC[34]. It has been found here that ligated PMe_3 facilitates the preparation of $Cp^*Ta(CO)_4$ under mild conditions and in reasonable yield.

The reduction of $Cp^*TaCl_2(PMe_3)(CO)_2$ (8) by sodium amalgam (2.5 equivalents) in THF solution under *ca.* 1.5 atmospheres of CO resulted in a dark orange solution from which $Cp^*Ta(CO)_4$ (10) was obtained in *ca.* 65% yield (characterised by elemental analysis, infrared, ^1H NMR and mass spectrometries, Chapter 7, section 7.2.11). The remaining supernatant solution was found to contain an additional reaction product which was formulated as $Cp^*Ta(CO)_3(PMe_3)$ (11) on the basis of its ^1H NMR spectrum. In particular, a singlet resonance is observed at 1.85 ppm for the ring methyl hydrogens and a doublet resonance at 1.03 ppm [$^2J(PH)$ = 8.1 Hz] is indicative of a single, metal bound PMe_3 ligand. However, (10) and (11) were readily separated by fractional crystallisation. It is likely that the two compounds are formed by competing pathways since (11) does not react with CO to produce (10) under the experimental conditions employed. Indeed the use of a lower CO pressure or excess PMe_3 in the reaction mixture led to a corresponding

increase in the proportion of (11) in the product mixture (by ^{1}H NMR spectroscopy).

The success of this reaction prompted us to attempt a direct "one-pot" synthesis of (10). Thus, Cp^*TaCl_4 was reacted over 21h. at room temperature with 4 equivalents of sodium amalgam in THF solvent under 1.5 atmospheres of CO, in the presence of 1 equivalent of PMe_3. Upon work-up, (10) was isolated cleanly in 47% yield. Thus, although previously prepared in 70% yield (under 380 bar of CO at 100°C)[34], the method described here has made accessible, $Cp^*Ta(CO)_4$ by a mild synthetic procedure and in reasonable yield.

Although the available data do not allow precise delineation of the reduction pathway followed in the conversion of Cp^*TaCl_4 to $Cp^*Ta(CO)_4$, Scheme 2.3 incorporates essential features consistent with the data.

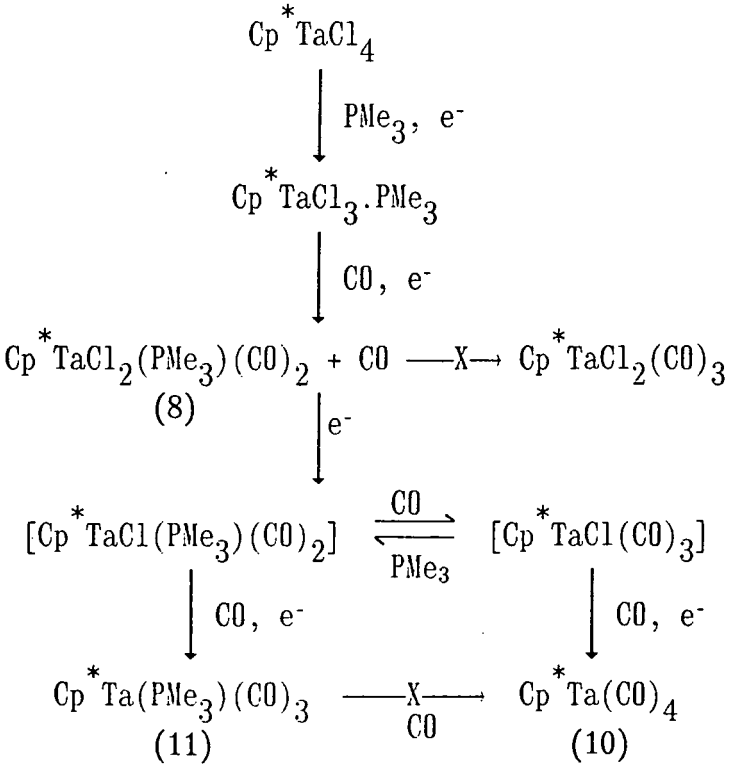

Scheme 2.3 *Potential reaction pathway for the conversion of Cp^*TaCl_4 to $Cp^*Ta(CO)_4$ in the presence of PMe_3.*

The presence of ligated PMe_3 is clearly crucial to the success of

this reaction, since previous attempts to prepare $CpM(CO)_4$ (M = Nb, Ta) from $CpMCl_4$ under mild conditions have proved unsuccessful[19]. The assistance of PMe_3 in the preparation of otherwise inaccessible species has been noted on previous occassions[20,23]. Of particular relevance is the synthesis of $CpV(CO)_3(PEt_3)$ from $CpVCl_2(PEt_3)_2$[20] (Chapter 1, section 1.4.5), although in this system, $CpV(CO)_4$ is only a minor side product.

While the precise role of the coordinated PMe_3 remains obscure, an important influence may be the coordinative stabilisation of mononuclear intermediates (both $Cp^*TaCl_3.PMe_3$ and $Cp^*TaCl_2(PMe_3)(CO)_2$ have been shown in this chapter to be mononuclear by X-ray diffraction studies). Furthermore, the effect of coordinated PMe_3 on the reduction potentials of the intermediates may facilitate a more controlled conversion from the Ta(V) starting material to the Ta(I) product.

2.5 THE MOLECULAR STRUCTURE OF $Cp^*TaCl_2(PMe_3)(CO)_2$ (8)

Purple prisms of $Cp^*TaCl_2(PMe_3)(CO)_2$ (8) were obtained by cooling a saturated toluene solution to -35°C for several days. The X-ray diffraction study was performed by Dr. W. Clegg at the University of Newcastle-upon-Tyne. The crystal data for (8) are reproduced in Appendix 1B and the molecular structure is illustrated in Figures 2.13 and 2.14. Selected bond distances and angles are given in Table 2.10.

If the (η^5-C_5Me_5) ligand is assumed to occupy a single coordination site, the molecule may be described as a distorted octahedron with the ring and phosphine ligands lying mutually *trans* (angle RC-Ta-P = 170.9°). The chloro and carbonyl ligands also adopt a mutually *trans* orientation resulting in a *cis*-dichloro/*cis*-dicarbonyl arrangement, as predicted in section 2.4.6 on the basis of NMR and infrared data. The

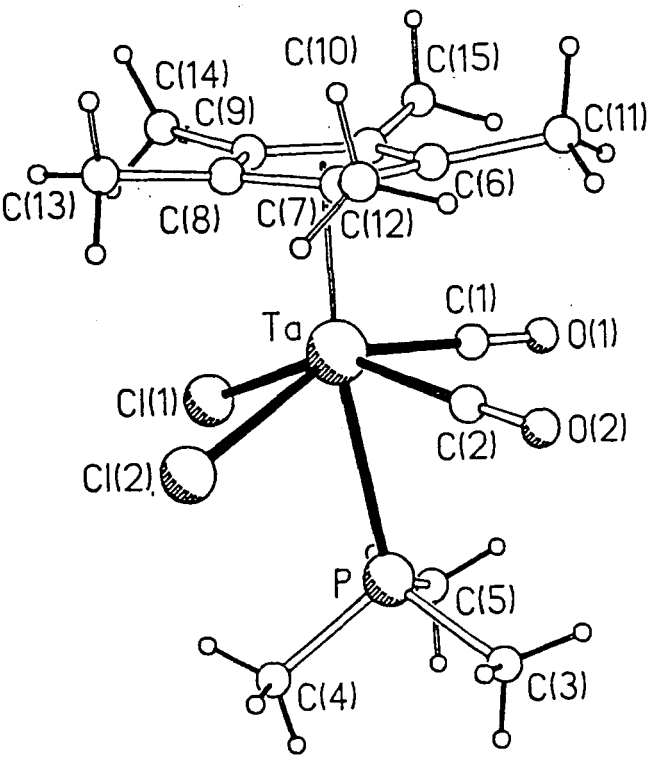

Figure 2.13 *The Molecular Structure of $Cp^*TaCl_2(PMe_3)(CO)_2$ (8)*

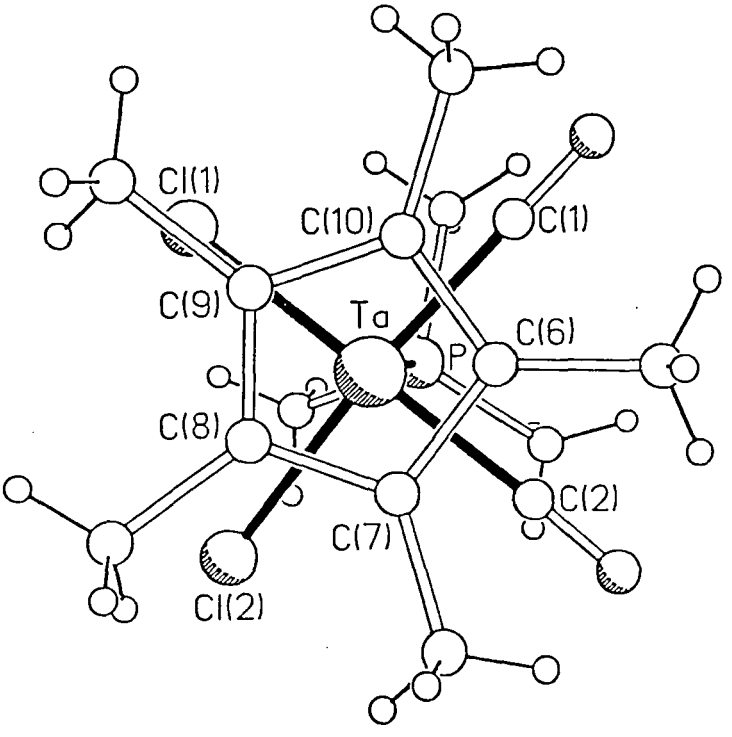

Figure 2.14 *View of $Cp^*TaCl_2(PMe_3)(CO)_2$ (8) along the Ring Centroid-Tantalum Vector.*

tantalum-RC distance of 2.094(6)Å is comparable to those reported for other Cp^*Ta complexes and is, as expected, slightly longer than that for $Cp^*TaCl_3(PMe_3)$ (2.053Å) due to the more electron rich nature of the metal centre in (8).

Ta-Cl(1)	2.504(2)	Cl(1)-Ta-Cl(2)	84.2(1)
Ta-Cl(2)	2.512(2)		
		Cl(1)-Ta-P	75.2(1)
Ta-P	2.707(2)	Cl(2)-Ta-P	78.7(1)
		C(1)-Ta-C(2)	83.9(3)
Ta-C(1)	2.070(6)		
Ta-C(2)	2.079(7)	C(1)-Ta-P	74.0(2)
Ta-C(6)	2.386(6)	C(2)-Ta-P	76.9(2)
Ta-C(7)	2.373(6)		
Ta-C(8)	2.438(6)	C(1)-Ta-Cl(1)	92.2(2)
Ta-C(9)	2.474(6)	C(1)-Ta-Cl(2)	152.4(2)
Ta-C(10)	2.426(6)	C(2)-Ta-Cl(1)	151.8(2)
		C(2)-Ta-Cl(2)	86.5(3)
C(1)-O(1)	1.136(7)		
C(2)-O(2)	1.117(8)	Ta-C(1)-O(1)	179.5(8)
		Ta-C(2)-O(2)	176.1(7)
P-C(3)	1.812(7)		
P-C(4)	1.776(9)	Ta-P-C(3)	118.4(3)
P-C(5)	1.812(10)	Ta-P-C(4)	114.7(3)
		Ta-P-C(5)	114.6(3)
C(6)-C(7)	1.475(9)		
C(6)-C(10)	1.420(9)	C(3)-P-C(4)	103.6(5)
C(6)-C(11)	1.508(11)	C(3)-P-C(5)	101.5(5)
C(7)-C(8)	1.417(9)	C(4)-P-C(5)	101.8(4)
C(7)-C(12)	1.481(11)		
C(8)-C(9)	1.379(9)	Ta-C(6)-C(7)	71.5(3)
C(8)-C(13)	1.513(10)		
C(9)-C(10)	1.438(9)	X-Ta-P	163.4
C(9)-C(14)	1.528(8)		
C(10)-C(15)	1.518(9)	Y-Ta-C(1)	97.7
		Y-Ta-C(2)	98.9
X-Ta	2.537		
Y-Ta	2.094	Y-Ta-P	170.9
Z-Ta	2.091	Y-Ta-Cl(1)	109.3
Y-Z	0.118	Y-Ta-Cl(2)	109.4

Table 2.10 *Bond Lengths (Å) and Angles (°) for $Cp^*TaCl_2(PMe_3)(CO)_2$ (8); X=Midpoint of C(8)-C(9); Y=Ring centroid; Z=Point in plane of ring where normal from tantalum intersects.*

Although the average inter-ring carbon-carbon and carbon-tantalum distances of 1.426(16)Å and 2.419(18)Å respectively are normal[38], the individual values cover quite a large range, with ΔR = 0.096Å and ΔM =

0.101Å (*cf.* Table 2.3). Indeed, a principal feature of interest in the molecular structure is a ring-slip distortion of the (η^5-C_5Me_5) ligand. The vector from tantalum, normal to the (η^5-C_5Me_5) ring is displaced 0.118Å from the ring centroid towards ring carbon atoms C(6) and C(7) (Figure 2.14). Consequently, the Ta-C(6) and and Ta-C(7) distances of 2.386(6)Å and 2.373(6)Å respectively are significantly shorter than the other Ta-ring carbon distances [av. 2.446(6)Å]. The ring slippage also results in an elongated C(6)-C(7) bond [1.475(9)Å] and a shortened C(8)-C(9) distance [1.379(9)Å]. Similar, although much larger distortions have been noted in half-sandwich oxo-rhenium systems[62], and correlated with the strong *trans* influence of the oxo ligand. A similar effect may operate in (8) as Figure 2.14 indicates the PMe_3 ligand to be directed approximately *trans* (angle X-Ta-P = 163.4°) to the C(8)-C(9) bond [X = midpoint of C(8)-C(9)].

Another interesting feature of this molecule is the distortion of the axial PMe_3 ligand away from linearity with the ring centroid (RC) tantalum vector. This has also been observed in the isoelectronic complex, $Cp^*ReCl_4.PMe_3$[22] although no explanation was offered.

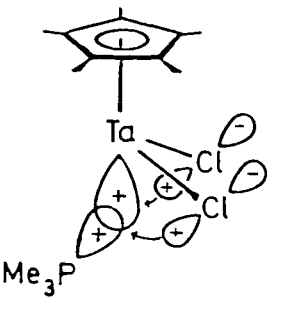

Figure 2.15 *Competitive Frontier Orbital interactions in (8).*

It is possible that the distortion arises to maximise overlap between the [$Cp^*MCl_2(CO)_2$] LUMO (dz^2), and the PMe_3 σ-donor orbital and pπ

interactions with chlorine lone pairs (Figure 2.15). This distortion also results in an expanded angle RC-Ta-Cl of 109.4° compared to RC-Ta-CO of 98.3° (average). Inter-ligand steric interactions between the halogens, the (η^5-C_5Me_5) methyls and the PMe_3 ligand are likely to accentuate this distortion. A more detailed study of these distortions is currently in progress *via* electronic structure calculations.

The tantalum chlorine bond distances of 2.504(2)Å [Cl(1)] and 2.512(2)Å [Cl(2)] are *ca.* 0.1Å longer than those of $Cp^*TaCl_3(PMe_3)$ (see section 2.3) presumably due to the lower tantalum oxidation state and electronic saturation of (8). Furthermore, the distances are somewhat longer than those of many other Ta(III) chloro complexes (Table 2.11), reflecting the electron rich nature of (8) and the fact that the chlorine atoms are displaced mutually *trans* to strongly *trans* influencing carbonyl ligands[43] with angles Cl(1)-Ta-C(2) and Cl(2)-Ta-C(1) of 151.8° and 152.4° respectively.

Of those complexes in Table 2.11, only the latter is electronically saturated with no potential for further M ← L pπ-dπ interactions.

COMPLEX	d(Ta-Cl) (Å)	REF
$Ta_2Cl_6(dmpe)_2$	2.415	70
$Ta_2Cl_4H_2(PMe_3)_4$	2.418	63
$TaClH_2(PMe_3)_4$	2.472	45
$[PyH]^+[TaCl_4(PhC_2Ph)(Py)]^-$	2.438 2.067	64 65
$CpTaCl_2(PMe_2Ph)_2(CO)$	2.539 2.518	19

Table 2.11 *Representative (Ta-Cl) Distances for Ta(III) Complexes.*

Significantly, it is the chlorine atom *trans* to the carbonyl ligand (the other is *trans* to Cp) that has the longer bond length in this complex.

Similarly the electron-rich nature of the tantalum atom in (8) results in a significantly longer tantalum-phosphorus bond [2.707(2)Å] than is usually found in Ta(III)-PMe_3 complexes, some representative examples of which are given in Table 2.12.

Interestingly, the tantalum-phosphorus distance for (8) is *ca.* 0.17Å (average) longer than those for the electronically saturated, formally seven coordinate complex, $Ta^{III}(PMe_3)_3(\eta\text{-}CH_2PMe_2)(\eta\text{-}CHPMe_2)$ and is also considerably longer than the tantalum-phosphorus distances in a number of lower oxidation state complexes, *eg.* $Ta^{I}(H)(CO)_2(dmpe)_2$ [2.514Å][66], $Ta^{0}(dmpe)_3$ [2.500Å][67] and $Ta^{II}Cl_2(PMe_3)_4$ [2.540Å][45] although a reduction in d(Ta-P) for the latter two compounds may result from their electronic unsaturation.

The two carbon monoxide ligands are essentially linear [Ta-C(1)-O(1) = 179.5°; Ta-C(2)-O(2) = 176.1°] with tantalum-carbon distances of 2.070(6)Å [C(1)] and 2.079(7)Å [C(2)].

COMPLEX	d(Ta-P) (Å)	REF
$Ta_2Cl_4H_2(PMe_3)_4$	2.600	63
$TaClH_2(PMe_3)_4$	2.517	45
$Ta_2Cl_6(PMe_3)_4$	2.666 (e) 2.598 (a)	49
$Ta(PMe_3)_3(\eta\text{-}CH_2PMe_2)(\eta\text{-}CHPMe_2)$	2.516 (e) 2.552 (a)	68
$Cp^*Ta(CHCMe_3)(\eta\text{-}C_2H_4)(PMe_3)$	2.507	36

Table 2.12 *Representative (Ta-P) Distances for Ta(III) Complexes; e=equitorial; a=axial.*

These are, as expected, longer than the tantalum-carbon distance in $CpTaCl_2(PMe_2Ph)_2(CO).THF$ [2.01(2)Å][19] since in the latter complex only one carbonyl ligand is available to accept π-charge density from tantalum. This is also reflected in the carbon-oxygen distances of (8)

being shorter than that in $CpTaCl_2(PMe_2Ph)_2(CO)$ (*viz.* 1.136(7)Å and 1.117(8)Å versus 1.20(2)Å respectively).

2.6 SUMMARY

A number of half-sandwich chloro-phosphine compounds of tantalum have been described. The paramagnetic d^2-complex, $Cp^*TaCl_2(PMe_3)_2$ has been shown to be a most useful synthetic precursor to both new and known organo-tantalum compounds. Some of its derivative chemistry developed in this Chapter is illustrated in Scheme 2.4.

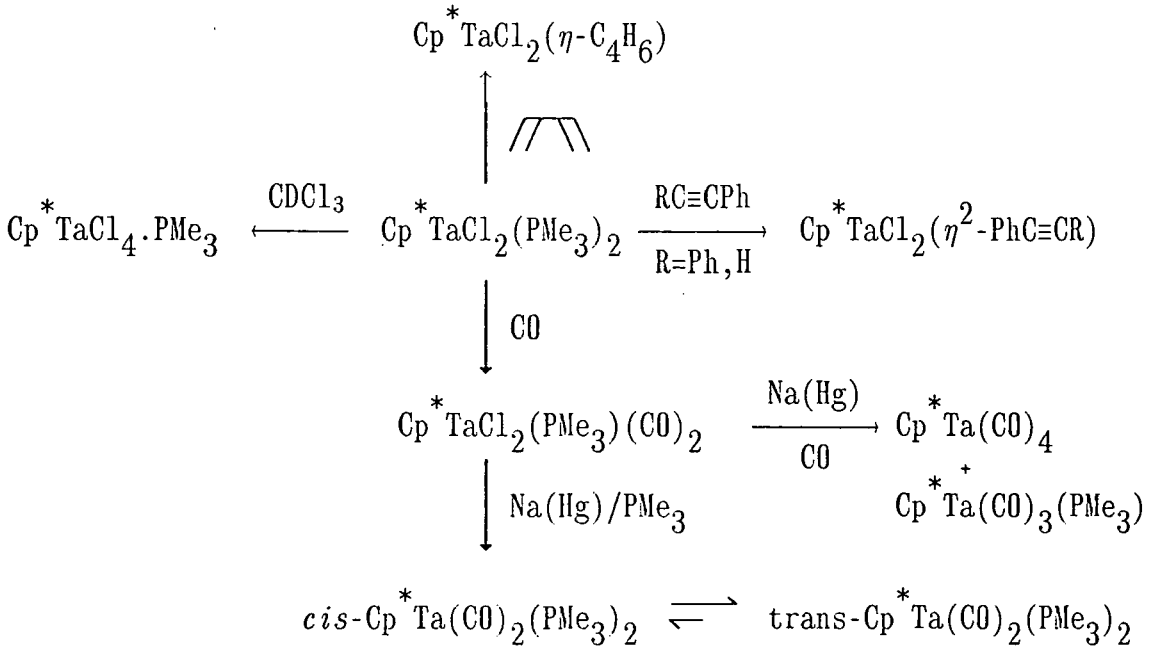

Scheme 2.4 *Some Derivative Chemistry of $Cp^*TaCl_2(PMe_3)_2$.*

Moreover, convenient syntheses of $Cp^*Ta(CO)_4$ and Cp^*NbCl_4 have been developed such that further exploitation of the chemistry of half-sandwich pentamethylcyclopentadienyl tantalum and niobium is now feasible throughout a range of oxidation states. Aspects of this work have been communicated[69] and further uses of $Cp^*TaCl_2(PMe_3)_2$ as a

synthetic precursor are described in Chapter 6.

2.7 REFERENCES

1. A.M. Cardoso, R.J.H. Clark and S. Moorhouse, *J.Chem.Soc.Dalton Trans.*, 1980, 1156.

2. G. Hidaleo Llinás, M. Mena, F. Palacios, P. Royo and R. Serrano, *J.Organometallic Chem.*, 1988, 340, 37.

3. D.F. Foust and M.D. Rausch, *J.Organometallic Chem.*, 1985, 287, 195.

4. R.B. King and C.D. Hoff, *J.Organometallic Chem.*, 1982, 225, 245.

5. M.J. Bunker, A. De Cian, M.L.H. Green, J.J.E. Moreau and N. Siganporia, *J.Chem.Soc.Dalton Trans.*, 1980, 2155.

6. R.J. Burt, J. Chatt, G.J. Leigh, J.H. Teuben and A. Westerhof, *J.Organometallic Chem.*, 1977, 129, C33.

7. S.J. McLain, C.D. Wood and R.R. Schrock, *J.Am.Chem.Soc.*, 1979, 101, 4558.

8. M. Moran, *Transition Metal Chem.*, 1981, 6, 173.

9. M.J. Bunker, A. De Cian and M.L.H. Green, *J.C.S. Chem Commun.*, 1977, 59.

10. R.C. Murray, L. Blum, A.H. Liu and R.R. Schrock, *Organometallics*, 1985, 4, 953.

11. W.A. Herrmann, J.K. Felixberger, E. Herdtweck, A. Schäfer and J. Okuda, *Angew.Chem.Int.Ed.Engl.*, 1987, 26, 466.

12. J.W. Kang, K. Moseley and P.M. Maitlis, *J.Am.Chem.Soc.*, 1969, 91, 5970.

13. J.W. Kang and P.M. Maitlis, *J.Organometallic Chem.*, 1971, 30, 127.

14. S.H. Taylor and P.M. Maitlis, *J.Organometallic Chem.*, 1977, 139, 121.

15. G.E. Coates, M.L.H. Green, P. Powell and K. Wade, "*Principles of Organometallic Chemistry*", Methuen, London (1968), page 175.

16. F.A. Cotton and G. Wilkinson, "*Advanced Inorganic Chemistry*", 4th Edition, Wiley-Interscience, New-York (1980).

17. R.R. Schrock, S.F. Pederson, M.R. Churchill and J.W. Ziller, *Organometallics*, 1984, 3, 1574.

18. a) J.C. Green, C.P. Overton, K. Prout and J.M. Marín, *J.Organometallic Chem.*, 1983, 241, C21.

b) J.M. Marín, V.S.B. Mtetwa and K. Prout, *Acta Cryst.*, 1985, C41, 58.

19. R.J. Burt, G.J. Leigh and D.L. Hughes, *J.Chem.Soc.Dalton Trans.*, 1981, 793.

20. J. Nieman, J.H. Teuben, J.C. Huffman and K.G. Caulton, *J.Organometallic Chem.*, 1983, 255, 193.

21. C.A. Tolman, *Chem.Rev.*, 1977, 77, 313.

22. W.A. Herrmann, U. Küsthardt and E. Herdtweck, *J.Organometallic Chem.*, 1985, 294, C37.

23. V.C. Gibson, J.E. Bercaw, W.J. Bruton, Jr. and R.D. Sanner, *Organometallics*, 1986, 5, 976.

24. S.M. Rocklage, H.W. Turner, J.D. Fellmann and R.R. Schrock, *Organometallics*, 1982, 1, 703.

25. A.M. Andreu, F.A. Jalón, A. Otero, P.Royo, A.M. Manotti Lanfredi and A. Tiripicchio, *J.Chem.Soc.Dalton Trans.*, 1987, 953.

26. D.F. Evans, *J.Chem.Soc.*, 1959, 2003.

27. J.C. Daran, K. Prout, A. De Cian, M.L.H. Green and N. Siganporia, *J.Organometallic Chem.*, 1977, 136, C4.

28. A.M. Cardoso, R.J.H. Clark and S. Moorhouse, *J.Organometallic Chem.*, 1980, 186, 237.

29. D.A. Redfield, J.H. Nelson and L.W. Cary, *Inorg.Nucl.Chem.Letts.*, 1974, 10, 727.

30. S.A. Best, T.J. Smith and R.A. Walton, *Inorg.Chem.*, 1978, 17, 99.

31. R.D. Sanner, S.T. Carter and W.J. Bruton, Jr., *J.Organometallic Chem.*, 1982, 240, 157.

32. N. Hovnanian, L.G. Hubert-Pfalzgraf and G. Le Borgne, *Inorg.Chem.*, 1985, 24, 4647.

33. a) C. Ting, N.C. Baenziger and L. Messerle, *J.C.S. Chem Commun.*, 1988, 1133.

b) L.G. Hubert-Pfalzgraf, M. Tsunoda and J.G. Riess, *Inorg. Chim. Acta.*, 1981, 52, 231.

34. W.A. Herrmann, W. Kalcher, H. Biersack, I. Bernal and M. Creswick, *Chem.Ber.*, 1981, 114, 3558.

35. a) J. Rajaram and J.A. Ibers, *Inorg.Chem.*, 1973, 12, 1313.

b) P.J. Vergamini, H. Vahrenkamp and L.F. Dahl, *J.Am.Chem.Soc.*, 1971, 93, 6326.

c) M.R. Churchill and J. Fennessey, *Inorg.Chem.*, 1967, 6, 1213.

d) C. Bueno and M.R. Churchill, *Inorg.Chem.*, 1981, 20, 2197.

36. A.J. Schultz, R.K. Brown, J.M. Williams and R.R. Schrock, *J.Am. Chem.Soc.*, 1981, 103, 170.

37. J.E. Huheey, "*Inorganic Chemistry - Principles of Structure and Reactivity*", 3rd Edition, Harper (1983) page 258.

38. J.M. Mayer, P.T. Wolczanski, B.D. Santarsiero, W.A. Olson and J.E. Bercaw, *Inorg.Chem.*, 1983, 22, 1149.

39. P. Kubácek, R. Hoffmann and Z. Havlas, *Organometallics*, 1982, 1, 180.

40. L.W. Messerle, P. Jennische, R.R. Schrock and G. Stucky, *J.Am.Chem. Soc.*, 1980, 102, 6744.

41. M.R. Churchill and W.J. Youngs, *Inorg.Chem.*, 1979, 18, 171.

42. G. Smith, R.R. Schrock, M.R. Churchill and W.J. Youngs, *Inorg. Chem.*, 1981, 20, 387.

43. M.L. Tobe, "*Inorganic Reaction Mechanisms*", Nelson, London (1972).

44. F.A. Cotton, S.A. Duraj and W.J. Roth, *Inorg.Chem.*, 1984, 23, 4046.

45. M.L. Leutkens, Jr., J.C. Huffman and A.P. Sattelberger, *J.Am.Chem. Soc.*, 1983, 105, 4474.

46. F.A. Cotton, L.R. Falvello and R.C. Najjar, *Inorg.Chem.*, 1983, 22, 770.

47. M.L. Leutkens, Jr., W.L. Elcesser, J.C. Huffman and A.P. Sattelberger, *J.C.S. Chem Commun.*, 1983, 1072.

48. P.D.W. Boyd, T.C. Jonks, A.J. Nielson and C.E.F. Rickard, *J.C.S. Chem Commun.*, 1984, 1086.

49. A.P. Sattelberger, R.B. Wilson, Jr. and J.C. Huffman, *J.Am.Chem. Soc.*, 1980, 102, 7113.

50. a) For $CpTaCl_4.PMe_3$ see section 2.2.1 of this thesis.

b) For $Cp^*TaCl_4.PMe_3$: See reference 31.

51. R.M. Silverstein, G.C. Bassler and T.C. Morrill, "*Spectrometric Identification of Organic Compounds*", 4th Edition, John Wiley, New York (1981).

52. S. Fredericks and J.L. Thomas, *J.Am.Chem.Soc.*, 1978, 100, 350.

53. H. Yasuda, K. Tatsumi, T. Okamoto, K. Mashima, K. Lee, A. Nakamura, Y. Kai, N. Kanehisa and N. kasai, *J.Am.Chem.Soc.*, 1985, 107, 2410.

54. V.C. Gibson, G. Parkin and J.E. Bercaw, *J.Am.Chem.Soc.*, In press.

55. F.A. Cotton and G. Wilkinson, "*Advanced Inorganic Chemistry*", 4th Edition, Wiley-Interscience, New-York (1980), page 1074.

56. J.M. Mayer and J.E. Bercaw, *J.Am.Chem.Soc.*, 1982, 104, 2157.

57. E.L. Muetterties, *J.Am.Chem.Soc.*, 1969, 91, 1636.

58. P.W. Atkins, "*Physical Chemistry*", 2nd Edition, Oxford University Press, Oxford (1982), Chapter 27.

59. J.W. Faller and A.S. Anderson, *J.Am.Chem.Soc.*, 1970, 92, 5852.

60. See for example:

a) H.-C. Bechthold and D. Rehder, *J.Organometallic Chem.*, 1981, 206, 305.

b) B.V. Lokshin, A.A. Pasinsky, N.E. Kolobova, K.N. Anisimov and Yu. V. Makarov, *J.Organometallic Chem.*, 1973, 55, 315.

c) W.A. Herrmann, M.L. Ziegler, K. Weidenhammer and H. Biersack, *Angew.Chem.Int.Ed.Engl.*, 1979, 19, 960.

d) A.N. Nesmeyanov, A.I. Gusev, A.A. Pasynskii, K.N. Anisimov, N.E. Kolobova and Yu. T. Struchkov, *J.C.S. Chem Commun.*, 1969, 739.

61. R.J. Kinney, W.D. Jones and R.G. Bergman, *J.Am.Chem.Soc.*, 1978, 100, 7902.

62. W.A. Herrmann, E. Herdtweck, M. Flöel, J. Kulpe, U. Küsthardt and J. Okuda, *Polyhedron*, 1987, 6, 1165.

63. R.B. Wilson, Jr., A.P. Sattelberger and J.C. Huffman, *J.Am.Chem. Soc.*, 1982, 104, 858.

64. F.A. Cotton and W.T. Hall, *J.Am.Chem.Soc.*, 1979, 101, 5094.

65. F.A. Cotton and W.T. Hall, *Inorg.Chem.*, 1980, 19, 2352.

66. P. Meakin, L.J. Guggenberger, F.N. Tebbe and J.P. Jesson, *Inorg. Chem.*, 1974, 13, 1025.

67. F.G.N. Cloke, P.J. Fyne, V.C. Gibson, M.L.H. Green, M.J. Ledoux, R.N. Perutz, A. Dix, A. Gourdon and K. Prout, *J.Organometallic Chem.*, 1984, 277, 61.

68. V.C. Gibson, P.D. Grebenik and M.L.H. Green, *J.C.S. Chem Commun.*, 1983, 1101.

69. V.C. Gibson, T.P. Kee and W. Clegg, *J.Organometallic Chem.*, 1988, 353, C23.

70. F.A. Cotton, L.R. Favello and R.C. Najjar, *Inorg. Chem.*, 1983, 22, 375.

CHAPTER THREE

CHARACTERISATION OF RING AND PHOSPHINE-METALLATED ISOMERS OF $(\eta^5\text{-}C_5Me_5)Ta(PMe_3)_2$: COMPETITIVE LIGAND C-H BOND ACTIVATIONS.

3.1 INTRODUCTION

The studies presented in Chapter 2 provided a convenient entry into half-sandwich halide derivatives of tantalum. It was envisaged that the removal of all attendant halide ligands and stabilisation of a compound of general formula $(\eta^5\text{-}C_5R_5)Ta(PMe_3)_n$ (R = H, Me; $n \leq 4$), would provide a most highly reactive and synthetically useful synthetic precursor to half-sandwich derivatives in which some or all of the phosphine ligands are displaced. Isolation of the 18-electron tetrakis-PMe_3 derivative (n=4) was considered unlikely for steric reasons, a more reasonable outcome being metallation reactions involving either the phosphine or ring methyls (Scheme 3.1).

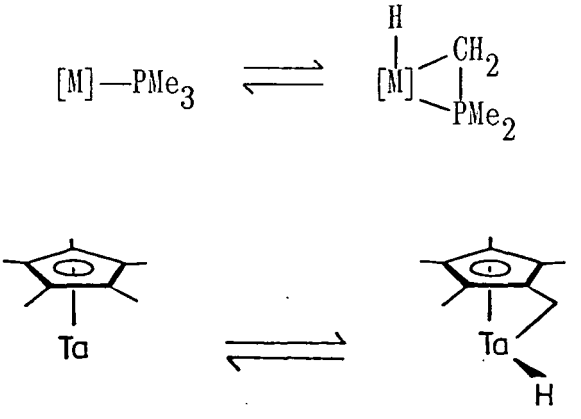

Scheme 3.1

However, since there is considerable precedence for both the reversibility of the above processes (see, for example, Chapter 1, section 1.4.4) and the lability of the PMe_3 ligands in phosphine rich compounds[1], we did not envisage metallation to be problematical.

In this chapter we describe studies culminating in the characterisation of two isomeric complexes with the empirical formula, $Cp^*Ta(PMe_3)_2$ in which, as anticipated, ligand metallation processes are favoured. Moreover, the two isomers reflect the two forms of ligand

metallation illustrated in Scheme 3.1, such that judicious modification of the reaction conditions allow both ring metallated and phosphine metallated isomers to be synthesised selectively and in good yield.

3.2 THE REACTION OF $CpTaCl_4$ WITH SODIUM IN PURE TRIMETHYLPHOSPHINE

The complete dehalogenation of transition metal halides by sodium metal in pure PMe_3 has been shown to facilitate the synthesis of low valent, PMe_3-rich complexes[1].

Thus, the reaction of $CpTaCl_4$ with excess sodium sand in neat PMe_3 solvent, proceeded smoothly over the course of 2 days at room temperature to afford a brown PMe_3 solution. Removal of unreacted PMe_3 by reduced pressure distillation into a receiving vessel, followed by extraction of the residue into light petroleum ether produced a deep red-orange solution. Concentration and cooling of this solution to -35^oC afforded a small crop of orange crystals. Infrared and NMR spectroscopies facilitated the characterisation of this compound as $Cp_2Ta(H)(PMe_3)$ (1). In particular, an absorption at 1700 cm^{-1} in the Nujol mull IR spectrum is assignable to a metal hydride stretching vibration, which compares well with analogous niobium and tantalum derivatives (Table 3.1).

Furthermore, the 250 MHz ^1H NMR spectrum (d^6-benzene) reveals the equivalent cyclopentadienyl hydrogens as a singlet at 4.39 ppm. A doublet resonance at 1.07 ppm ($^2J(PH)$=7.0 Hz) is assignable to the hydrogens of a single coordinated PMe_3 ligand. Most characteristic, however, is the low frequency-shifted resonance of the metal hydride ligand at -9.39 ppm ($^2J(PH)$=20.8 Hz) (Table 3.1). Finally, a single resonance is found at -25.60 ppm in the $^{31}P\{^1H\}$ NMR spectrum (d^6-

benzene).

COMPLEX	ν(M-H) cm^{-1}	δ(M-H) *ppm*	^{2}J(PH) *Hz*	REF
$Cp_2Ta(H)(PMe_3)$	1700	-9.39	20.8	#
$Cp_2Ta(H)(PEt_3)$	1705	-9.54	21	2
$Cp_2Nb(H)(PMe_3)$	1635	-7.84	27	2
$Cp_2Nb(H)(PEt_3)$	1650	-7.69	29	2
$Cp_2Nb(H)(PMe_2Ph)$		-7.53	28.6	3
$Cp_2Nb(H)(PPh_3)$		-6.65	27.0	4
$Cp_2Nb(H)(PMePh_2)$		-7.70	29	5

Table 3.1 *Spectroscopic Parameters for Compounds $Cp_2M(H)(PR_3)$; #=This Work.*

The crude product from the above reaction was found to comprise two additional Cp-containing products, although attempts at separation by fractional crystallisation proved unsuccessful. One of the products exhibits resonances in the ^{1}H NMR spectrum (d^6-benzene) at 0.44, -0.48 and -3.02 ppm, consistent with the presence of a metallated PMe_3 ligand (Figure 3.1).

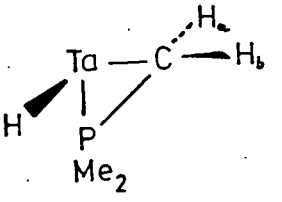

Figure 3.1

The signal at -3.02 ppm may be assigned to the metal bound hydride ligand and the two remaining signals to the diastereotopic methylene hydrogens H_a and H_b. This assignment is supported by analogy with the metal bound methylene shifts found in $W(H)(\eta^2\text{-}CH_2PMe_2)(PMe_3)_4$ (0.43 ppm) and $Ta(PMe_3)_3(\eta^2\text{-}CH_2PMe_2)(\eta^2\text{-}CHPMe_2)$ (-0.87 ppm)[1]. Furthermore the

$^{31}P\{^{1}H\}$ NMR spectrum of the crude product mixture displayed a triplet resonance at -69.51 ppm ($^{2}J(PP)$=27.5 Hz), consistent with the presence of a three-membered metallaheterocycle [*cf.* $W(H)(\eta^{2}\text{-}CH_2PMe_2)(PMe_3)_4$[1] (-80.30 ppm); $Os(H)(\eta^{2}\text{-}CH_2PMe_2)(PMe_3)_3$[6] (-71.43 ppm) and $Re(\eta^{2}\text{-}CH_2PMe_2)(PMe_3)_4$[7] (-73.6 ppm)].

SHIFT (ppm)	REL.INT	MULT.	J (Hz)	ASSIGNMENT
4.40	5	s	---	$C_5\underline{H}_5$
1.82	3	d	$^{2}J(PH)$=9.3	$P\underline{Me}_2$
1.46	3	d	$^{2}J(PH)$=8.0	$P\underline{Me}_2$
1.07	9	d	$^{2}J(PH)$=6.9	$P\underline{Me}_3$
1.05	9	d	$^{2}J(PH)$=5.7	$P\underline{Me}_3$
0.44	1	m	---	$C\underline{H}_2$
-0.48	1	m	---	$C\underline{H}_2$
-3.02	1	m	---	M-$\underline{H}$

Table 3.2 *^{1}H NMR Data For (2) (250 MHz, d^{6}-benzene).*

The ^{1}H NMR data for this complex are reproduced in Table 3.2 and are consistent with the formula, $CpTa(PMe_3)_2(H)(\eta^{2}\text{-}CH_2PMe_2)$ (2). Although the available data do not permit distinction between the various possible isomers, a full NMR study on an analogue, $Cp^{*}Ta(dmpe)(H)(\eta^{2}\text{-}CH_2PMe_2)$, is presented in Chapter 4, which indicates it to have the structure illustrated in Figure 3.2. (2) is presumed to be isostructural.

The nature of the third ($\eta^{5}\text{-}C_5H_5$) component in the reaction mixture remains unclear. A singlet ($\eta^{5}\text{-}C_5\underline{H}_5$) resonance is found at 4.22 ppm and a broad signal at *ca.* 1.35 ppm may be assigned to coordinated PMe_3 ligands. Furthermore a broad, unresolved signal at -0.69 ppm remains unassigned.

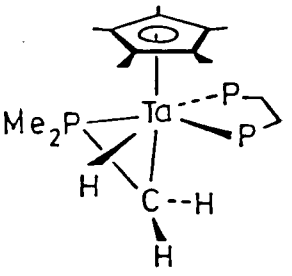

Figure 3.2

Although the reaction described above produces a mixture of products, it is of interest to note that a Cp-ring transfer must have occurred to form (1). Such a process is not common but has been reported on one occasion for tantalum (Equation 3.1)[8], and has also been observed in vanadium systems[9].

$$CpTaCl_4 \xrightarrow[2.\ EtOH]{1.EtAlCl_2/Toluene} Cp_2TaCl_2 \qquad (3.1)$$

In the sodium metal/pure PMe_3 reaction it is probable that the sequence of one-electron redox reactions proceeds initially according to Scheme 3.2.

$$CpTaCl_4 \xrightarrow{PMe_3} CpTaCl_4.PMe_3 \xrightarrow[e^-]{PMe_3} CpTaCl_3.PMe_3 \xrightarrow{PMe_3;\ e^-} CpTaCl_2(PMe_3)_3$$

Scheme 3.2

That these compounds are indeed intermediates in the reaction is supported by the treatment of pure samples of each with sodium metal and pure PMe_3; in each case the same product mixture was obtained, identical to that produced with $CpTaCl_4$.

Therefore, as $CpTaCl_2(PMe_3)_3$ is an electronically saturated monomer, cyclopentadiene transfer presumably occurs *via* reduction of $CpTaCl_2(PMe_3)_3$ in which Cp displacement is competitive with chloride loss. Formation of NaCp which would then be capable of reacting with earlier intermediates to generate a bis(cyclopentadienyl) system is not unreasonable. Independent evidence for the feasibility of this is provided by the preparation of $Cp^*_2TaCl_2$ from $Cp^*TaCl_3.PMe_3$ (Equation 3.2)[10].

$$Cp^*TaCl_3.PMe_3 \xrightarrow[100^0C;\ 24h]{KCp^*/Toluene} Cp^*_2TaCl_2 \qquad (3.2)$$

The formation of $CpTa(PMe_3)_2(H)(\eta^2\text{-}CH_2PMe_2)$ (2) from $CpTaCl_2(PMe_3)_3$ may then result from competitive chloride rather than Cp displacement. A reasonable pathway is illustrated in Scheme 3.3.

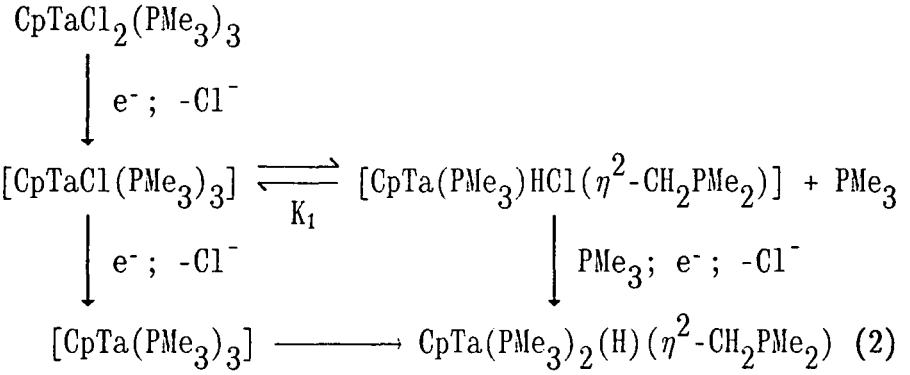

Scheme 3.3

In pure PMe_3 solvent, equilibrium K_1 should lie predominantly to the left-hand side.

Thus, although the reduction of $CpTaCl_4$ in pure PMe_3 afforded a mixture of products, it did produce a compound of empirical formula, $CpTa(PMe_3)_3$ in which phosphine metallation had occurred. Encouraged by these observations it was considered desirable to extend this synthetic strategy to the analogous pentamethylcyclopentadienyl system.

3.3 THE REACTION OF Cp^*TaCl_4 WITH SODIUM IN PURE TRIMETHYLPHOSPHINE: PREPARATION OF $Cp^*Ta(PMe_3)(H)_2(\eta^2\text{-}CHPMe_2)$ (3).

The dehalogenation of Cp^*TaCl_4 with sodium sand in pure PMe_3 solvent proceeded slowly over the course of 4 days at room temperature to afford a dark brown PMe_3 solution. Vacuum distillation of the unreacted PMe_3 into a receiving vessel followed by extraction of the crude residue with petroleum ether afforded an orange solution from which off-white crystals were obtained upon concentration and cooling to -78^oC. Purification of this crude product was achieved by vacuum sublimation at 75-80^oC (5×10^{-3} Torr), affording a white crystalline solid (3). Elemental analysis was consistent with a stoichiometry of $C_{16}H_{33}P_2Ta$:

Found (Required): %C, 40.94 (41.03); %H, 7.15 (7.12)

suggesting (3) to possess the empirical formula, $Cp^*Ta(PMe_3)_2$. This assignment was further corroborated by the low resolution mass spectrum which revealed a parent ion peak at m/e 468 with additional fragments at m/e 466 $[M\text{-}2H]^+$, 390 $[M\text{-}2H\text{-}PMe_3]^+$ and 374 $[M\text{-}2H\text{-}PMe_3\text{-}CH_4]$ respectively.

However, if the ligands are assumed to coordinate in classical fashion, the above empirical formula would allow the metal only 14 valence electrons and would be consequently highly coordinatively unsaturated. Such a complex would be expected to be unstable under ambient conditions.

The first indication that the structure of compound (3) is of a more complex nature was provided by infrared spectroscopy. The Nujol mull spectrum revealed strong, broad bands at 1710 and 1650 cm^{-1} which may be assigned to metal-bound hydride ligands, as well as bands at 962 cm^{-1} and 925 cm^{-1} attributable to the $\rho(CH_3)$ modes of coordinated PMe_3

groups[11].

An X-ray structural determination on a single crystal of (3) confirmed that activation of C-H bonds had occurred but had not resulted in the $MH(\eta^2\text{-}CH_2PMe_2)$ moiety. Rather a double metallation had taken place, with the metal inserting into two C-H bonds of a metal-bound PMe_3 methyl substituent to give the $TaH_2(\eta^2\text{-}CHPMe_2)$ moiety (Equation 3.3).

$$M\text{-}PMe_3 \rightleftharpoons MH(\eta^2\text{-}CH_2PMe_2) \rightleftharpoons MH_2(\eta^2\text{-}CHPMe_2) \quad (3.3)$$

A full description of the molecular structure of (3) is presented in the following section.

3.4 THE MOLECULAR STRUCTURE OF $Cp^*Ta(PMe_3)(H)_2(\eta^2\text{-}CHPMe_2)$ (3).

Colourless crystals of (3) were obtained by slow cooling of a saturated petroleum ether (40-60°C) solution to *ca.* -60°C. Crystal data were collected and analysed by Dr. W. Clegg at the University of Newcastle Upon Tyne, and are summarised in Appendix 1C. The molecular structure is illustrated in Figures 3.3 and 3.4, and selected bond distances and angles are displayed in Table 3.3.

Analysis of the crystallographic data reveals η^5-coordination of the C_5Me_5 ligand with a plane of symmetry passing through the ring centroid (RC) and atoms C(23),P(1) and P(2) (rms deviation = 0.005Å). The tantalum atom lies only 0.015Å out of this plane. Figure 3.4 illustrates the pseudo mirror symmetry of the molecule.

Unfortunately the metal hydride and metallacycle hydrogens were not detected in the crystal structure determination, but the presence of a single hydrogen on C(23) and two equivalent metal hydride ligands has been confirmed by NMR spectroscopy (*vide infra*). On the basis of these

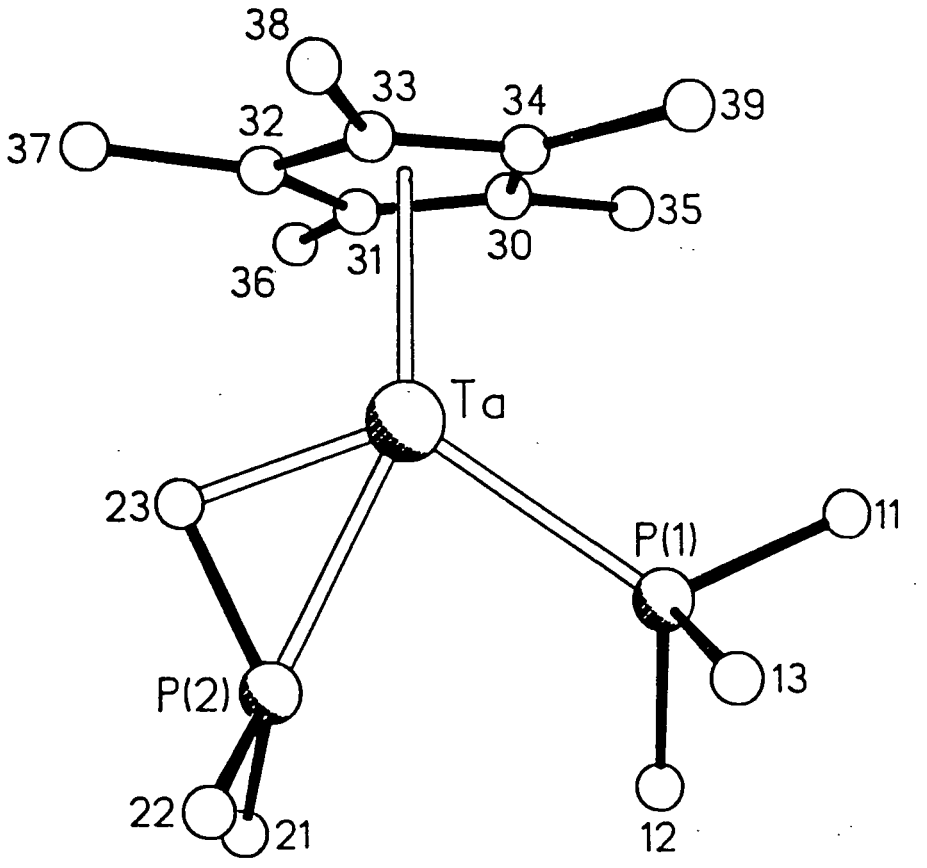

Figure 3.3 *The Molecular Structure of* $Cp^*Ta(PMe_3)(H)_2(\eta^2\text{-}CHPMe_2)$.

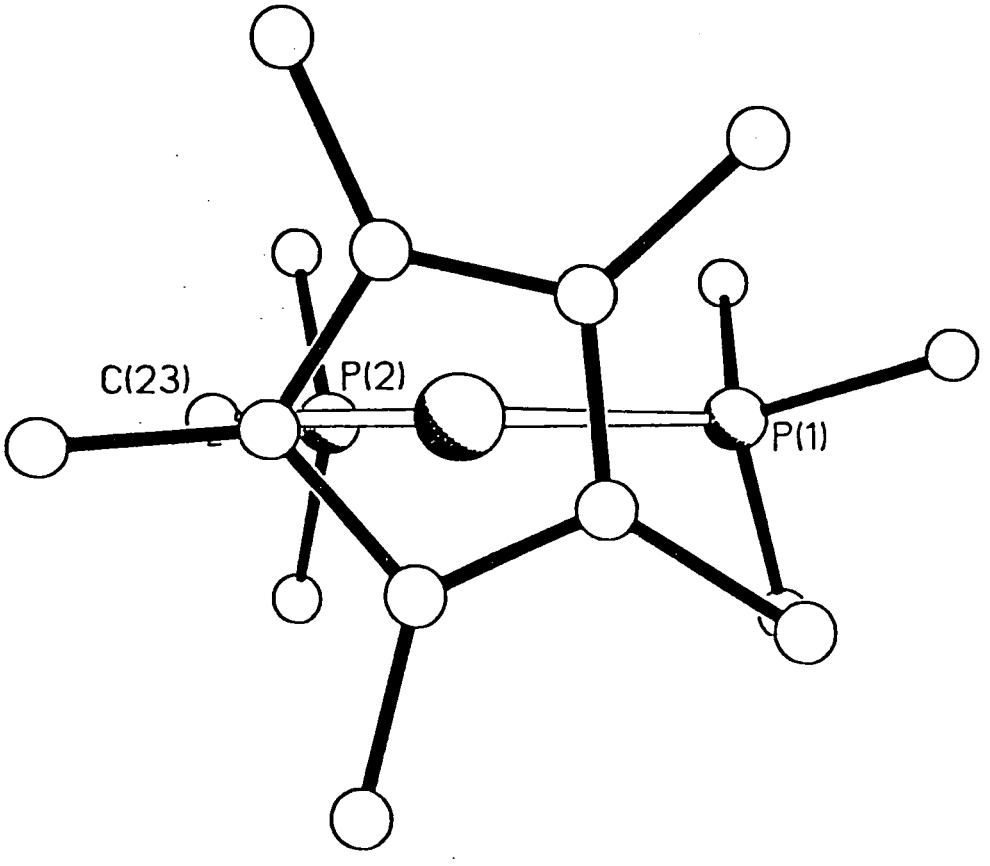

Figure 3.4 *View down the* $C_5Me_5\text{-}Ta$ *Vector of* $Cp^*Ta(PMe_3)(H)_2(\eta^2\text{-}CHPMe_2)$.

Ta-P(1)	2.590(3)	P(1)-Ta-P(2)	82.3(1)
Ta-P(2)	2.480(2)		
		P(1)-Ta-C(23)	125.6(3)
Ta-C(23)	2.005(10)	P(1)-Ta-C(30)	101.3(2)
Ta-C(30)	2.446(8)	P(2)-Ta-C(23)	43.4(3)
Ta-C(31)	2.405(7)		
Ta-C(32)	2.436(8)	Ta-P(1)-C(11)	118.7(4)
		Ta-P(1)-C(12)	116.3(4)
Ta-C(33)	2.412(7)	Ta-P(1)-C(13)	116.6(5)
Ta-C(34)	2.444(8)	Ta-P(2)-C(21)	125.9(4)
		Ta-P(2)-C(22)	126.5(4)
P(1)-C(11)	1.850(14)	Ta-P(2)-C(23)	53.4(3)
P(1)-C(12)	1.860(15)		
P(1)-C(13)	1.828(16)	C(11)-P(1)-C(12)	98.6(6)
P(2)-C(21)	1.860(13)	C(11)-P(1)-C(13)	101.5(6)
P(2)-C(22)	1.851(13)	C(12)-P(1)-C(13)	102.1(7)
P(2)-C(23)	1.714(9)	C(21)-P(2)-C(22)	106.6(6)
		C(21)-P(2)-C(23)	115.3(5)
C(30)-C(31)	1.390(12)	C(22)-P(2)-C(23)	115.1(6)
C(30)-C(34)	1.455(13)		
C(30)-C(35)	1.519(15)	Ta-C(23)-P(2)	83.2(4)
C(31)-C(32)	1.422(14)		
C(31)-C(36)	1.511(14)	X-Ta-P(1)	124.6
C(32)-C(33)	1.462(14)	X-Ta-P(2)	153.1
C(32)-C(37)	1.510(14)	X-Ta-C(23)	109.7
C(33)-C(34)	1.390(13)		
C(33)-C(38)	1.492(13)	Y-C(30)-C(35)	5.0
C(34)-C(39)	1.523(14)	Y-C(31)-C(36)	2.3
		Y-C(32)-C(37)	7.7
X-Ta	2.105	Y-C(33)-C(38)	4.3
		Y-C(34)-C(39)	3.6

Table 3.3 *Bond Lengths (Å) and Angles (°) for Cp*Ta(PMe_3)-$(H)_2(\eta^2$-$CHPMe_2)$ (3) [X=Centre of Cp* ring; Y=best plane through Cp* ring].*

observations, the established geometry of the other ligands around the metal centre, and consideration of the remaining available space, we favour placement of the two hydride ligands either side of the pseudo mirror plane as represented in Figure 3.5.

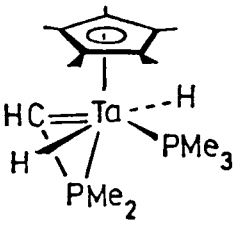

Figure 3.5 *Representation of the Structure of* $Cp^*Ta(PMe_3)(H)_2(\eta^2\text{-}CHPMe_2)$.

A consideration of the η^5-C_5Me_5 ring shows it to be unexceptional, with average values for inter-ring carbon-carbon, ring carbon-ring methyl and ring carbon-tantalum distances of 1.424(15)Å, 1.511(5)Å and 2.429(8)Å respectively, which are within the ranges found for other Cp^*Ta complexes[12]. As observed in other (η^5-C_5R_5) complexes, there is a degree of asymmetry in the inter-ring carbon distances (see Chapter 2, sections 2.3 and 2.5). The C(30)-C(31) [1.390(12)Å] and C(33)-C(34) [1.390(13)Å] bond lengths are somewhat shorter than the others [average = 1.446(12)Å] suggesting a predominant diene-like bonding interaction. This type of cyclopentadienyl bonding mode has been found in 18-electron systems of the form (η^5-C_5R_5)ML_2, where, depending on the orientation of the [ML_2] fragment with respect to the ring, the (η^5-C_5R_5) bonding may possess either allyl-ene or diene character, mirroring the nodal characteristics of the C_5R_5 HOMO, as illustrated in Figure 3.6. An example of each bonding type is provided by (η^5-C_5Me_5)$Co(CO)_2$[13] (allyl-ene) and (η^5-C_5Cl_5)Rh(1,5-C_8H_{12})[14] (diene).

(a) Diene-like (b) Allyl-ene like

Figure 3.6 *Modes of C_5R_5 Bonding in $(\eta^5\text{-}C_5R_5)ML_2$ Complexes*

The Ta-P(1) bond length of 2.590(3)Å is within the range of Ta(V)-PMe_3 distances previously observed (*ca.* 2.51-2.60Å)[15], and the carbon-phosphorus-carbon angles average 101°, significantly lower than the tetrahedral value of 109.5°. The orientation of the PMe_3 ligand methyls can be seen from Figure 3.4 to be staggered with respect to the (η^5-C_5Me_5) methyls, presumably to reduce close contacts.

The metallaheterocycle represents a most interesting feature of the structure. To date, this type of ligand has been observed exclusively in tantalum complexes, for example, $Ta(PMe_3)_3(\eta^2\text{-}CH_2PMe_2)(\eta^2\text{-}CHPMe_2)$[1], $Ta(\eta^2\text{-}CHPMe_2)(PMe_3)_4Cl$[16], $Ta(\eta\text{-}C_4H_6)(\eta^2\text{-}CHPMe_2)(PMe_3)_2Cl$[16] and $Ta(PMe_3)_2(H_2)(\eta^2\text{-}CH_2PMe_2)(\eta^2\text{-}CHPMe_2)$[16]. Two of these compounds have been studied by X-ray diffraction and a comparison of the metallacycle parameters to those of (3) and to the (η^2-CH_2PMe_2) metallacycle are informative.

A consideration of the data in Table 3.4 shows that the tantalum carbon distances are all shorter than those found for the Ta-C single bonds in the complexes of Table 3.5 and are more comparable to the Ta=C

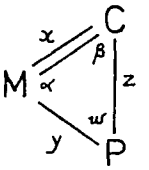

COMPLEX	x (Å)	y (Å)	z (Å)	α (^{o})	β (^{o})	ω (^{o})	REF
$Cp^*Ta(PMe_3)(H_2)(\eta^2\text{-}CHPMe_2)$	2.005(10)	2.480(2)	1.714(9)	43.4(3)	83.2(4)	53.4(3)	#
$Ta(PMe_3)_3(\eta^2\text{-}CH_2PMe_2)(\eta^2\text{-}CHPMe_2)$	2.015(4)	2.516(1)	1.716(5)	42.75(13)	84.39(19)	52.86(14)	1
$Ta(\eta\text{-}C_4H_6)(\eta^2\text{-}CHPMe_2)(PMe_3)_2Cl$	2.026(3)	2.495(1)	1.704(4)	42.72(10)	85.51(14)	53.77(12)	16

Table 3.4 *Comparison of (η^2-$CHPMe_2$) Metallacycles; # = This work.*

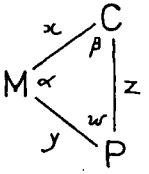

COMPLEX	x (Å)	y (Å)	z (Å)	α (^{o})	β (^{o})	ω (^{o})	REF
$Ta(PMe_3)_3(\eta^2\text{-}CH_2PMe_2)(\eta^2\text{-}CHPMe_2)$	2.324(4)	2.435(1)	1.776(5)	43.74(11)	71.46(15)	64.80(14)	1
$Re(\eta^2\text{-}CH_2PMe_2)(PMe_3)_4$	2.277(8)	2.332(2)	1.755(7)	44.8(2)	69.2(3)	66.0(3)	7
$IrCl_2(\eta^2\text{-}CH_2PMePh)(PMe_2Ph)_2$	2.19(2)	2.276(6)	1.90(3)	50.3(7)	67.2(10)	62.5(8)	17
$Pt[(\eta^2\text{-}CHPhP(CH_2Ph)_2]\text{-}(C_2B_{20}H_{20}Me)P(CH_2Ph)_3$	2.15(1)	2.235(4)	1.76(2)	47.3(4)	68.8(5)	63.9(4)	18
$Pt[(^nPr_3P)(\eta^2\text{-}CH(CH_2CH_3)PPr_2^n)]\text{-}2\text{-}C_6H_5\text{-}1,2\text{-}(O\text{-}B_{10}C_2H_{10})$	2.17(2)	2.202(5)	1.76(2)	---	---	---	19
$WH(\eta^2\text{-}CH_2PMe_2)(PMe_3)_4$	2.307(5)	2.375(1)	1.760(6)	44.14(15)	69.96(18)	65.90(18)	1

Table 3.5 *Comparison of (η^2-CH_2PR_2) Metallacycles.*

double bonds of electronically saturated alkylidene complexes (Table 3.6).

COMPLEX	Ta=C (Å)	Ta-C (Å)	∠TaCαCβ (°)	∠TaCαHα (°)	REF
$Cp_2Ta(CH_2)(CH_3)$	2.026(10)	2.246(12)	126(4)‡	126(4)	20
$Cp_2Ta(CHPh)(CH_2Ph)$	2.07(1)	2.30(1)	135.2(7)	---	21
$Cp_2Ta(CHCMe_3)Cl$	2.030(6)	---	150.4(5)	111(4)	22

Table 3.6 *Tantalum-Carbon Distances in Some 18-Electron Alkylidene Complexes; [‡In the (CH_2) ligand ∠TaCαCβ ≡ ∠TaCαHα].*

An important phenomenon has been recognised to operate in electronically unsaturated alkylidene complexes, which may have significant structural and spectroscopic implications for (3). Within the M=CH(R) moiety, a rehybridisation of the Cα atom occurs, resulting in an increased Ta-Cα-Cβ angle and a reduced Ta-Cα-Hα angle. This is illustrated schematically in Figure 3.7(b).

(a) (b)

Figure 3.7

Similar observations have been reported for electronically saturated complexes as in Table 3.6, and here, the reason is presumably due to unfavourable steric interactions between a Cp ring and the Cα-alkyl substituent[20-22]. It appears however, that in electronically unsaturated

complexes the reasons for distortion are primarily electronic[23] and reminiscent of the CH...M agostic interactions in electronically unsaturated alkyls. As the Ta-Cα-Cβ angle increases, so the alkylidene ligand more resembles a hydrogen-bridged alkylidyne and consequently the Ta-Cα distances are intermediate between those of saturated alkylidene (Table 3.6) and alkylidyne compounds (Table 3.7).

COMPLEX	Ta=C (Å)	∠TaCαCβ (^{0})	REF
$Cp^*Ta(PMe_3)(\eta^2\text{-}C_2H_4)(CHCMe_3)$	1.946(3)	170.0	15b
$Cp^*Ta(CH_2Ph)_2(CHPh)$	1.883(14)	166.0	23
$[Ta(CHCMe_3)Cl_3(PMe_3)]_2$	1.898(2)	161.2	15b
$Ta(MES)(PMe_3)_2(CHCMe_3)_2$	1.932(7)	168.90	15c
	1.955(7)	154.02	15c
$Ta(CH_2CMe_3)_3(CCMe_3)Li(DMP)$	1.76(2)	165	24
$Cp^*TaCl(PMe_3)_2(CPh)$	1.849(8)	171.8	15a

Table 3.7 *Parameters For Alkylidyne and Electronically Unsaturated Alkylidene Complexes; [MES = mesityl; DMP = 2,6-dimethylpiperazine].*

Thus the slightly shorter (Ta=C) distance in **(3)**, compared to those of saturated alkylidene complexes (Table 3.6) may be due to a rehybridisation of Cα upon coordination of the PMe_2 moiety to the metal centre (Figure 3.7a) thus increasing the TaCαHα angle and leading to a certain degree of Ta-C triple bond character in the $Ta(\eta^2\text{-}CHPMe_2)$ metallacycle (Hα was not located in the X-ray analysis but the TaCαHα angle is not anticipated to be too dissimilar to the corresponding angle of $145(3)^0$ found in $Ta(PMe_3)_3(\eta^2\text{-}CH_2PMe_2)(\eta^2\text{-}CHPMe_2)$[1]).

Consideration of the tantalum-phosphorus distances (y) in Table 3.4 shows them to be, in all cases, shorter by *ca.* 0.1Å than the Ta-PMe_3 distances in the same complex. This may reflect a change in phosphorus

hybridisation, increasing the % s-character in the (P-Ta) bond (Figure 3.3). Support for this is provided by the angles Ta-P(2)-C(21) (125.9(4)^{o}) and Ta-P(2)-C(22) (126.5(4)^{o}) being considerably larger than those for the Ta-PMe_3 ligand (average = 117.2^{o}) and by the fact that the dihedral angle between the planes defined by TaC(21)C(22) and P(2)C(21)C(22) is 6.2^{o}, whereas the analogous planes within the PMe_3 ligand are separated by 31.9^{o} (average).

A particularly notable facet of the (η^2-$CHPMe_2$) metallacycle is a significant shortening of the phosphorus-carbon distance (z) by *ca.* 0.1Å over P-C distances in normal coordinated PMe_3 ligands (1.82-1.86Å)[12]. For **(3)**, z = 1.714(9)Å and the average P-C distance around P(1) (Figure 3.3) is 1.850(16)Å. These results suggest a certain amount of phosphorus-carbon double bond character implying a significant contribution from canonical form II in which the $HC{=}PMe_2$ residue may be perceived as a coordinated λ^5-phosphaalkyne (Figure 3.8). Form (III) is a delocalised representation of the bonding reminiscent of a bridging carbyne ligand.

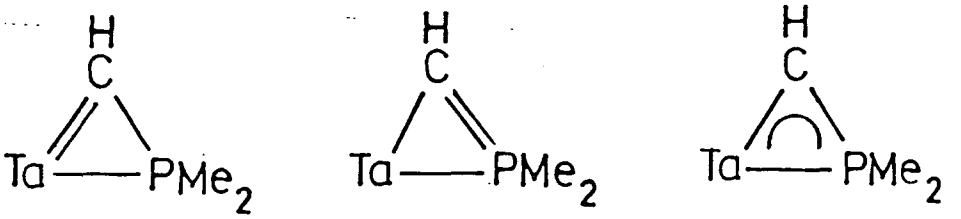

(I) (II) (III)

Figure 3.8 *Bonding Forms of* (η^2-$CHPMe_2$)

There has been much interest in the stabilisation of λ^5-phosphaalkynes and this has recently been achieved by thermolysis of substituted diazomethanes (Equation 3.4).

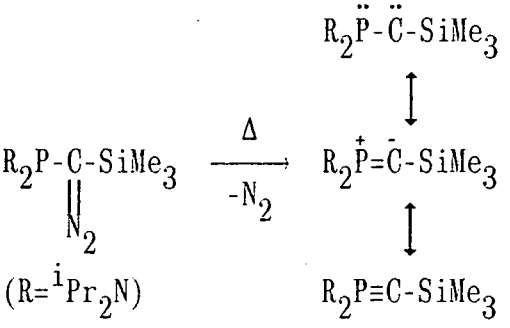

(3.4)

The chemical reactivity of the λ^5-phosphaalkyne mirrors the canonical forms above in that both cycloaddition and carbene reactions are possible[26]. A related tungsten carbene metallacycle has been prepared according to Scheme 3.4[25].

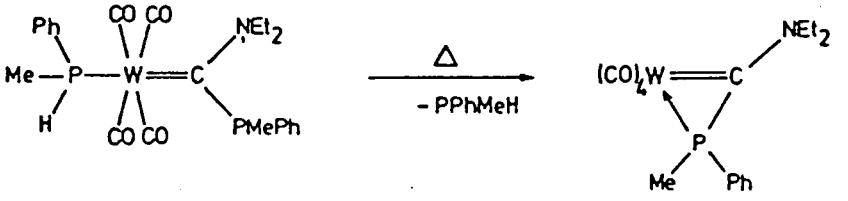

Scheme 3.4

The presence of a short C-N bond was interpreted in terms of electron delocalisation through the amino group as indicated in Figure 3.9.

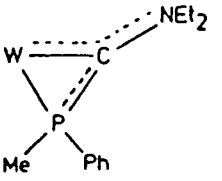

Figure 3.9

3.5 THE NMR SPECTROSCOPY OF $Cp^*Ta(PMe_3)(H)_2(\eta^2\text{-}CHPMe_2)$ (3)

The NMR data for (3) can be interpreted on the basis of the core solid state structure persisting in solution. The 250 MHz, ^1H NMR spectrum (d^6-benzene) of (3) is reproduced in Figure 3.10. The equivalent (η^5-C_5Me_5) hydrogens are found to resonate at 2.18 ppm. Two distinct resonances, attributable to the hydrogens of phosphorus methyls, are observed at 1.44 ppm ($^2J(P_2H)$=10.2 Hz) and 1.41 ppm ($^2J(P_1H)$=6.4 Hz) in the ratio 2:3 consistent with PMe_2 and PMe_3 moieties respectively. In the room temperature ^1H NMR spectrum (d^6-benzene) these signals are not completely resolved but become so upon resolution enhancement (Figure 3.10) which also appears to resolve secondary coupling of the PMe_3 hydrogens to P(2) (see Figure 3.3).

Interestingly, the $^2J(P_2H)$ value is significantly larger than that usually observed for a normal PMe_3 ligand, providing further support for rehybridisation at the P_2 phosphorus leading to increased s-character in the Ta-P and PMe_2 bonds. The equivalent metal hydride ligands occur as a doublet of doublets resonance at 3.87 ppm with couplings to both phosphorus nuclei ($^2J(PH)$=17.9 Hz and 54.9 Hz). Selective ^{31}P-decoupling experiments (*vide infra*) have allowed the assignment of these couplings to P_2 and P_1 respectively. The occurrence of the metal hydride resonance to high frequency of tetramethylsilane is not unusual for Ta(V), d^0 complexes [see for example: $Cp^*TaHCl(PMe_3)(CHCMe_3)$ (7.53 ppm)[27], $Cp^*Ta(PMe_3)_2H_4$ (1.08 ppm)[12], $TaHCl_2(PMe_3)_3(CHCMe_3)$ (10.00 ppm)[27] and $Cp^*_2Ta(CH_2)(H)$ (1.75 ppm)[28]]. The CHα hydrogen is located at 9.13 ppm which is not unusual for electronically saturated alkylidene CHα hydrogens[20-22]. For electronically saturated compounds containing the (η^2-$CHPMe_2$) moiety, the CHα signal is found over a range of *ca.* 1.4 ppm (Table 3.8).

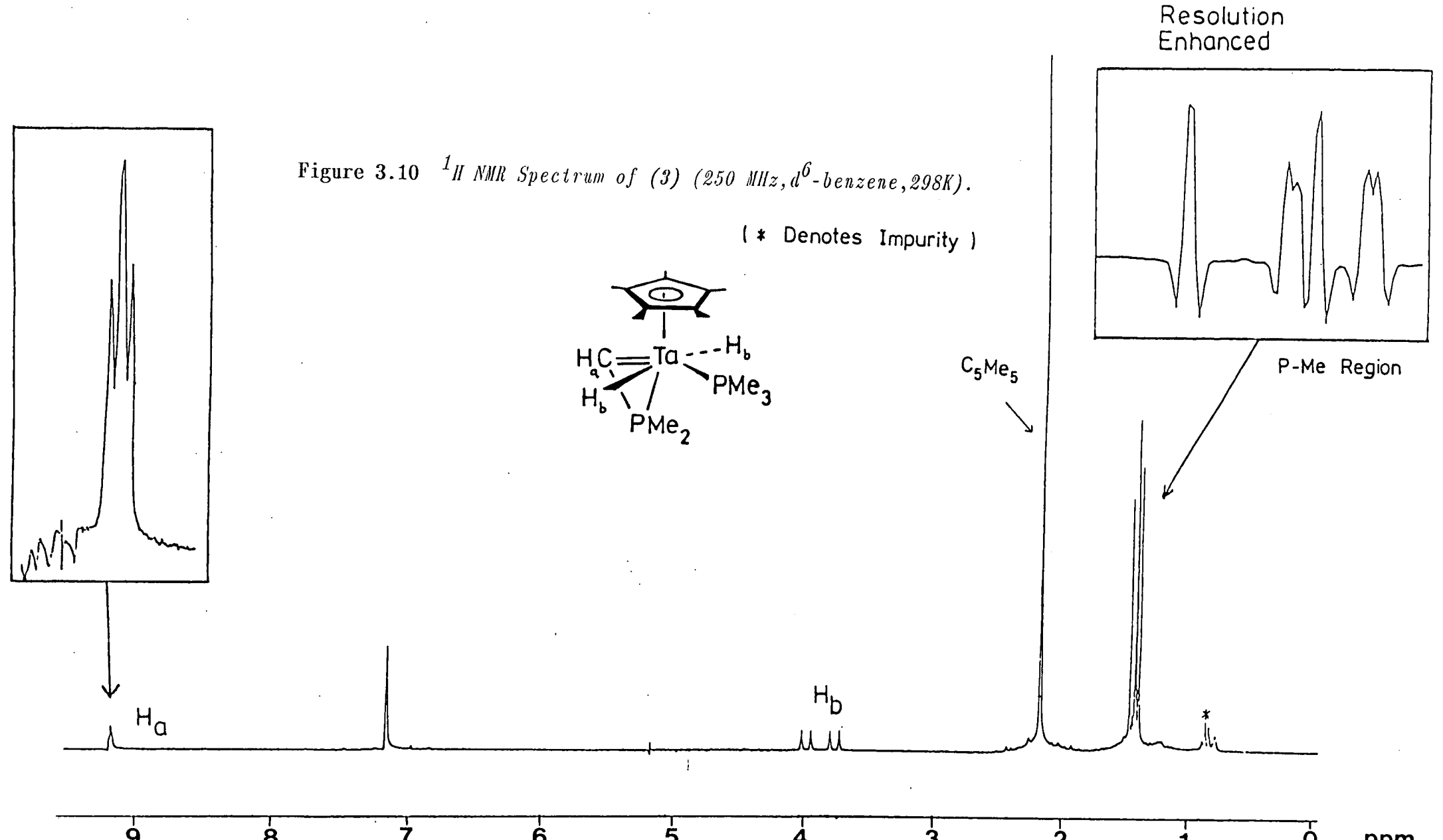

Figure 3.10 *^{1}H NMR Spectrum of (3) (250 MHz, d^6-benzene, 298K).*

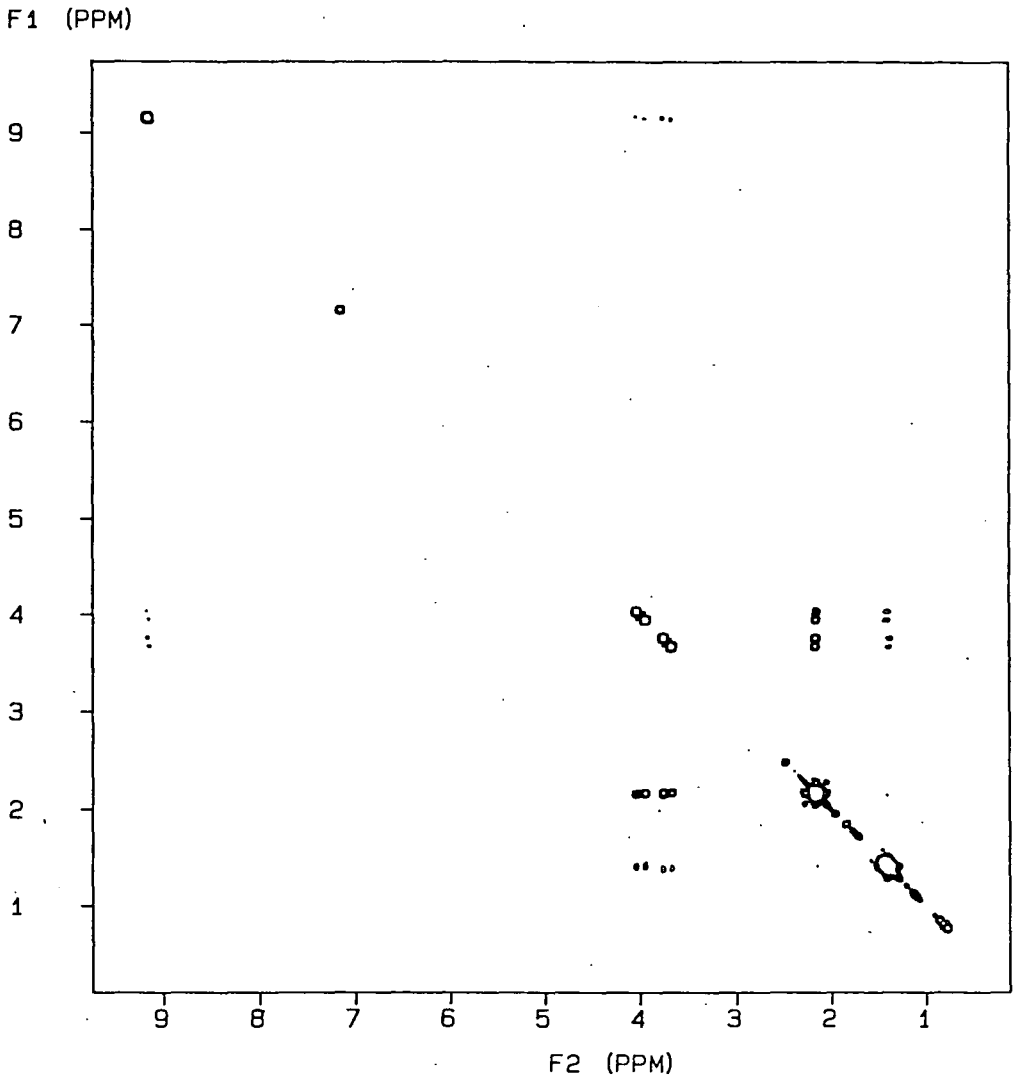

Figure 3.11 *COSY 2D ^{1}H NMR Spectrum of (3) (250 MHz, d^{6}-benzene, 298K).*

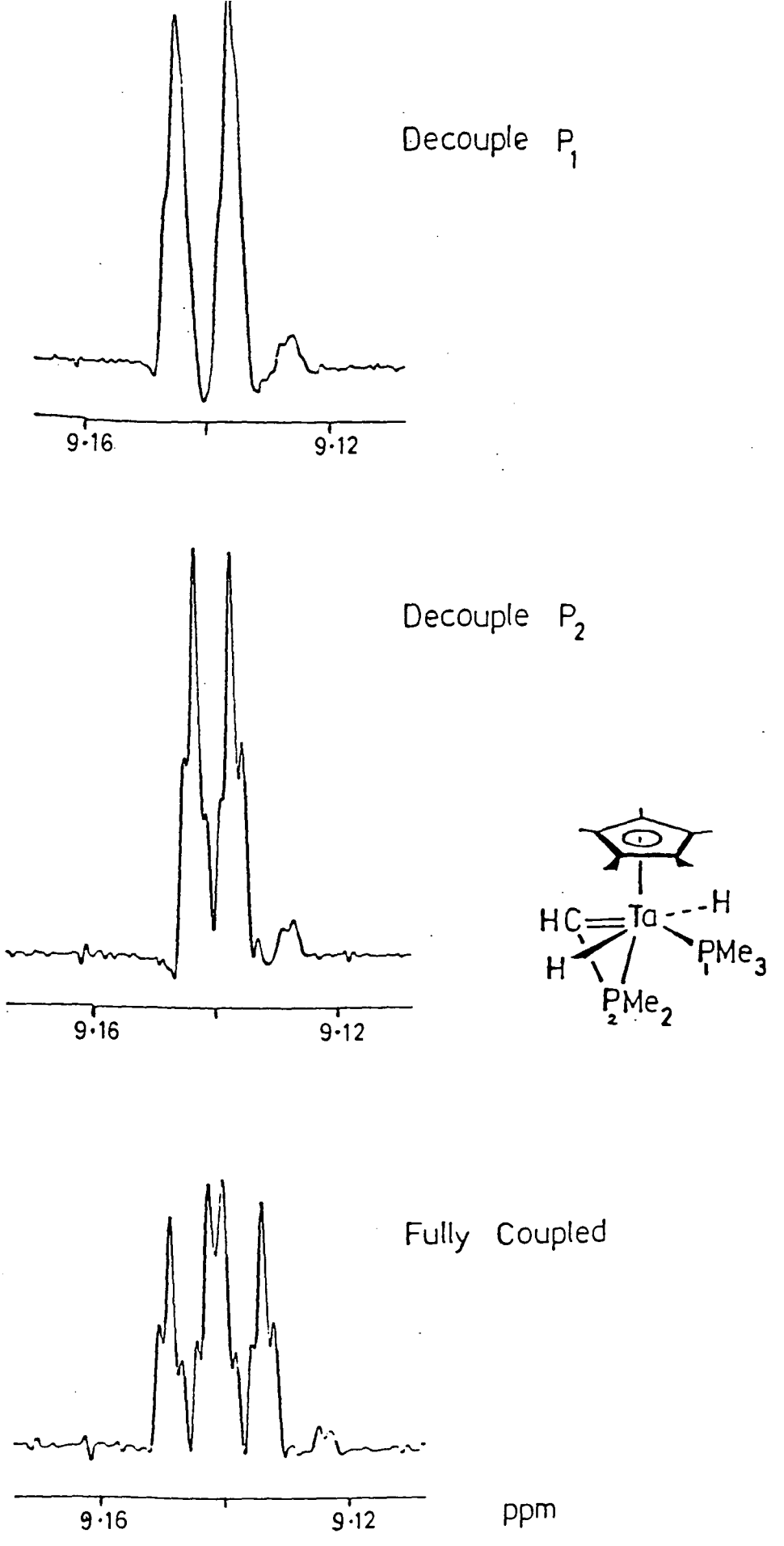

Figure 3.12 *Methine Hydrogen resonances at 360 MHz.*

COMPLEX	δ(CαH) (ppm)	δ ^{31}P (cycle)	δ ^{13}C (cycle)	^{1}J(CHα) (Hz)	REF
$Cp^*Ta(PMe_3)(H)_2(\eta^2\text{-}CHPMe_2)$	9.13	-112.35	192.07	171.0	#
$Ta(PMe_3)_3(\eta^2\text{-}CH_2PMe_2)(\eta^2\text{-}CHPMe_2)$	9.46	-135.31	193.51	---	1
$Ta(H)_2(PMe_3)_2(\eta^2\text{-}CH_2PMe_2)$-$(\eta^2\text{-}CHPMe_2)$	8.10	-124.0	170	---	16
$Ta(\eta\text{-}C_4H_6)(\eta^2\text{-}CHPMe_2)(PMe_3)_2Cl$	8.85	-118.2	173.1	158	16
$Ta(\eta^2\text{-}CHPMe_2)(PMe_3)_4Cl$	9.56	-139.6	187.8	161	16

Table 3.8 *Spectroscopic Parameters For (η^2-CHPMe$_2$) Compounds; [#This Work].*

At 250 MHz, the CHα resonance is an apparent triplet, presumably due to couplings of similar magnitude to both phosphorus nuclei. The presence of additional coupling to the equivalent hydride ligands was inferred from a COSY 2-D experiment (Figure 3.11), which also highlighted unresolved couplings of the hydrides to both the (η^5-C_5Me_5) hydrogens and phosphorus methyl hydrogens. In an attempt to further resolve the CHα resonance, a ^{1}H-NMR spectrum was recorded at 360 MHz, whereupon a doublet of doublet of triplets pattern was clearly discernable (Figure 3.12). The coupling constants have been assigned by selective ^{31}P-decoupling experiments. At this frequency, the signal for the PMe_3 hydrogens is clearly shown as a doublet of doublets with the smaller coupling arising due to long range ^{31}P coupling to the metallacycle phosphorus (confirmed by selective decoupling). The full ^{1}H-NMR data for $Cp^*Ta(PMe_3)(H)_2(\eta^2\text{-}CHPMe_2)$ (3) is presented in Table 3.9. The $^{31}P\{^{1}H\}$ NMR spectrum consists of two doublets, with ^{2}J(PP)=57.2 Hz. The PMe_3 phosphorus nucleus resonates at -24.88 ppm, within the usual range for PMe_3 coordinated to tantalum (typically *ca.* 20 to -40 ppm). The phosphorus nucleus (P_2) of the metallacycle, however, exhibits a significant low frequency shift (-112.35 ppm).

SHIFT (ppm)	REL.INT	MULT.	J (Hz)	ASSIGNMENT
9.13	1	ddt	$^2J(P_2H)$=3.3 $^3J(P_1H)$=2.2 J(HH) =0.7	M=C-H
3.87	2	dd	$^2J(P_2H)$=17.9 $^2J(P_1H)$=54.9	M-H
2.18	15	s	---	C_5Me_5
1.44	6	d	$^2J(P_2H)$=10.2	P_2Me_2
1.41	9	dd	$^2J(P_1H)$=6.4 $^4J(P_2H)$=0.7	P_1Me_3

Table 3.9 *^1H NMR Data For (3) (360 MHz, d^6-benzene).*

Similar chemical shifts have been reported for the other complexes containing the (η^2-$CHPMe_2$) moiety (Table 3.8).

The $^{13}C\{^1H\}$-NMR spectrum (Figure 3.13) concurs with the ^1H and $^{31}P\{^1H\}$-NMR data, and is collected in Table 3.10. The notable feature of the spectrum is the high frequency signal found for the metallacyclic carbon, Cα (192.07 ppm), consistent with shifts noted for other (η^2-$CHPMe_2$) complexes (Table 3.8) and alkylidene carbons in general. A most likely explanation for such shifts is the magnetic anisotropy of the M=C bond, since M-C single bonds do not generally display high frequency resonances.

Also of interest is the value of $^1J(C\alpha H\alpha)$, being significantly larger than those of electronically saturated alkylidene complexes (*ca.* 120-130 Hz)[29] and somewhat higher than those of normal sp^2 hybridised C-H bonds (*ca.* 150-160 Hz)[30]. But it is comparable with reported $^1J(CH)$ values for bridging methylidyne ligands[31,32] (*cf.* bonding form III, Figure 3.8).

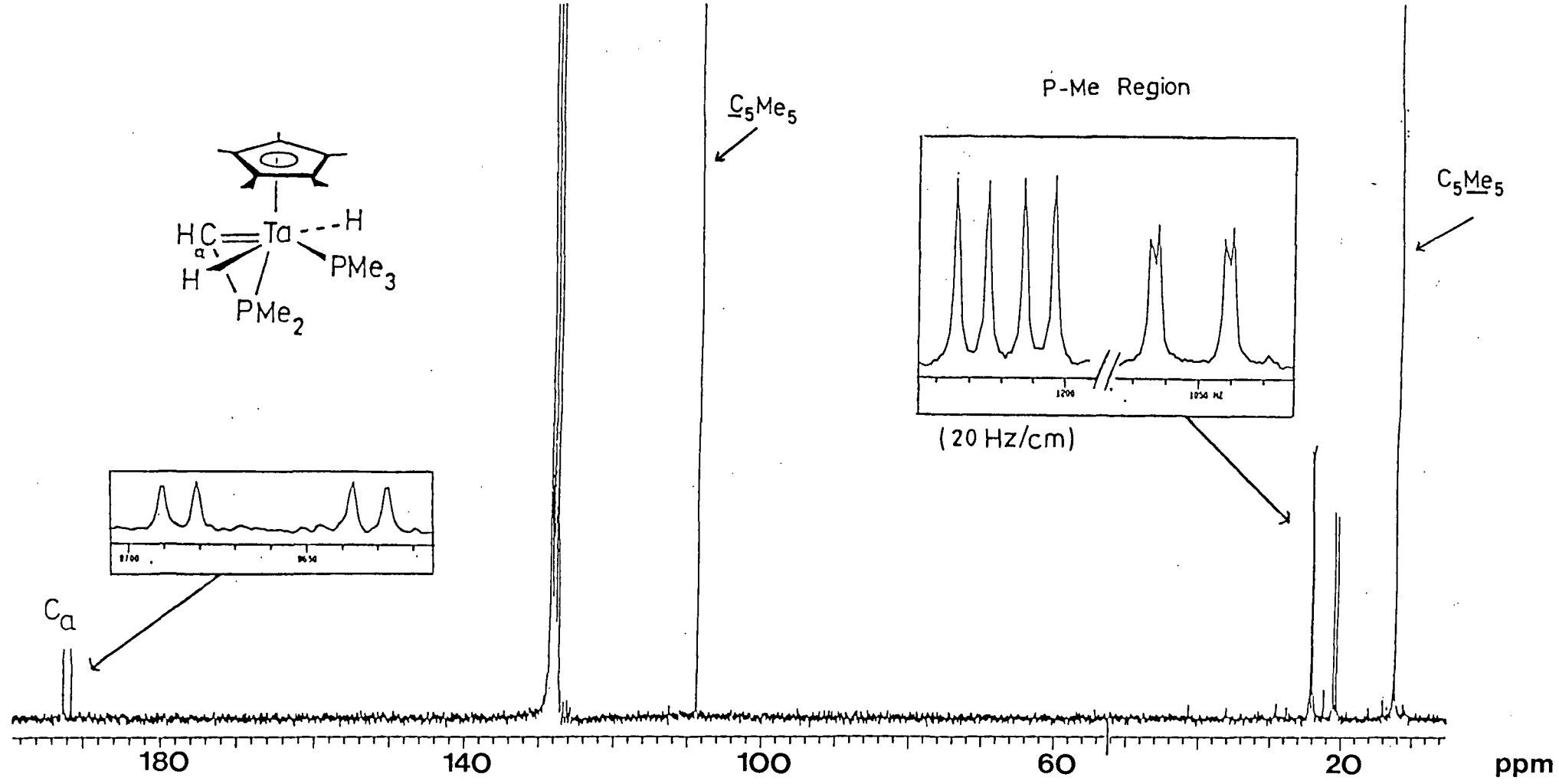

Figure 3.13 $^{13}C\{^{1}H\}$ *NMR Spectrum of (3) (50 MHz, d^6-benzene, 298K).*

SHIFT (ppm)	MULT.	J (Hz)	ASSIGNMENT
192.07	dd	$^1J(P_2C)$=53.2 $^2J(P_1C)$= 9.6 $^1J(C\alpha H\alpha)$=171.0‡	M=C-H
108.79	s	---	$\underline{C}_5Me_5$
24.24	dd	$^1J(P_1C)$=21.0 $^3J(P_2C)$= 9.6	$P(\underline{C}H_3)_3$
20.93	dd	$^1J(P_2C)$=22.8 $^3J(P_1C)$= 2.4	$P(\underline{C}H_3)_2$
12.57	s	---	$C_5\underline{Me}_5$

Table 3.10 *$^{13}C\{^1H\}$-NMR Data For (3) (d^6-benzene); [‡From fully coupled spectrum].*

3.6 THE REACTION OF Cp^*TaCl_4 WITH SODIUM AMALGAM IN THF IN THE PRESENCE OF PMe_3: PREPARATION OF $(\eta^7\text{-}C_5Me_3(CH_2)_2)Ta(H)_2(PMe_3)_2$ (4)

During the course of our studies on the reduction of Cp^*TaCl_4 with sodium sand in neat PMe_3, we became aware of a closely related reaction carried out in the laboratory of Prof. R.D. Sanner at Arizona State University. A compound of identical empirical formula had been isolated from the reduction of Cp^*TaCl_4 by sodium amalgam in THF solvent in the presence of PMe_3. However, preliminary X-ray data suggested that rather than activation of a PMe_3 ligand, cleavage of two ring-methyl C-H bonds had occurred to give a new ring system. Unfortunately, systematic flaws in the X-ray data prevented an accurate structure determination and the study had since been discontinued by the Arizona group. The relevance of this product to complex (3) led us to repeat this work and redetermine the X-ray structure in collaboration with the Arizona group.

Thus, the reaction of Cp^*TaCl_4 with four equivalents of sodium amalgam in THF solvent in the presence of five equivalents of PMe_3,

proceeded smoothly over 24 hrs. at room temperature to afford an orange-brown solution. Removal of the volatiles under reduced pressure, followed by recrystallisation of the residue from light petroleum ether, resulted in off-white crystals. Purification by slow vacuum sublimation at 75°C (5 x 10^{-3} Torr) afforded pure white crystalline (4). Elemental analysis was supportive of the stoichiometry, $C_{16}H_{33}P_2Ta$:

Found (Required): %C, 40.99 (41.03); %H, 7.16 (7.12)

The low resolution mass spectrum reveals a weak parent ion at m/e 468 and fragments at m/e 466, 407 and 390 due to loss of [2H], [PMe_2] and [2H+PMe_3] respectively. The infrared spectrum of compound (4) shows bands assignable to coordinated PMe_3 ligands, in particular, 1303, 1297 cm^{-1} ($\delta(CH_3)$), 948, 930 cm^{-1} (ρ(PMe)) and 733, 720 cm^{-1} ($\nu_a(PC_3)$). Furthermore, the presence of metal-bound hydride ligands is indicated by a strong, broad absorption at 1635 cm^{-1}. Thus, despite the close appearance and stoichiometry of (3) and (4), their infrared spectra are significantly different.

The single crystal, X-ray structural determination of (4), performed by Dr. W. Clegg at the University of Newcastle-Upon-Tyne, confirmed that (3) and (4) were structural isomers and that (4) had indeed resulted from ring metallation, wherein the metal had inserted into two C-H bonds of adjacent ring methyl substituents (Scheme 3.5).

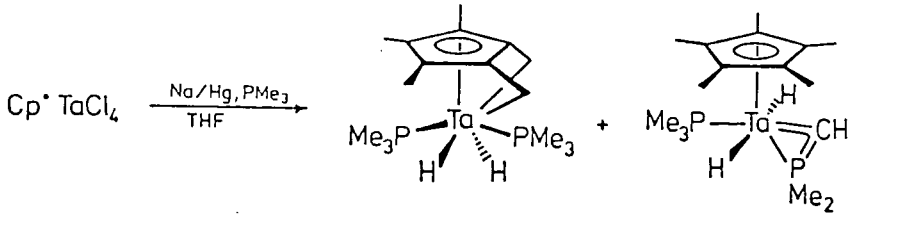

Scheme 3.5

A number of complexes have been reported in which, formally, the metal

has undergone intramolecular insertion into the C-H bond of a ring methyl substituent. Several examples of hydrogen abstraction from one methyl group to give η^6-1,2,3,4-tetramethylfulvene (or η^5,η^1-$C_5Me_4CH_2$) complexes have been reported, all of which occur in bis-Cp^* systems. For example, the thermal decomposition of $Cp^*_2TiMe_2$ results in the complex $Cp^*(\eta^6$-$C_5Me_4CH_2)TiMe$[33]; $Cp^*(\eta^6$-$C_5Me_4CH_2)WH$ is produced upon the photolysis of $Cp^*_2WH_2$[34]; $Cp^*(\eta^6$-$C_5Me_4CH_2)TiH$ is observed in solutions of Cp^*_2Ti[35] and $Cp^*(\eta^5,\eta^1$-$C_5Me_4CH_2)Hf(CH_2C_6H_5)$ is formed as an intermediate in the thermal decomposition of $Cp^*_2Hf(CH_2C_6H_5)_2$[36]. However, the abstraction of a hydrogen atom from a second methyl substituent to afford a double ring metallated product has been observed on only rare occasions. Specifically, the photochemical decomposition of $Cp^*_2WH_2$ has been shown to proceed according to Scheme 3.6[34].

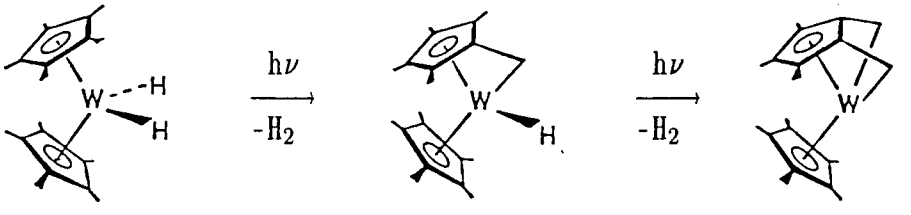

Scheme 3.6 *Photolysis of $Cp^*_2WH_2$*

The thermolysis of Cp^*_2TiR (R = H, Me) in aromatic solvents has been shown to undergo similar, stepwise insertions (Scheme 3.7).

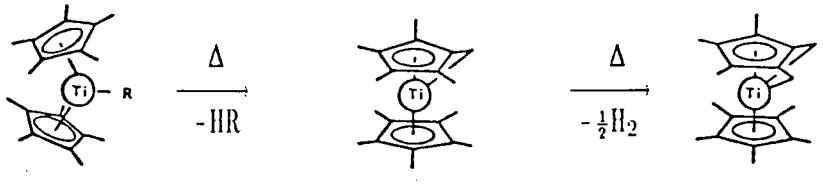

Scheme 3.7 *Thermolysis of Cp^*_2TiR (R=H,Me)*

Furthermore, pyrolysis of the permethyltantalacene complex, $Cp^*_2Ta(=CH_2)H$ has been interpreted in terms of the following reaction (Scheme 3.8)[38].

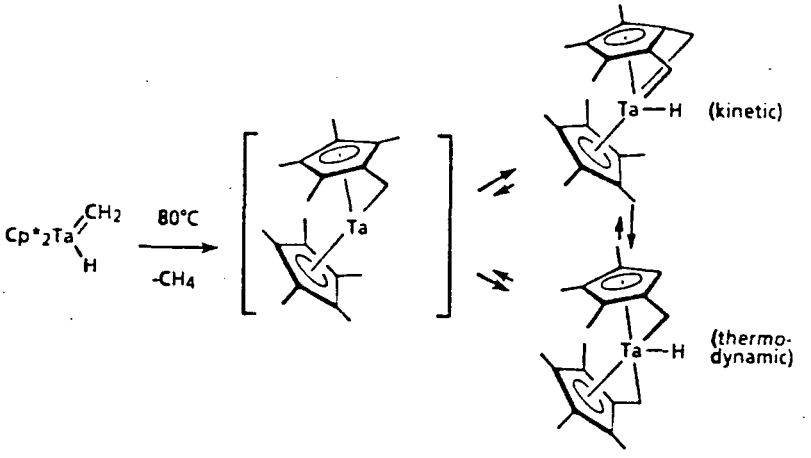

Scheme 3.8

3.7 THE MOLECULAR STRUCTURE OF $(\eta^7\text{-}C_5Me_3(CH_2)_2)Ta(H)_2(PMe_3)_2$ (4)

Colourless crystals of $(\eta^7\text{-}C_5Me_3(CH_2)_2)Ta(H)_2(PMe_3)_2$ (4) were grown from a saturated, light petroleum ether solution cooled to -35°C. The crystal data were collected and analysed by Dr. W. Clegg at the University of Newcastle-Upon-Tyne, and are summarised in Appendix 1D

The molecular structure is illustrated in Figure 3.14 and 3.15, selected bond distances and angles are collected in Table 3.11. The molecule possesses a crystallographic mirror plane (Figure 3.15) containing the tantalum atom, P(1), P(2) and C(31), and bisects the C_5-ring through the C(33)-C(33') bond.

The two tantalum-PMe_3 distances of 2.567(1)Å [P(1)] and 2.568(1)Å [P(2)] are within the range expected for single phosphorus bonds to tantalum[39]. Both PMe_3 ligands have their methyl substituents orientated to reduce interactions with the ring methyls (*cf.* $Cp^*TaCl_3.PMe_3$,

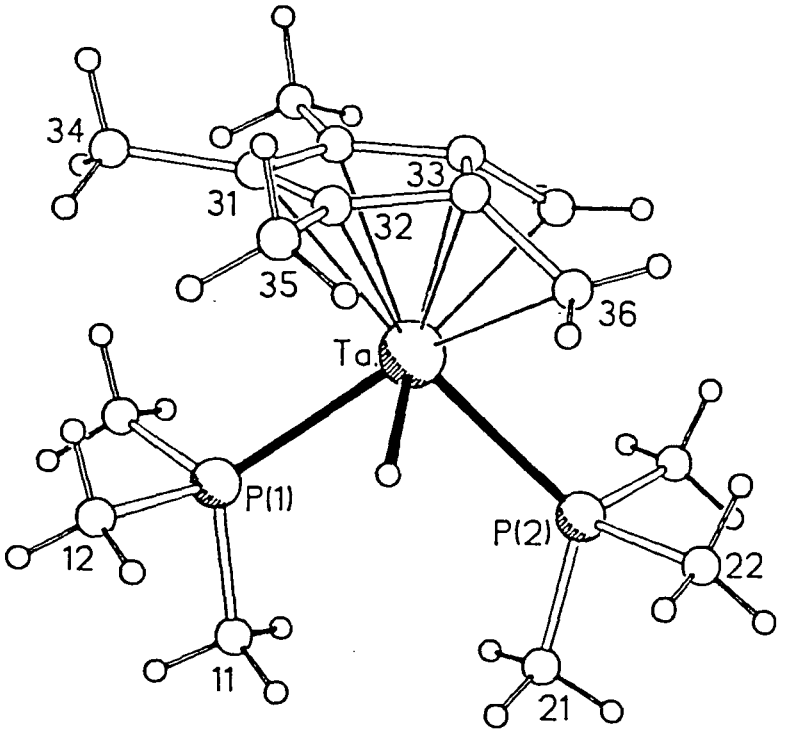

Figure 3.14 *Molecular Structure of* $(\eta^7\text{-}C_5Me_3(CH_2)_2)Ta(H)_2(PMe_3)_2$ *(4).*

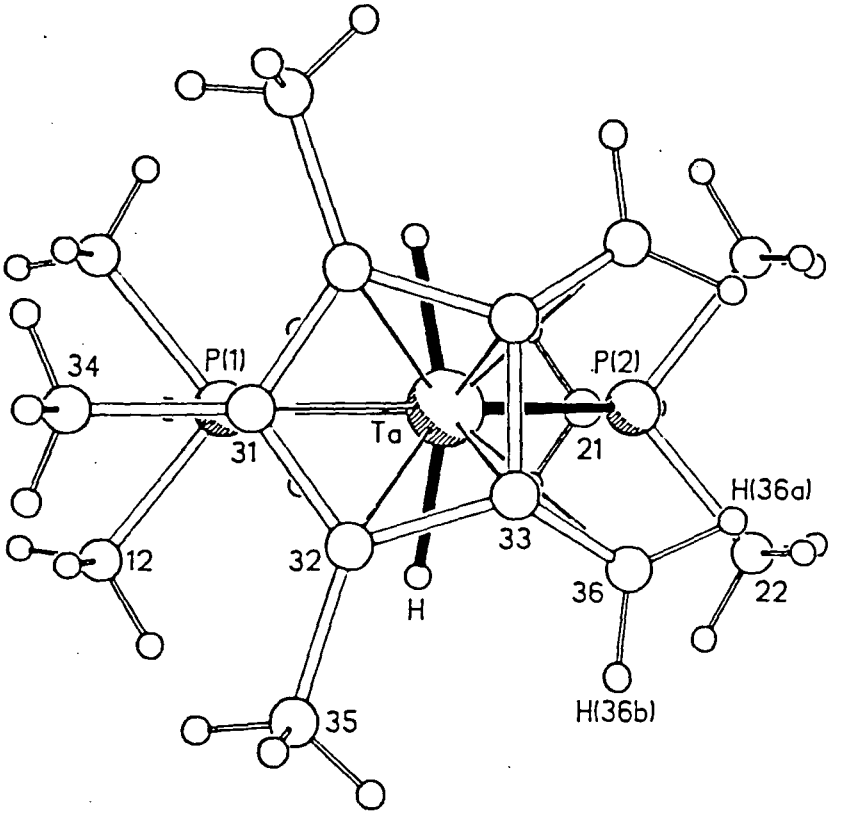

Figure 3.15 View down the C_5-Ta Vector of $(\eta^7\text{-}C_5Me_3(CH_2)_2)Ta(H)_2(PMe_3)_2$.

Ta-H	1.735(42)	P(1)-Ta-P(2)	100.1(1)
Ta-P(1)	2.567(1)	P(1)-Ta-C(36)	144.4(1)
Ta-P(2)	2.568(1)	P(2)-Ta-C(36)	84.0(1)
Ta-C(31)	2.569(5)	C(31)-Ta-C(36)	91.8(1)
Ta-C(32)	2.409(4)	C(32)-Ta-C(36)	63.0(1)
Ta-C(33)	2.172(3)	C(33)-Ta-C(36)	36.1(1)
Ta-C(36)	2.394(4)		
		Ta-P(1)-C(11)	119.8(3)
P(1)-C(11)	1.814(8)	Ta-P(1)-C(12)	116.4(2)
P(1)-C(12)	1.831(5)	Ta-P(2)-C(21)	122.8(2)
P(2)-C(21)	1.822(8)	Ta-P(2)-C(22)	115.2(1)
P(2)-C(22)	1.830(4)		
		C(11)-P(1)-C(12)	99.5(2)
C(31)-C(32)	1.407(5)	C(12)-P(1)-C(12')	102.3(3)
C(31)-C(34)	1.502(8)	C(21)-P(2)-C(22)	99.6(2)
C(32)-C(33)	1.445(5)	C(22)-P(2)-C(22')	101.0(3)
C(32)-C(35)	1.503(6)		
C(33)-C(36)	1.429(6)	Ta-C(36)-C(33)	63.5(2)
C(33)-C(33')	1.460(8)	Ta-C(36)-H(36a)	113.5(32)
		Ta-C(36)-H(36b)	114.9(35)
C(36)-H(36a)	0.997(58)		
C(36)-H(36b)	0.949(65)	H(36a)-C(36)-C(33)	111.9(32)
		H(36a)-C(36)-H(36b)	121.6(47)
X-Ta	2.011	H(36b)-C(36)-C(33)	117.7(35)
Y-Ta	1.963		
		X-Ta-H	111.5
X-Y	0.436	X-Ta-P(1)	112.1
		X-Ta-P(2)	147.8
H-Ta-P(1)	69.2(14)		
H-Ta-P(2)	79.4(13)	Y-Ta-X	12.5
		Y-Ta-P(1)	124.6
H-Ta-C(36)	77.1(14)	Y-Ta-P(2)	135.3
H-Ta-H'	128.4(28)	Z-C(31)-C(34)	8.8
		Z-C(32)-C(35)	3.9
H'-Ta-C(33)	135.4(14)	Z-C(33)-C(36)	33.4

Table 3.11 *Bond Lengths (Å) and Angles (°) for (η^7-$C_5Me_3(CH_2)_2$)-$Ta(H)_2(PMe_3)_2$ (4) [X=Centre of Cp* ring; Y=Point in plane of ring where normal from tantalum intersects; Z=best plane through C_5 ring].*

Chapter 2, section 2.3). The P(1)TaP(2) angle of 100.1(1)^{o} is smaller than the *trans* ClTaP angle of 135.8^{o} found in $Cp^{*}TaCl_3.PMe_3$, presumably reflecting the less crowded coordination sphere in (4).

The hydride ligands were located in the structure determination and are found to be symmetrically displaced on either side of the mirror plane, with a bond length of 1.735(42)Å. This is, as expected, slightly shorter than the corresponding distance in $TaCl_2H_2(PMe_3)_4$[40], [1.94(11)Å], due to the lower metal oxidation state in the latter, but is comparable to the tantalum-hydrogen distance in Cp_2TaH_3[41], [1.774(2)Å], which has been studied by neutron diffraction, and which has the same formal metal oxidation state (+5) to that of (4). The large e.s.d. value of the Ta-H distance however, precludes a more detailed comparison.

The most intriguing feature of the molecule is the coordination of the C_5 ring to tantalum. Figure 3.15 shows clearly that the tantalum atom is displaced away from C(31) towards the C(33)-C(33') edge (0.44Å from the ring centroid as determined by a normal from the ring plane through the metal atom). This distortion results in an elongated ring carbon-tantalum distance for C(31) of 2.569(5)Å (*cf.* average ring carbon-tantalum distance for (3) is 2.429(8)Å), and a significantly shortened Ta-C(33) (Ta-C(33')) distance of 2.172(3)Å. The ring slippage is caused by interaction of the tantalum atom with two adjacent ring methylene ligands, C(36) and C(36'). The Ta-C(36) distance of 2.394(4)Å is more than 1Å shorter than the metal-methyl distances found in (η^5-C_5Me_5)Ta compounds[15b], and is comparable to normal ring carbon-tantalum distances. Furthermore, the methylene carbon atoms, which are closer to the metal atom partially by virtue of the 0.44Å ring displacement, are also bent below the mean plane by an angle (ϕ) of 33.4^{o} (Figure 3.14). Similar bending of a methylene group towards a metal atom has been

observed in the molecular structures of related fulvene complexes, which are tabulated in Table 3.12. This is in direct contrast to the usual disposition of ring methyl substituents, being bent *ca.* 5^{o} from the mean C_5 ring plane, *away* from the metal atom[15b]. The relevant displacements from the ring plane in (4) are 8.8^{o} (C(34)-C(31)) and 3.9^{o} (C(35)-C(32)). Figure 3.14 also clearly shows the usual dispositions of the ring methyl hydrogens with one atom approximately parallel to the tantalum-ring centroid vector[15b].

COMPLEX	ϕ (^{o})	C(1)-C(α) (Å)	REF
$(C_5Me_3(CH_2)_2)Ta(H)_2(PMe_3)_2$ (4)	33.4	1.429(6)	#
$(C_5H_4CPh_2)Cr(CO)_3$	31.0	1.40	42
$[(C_5H_5)(C_5H_4CPh_2)Fe]BF_4$	20.7	1.416(9)	43
$(C_5H_4CH_2)Cr(CO)_3$	35	1.37(1)	44,45
$Cp^*(C_5Me_4CH_2)ZrPh$	37	1.468(9)	46
$(C_6H_6)(C_5H_4CMe_2)Mo$ (a)	39	1.42(2)	47
$(C_6H_6)(C_5H_4CPh_2)Mo$ (b)	38	1.437(4)	47
$(C_7H_8)(C_5H_4CMe_2)W$ (c)	37	1.45(3)	47
$(C_7H_8)(C_5H_4CPh_2)W$ (d)	39	1.44(2)	47
$(C_5H_4CPh_2)_2Ti$ (e)	36,37	1.446(11) 1.458(11)	47

Table 3.12 *Structural Parameters For Fulvene-like Complexes; [#=This Work].*

A number of limiting structures may be proposed to account for the ring π-bonding and the ring-to-metal interactions (Figure 3.16).

[A] [B] [C] [D]

Figure 3.16

Structure [A] may be described as a fused η^4-butadiene/η^3-allyl system, [B] and [C] are equivalent resonance forms of an η^7-heptatrienyl anion and [D] is a normal cyclopentadienyl ring with two additional sp^3-type methylene bridges to the metal atom.

Structurally, it has been found that in fulvene complexes the C(1)-C(α) distance increases and ϕ increases (Figure 3.17) as the C(α) atom develops more sp^3 character[46].

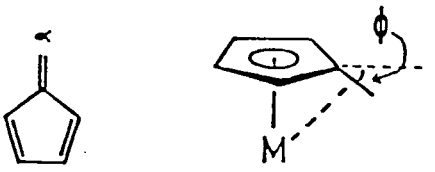

Figure 3.17

On the basis of these data and NMR spectroscopy, the bonding in $Cp^*(C_5Me_4CH_2)ZrPh$[46] was proposed to be mainly of η^5,η^1 character, rather than η^6-fulvene. Conversely, the η^6-fulvene mode is more prominent in $(C_5H_4CR_2)Cr(CO)_3$ complexes[46], for which the C(1)-C(α) distances average *ca.* 1.39Å (Table 3.12) (*cf.* C(1)-C(α) = 1.348(1)Å for uncoordinated fulvene)[46].

Considerable structural data have been compiled by Green *et al.*[47] on the fulvene compounds of molybdenum, tungsten and titanium, illustrated in Figure 3.18. Relevant structural parameters for (a)-(e) are collected in Table 3.12, along with data for several other complexes. The bonding of the fulvene ligands in complexes (a)-(e) has been described as predominantly η^5,η^1 on the basis of the large C(1)-C(α) distances, the large ϕ values and the results of photoelectron spectroscopy[47].

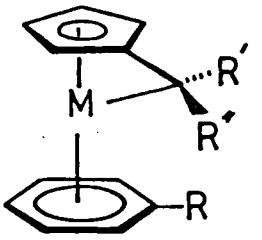

M=Mo; R=H; R'=R''=Me (a)
M=Mo; R=H; R'=R''=Ph (b)
M=W; R=Me; R'=R''=Me (c)
M=W; R=Me; R'=R''=Ph (d)

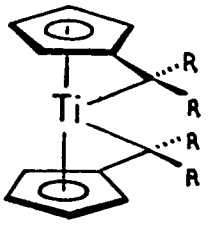

(e)

R=Ph

Figure 3.18

Clearly, compound (4) does not show the same degree of distortion as (a)-(e) and must therefore contain more C(1)-C(α) olefin character. Moreover, the Ta-C(α) distance of 2.394(4)Å in (4) is considerably longer than normal Ta-C(sp^3) distances (*eg.* 2.217(8)Å in $Cp^*TaCl_2(CH_2CH_2CH_2CH_2)$)[48]. Yet the ϕ and C(1)-C(α) values are both larger than those for the true η^6-fulvene complex, $(C_5H_4CH_2)Cr(CO)_3$, indicating at least some dilution of olefin character through forms [B] and [C] (Figure 3.16).

In summary, although the structural data do not definitely favour one particular bonding mode, the $C_5Me_3(CH_2)_2$ ligand in complex (4) appears to be of predominantly fused η^4-butadiene-η^3-allyl character [A] with contributions from η^7-heptatrienyl forms [B]/[C]. Indeed, further support for this description is provided by infrared and NMR data. For example, in the infrared spectrum an absorption at 3040 cm^{-1} may be assigned to an olefinic C-H stretching vibration. A similar band at 3040 cm^{-1} was observed for $Cp^*(C_5Me_4(CH_2))TiMe$[33].

3.8 THE NMR SPECTROSCOPY OF (η^7-$C_5Me_3(CH_2)_2$)$Ta(H)_2(PMe_3)_2$ (4)

The NMR data for (4) are fully consistent with the retention of the solid state geometry in solution at room temperature. Figure 3.19 shows the 250 MHz ^1H NMR spectrum of (4) in d^6-benzene solvent. Two singlets, assignable to the ring methyl groups at 1.97 ppm (6H, $C_5\underline{Me}_2Me(CH_2)_2$) and 1.86 ppm (3H, $C_5Me_2\underline{Me}(CH_2)_2$) are observed, and two doublets at 1.32 ppm and 1.14 ppm (both 9H and $^2J(PH)$=7.0 Hz, 6.7 Hz respectively), are present for the inequivalent phosphine ligands.

The two equivalent metal hydride ligands are found as a doublet of doublets resonance at 2.64 ppm ($^2J(PH)$=55.9 Hz, 25.7 Hz). The diastereotopic hydrogens of the equivalent methylene groups exhibit complex multiplets at 2.66 ppm and 1.30 ppm. The assignment of the methylene hydrogens was facilitated by difference NOE experiments. Specifically, irradiation of the signal at 1.97 ppm (Me_1) led to considerable enhancement (3.4%) of the signal at 2.66 ppm and had no detectable effect on the signal at 1.30 ppm. Thus, the multiplet at 2.66 ppm is assigned to the *exo*-enantiotopic hydrogens, Hb (Figure 3.19).

The *endo*-enantiotopic hydrogens at 1.30 ppm consist of a doublet of doublets which was shown from selective ^{31}P decoupling experiments to be due to coupling to only one of the PMe_3 phosphorus nuclei (J(PH) = 4.9 Hz) and a small geminal (H_aH_b) coupling of 2.7 Hz (Figure 3.20). The H_b hydrogens at 2.66 ppm show a complex multiplet when fully coupled (Figure 3.20). Heteronuclear decoupling experiments revealed coupling to both PMe_3 phosphorus nuclei, with J(PH)=2.0 and 3.0 Hz. Further coupling to the geminal hydrogens, H_a, must be present with $^2J(H_aH_b)_{gem}$= 2.7 Hz, and possibly additional coupling to the metal hydride ligands. Attempts to further simplify the spectrum by decoupling both phosphorus

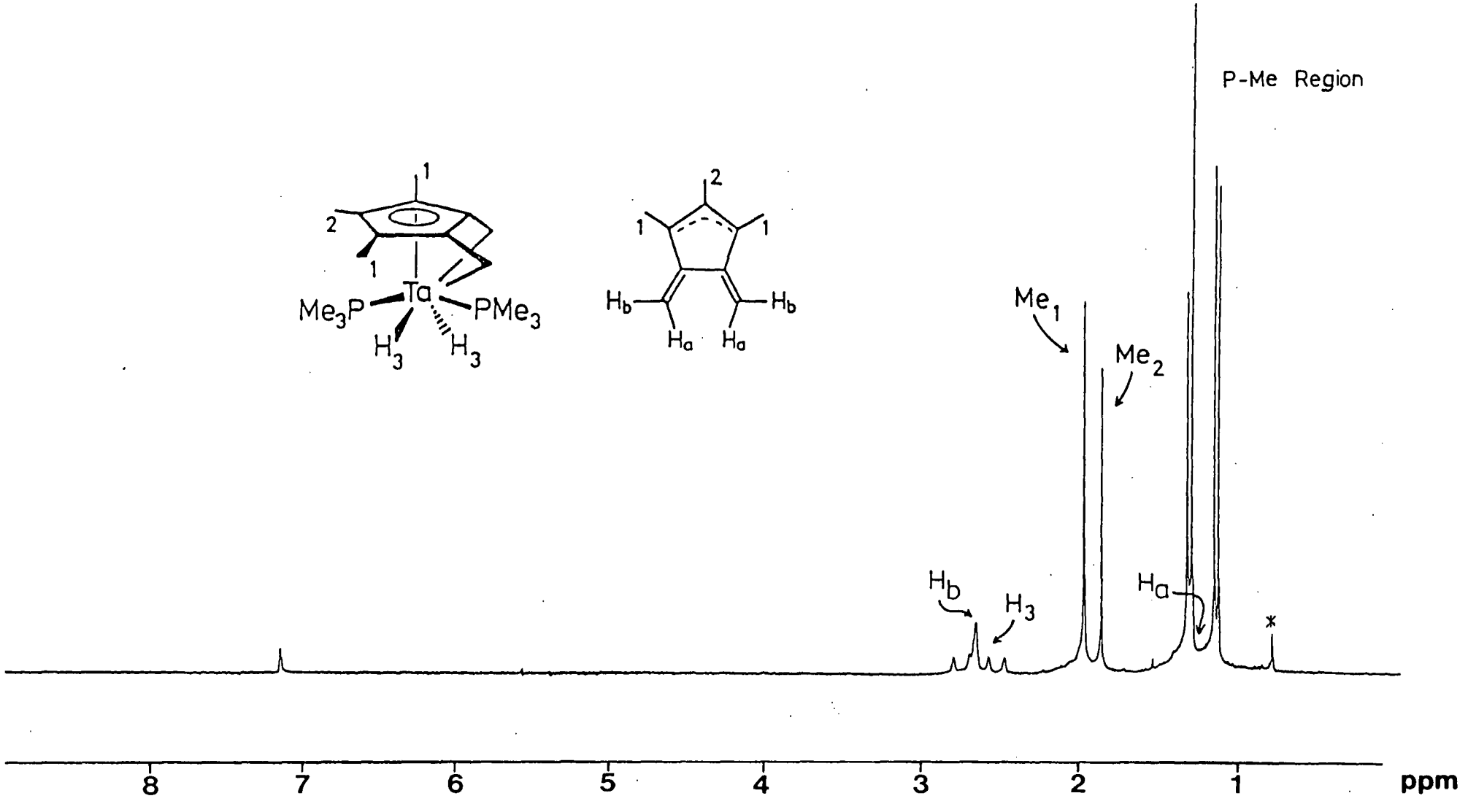

Figure 3.19 *^{1}H NMR Spectrum of (4) (250 MHz, d^6-benzene, 298K).* (* Denotes Impurity)

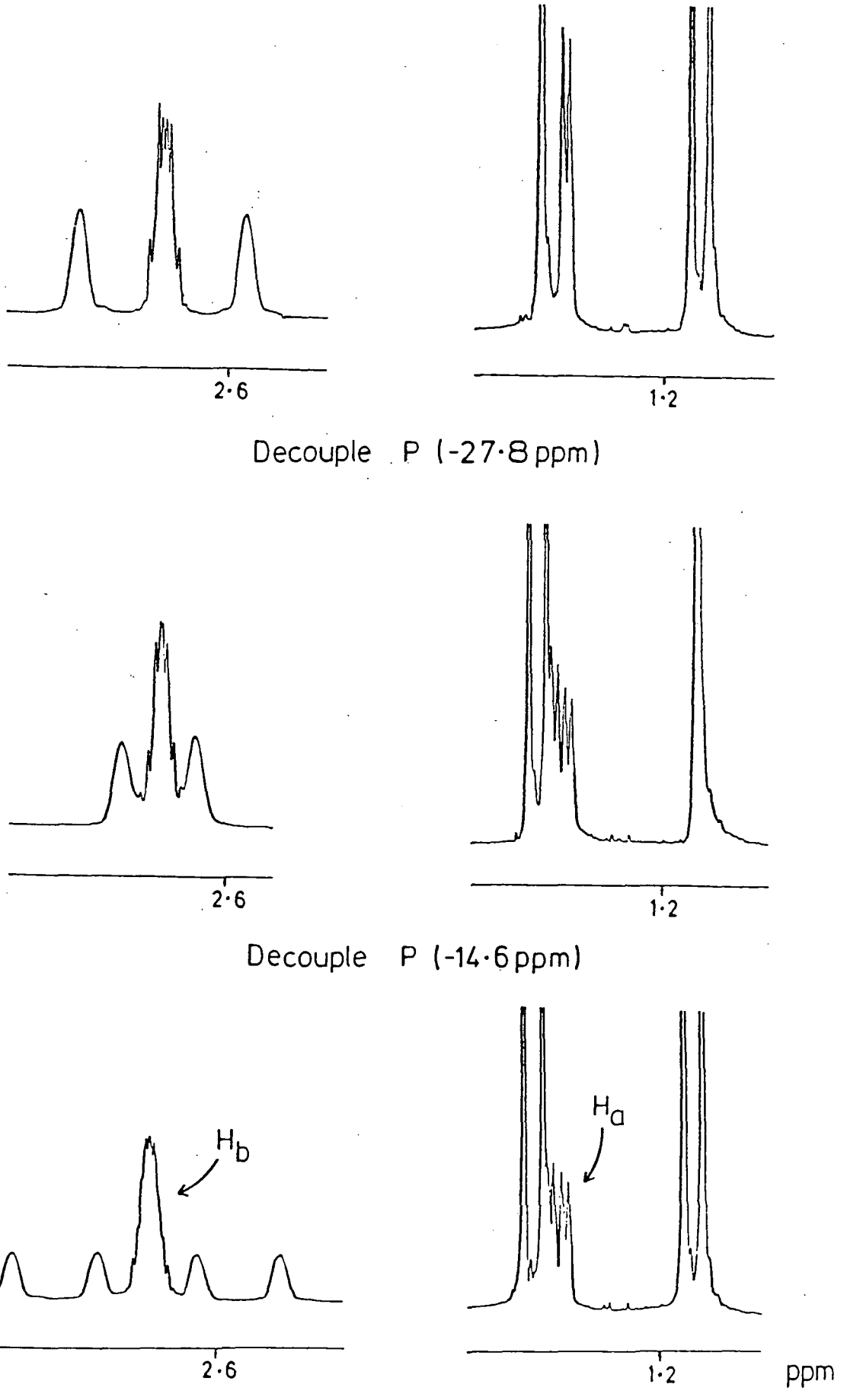

Figure 3.20 *Diastereotopic methylene hydrogens at 360 MHz.*

nuclei simultaneously, leaving only J(HH) couplings, were unsuccessful due to chemical shift overlap with the metal hydride signal. The full ^{1}H-NMR data is presented in Table 3.13.

SHIFT (ppm)	REL.INT.	MULT.	J (Hz)	ASSIGNMENT
2.66	2	m	$^2J(H_aH_b)_{gem}$=2.7 ^3J(PH)=2.0 (P,-14.6) ^3J(PH)=3.0 (P,-27.8)	H_b
2.64	2	dd	^2J(PH)=25.7 (P,-27.8) ^2J(PH)=55.9 (P,-14.6)	M-H
1.97	6	s	---	C_5Me_2MeR
1.86	3	s	---	C_5Me_2MeR
1.32	9	d	^2J(PH)=7.0 (P,-27.8)	PMe_3
1.30	2	dd	^3J(PH)=4.9 (P,-27.8) $^2J(H_aH_b)$=2.7	H_a
1.14	9	d	^2J(PH)=6.7 (P,-14.6)	PMe_3

Table 3.13 *^{1}H NMR Data For (4) (360 MHz, d^6-benzene); R=$(CH_2)_2$.*

Of particular relevance to the analysis of ring bonding contributions is the $^2J(H_aH_b)_{gem}$ coupling of 2.7 Hz. This value is more consistent with hydrogens on sp^2-hybridised carbon atoms of forms [A], [B] or [C] (Figure 3.16) (typical $^2J(HH)_{gem}$ values for sp^2 hybridised carbons are 0-3 Hz, *cf*: 12-15 Hz for geminal hydrogens attached to sp^3-hybridised carbon[30]). Geminal J(HH) coupling constants of 1.8 Hz and 4.4 Hz have been reported for $Cp^*(C_5Me_3(CH_2)_2)W$[34] and $Cp^*(C_5Me_3(CH_2)_2)Ti$[37] respectively, whereas a value of 6.59 Hz was reported for $Cp^*(C_5Me_4CH_2)$-Zr(Ph)[46], which was proposed to contain a predominantly sp^3-hybridised C(α) atom.

The $^{31}P\{^1H\}$-NMR spectrum in d^6-benzene solvent gives rise to phosphorus resonances at -14.6 ppm and -27.8 ppm with ^2J(PP)=28.3 Hz.

These values are quite normal for coordinated PMe_3 ligands.

The ^{13}C-NMR data (d^6-benzene) is reproduced in Table 3.14. Most importantly, the chemically equivalent methylene carbon atoms (C(α)) are located at 45.0 ppm with a one-bond C-H coupling constant of 151.1 Hz. This value is more consistent with sp^2-hybridisation of C(α) (typically 150-160 Hz[30]).

SHIFT (ppm)	MULT.	J (Hz)	ASSIGNMENT
123.8	s	---	C(ring)
113.5	s	---	C(ring)
105.2	s	---	C(ring)
45.0	tdd	$^1J(CH)=151.1$ $^2J(PC)=4.4, 8.8$	C(α)
24.0	qd	$^1J(CH)=129.6$ $^1J(PC)=22.1$	PMe_3
21.5	qd	$^1J(CH)=130.2$ $^1J(PC)=22.8$	PMe_3
13.1	q	$^1J(CH)=126.5$	$C_5\underline{Me_2}Me$
11.9	q	$^1J(CH)=126.5$	$C_5Me_2\underline{Me}$

Table 3.14 *^{13}C-NMR Data For (4) (50 MHz, d^6-benzene).*

Quite similar $^1J(CH)$ values have been reported for $Cp^*(C_5Me_4CH_2)TiMe$ (150 Hz)[33], $Cp^*(C_5Me_4CH_2)WH$ (151.3 Hz)[34], $Cp^*(C_5Me_3(CH_2)_2)W$ (152 Hz)[34] and $Cp^*(C_5Me_3(CH_2)_2)Ti$ (160 Hz)[37] whereas for the more sp^3-hybridised compound, $Cp^*(C_5Me_4CH_2)Zr(Ph)$, $^1J(C_\alpha H)$ was significantly lower at 144.8 Hz[46].

Thus spectroscopic investigations also support the fused η^4-butadiene-η^3-allyl character [A] for the bonding in (4) with additional contributions from η^7-heptatrienyl resonance forms [B] and [C]. For convenience however, the ring bonding in (4) is figuratively represented as form [D] of Figure 3.16.

3.9 MECHANISTIC CONSIDERATIONS ON THE FORMATION OF (3) AND (4)

The close relationship of the two isomeric products (3) and (4), differing only in the site of ligand activation, which in turn appears to be dependent upon only minor changes in the reducing conditions employed, led us to attempt to probe the mechanism(s) resulting in these selective, competitive ligand C-H bond activations. Indeed, given the isomeric nature of (3) and (4) and the nature of the reducing media it is not unreasonable that the initial stages of reduction in both pure PMe_3 and ethereal solvents would proceed in the sequence shown in Scheme 3.9.

$$Cp^*TaCl_4$$
$$\downarrow PMe_3$$
$$Cp^*TaCl_4.PMe_3 \quad (I)$$
$$\downarrow e^-$$
$$Cp^*TaCl_3.PMe_3 \quad (II)$$
$$\downarrow e^-, PMe_3$$
$$Cp^*TaCl_2(PMe_3)_2 \quad (III)$$

Scheme 3.9

The observation of an initial yellow solution in both pure PMe_3 and THF mediated reductions followed by conversion to red-brown solutions is supportive of the presence of (I) and (II)/(III) respectively. Furthermore, it has been specifically demonstrated that (III) can be converted to either (3) or (4).

The reduction of $Cp^*TaCl_2(PMe_3)_2$ (III) has been investigated under a variety of conditions employing different reducing agents and solvents. The results are collected in Table 3.15 and compared with

similar, small scale reductions of Cp^*TaCl_4. Reactions were carried out on a 50mg scale, over 48h. at room temperature with an excess of reducing agent (*ca.* 10 equivalents) and the petroleum ether soluble products were analysed by ^1H NMR spectroscopy in d^6-benzene.

SUBSTRATE	REDUCTANT	SOLVENT	% (3)	% (4)	OTHERS (%)
Cp^*TaCl_4	Na(sand)	PMe_3	100	---	---
Cp^*TaCl_4 [+]	Na/Hg	THF	27	43	30
Cp^*TaCl_4 [+]	Na/Np	THF	trace	~95	~5
(III)	Zn,Al,Mg†	THF,PMe_3	---	---	‡
(III)	Na(sand)	PMe_3	100	---	---
(III)	Na(sand)	THF	80	20	---
(III)	Na(sand)	Et_2O	60	40	---
(III)	Na/Hg	PMe_3	40	trace	60‡
(III)	Na/Hg	THF	24	48	28
(III)	K,Na/K	THF	---	---	---
(III)	Na/Np	THF	70	20	10

Table 3.15 *Reductions of Cp^*TaCl_4 and $Cp^*TaCl_2(PMe_3)_2$ (III) [Np=Naphthalene; †Magnesium reduction in pure PMe_3 does produce some (3) but the reaction is unclean; ‡Starting material detected; +Mixture contains ca. 5 equivalents PMe_3].*

The results show that:

(I) The strong reducing agents, potassium metal and sodium-potassium alloy, react to form petroleum ether insoluble products, possibly including anionic organo-tantalum species.

(II) The weaker reducing agents, zinc and aluminium do not completely dehalogenate $Cp^*TaCl_2(PMe_3)_2$ in either THF or pure PMe_3. Magnesium does produce a small amount of (3) in neat PMe_3 but the reaction is unclean. No reduction products are observed in THF solvent.

(III) The sodium sand reductions in pure PMe_3 solvent invariably

yield (3) as the sole petroleum ether soluble product.

(IV) The reductions in ethereal solvents produce mixtures of (3) and (4) whose composition is strongly dependent upon the nature of the reducing agent.

(V) (3) and (4) do not equilibrate under the reducing conditions employed. Thus, THF and PMe_3 solutions of (3) and (4) remain unchanged at room temperature. The addition of mercury to these solutions produces no change.

(VI) The degree of intimate mixing appears to be important as indicated by the reductions of Cp^*TaCl_4 with Na(Hg) and Na(Np), the homogeneous reducing agent Na(Np) providing a higher yield of (4).

While these experiments clearly show the dependence of the reaction pathway on both the nature of the reducing agent and the solvent medium, they have not served to clarify the reduction pathway beyond $Cp^*TaCl_2(PMe_3)_2$. In view of the latter's complex solution behaviour (Chapter 2, section 2.2.5) and the heterogeneous nature of many of the reduction steps a discussion of likely mechanisms leading to the selective formation of (3) and (4) would be speculative, and further studies were not pursued.

3.10 SUMMARY

Our efforts to find a convenient entry into half-sandwich tantalum chemistry *via* a compound of the general type, $Cp'Ta(PMe_3)_n$ have been realised through the synthesis of two isomers which, remarkably, differ only in their site of ligand activation. The first isomer, $Cp^*Ta(PMe_3)$-

$(H)_2(\eta^2\text{-}CHPMe_2)$ (3) was obtained using a sodium metal-pure PMe_3 reducing medium, whilst the more familiar sodium amalgam-ether(THF) reducing medium allowed access to the other isomer $(\eta^7\text{-}C_5Me_3(CH_2)_2)Ta(H)_2(PMe_3)_2$ (4). Both have been characterised by detailed NMR and X-ray crystallographic studies and preliminary accounts of the synthesis and characterisation of these compounds have been communicated[49,50].

3.11 REFERENCES

1. V.C. Gibson, C.E. Graimann, P.M. Hare, M.L.H. Green, J.A. Bandy, P.D. Grebenik and K. Prout, *J.Chem.Soc.Dalton Trans.*, 1985, 2025.
2. F.N. Tebbe and G.W. Parshall, *J.Am.Chem.Soc.*, 1971, 93, 3793.
3. C.R. Lucas, *Inorg.Synth.*, 1976, 16, 107.
4. C.R. Lucas and M.L.H. Green, *J.C.S. Chem Commun.*, 1972, 1005.
5. J.A. Labinger and K.S. Wong, *J.Organometallic Chem.*, 1979, 170, 373.
6. H. Werner and J. Gotzig, *Organometallics*, 1983, 2, 547.
7. K.W. Chiu, C.G. Howard, H.S. Rzepa, R.N. Sheppard, G. Wilkinson, A.M.R. Galas and M.B. Hursthouse, *Polyhedron*, 1982,1,441.
8. M.J. Bunker, A. De Cian, M.L.H. Green, J.J.E. Moreau and N. Siganporia, *J.Chem.Soc.Dalton Trans.*, 1980, 2155.
9. J. Hieman, J.H. Teuben, J.C. Huffmann and K.G. Caulton, *J.Organometallic Chem.*, 1983, 255, 193.
10. V.C. Gibson, J.E. Bercaw, W.J. Bruton and R.D. Sanner, *Organometallics*, 1986, 5, 986.
11. J. Nieman and J.H. Teuben, *Organometallics*, 1986, 5, 1149.
12. J.M. Mayer, P.T. Wolczanski, B.D. Santarsiero, W.A. Olson and J.E. Bercaw, *Inorg.Chem.*, 1983, 22, 1149.
13. L.R. Byers and L.F. Dahl, *Inorg.Chem.*, 1980, 19, 277.
14. V.W. Day, K.J. Reimer and A. Shaver, *J.C.S. Chem Commun.*, 1975, 403.
15. a) M.R. Churchill and W.J. Youngs, *Inorg.Chem.*, 1979, 18, 171.

b) A.J. Schultz, R.K. Brown, J.M. Williams and R.R. Schrock, *J.Am. Chem.Soc.*, 1981, 103, 169.

c) M.R. Churchill and W.J. Youngs, *Inorg.Chem.*, 1979, 18, 1930.

16. M.L.H. Green, P.M. Hare and J.A. Bandy, *J.Organometallic Chem.*, 1987, 330, 61.

17. S.Al-Jibori, C. Crocker, W.S. McDonald and B.L. Shaw, *J.Chem.Soc. Dalton Trans.*, 1981, 1572.

18. S. Bresadola, N. Bresciani-Pahor and B. Longato, *J.Organometallic Chem.*, 1979, 179, 73.

19. N. Bresciani, M. Calligaris, P. Delise, G. Nardin and L. Randaccio, *J.Am.Chem.Soc.*, 1974, 96, 5642.

20. R.R. Schrock and L.J. Guggenberger, *J.Am.Chem.Soc.*, 1975, 97, 6578.

21. R.R. Schrock, L.J. Guggenberger, L.W. Messerle and C.D. Wood, *J.Am.Chem.Soc.*, 1978, 100, 3793.

22. M.R. Churchill and F.J. Hollander, *Inorg.Chem.*, 1978, 17, 1957.

23. L.W. Messerle, P. Jennische, R.R. Schrock and G. Stucky, *J.Am. Chem.Soc.*, 1980, 102, 6744.

24. L.J. Guggenberger and R.R. Schrock, *J.Am.Chem.Soc.*, 1975, 97, 2935.

25. E.O. Fischer, R. Reitmeier and K. Ackermann, *Angew.Chem.Suppl.*, 1983, 488.

26. A. Igau, H. Grutzmacher, A. Baceiredo and G. Bertrand, *Proc. Euchem. PSIBLOCS Conf.Paris.*, 1988.

27. J.D. Fellmann, H.W. Turner and R.R. Schrock, *J.Am.Chem.Soc.*, 1980, 102, 6608.

28. A. Van Asselt, B.J. Burger, V.C. Gibson and J.E. Bercaw, *J.Am. Chem.Soc.*, 1986, 108, 5347.

29. R.R Schrock, "*Reactions of Coordinated Ligands*", Ed. P.S. Braterman, Plenum, New York, Chapter 3 (1986).

30. R.M. Silverstein, G.C. Bassler and T.C. Morril, "*Spectrometric Identification Of Organic Compounds*", 4th Edition, John Wiley, New York (1981).

31. R.B. Calvert and J.R. Shapley, *J.Am.Chem.Soc.*, 1977, 99, 5225.

32. J.R. Shapley, M.E. Cree-Uchiyama and G.M. St.George, *J.Am.Chem. Soc.*, 1983, 105, 140.

33. C. McDade, J.C. Green and J.E. Bercaw, *Organometallics*, 1982, 1, 1629.

34. F.G.N. Cloke, J.C. Green, M.L.H. Green and C.P. Morley, *J.C.S. Chem Commun.*, 1985, 945.

35. a) J.E. Bercaw, R.H. Marvich, L.G. Bell and H.H. Brintzinger, *J.Am.Chem.Soc.*, 1972, 94, 1219.

b) J.E. Bercaw, *J.Am.Chem.Soc.*, 1974, 96, 5087.

36. A.R. Bulls, W.D. Schaefer, M. Serfas and J.E. Bercaw, *Organometallics*, 1987, 6, 1219.

37. J.W. Pattiasina, C.E. Hissink, J.L. DeBoer, A. Meetsma and J.H. Teuben, *J.Am.Chem.Soc.*, 1985, 107, 7758.

38. G. Parkin, E. Bunel, B.J. Burger, M.S. Trimmer, A. Van Asselt and J.E. Bercaw, *J.Mol.Cat.*, In Press.

39. C.E. Holloway and M. Melnik, *Rev.Inorg.Chem.*, 1985, 7, 1.

40. M.L. Luetkens, Jr., J.C. Huffman and A.P. Sattelberger, *J.Am.Chem. Soc.*, 1983, 105, 4474.

41. R.D. Wilson, T.F. Koetzle, D.W. Hart, A. Kvick, D.L. Tipton and R. Bau, *J.Am.Chem.Soc.*, 1987, 19, 1775.

42. V.G. Andrianov, Y.T. Struchkov, V.N. Setkina, V.I. Zdanovich, A. Zh. Zhakaeva and D.N. Kursanov, *J.C.S. Chem Commun.*, 1975, 117.

43. U. Behrens, *J.Organometallic Chem.*, 1979, 182, 89.

44. F. Edelmann, B. Lubke and U. Behrens, *Chem.Ber.*, 1982, 115, 1325.

45. B. Lubke, F. Edelmann and U. Behrens, *Chem.Ber.*, 1983, 116, 11.

46. L.E. Schock, C.P. Brock and T.J. Marks, *Organometallics*, 1987, 6, 232.

47. J.A. Bandy, V.S.B. Mtetwa, K. Prout, J.C. Green, C.E. Davies, M.L.H. Green, N.J. Hazel, A. Izquierdo and J.J. Martin-Polo, *J.Chem.Soc.Dalton Trans.*, 1985, 2037.

48. M.R. Churchill and W.J. Youngs, *J.Am.Chem.Soc.*, 1979, 101, 6462.

49. T.P. Kee, V.C. Gibson and W. Clegg, *J.Organometallic Chem.*, 1987, 325, C14.

50. S.T. Carter, W. Clegg, V.C. Gibson, T.P. Kee and R.D. Sanner, *Organometallics*, In Press.

CHAPTER FOUR

REACTIVITY STUDIES AND DERIVATIVE CHEMISTRY OF $Cp^*Ta(PMe_3)(H)_2(\eta^2\text{-}CHPMe_2)$.

4.1 INTRODUCTION

The previous chapter described the synthesis and characterisation of two isomeric species $Cp^*Ta(PMe_3)(H)_2(\eta^2\text{-}CHPMe_2)$ and $(\eta^7\text{-}C_5Me_3(CH_2)_2)\text{-}Ta(H)_2(PMe_3)_2$. This chapter describes aspects of the reactivity and derivative chemistry of one of these compounds, $Cp^*Ta(PMe_3)(H)_2(\eta^2\text{-}CHPMe_2)$ (1) along two main lines of approach:

(1) The promotion of reversible hydrogen migrations and the potential for exploiting (1) as a source of the 14-electron $[Cp^*Ta(PMe_3)_2]$ and 10-electron $[Cp^*Ta]$ fragments.

(2) The development of the derivative chemistry in which the $(\eta^2\text{-}CHPMe_2)$ metallacycle is retained and its influence upon the products formed.

4.2 $Cp^*Ta(PMe_3)(H)_2(\eta^2\text{-}CHPMe_2)$ (1) AS A SOURCE OF $[Cp^*Ta(PMe_3)_2]$

4.2.1 Introduction

The primary objective of the work discussed in Chapter 3 was the synthesis of a complex of the form, $Cp^*Ta(PMe_3)_n$. Complex (1) may be viewed as a potential source of the $Cp^*Ta(PMe_3)_2$ fragment *via* the reversible hydrogen migrations outlined in Scheme 4.1.

Reversible hydrogen migrations have been shown to occur in the complex, $Fe(PMe_3)_4$ (Equation 4.1)[1], and hydride to alkylidene migrations have been observed on a number of occasions[2,3].

$$Fe(PMe_3)_4 \rightleftharpoons FeH(\eta^2\text{-}CH_2PMe_2)(PMe_3)_3 \qquad (4.1)$$

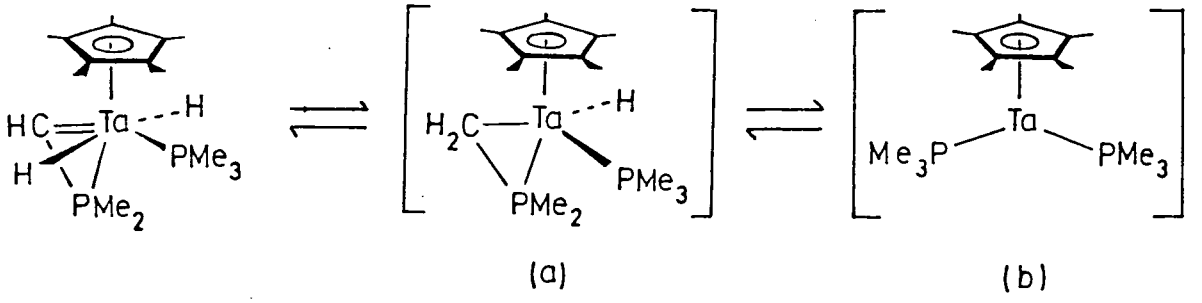

Scheme 4.1 *Reversible Hydrogen Migrations in (1).*

Thus it was of interest to establish the configurational stability of (1) with respect to hydrogen migration processes and the influence of these upon its reactivity towards a variety of reagents.

4.2.2 The Configurational stability of (1) on the NMR Timescale.

The ^1H NMR spectrum of (1) was discussed in detail in Chapter 3, section 3.5. There is no evidence for rapid hydrogen migrations at room temperature. Moreover, double resonance experiments[4] gave no indication of saturation transfer between the metal hydride and the metallacycle methine hydrogen sites up to 360K, at which point decomposition becomes significant suggesting that any migration processes must be occurring at a rate significantly less than $1/T_1$ (where T_1 is the longitudinal relaxation time of the methine hydrogen). Similar results have been reported for the complex, $Ta(H)_2(\eta^2\text{-}CHPMe_2)(\eta^2\text{-}CH_2PMe_2)(PMe_3)_2$[5] which did not show saturation transfer between the hydride site and any other sites at room temperature.

The only significant result of raising the temperature is to

promote exchange between coordinated and free PMe_3.

4.2.3 The Configurational Stability of (1) on the Chemical Reactivity Timescale: Reactions of (1) with tertiary phosphines and phosphites.

The above observation of PMe_3 exchange suggested that (1) would react with other $2e^-$ donor ligands by phosphine displacement. Accordingly, complex (1) was found to react with a range of tertiary phosphines and phosphites according to Equation 4.2.

$$Cp^*Ta(PMe_3)(H)_2(\eta^2\text{-}CHPMe_2) + PR_3 \underset{}{\overset{K_p}{\rightleftharpoons}} Cp^*Ta(PR_3)(H)_2(\eta^2\text{-}CHPMe_2) + PMe_3$$

$$R_3 = Me_2Ph,\ Et_3,\ MePh_2,\ OMe_3 \qquad (4.2)$$

Equilibrium was reached within 6 days at room temperature and there was no evidence for the formation of $Cp^*TaH(\eta^2\text{-}CH_2PMe_2)(PR_3)_2$ or $Cp^*Ta(PMe_3)_2(PR_3)_2$. The above equilibria were stable over several months for the tertiary phosphine ligands but with $P(OMe)_3$ decomposition to undefined products occurred within 3-4 weeks at 25°C.

LIGAND	K_p †	ν (cm^{-1})	Θ (°)
PMe_3	1	2064.1	118
PMe_2Ph	$1.50(5)\times10^{-1}$	2065.3	122
$PMePh_2$	$1.8(3)\times10^{-3}$	2067.0	136
PEt_3	$2.0(3)\times10^{-2}$	2061.7	132
$P(OMe)_3$	$1.47(7)\times10^{-1}$	2079.5	107
$P(OPh)_3$	a	2085.3	128

Table 4.1 *Equilibrium Constants for Phosphine Exchange Reactions of (1) (d^6-benzene,298K); †=Values are the mean of three determinations; a=Too small to measure under the conditions employed.*

The equilibrium constants, K_p have been calculated in d^6-benzene solvent at 298K, and are collected in Table 4.1, along with values of ν and Θ (see Chapter 1, section 1.2) as a measure of the electronic and steric properties of the phosphine ligands employed[6]. From the table the order of decreasing K_p is:

$$PMe_3 > PMe_2Ph \approx P(OMe)_3 > PEt_3 > PMePh_2 > P(OPh)_3$$

while on the basis of steric requirements alone, the predicted order would be:

$$P(OMe)_3 > PMe_3 > PMe_2Ph > P(OPh)_3 > PEt_3 > PMePh_2$$

Thus although the observed ordering is in accord with the steric requirement of the phosphine ligands, the two phosphite ligands have significantly lower K_p values than would be predicted upon the basis of ligand size alone. This discrepancy is presumably the result of electronic factors. The Ta(V) metal centre in (1) may be regarded as a hard acid and consequently will be stabilised most favourably by a hard, electron releasing base[7]. The ν parameters in Table 4.1 are a measure of the basicity of the phosphorus ligands, consideration of which leads to the following order of decreasing K_p:

$$PEt_3 > PMe_3 > PMe_2Ph > PMePh_2 > P(OMe)_3 > P(OPh)_3$$

In this series, the phosphite ligands show the smallest K_p values. Thus, the observed ordering of equilibrium constants may be regarded as a combination of the sterically and electronically determined series of which, for the phosphine ligands, steric effects are probably dominant.

The ^1H NMR data for the derivatives, $Cp^*Ta(PR_3)(H)_2(\eta^2\text{-}CHPMe_2)$ are summarised in Appendix 2.

4.2.4 Reaction of (1) with dmpe.

Tertiary monophosphines, PR_3, although participating in ligand

exchange equilibria, did not trap the products resulting from reversible hydrogen migrations *ie.* (a) and (b) in Scheme 4.1. It was therefore envisaged that a chelating diphosphine would be better able to stabilise the $MH(\eta^2\text{-}CH_2PMe_2)$ moiety towards swift regeneration of $MH_2(\eta^2\text{-}CHPMe_2)$ since a vacant coordination site is required for such a process and the chelating phosphines dppe and dmpe have been generally shown to be less labile than their monophosphine counterparts[8].

The reaction between (1) and dppe in d^6-benzene solvent did not occur at room temperature and no evidence was obtained for phosphine ligand exchange (^1H NMR). Although reaction occurred upon prolonged pyrolysis at 70°C no tractable products could be isolated. However, a toluene solution of (1) reacted smoothly with dmpe (1 equivalent) at 70°C over the course of 3h. to afford an orange solution from which orange crystals were obtained upon concentration and cooling to -78°C.

Elemental analysis and mass spectrometry were consistent with the empirical formula, $Cp^*Ta(PMe_3)(dmpe)$ (Chapter 7, section 7.4.1). Ions at m/e 542 and 464 may be assigned to $[M]^+$ and $[M\text{-}PMe_3\text{-}2H]^+$ respectively. However, infrared spectroscopy indicates the presence of a metal hydride ligand [ν(Ta-H), 1650(m,br)] and detailed NMR studies (*vide infra*) have facilitated characterisation of the compound as $Cp^*Ta(dmpe)(H)(\eta^2\text{-}CH_2PMe_2)$ (2). The formation of (2) can be envisaged to result from the trapping of $[Cp^*Ta(PMe_3)(H)(\eta^2\text{-}CH_2PMe_2)]$ [compound (a) in Scheme 4.1] by dmpe and confirms that hydrogen migrations do indeed occur on the chemical reaction timescale.

When the reaction between (1) and dmpe was monitored by ^1H NMR spectroscopy in d^6-benzene at room temperature an intermediate was observed which exhibited an apparent triplet signal at 9.18 ppm [J(PH) = 2.8 Hz] assignable to the methine hydrogen of a $(\eta^2\text{-}CHPMe_2)$ ligand, a doublet of doublets at 3.75 ppm [^{2}J(PH) = 53.5, 17.7 Hz] attributable to

two metal hydride ligands and a (η^5-C_5Me_5) resonance at 2.18 ppm. These data are consistent with an adduct of the form $Cp^*Ta(dmpe)(H)_2(\eta^2$-$CHPMe_2$) in which PMe_3 has been replaced by dmpe, which is presumed to coordinate *via* only one phosphorus atom. The reaction is believed to proceed according to Scheme 4.2.

$$Cp^*Ta(PMe_3)(H)_2(\eta^2\text{-}CHPMe_2) + dmpe \rightleftharpoons Cp^*Ta(dmpe)(H)_2(\eta^2\text{-}CHPMe_2) + PMe_3$$
(1)

$$\downarrow$$

$$Cp^*Ta(dmpe)(H)(\eta^2\text{-}CH_2PMe_2)$$
(2)

Scheme 4.2

Strictly therefore, the hydrogen migration occurs for the dmpe adduct rather than (1). Several structures are possible for (2) as illustrated schematically in Figure 4.1.

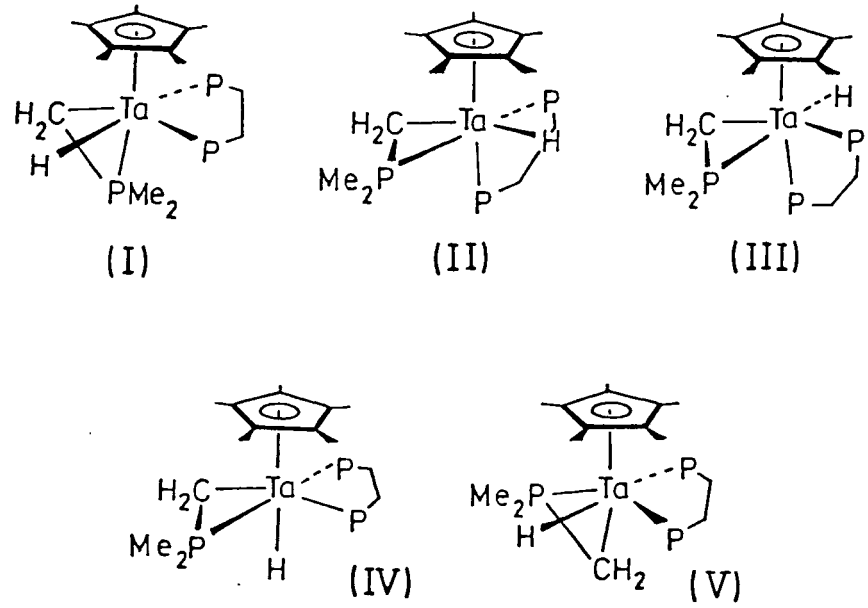

Figure 4.1 *Possible geometries for (2).*

The $^{31}P\{^1H\}$ NMR spectrum reveals the expected AMX pattern (Table 4.2). The (η^2-CH_2PMe_2) phosphorus nucleus resonates at significantly higher

frequency than in the (η^2-$CHPMe_2$) moiety and in a similar region to analogous tantalum systems *eg.* Ta(η^2-$CHPMe_2$)(η^2-$CH_2\underline{P}Me_2$)$(PMe_3)_3$, -77.5 ppm[9], Ta(H)$_2$(η^2-$CHPMe_2$)(η^2-$CH_2\underline{P}Me_2$)$(PMe_3)_2$, -59.3 ppm[5].

SHIFT (ppm)	REL.INT.	MULT.	J (Hz)	ASSIGNMENT
25.60	1	dd	$J(P_AP_B)$=38.8 $J(P_AP_C)$=18.6	P_A
21.51	1	dd	$J(P_AP_B)$=38.8 $J(P_BP_C)$=10.3	P_B
-53.57	1	dd	$J(P_AP_C)$=18.6 $J(P_BP_C)$=10.3	P_C

Table 4.2 *$^{31}P\{^1H\}$-NMR Data For (2) (d^6-benzene); P_A,P_B=nuclei of dmpe; P_C=metallacycle P-nucleus.*

The 250 MHz ^{1}H NMR spectrum (Figure 4.2) consists of a single (η^5-C_5Me_5) resonance at 2.26 ppm and six doublets between 1.84 and 0.92 ppm indicating all six phosphorus methyl substituents to be inequivalent. A broad multiplet at 1.33 ppm may be assigned to the four methylene hydrogens of the dmpe ligand.

Characteristic signals for the diastereotopic (η^2-$C\underline{H}_2PMe_2$) hydrogens are found at 0.26 ppm and -0.97 ppm in the same regions as those found for Ta(η^2-$CHPMe_2$)(η^2-CH_2PMe_2)$(PMe_3)_3$, -0.87 ppm[9] and WH(η^2-CH_2PMe_2)$(PMe_3)_4$[9], 0.43 ppm. Finally, the hydride ligand of (2) resonates at -2.96 ppm (*cf.* W$\underline{H}$(η^2-CH_2PMe_2)$(PMe_3)_4$[9], -3.75 ppm). Selective phosphorus decoupling experiments allow the assignment of all methyl groups to their respective phosphorus atoms (see Figure 4.3 and Table 4.3).

Although all the possible structures in Figure 4.1 possess six inequivalent phosphorus methyl groups. difference NOE experiments

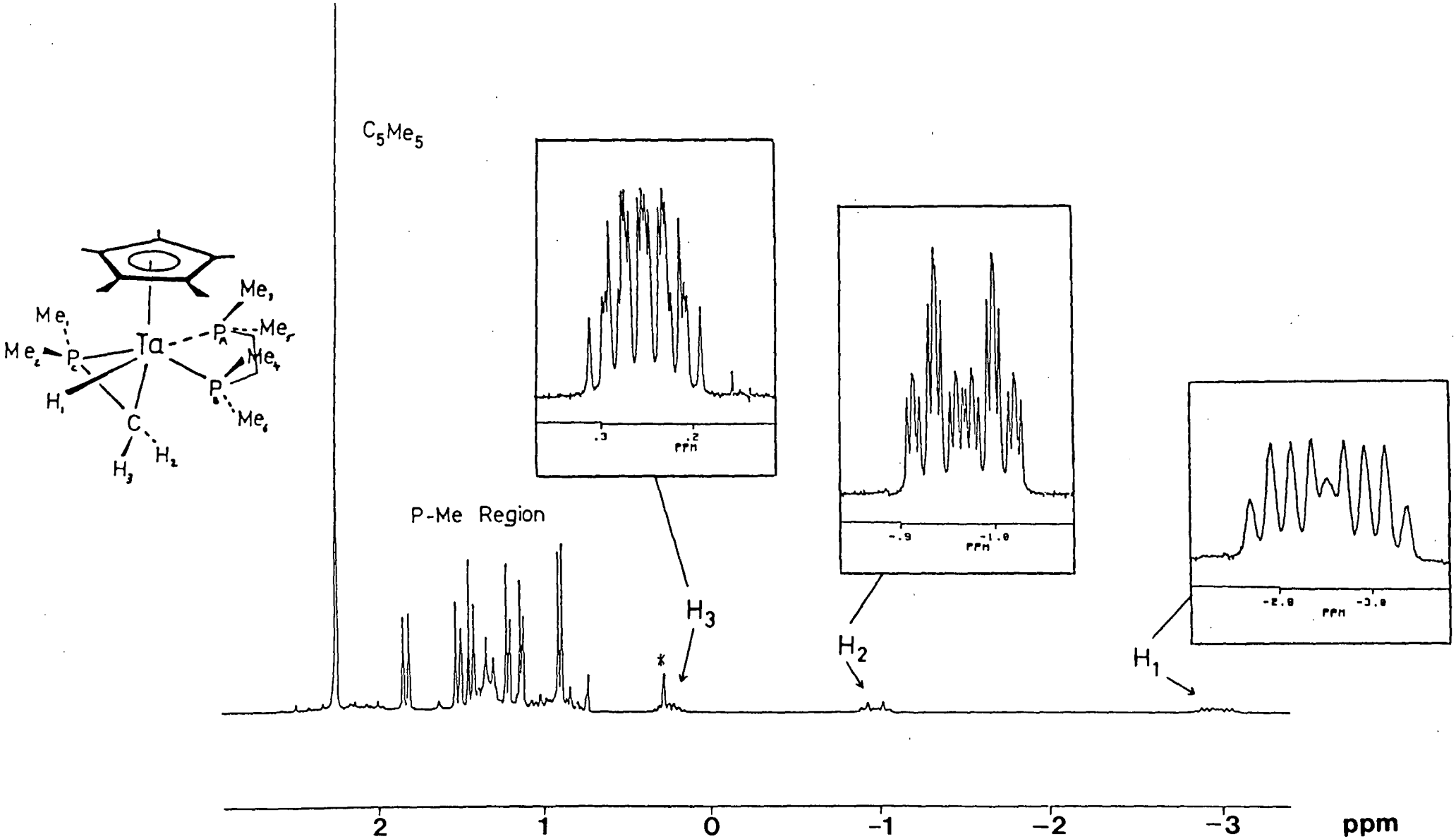

Figure 4.2 *^{1}H NMR Spectrum of (2) (250 MHz, d^6-benzene).* (* Denotes Impurity)

facilitate an assignment of the most likely structure. Specifically, irradiation of the (η^5-C_5Me_5) resonance results in an enhancement of the metal hydride signal (*ca.* 7%) and one methyl group on each dmpe phosphorus atom (*ca.* 3% each), thus eliminating structures (II), (III) and (IV). Furthermore, the observation of an NOE enhancement of the methyl hydrogens of the metallacycle (*ca.* 3% each) but no detectable effect upon the methylene hydrogens, suggests that the (η^2-CH_2PMe_2) ligand is orientated with the -PMe_2 terminus nearest to the Cp^* ring. Only structure (V) is consistent with all of the above results, and the NMR spectrum of (2) can be elucidated on the basis of this structure.

Selective phosphorus decoupling experiments allow the assignments of phosphorus coupling to the hydride ligand, with $J(P_AH)$ = 28.0 Hz, $J(P_BH)$ = 6.5 Hz and $J(P_CH)$ = 15.0 Hz (Figure 4.3).

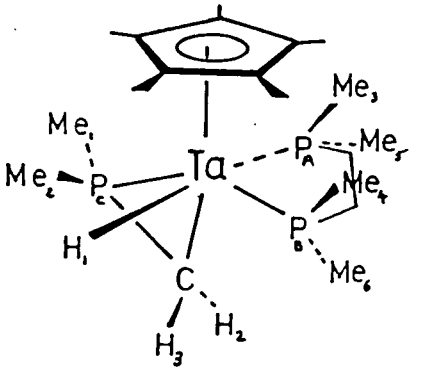

Figure 4.3 *Structure of (2)*

The hydride resonance exhibits further coupling to the (η^2-CH_2PMe_2) methylene hydrogens, resulting in an overall ddddd splitting pattern but the broad nature of the hydride signal prevents the complete resolution of these couplings. However, J-values can be obtained from an examination of the methylene resonances (*vide infra*).

Irradiation of the methylene hydrogen at 0.26 ppm results in NOE enhancement to H_1 (*ca.* 4%) whilst irradiation at -0.97 ppm does not

affect H_1, suggesting that the 0.26 ppm signal is assignable to H_3 which is on the same side of the metal as the hydride. Thus the resonance at -0.97 is assigned to H_2.

Hydrogens H_3 and H_2 are both ddddd multiplets for which selective phosphorus decoupling allows assignment of the J(PH) values, and by elimination, $J(H_1H_3)$, $J(H_1H_2)$ and $J(H_2H_3)$. The full ^1H NMR data are collected in Table 4.3 (see also Figure 4.3 for assignments).

SHIFT (ppm)	REL.INT.	MULT.	J (Hz)	ASSIGNMENT
2.27	15	s	---	$C_5\underline{Me}_5$
1.84	3	d	$^2J(P_CH)=9.0$	P_CMe_2
1.52	3	d	$^2J(P_BH)=7.8$	P_BMe_6
1.44	3	d	$^2J(P_CH)=7.6$	P_CMe_1
1.33	4	m	---	$PC\underline{H}_2C\underline{H}_2P$
1.22	3	d	$^2J(P_BH)=5.1$	P_BMe_4
1.14	3	d	$^2J(P_AH)=4.9$	P_AMe_3
0.92	3	d	$^2J(P_AH)=5.5$	P_AMe_5
0.26	1	ddddd	$^3J(P_AH_3)=8.0$	H_3
			$^3J(P_BH_3)=15.8$	
			$^3J(P_CH_3)=6.4$	
			$^3J(H_1H_3)=5.3$	
			$^2J(H_2H_3)=8.0$	
-0.97	1	ddddd	$^3J(P_AH_2)=8.4$	H_2
			$^3J(P_BH_2)=23.9$	
			$^3J(P_CH_2)=3.0$	
			$^3J(H_1H_2)=2.3$	
			$^2J(H_3H_2)=8.0$	
-2.96	1	ddddd	$^2J(P_AH_1)=28.0$	H_1
			$^2J(P_BH_1)=6.5$	
			$^2J(P_CH_1)=15.0$	
			$^3J(H_2H_1)=2.3$	
			$^3J(H_3H_1)=5.3$	

Table 4.3 *^1H NMR Data For (2) (360 MHz, d^6-benzene).*

The $^{13}C\{^1H\}$ NMR data (Table 4.4) are consistent with this structure. In particular, the metallacycle methylene carbon is found at 4.12 ppm as a broad signal for which the expected J(PC) coupling was not resolved. This shift is considerably lower than those found for the methine carbon of the (η^2-$CHPMe_2$) moiety (> 190 ppm) and is consistent with other complexes containing the (η^2-CH_2PMe_2) unit *eg.* Ta(η^2-$CHPMe_2$)-(η^2-$\underline{C}H_2PMe_2$)(PMe_3)$_3$, 3.6 ppm[9] and WH(η^2-CH_2PMe_2)(PMe_3)$_4$, -11.7 ppm[9].

SHIFT (ppm)	MULT.	J (Hz)	ASSIGNMENT
96.42	s	---	$\underline{C}_5Me_5$
37.23	dd	J(PC)=25.8, 13.3	$P\underline{C}H_2CH_2P'$
33.11	dd	J(PC)=23.1, 12.1	$PCH_2\underline{C}H_2P'$
26.78	d	J(PC)=32.0	PMe
26.65	d	J(PC)=32.0	PMe
25.55	d	J(PC)=20.1	PMe
19.23	d	J(PC)=11.7	PMe
18.60	m	---	PMe
16.57	d	J(PC)=14.0	PMe
14.26	s	---	$C_5\underline{Me}_5$
4.12	m	---	(η^2-$\underline{C}H_2PMe_2$)

Table 4.4 *$^{13}C\{^1H\}$-NMR Data For (2) (d^6-benzene).*

4.2.5 The Reaction of (1) with carbon monoxide

Complex (1) reacted slowly at 25°C with CO (1 atm.) over 3 days to afford exclusively three products which were identified as *cis* and *trans*-$Cp^*Ta(CO)_2(PMe_3)_2$ and $Cp^*Ta(CO)_3(PMe_3)$ by comparison of their ^1H NMR data to authentic samples[10]. These observations suggested that reversible hydrogen migrations had occurred to regenerate PMe_3.

However, the true situation is more complex. Upon monitoring the reaction by ^1H NMR spectroscopy in d^6-benzene solvent at 25°C, $Cp^*Ta(CO)_3(PMe_3)$ was observed to form first, with $Cp^*Ta(CO)_2(PMe_3)_2$ being produced subsequently. The product composition of the reaction mixture as a function of time is tabulated below and in graphical form

in Figure 4.4.

TIME (MIN.)	%CIS	%TRANS	%X	ln[TIME]
0	----	----	----	----
40	2.8	1.9	7.5	3.69
71	3.9	2.9	8.8	4.26
156	5.0	4.0	9.0	5.05
255	5.9	6.9	10.1	5.54
796	11.5	20.7	14.9	6.68
7days	15.4	32.7	51.9	----
14days	18.4	22.4	59.2	----
22days	12.7	18.5	68.8	----

Table 4.5 *Composition of the product mixture in the Reaction of (1) (20mg) with CO (1 atm.) at 25°C as a function of time; X=Cp*Ta(CO)$_3$(PMe$_3$).*

It can be clearly seen from Figure 4.4, that $Cp^*Ta(CO)_3(PMe_3)$ is formed at a faster rate during the early stages of reaction but that *trans*-$Cp^*Ta(CO)_2(PMe_3)_2$ becomes the dominant product after the first half-life of reaction (*ca.* 13h.). Prolonged reaction over several days leads to a steady growth of $Cp^*Ta(CO)_3(PMe_3)$ at the expense of both *cis* and *trans* $Cp^*Ta(CO)_2(PMe_3)_2$. Furthermore, the rate of reaction is inhibited by the presence of excess PMe_3.

These experimental observations may be interpreted on the basis of the mechanism outlined in Scheme 4.3. The phosphine dependency of the reaction rate suggests PMe_3 displacement to be the rate determining step, presumably generating an unstable d^0 carbonyl complex (I). Similar d^0 carbonyls, such as $Cp^*_2ZrH_2(CO)$[11], have been proposed in the transition metal mediated reduction of CO by H_2.

In the presence of CO, hydrogen migrations can then occur to produce the intermediate (II). Formally the tantalum atom has been reduced from Ta(V) to Ta(III), a process expected to be favoured by the coordination of carbonyl ligands.

Figure 4.4 *Plot of % versus Ln(Time) for each Product in the Reaction of (1) (20mg) with CO (1 atm.), 298K.*

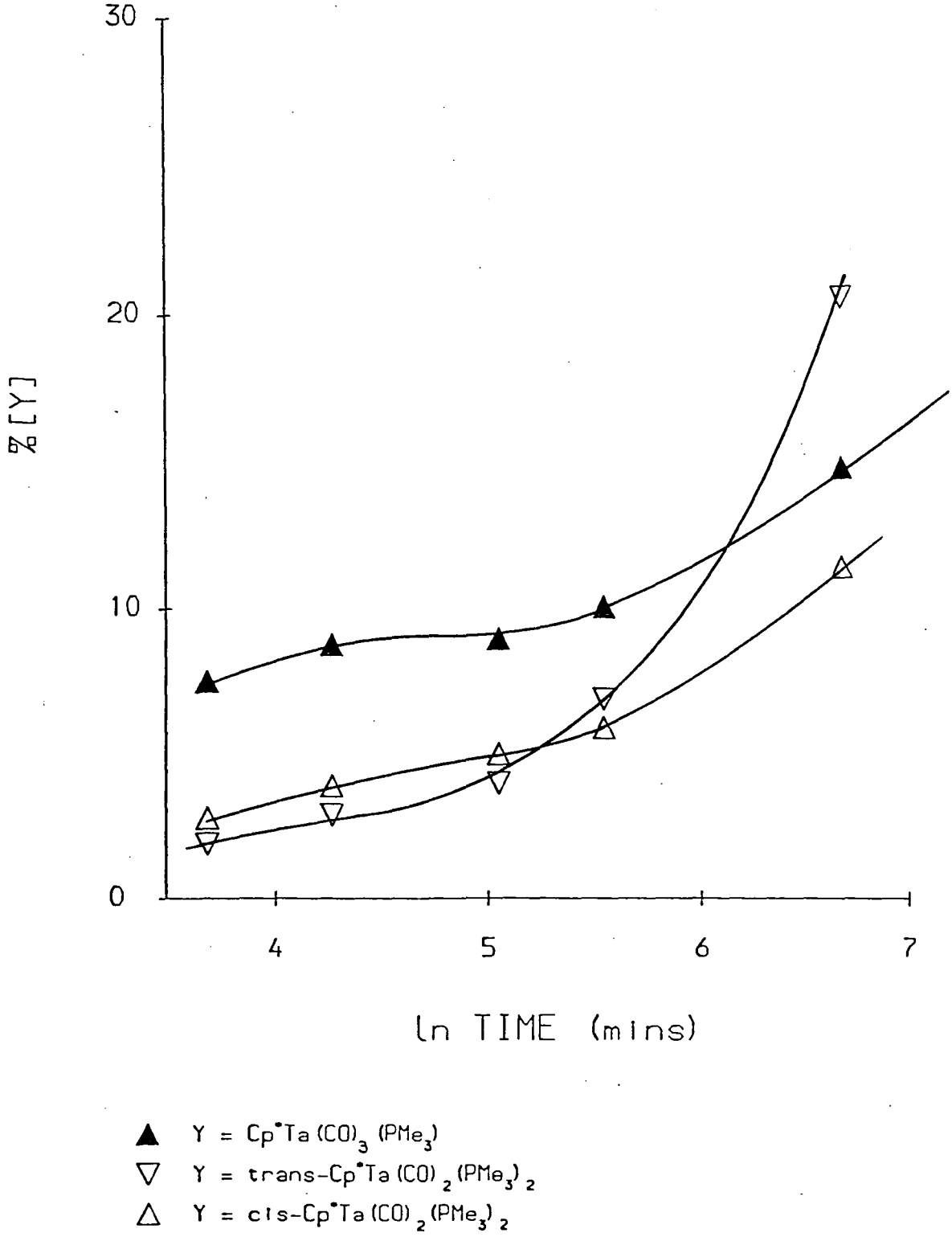

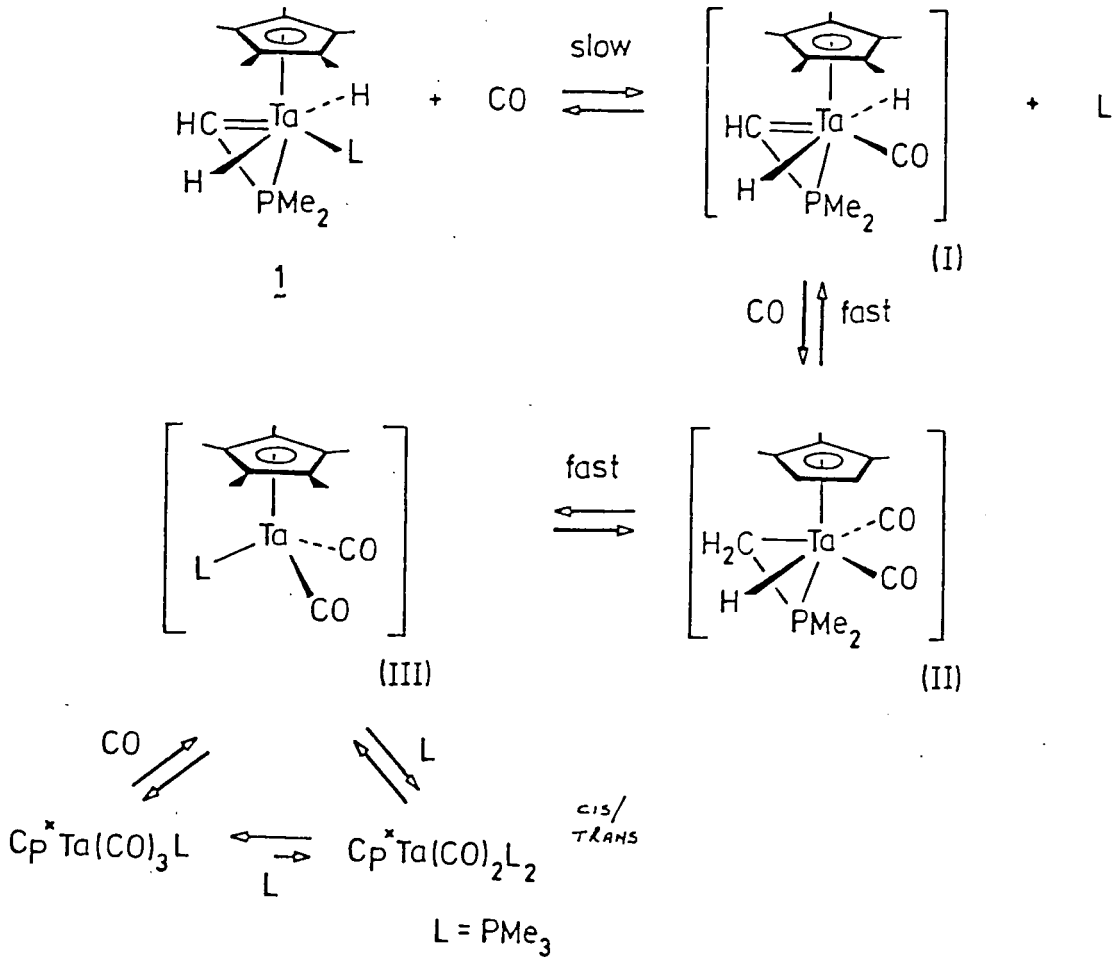

Scheme 4.3 *Proposed Mechanism for the Reaction of (1) with CO.*

Intermediates (I) and (II) were not observed by ^{1}H NMR spectroscopy although (II) is an analogue of (2) described in section 4.2.4. Presumably, with the more π-acidic CO ligands, further hydrogen migrations to form (III) may be more facile. Intermediate (III) is electronically unsaturated and would be expected to react rapidly with any donor molecules in solution. During the early stages of reaction, [CO] > [PMe_3] and (III) is preferentially trapped by CO to form $Cp^*Ta(CO)_3(PMe_3)$ as the major product. As the reaction proceeds however, [CO] decreases and [PMe_3] increases such that trapping by PMe_3 becomes more competitive. Indeed, after the first half-life, *trans*-$Cp^*Ta(CO)_2(PMe_3)_2$ is the major product. When the reaction is performed using 2 atm. of CO, the first half-life falls to *ca.* 3h. and

$Cp^*Ta(CO)_3(PMe_3)$ remains the dominant product throughout the reaction.

After 3 days at 25°C, the starting compound (1) has been exhausted and Scheme 4.3 is no longer valid. The fact that reaction still occurs several days beyond this point indicates the presence of a secondary, much slower reaction responsible for the conversion of $Cp^*Ta(CO)_2(PMe_3)_2$ to $Cp^*Ta(CO)_3(PMe_3)$. This reaction was recognised in Chapter 2, section 2.4.9, as proceeding according to Equation 4.3.

$$Cp^*Ta(CO)_2(PMe_3)_2 + CO \rightleftharpoons Cp^*Ta(CO)_3(PMe_3) + PMe_3 \quad (4.3)$$

In conclusion, compound (1) has been shown to give rise to products resulting from α-hydrogen migration reactions. Such reactions usually proceed *via* PMe_3 displacement in which case the hydrogen migration may be more facile for coordinatively unsaturated $Cp^*Ta(H)_2(\eta^2\text{-}CHPMe_2)$ or the adduct $Cp^*Ta(L)(H)_2(\eta^2\text{-}CHPMe_2)$. However, there is some evidence that hydrogen migrations do occur in (1), since heating a sample of (1) with excess (*ca.* 9 equivalents) of $P(CD_3)_3$ in d^6-benzene at 90°C for 14h. results in deuterium incorporation in both the hydride and metallacycle methine sites (by ^2H-NMR) although the degree of incorporation is low.

4.3 SYNTHESIS AND CHARACTERISATION OF $Cp^*Ta(PMe_3)HX(\eta^2\text{-}CHPMe_2)$ AND $Cp^*TaX_2(\eta^2\text{-}CHPMe_2)$ (X=Cl, Br, I)

4.3.1 Synthesis of $Cp^*Ta(PMe_3)HX(\eta^2\text{-}CHPMe_2)$ (X=Cl, Br, I)

Compound (1) reacted smoothly with both methyl bromide and methyl iodide at room temperature in toluene solvent to give the compounds $Cp^*Ta(PMe_3)HBr(\eta^2\text{-}CHPMe_2)$ (3) and $Cp^*Ta(PMe_3)HI(\eta^2\text{-}CHPMe_2)$ (4) in 88%

and 69% isolated yields respectively (Equation 4.4). Both compounds have been characterised by microanalytical and spectroscopic techniques (Chapter 7, section 7.4).

$$Cp^*Ta(PMe_3)(H)_2(\eta^2\text{-}CHPMe_2) + MeX \longrightarrow Cp^*Ta(PMe_3)HX(\eta^2\text{-}CHPMe_2) + CH_4 \qquad (4.4)$$
$$X = Br\ (3),\ I\ (4)$$

The metallacycle has been retained in these reactions and its presence is clearly indicated by ^1H NMR spectroscopy. Selected spectroscopic data for (3) and (4) are presented in Table 4.6.

COMPOUND	SPECTROSCOPIC DATA‡
(3)	^1H NMR: 9.22(1H,s,M=C<u>H</u>);
	^{31}P NMR: -104.20(1P,d,^2J(PP)=47.7Hz,<u>P</u>Me$_2$);
	^{13}C NMR: 196.69(1C,d,^1J(PC)=48.7Hz,M=<u>C</u>H);
	ν(M-H): 1710(m,br);
	m/e: 470,[M-PMe$_3$-H]$^+$.
(4)	^1H NMR: 9.53(1H,s,M=C<u>H</u>);
	^{31}P NMR: -107.83(1P,d,^2J(PP)=46.1Hz);
	^{13}C NMR: 202.11(1C,d,^1J(PC)=50.1Hz,M=<u>C</u>H);
	ν(M-H): 1755(m,br), 1730(m,sh);
	m/e: 518,[M-PMe$_3$]$^+$.

Table 4.6 *Selected Spectroscopic Data for (3) and (4)*
‡250 MHz ^1H NMR, d^6-benzene; ν(IR) cm^{-1}.

Compounds (3) and (4) are white, crystalline materials, soluble in aromatic solvents and slightly soluble in aliphatic hydrocarbon solvents. The coordinated PMe$_3$ in (3) and (4) appears to be somewhat more labile than that in (1) as indicated by the temperature dependent broadening of the PMe$_3$ resonances in the ^1H NMR spectra. This may be the result of the greater steric demand of halide over hydride ligands and a lower Lewis acidity of the metal in (3) and (4) due to pπ-dπ interactions with the halogen atoms. Similar explanations were offered to account for the more facile PMe$_3$ dissociation in $Cp^*Ta(PMe_3)_2ClH_3$

over $Cp^*Ta(PMe_3)_2H_4$[8].

Furthermore, the steric and electronic arguments above may be the cause of the smaller equilibrium constants for phosphine ligand exchange in (3) and (4) over (1) (Equation 4.5).

$$Cp^*Ta(PMe_3)HX(\eta^2\text{-}CHPMe_2) + PR_3 \underset{298K}{\overset{K_p}{\rightleftharpoons}} Cp^*Ta(PR_3)HX(\eta^2\text{-}CHPMe_2) + PMe_3 \qquad (4.5)$$

K_p for $PR_3 = PMe_2Ph$: $1.50(5) \times 10^{-1}$ (X = H)

$4.3(3) \times 10^{-2}$ (X = Br)

$2.7(3) \times 10^{-2}$ (X = I)

Compound (1) also reacted with methyl chloride (1 equivalent) slowly at 25°C but rapidly at 70°C to afford a mixture of unreacted (1) and two products, the major component of which was characterised as $Cp^*Ta(PMe_3)HCl(\eta^2\text{-}CHPMe_2)$ (5) by comparison of its ^{1}H-NMR data to those of (3) and (4) (Table 4.7).

SHIFT (ppm)	REL.INT.	MULT.	J (Hz)	ASSIGNMENT
9.00	1	s	---	M=C<u>H</u>
6.73	1	dd	$^2J(PH)=26.3$ $^2J(PH)=44.6$	M-H
2.03	15	s	---	$C_5\underline{Me}_5$
1.45	3	d	$^2J(PH)=10.6$	$P\underline{Me}_2$
1.42	3	d	$^2J(PH)=10.8$	$P\underline{Me}_2$
1.27	9	d	$^2J(PH)=6.1$	PMe_3

Table 4.7 *^{1}H NMR Data For (5) (250 MHz, d^6-benzene).*

The signal for the coordinated PMe_3 ligand of (5) is significantly broadened at room temperature presumably reflecting the more pronounced

lability of this ligand than that in either (3), (4) or (1).

4.3.2 Synthesis of $Cp^*TaX_2(\eta^2\text{-}CHPMe_2)$ (X = Cl, Br, I)

The reaction of (1) with excess methyl bromide or methyl iodide in toluene solvent proceeded cleanly *via* the monohalo complexes (3) and (4) to form, ultimately, the dihalo compounds (6) and (7) respectively (Equations 4.6 and 4.7).

$$Cp^*Ta(PMe_3)(H)_2(\eta^2\text{-}CHPMe_2) + MeX \longrightarrow Cp^*Ta(PMe_3)HX(\eta^2\text{-}CHPMe_2) + CH_4 \qquad (4.6)$$

$$Cp^*Ta(PMe_3)HX(\eta^2\text{-}CHPMe_2) + 2MeX \longrightarrow Cp^*TaX_2(\eta^2\text{-}CHPMe_2) + CH_4 + Me_4PX \qquad (4.7)$$
$$(X = Br(6),\ I(7))$$

Introduction of the second halide ligand results in displacement of the PMe_3 ligand which subsequently combines with MeX to produce the tetramethylphosphonium salt byproduct, which precipitates from the toluene solution. It is presumed that the second substitution renders the metal centre sterically and electronically reluctant to coordinate the PMe_3 ligand. However, the dihalo complexes do interact with PMe_3 in solution as indicated by the shift in the resonance frequency of PMe_3 when in contact with a d^6-benzene sample of pure (6) (0.87 ppm *vs* 0.79 ppm for uncomplexed PMe_3), indicating the equilibrium of Equation 4.8 to lie far to the left hand side.

$$Cp^*TaX_2(\eta^2\text{-}CHPMe_2) + PMe_3 \rightleftharpoons Cp^*Ta(PMe_3)X_2(\eta^2\text{-}CHPMe_2) \qquad (4.8)$$

The compounds (6) and (7) have been characterised by elemental analysis, infrared, ^1H, ^{31}P, ^{13}C NMR and mass spectroscopies (Chapter 7, section 7.4). No evidence of a hydride ligand remains in the infrared

or ^{1}H NMR spectra, although NMR spectroscopy supports the presence of the (η^2-CHPMe$_2$) metallacycle. Particularly, singlet resonances at 10.49 ppm [compound (6)] and 11.28 ppm [compound (7)] may be assigned to the methine hydrogens.

The available data are consistent with the dihalo complexes possessing structures of the form shown in Figure 4.5.

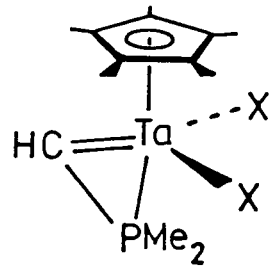

Figure 4.5 *Representation of the Structures of Cp*TaX$_2$(η^2-CHPMe$_2$) (X = Cl, Br, I).*

Although crystallographic or molecular weight data are not presently available, a monomeric structure may be argued by analogy to the isoelectronic compounds, Cp*TaCl$_2$(η^2-RC≡CR) (R = Me, Ph, H)[12]. The reaction between (1) and methyl chloride was found to afford a mixture of products. One component was identified as the monochloro derivative (5) (see section 4.3.1). The second component has been characterised as the dichloro compound (8), by comparison of ^{1}H NMR data to the bromo and iodo analogues (Table 4.8). Apparently, methyl chloride reacts with (1) and the monochloro complex (5) at comparative rates.

SHIFT (ppm)	REL.INT.	MULT.	J (Hz)	ASSIGNMENT
9.92	1	s	---	M=C<u>H</u>
1.87	15	s	---	C$_5$<u>Me$_5$</u>
1.52	6	d	^{2}J(PH)=11.1	P<u>Me$_2$</u>

Table 4.8 *^{1}H NMR Data For (8) (250 MHz, d^6-benzene).*

4.4 REACTION OF (1) WITH ISOCYANATES

(1) reacted smoothly with one equivalent of phenylisocyanate (PhNCO) in toluene solution over a period of 1h. at room temperature to afford a white solid which was indicated by elemental analysis (Chapter 7, section 7.4.6) to possess the empirical formula, $Cp^*Ta(PMe_3)(PhNCO)$ (9). Mass spectrometry reveals a parent ion at m/e 511 with concomitant fragmentation leading to ions at m/e 435 and 392 assignable to $[M-PMe_3]^+$ and $[M-PhNCO]^+$ respectively.

The infrared spectrum of (9) is informative. A broad absorption at 1738 cm^{-1} may be attributed to a metal bound hydride ligand whilst a band centred at 1560 cm^{-1} is consistent with the presence of a chelating formamide ligand[13] which presumably results from insertion of PhNCO into one of the hydride ligands of (1) according to Equation 4.9.

$$\underset{(1)}{Cp^*Ta(PMe_3)(H)_2(\eta^2\text{-}CHPMe_2)} \xrightarrow{PhNCO} \underset{(9)}{Cp^*Ta(\eta\text{-}PhNCHO)(H)(\eta^2\text{-}CHPMe_2)} + PMe_3 \quad (4.9)$$

The presence of the $(\eta^2\text{-}CHPMe_2)$ metallacycle was confirmed by ^1H NMR spectroscopy (*vide infra*). Monitoring the progress of reaction by ^1H NMR spectroscopy did not reveal any detectable intermediates. A probable structure for (9) is given in Figure 4.6.

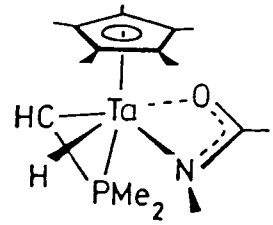

Figure 4.6 *Possible Structure of (9)*

A closely related product may be obtained from the reaction of (1) with p-tolyl isocyanate (p-$CH_3C_6H_4NCO$). $Cp^*Ta(\eta\text{-}CH_3C_6H_4NCHO)(H)(\eta^2\text{-}CHPMe_2)$ (10) displays infrared absorptions at 1738 cm^{-1} and 1550 cm^{-1} corresponding to ν(Ta-H) and ν(NCHO) respectively. A parent ion at m/e 525 is observed in the mass spectrum.

Both complexes (9) and (10) show unusual solution NMR behaviour. The $^{31}P\{^1H\}$ NMR spectrum of (9) consists of two moderately broadened resonances at -58.26 ppm and -72.23 ppm ($\Delta\frac{1}{2}$ *ca.* 40 Hz) in a 3:7 ratio suggesting the presence of two, possible interconverting, species in solution. Similarly, (10) displays two resonances, also in a 3:7 ratio, at -58.25 ppm and -72.04 ppm respectively.

The 250 MHz ^1H NMR spectrum of (9) (d^6-benzene) supports the presence of two compounds which appear to be isomers on the basis of the close similarity of their NMR parameters. At 298K, a single set of resonances is observed for the $[Cp^*Ta(\eta^2\text{-}CHPMe_2)]$ moiety (Table 4.9) although the phosphorus methyl signals are somewhat broadened. However, two metal hydride signals are observed at 12.79 ppm and 11.68 ppm respectively each of which reveal coupling to a single phosphorus nucleus with $^2J(PH)$ = 34.0 Hz and 25.9 Hz respectively. Moreover, two distinct formamide hydrogens are also observed (Table 4.9). Table 4.10 summarises the corresponding data for (10).

SHIFT (ppm)	MULT.	J (Hz)	ASSIGNMENT
12.79	d	$^2J(PH)$=34.0	M-H
11.68	d	$^2J(PH)$=25.9	M-H
9.17	d	$^2J(PH)$= 2.9	M=CH
9.01	s	---	PhNCHO
8.76	s	---	PhNCHO
7.2-6.6	m	---	PhNCHO
1.98	s	---	C_5Me_5
1.73	d	$^2J(PH)$=10.5	PMe_2
1.39	d	$^2J(PH)$=10.0	PMe_2

Table 4.9 *^1H-NMR Data For (9) (250 MHz, d^6-benzene, 298K).*

SHIFT (ppm)	MULT.	J (Hz)	ASSIGNMENT
12.81	d	$^2J(PH)=35.0$	M-H
11.70	d	$^2J(PH)=26.2$	M-H
9.17	d	$^2J(PH)= 2.3$	M=CH
9.05	s	---	Tol-NCHO
8.80	s	---	Tol-NCHO
7.2-6.5	m	---	CH_3PhNCHO
2.12	s	---	CH_3PhNCHO
2.00	s	---	C_5Me_5
1.75	d	$^2J(PH)=11.0$	PMe_2
1.40	d	$^2J(PH)=10.0$	PMe_2

Table 4.10 *^{1}H-NMR Data For (10) (250 MHz, d^6-benzene, 298K).*

The room temperature $^{13}C\{^1H\}$ NMR spectrum of (9) is further supportive of two formamido complexes in solution, with the observation of two distinct formamide carbon resonances in the region observed for other alkanamide complexes[14] (Table 4.11).

SHIFT (ppm)	MULT.	J (Hz)	ASSIGNMENT
206.17	d	$^1J(PC)=56.0$	M=CH
168.88	s	---	PhNCHO
166.61	s	---	PhNCHO
144.64	s	---	Ph-C(*ipso*)
124.10	s	---	Ph
120.95	s	---	Ph
113.15	s	---	C_5Me_5
20.26	d	$^1J(PC)=27.3$	PMe_2
13.10	s,br	---	PMe_2
11.63	s	---	C_5Me_5

Table 4.11 *$^{13}C\{^1H\}$-NMR Data For (9) (d^6-benzene, 298K, one Ph resonance obscured by solvent).*

The ^{1}H NMR spectrum of (9) has been collected at several temperatures between 235K and 335K in d^8-toluene solvent, and portions of the spectra are reproduced in Figure 4.7. At the high temperature limit (temperatures above 335K lead to decomposition) a single set of resonances is observed for each hydrogen environment. Lowering the

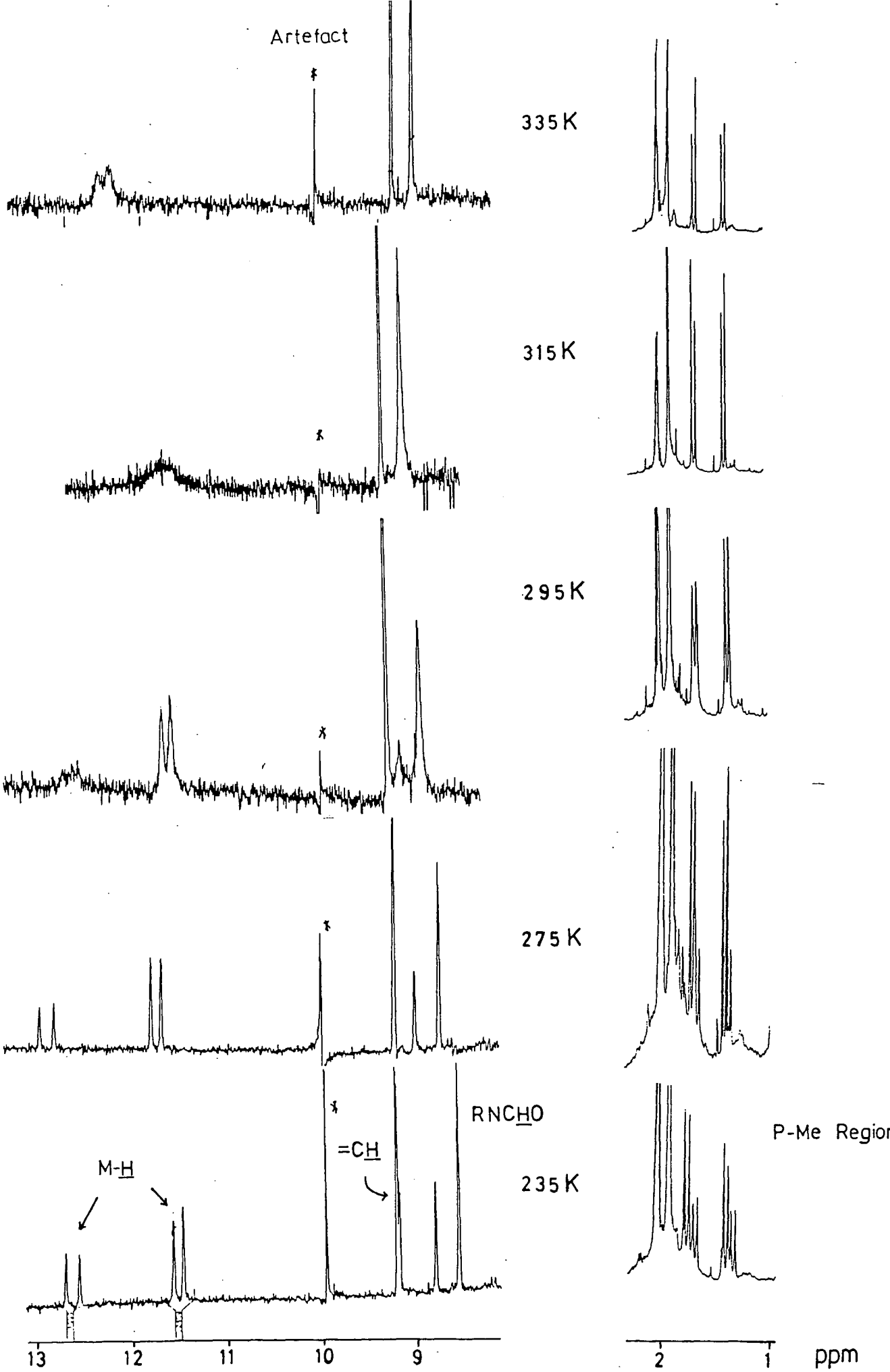

Figure 4.7 *Variable Temperature ^1H NMR Spectra of (9) (250 MHz, d^8-toluene).*

temperature to 315K results in slight broadening of the PMe_2 signals and considerable broadening of the formamide and hydride signals. At 295K, separate signals are observed for the formamide and hydride sites of each isomer as the rate of interconversion of the isomers decreases. At 275K, the PMe_2 resonances have become partially resolved whereas the hydride and formamide signals have sharpened considerably. Finally, at 235K the PMe_2 hydrogens are completely resolved for each isomer and two separate metallacycle methine resonances are observed. The full ^1H NMR data for each isomer at 235K are collected in Table 4.12. The tolylisocyanate product displays similar solution behaviour.

SHIFT‡ (ppm)	REL.INT.	MULT.	J (Hz)	ASSIGNMENT
ISOMER A				
12.54	1	d	$^2J(PH)=35.6$	M-H
9.09	1	d	$^2J(PH)= 3.2$	M=C<u>H</u>
8.71	1	s	---	PhNC<u>H</u>O
1.84	15	s	---	C_5<u>Me</u>$_5$
1.60	3	d	$^2J(PH)=10.1$	P<u>Me</u>$_2$
1.24	3	d	$^2J(PH)= 9.7$	P<u>Me</u>$_2$
ISOMER B				
11.42	1	d	$^2J(PH)=25.9$	M-H
9.12	1	d	$^2J(PH)= 2.6$	M=C<u>H</u>
8.47	1	s	---	PhNC<u>H</u>O
1.84	15	s	---	C_5<u>Me</u>$_5$
1.68	3	d	$^2J(PH)=10.6$	P<u>Me</u>$_2$
1.31	3	d	$^2J(PH)=10.0$	P<u>Me</u>$_2$

Table 4.12 *^1H NMR Data For Isomers A and B of (9) (250 MHz, d^8-toluene, 235K); ‡Phenyl hydrogens not resolved between 7.3-6.5 ppm.*

The most likely identity of the two isomers is illustrated in Figure 4.8. The tentative assignment of the isomers in Table 4.12 is based upon our observations that the chemical shift of the metal hydride ligand is strongly dependent upon the electronegativity of the ligand

trans to it, the more electronegative the *trans* substituent the higher the frequency of the hydride resonance (*cf.* the monohalide derivatives in section 4.3.1). Therefore isomer A, with a transoid oxygen atom is expected to possess the higher frequency hydride signal.

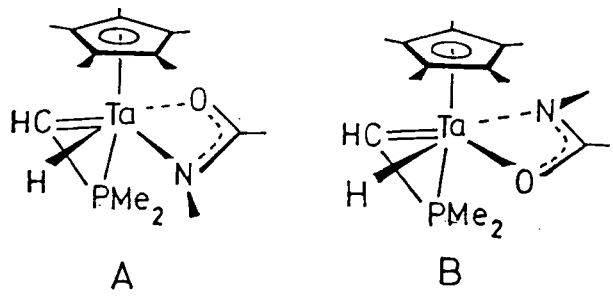

Figure 4.8 *Isomers of (9).*

At room temperature, the two isomers are present in the ratio A:B = 3:7. Presumably this reflects the presence of greater intramolecular repulsive interactions for A, between the hydride ligand and the N-phenyl hydrogens. The interconversion of isomers A and B presumably proceeds *via* dissociation of one arm of the chelating formamide ligand. Either ligand rotation or reversible β-hydrogen migration processes may then occur followed by chelation as illustrated in Scheme 4.4. It would be anticipated that pathway (II) would have the lower energy barrier since it involves only bond rotations whilst pathway (I) requires further bonds to be broken, in addition to rotations. This rationale is supported by saturation transfer studies. If pathway (II) is followed, then saturation transfer should be observed only between the hydride sites of each isomer, whereas the operation of pathway (I) would be indicated by saturation transfer between the hydride and formamide sites.

The saturation transfer experiment (performed in d^8-toluene) shows

that at 293K and 253K, there is saturation transfer only between the two hydride sites indicating that only pathway (II) operates under these conditions. This mechanism is analogous to the equilibration of the *syn* and *anti* hydrogens of a η^3-allyl ligand *via* bond rotation within an intermediate σ-allyl[15].

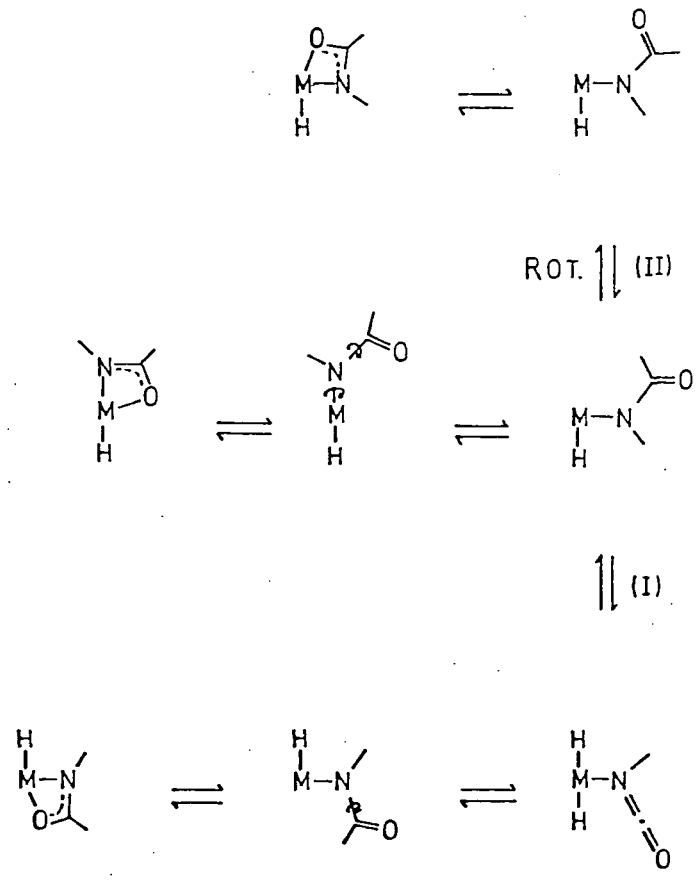

Scheme 4.4 *Possible Pathway for A ≒ B interconversion.*

4.5 REACTION OF (1) WITH CARBON DIOXIDE

The treatment of a petroleum ether solution of (1) with carbon dioxide (1 atms.) at room temperature led to the precipitation of a white solid over a period of 24h. The compound was found to be sparingly soluble in toluene and appreciably soluble in dichloromethane

in which it remained unchanged for at least 24h. Elemental analysis was consistent with the empirical formula $Cp^*Ta(PMe_3)(CO_2)_2$ (11), $C_{15}H_{24}O_4PTa$:

Found (Required): %C, 37.70 (37.51); %H, 5.14 (5.05)

The highest mass peak occurring in the mass spectrum was at m/e 448 corresponding to $[M-O_2]^+$.

The infrared spectrum gives a strong band at 955 cm^{-1} which may be assigned to a ρ(PMe) vibration whilst two strong absorptions at 1650 cm^{-1} and 1565 cm^{-1} are attributable to the $\nu_{as}(CO_2)$ vibrations of η^1 and η^2 formato ligands respectively, *cf.* $MoH(\eta^2\text{-}OCHO)(PMe_3)_4$[14], 1570 cm^{-1}; $(Ph_3P)_2Cu(\eta^2\text{-}OCHO)$[16], 1565 cm^{-1}; $[(Ph_2PCH_2)_3CMe]Cu(\eta^1\text{-}OCHO)$[17], 1620 cm^{-1} and $CpFe(CO)_2(\eta^1\text{-}OCHO)$[18], 1620 cm^{-1}. An absorption at 2720 cm^{-1} is assignable to the ν(CH) vibrations of the formato ligands[14].

The above data suggest that CO_2 has inserted into the metal hydride bonds of (1), a type of reaction that has been observed previously for CO_2[19]. Unfortunately, the room temperature ^1H NMR spectrum (250 MHz, d-chloroform) displayed only a single broad resonance at 2.0 ppm ($\Delta\frac{1}{2}$, 40 Hz), suggestive of fluxional processes possibly similar to those found in the formamido complexes (9) and (10). Studies are currently in progress to provide a more detailed characterisation of (11).

4.6 REACTIONS OF $Cp^*Ta(PMe_3)HX(\eta^2\text{-}CHPMe_2)$ (X = H, Br, I) WITH OLEFINS

4.6.1 Introductory Remarks

The insertion of olefins into metal hydride bonds is well documented[15] and is a fundamental reaction in processes such as olefin

hydrogenation, isomerisation and hydroformylation.

The interactions of olefins with the compounds $Cp^*Ta(PMe_3)HX(\eta^2\text{-}CHPMe_2)$ (X = H, Br, I) was of interest since these compounds contain both hydride ligands and the unusual metallacycle (η^2-$CHPMe_2$) which may be considered to possess a formal metal carbon double bond (see Chapter 3, section 3.4). Recent studies by Schrock and co-workers have shown that similar systems are capable of polymerising olefins[20].

4.6.2 Reaction of $Cp^*Ta(PMe_3)(H)_2(\eta^2\text{-}CHPMe_2)$ (1) With Olefins

Compound (1) reacted with ethylene (*ca.* 3 equivalents) slowly at room temperature to afford a mixture of products including tantalum alkyl species which were implicated by the observation of complex ^{1}H-NMR resonances at 0.15 ppm and -0.49 ppm assignable to metal coordinated alkyl hydrogens. Furthermore, new olefinic signals were observed in the region between 4.8-5.8 ppm. However, due to the apparent complexity of this reaction further studies were not pursued.

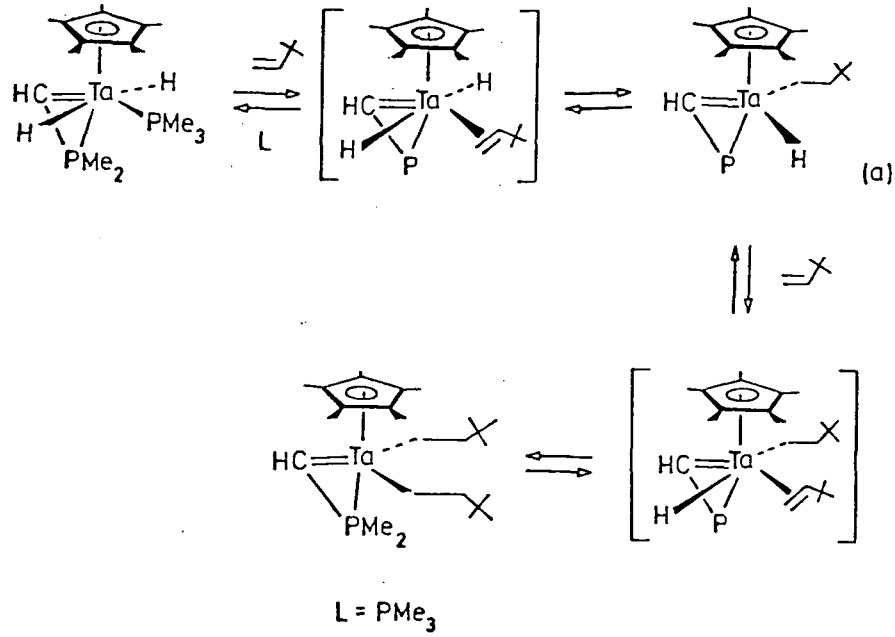

Scheme 4.5 *Reaction of (1) with Neohexene.*

In contrast, a clean reaction was observed between (1) and the sterically demanding olefin, 3,3-dimethylbut-1-ene (neohexene, CH_2=CH^tBu). Sequential insertion of neohexene into the metal hydride bonds led first to the mono-neohexyl complex which reacted with neohexene at a rate comparable to (1) to produce, as the ultimate product after 4 days at room temperature, the bis-neohexyl complex $Cp^*Ta(CH_2CH_2CMe_3)_2(\eta^2\text{-}CHPMe_2)$ (12) (Scheme 4.5).

The mono inserted product (a) was not isolated but characterised by ^1H NMR spectroscopy only (Table 4.13).

SHIFT‡ (ppm)	REL.INT.	MULT.	J (Hz)	ASSIGNMENT
8.71	1	d	$^2J(PH)$= 2.0	M=C<u>H</u>
4.74	1	d	$^2J(PH)$=12.0	M-<u>H</u>
2.05	15	s	---	C_5<u>Me</u>$_5$
1.52	3	d	$^2J(PH)$= 9.6	P<u>Me</u>$_2$
1.37	3	d	$^2J(PH)$=10.2	P<u>Me</u>$_2$
1.04	9	s	---	t-<u>Bu</u>

Table 4.13 *^1H NMR Data For $Cp^*Ta(CH_2CH_2CMe_3)(H)(\eta^2\text{-}CHPMe_2)$; (250 MHz, d^6-benzene); ‡Methylene signals not resolved.*

Presumably (a) interacts only weakly with PMe_3 as the methine hydrogen is observed as a doublet signal coupling only to the metallacycle phosphorus nucleus.

Conversely (12) was isolated as a colourless, crystalline solid in *ca.* 66% yield after recrystallisation from petroleum ether. Characterisation was provided by elemental analysis, infrared and mass spectrometry (Chapter 7, section 7.4.9), ^1H, ^{31}P and ^{13}C NMR spectroscopies and a single crystal X-ray diffraction study (*vide infra*).

The 250 MHz, ^1H NMR spectrum of (12) in d^6-benzene solvent (Figure 4.9) shows the α-methylene and β-methylene hydrogens as diastereotopic

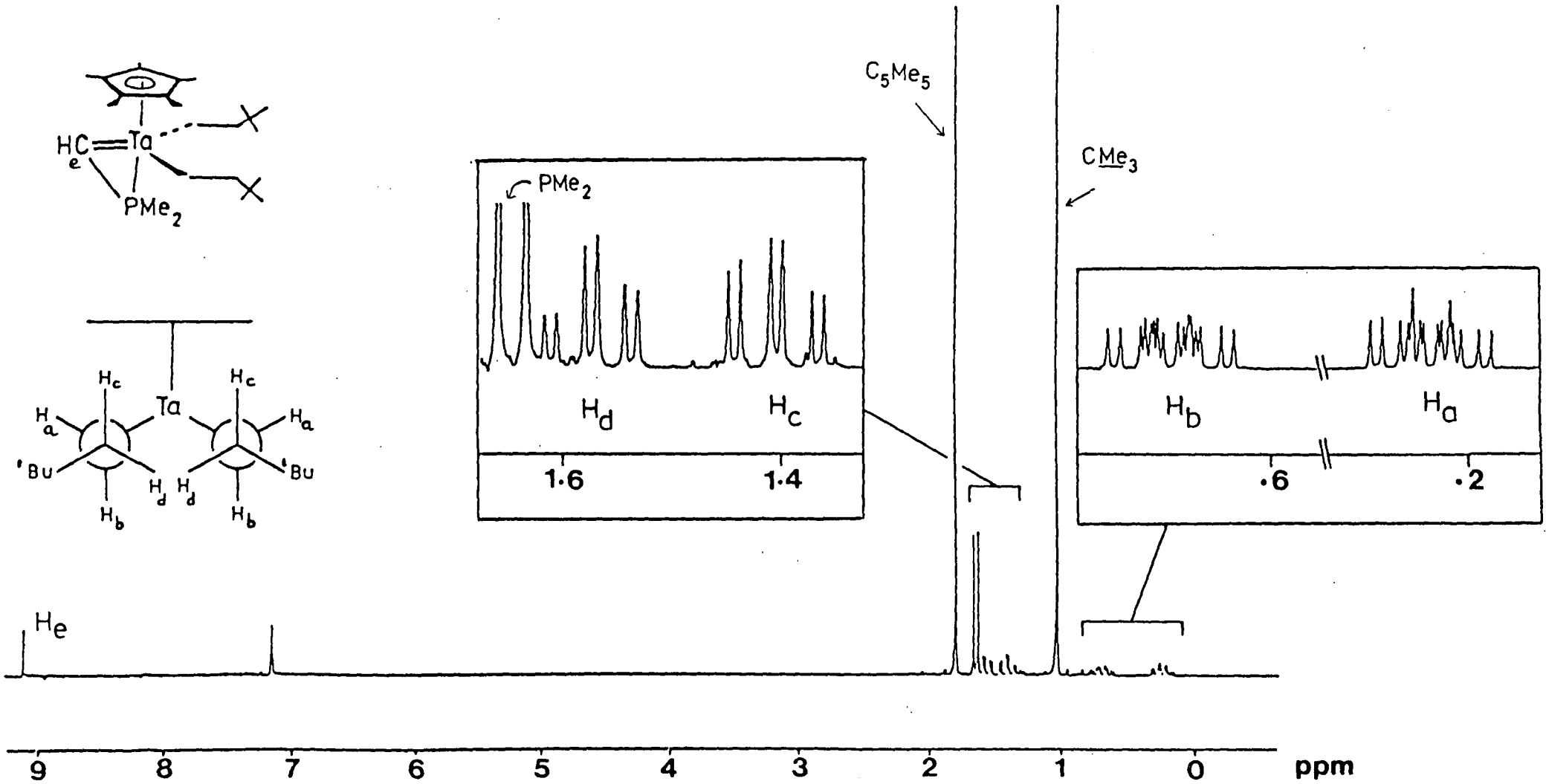

Figure 4.9 *^{1}H NMR Spectrum of (12) (250 MHz, d^6-benzene).*

pairs. The β-CH_2 signals centred at 1.53 ppm and 1.35 ppm respectively are triplets of doublets due to coupling to both *vicinial* and *geminal* hydrogens (Table 4.14). The α-CH_2 hydrogens resonate to lower frequency (0.64 ppm and 0.20 ppm respectively) and both have dddd splitting patterns due to coupling to the phosphorus nucleus (which resonates at -46.85 ppm in the $^{31}P\{^1H\}$ NMR spectrum), and both *geminal* and *vicinial* neohexyl hydrogens. For the purpose of explaining the ^1H NMR data the projection diagram shown in Figure 4.10 is particularly useful.

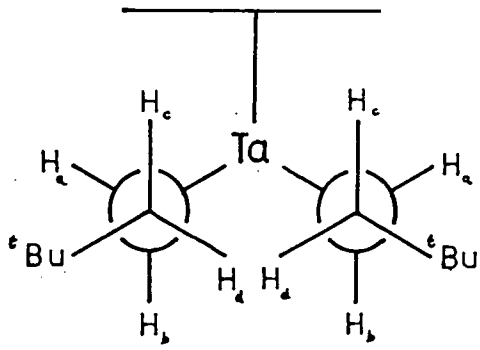

Figure 4.10 *Representation of Most Stable Conformation of (12).*

Difference NOE experiments suggest a conformationally rigid (Ta-CH_2) bond since irradiation of the (η^5-C_5Me_5) hydrogens results in a 2.5% enhancement of the α-CH_2 signal at 0.20 ppm whilst having no effect upon the other α-CH_2 resonance. Conversely, irradiation of the PMe_2 methyl resonance at 1.62 ppm (Table 4.14) selectively enhances the α-CH_2 signal at 0.64 ppm by 2.5% but does not affect the lower frequency, 0.20 ppm resonance.

These experiments permit the assignment of H_a at 0.20 ppm and H_b at 0.64 ppm (Figure 4.10). Neither experiment had any effect upon the β-CH_2 hydrogens H_c and H_d, but (η^5-C_5Me_5) irradiation did produce a strong enhancement (8.5%) of the methine hydrogen of the metallacycle

confirming that the orientation of this ligand is the same as in (1), with the CH terminus nearest to the Cp^* ring.

The coupling pattern observed between the α- and β-methylene hydrogens suggests there to be hindered rotation about the Cα-Cβ bond, such that $^3J(H_aH_c)$ = 4.0 Hz and $^3J(H_bH_d)$ = 4.1 Hz, whilst a non-rigorous examination of the *vicinial* and *geminal* Karplus correlations[21] indicates $^2J(H_cH_d) \approx {}^3J(H_bH_c) \approx {}^3J(H_aH_d)$. The fully assigned ^1H NMR spectral data for (13) are presented in Table 4.14 (*re.* Figure 4.10).

SHIFT (ppm)	REL.INT.	MULT.	J (Hz)	ASSIGNMENT
9.05	1	s	---	M=C<u>H</u>
1.79	15	s	---	C_5<u>Me_5</u>
1.62	6	d	$^2J(PH)$=8.9	P<u>Me_2</u>
1.53	2	td	$^3J(H_bH_d)$=4.1 $^3J(H_aH_d)$=13.4 $^2J(H_dH_c)$=13.4	H_d
1.35	2	td	$^3J(H_aH_c)$=4.0 $^3J(H_bH_c)$=13.7 $^2J(H_dH_c)$=13.7	H_c
1.00	18	s	---	t-<u>Bu</u>
0.64	2	dddd	$^3J(PH_b)$=10.8 $^3J(H_bH_d)$=4.1 $^3J(H_bH_c)$=13.9 $^2J(H_aH_b)$=12.2	H_b
0.20	2	dddd	$^3J(PH_b)$=9.9 $^3J(H_aH_c)$=4.0 $^3J(H_aH_d)$=13.3 $^2J(H_aH_b)$=12.2	H_a

Table 4.14 *^1H NMR Data For (12) (250 MHz, d^6-benzene).*

The ^{13}C NMR spectrum is consistent with the structure outlined in

Figure 4.10. The data are summarised in Table 4.15 and the spectrum is shown in Figure 4.11.

SHIFT (ppm)	MULT.	J (Hz)	ASSIGNMENT
204.88	dd	$^1J(CH)=166.9$ $^1J(PC)=58.9$	M=<u>C</u>H
112.53	s	---	<u>C</u>$_5$Me$_5$
53.92	t	$^1J(CH)=116.8$	-CαH$_2$- ‡
44.66	t	$^1J(CH)=124.6$	-CβH$_2$- ‡
34.02	s	---	-<u>C</u>(CH$_3$)$_3$
15.83	qd	$^1J(CH)=125.4$ $^1J(PC)=17.5$	P<u>Me</u>$_2$
29.61	q	$^1J(CH)=123.9$	-C(<u>C</u>H$_3$)$_3$
10.97	q	$^1J(CH)=126.9$	C$_5$<u>Me</u>$_5$

Table 4.15 *$^{13}C\{^1H\}$-NMR Data For (12) (d^6-benzene); ‡Assigned by Selective Proton Decoupling Expts.*

Inert atmosphere solutions of (12) in aromatic or aliphatic hydrocarbons are stable to decomposition over several weeks at room temperature, whilst solid samples remain unchanged over several months in an argon-filled drybox.

Solutions of (12) in d^6-benzene decompose slowly at 50°C to liberate both neohexene and neohexane (^{1}H NMR). It appears that the relatively high barrier to β-elimination in this formally electronically unsaturated dialkyl complex is related to the rigidity of the alkyl substituents in solution such that interligand steric interactions prevent the ready attainment of a conformation suitable for β-elimination. A similar explanation has been offered for the stability of the complex, Cr^tBu_4[22].

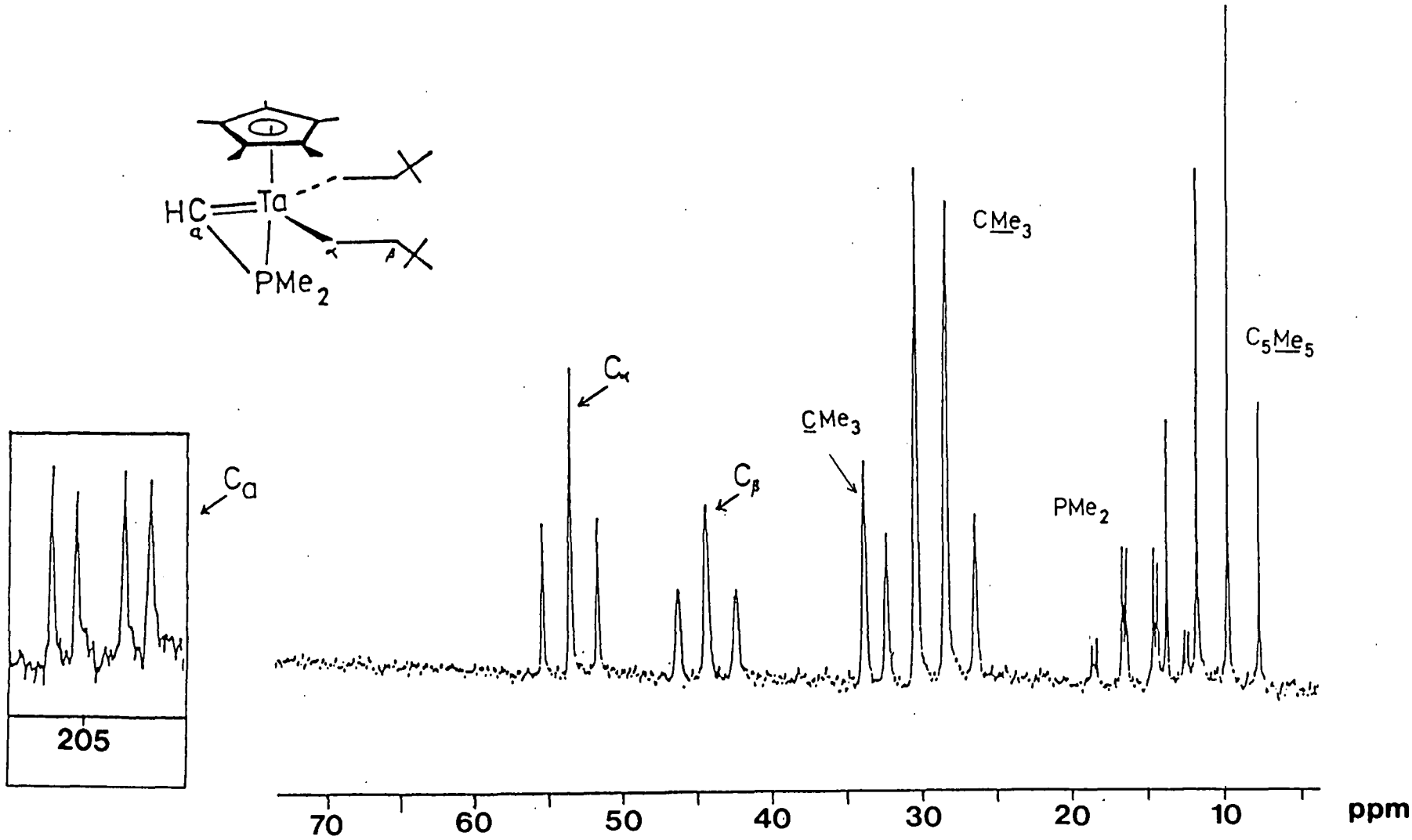

Figure 4.11 *^{13}C NMR Spectrum of (12) (d^6-benzene).*

$\underline{C}Me_3$ Not Shown

4.6.3 The Molecular Structure of $Cp^*Ta(CH_2CH_2CMe_3)_2(\eta^2\text{-}CHPMe_2)$ (12)

Colourless prisms of (12) were obtained by prolonged cooling of a saturated petroleum ether solution at -35°C. A crystal of dimensions 0.19 x 0.23 x 0.38 mm, mounted in a Lindemann capillary was chosen for study. The data were collected and analysed by Dr. W. Clegg of the University of Newcastle-upon-Tyne (Appendix 1E) and the results are described below. The molecular structure is illustrated in Figures 4.12 and 4.13 and selected bond distances and angles are given in Table 4.16.

The coordination sphere of (12) consists of a η^5-coordinated (C_5Me_5) ligand, two neohexyl ligands and a three membered $Ta(\eta^2\text{-}CHPMe_2)$ metallacycle. Consideration of the ($\eta^5\text{-}C_5Me_5$) ligand reveals average C(ring)-C(ring), C(ring)-C(methyl) and C(ring)-Ta distances of 1.407(1)Å, 1.521(7)Å and 2.449(7)Å respectively.

A comparison of the metallacycle parameters of (12) and (1) (Table 4.17) shows there to be essentially no difference in the inter-ligand angles. The tantalum-carbon distances, x are not statistically different, the tantalum-phosphorus distance (y) is slightly longer for (12) but the phosphorus-carbon distances (z) are essentially identical.

PARAMETER	(12)	(1)
x†	1.983(13)	2.005(10)
y†	2.501(2)	2.480(2)
z†	1.715(13)	1.714(9)
α‡	43.1(4)	43.4(3)
β‡	84.8(6)	83.2(4)
ϕ‡	52.1(4)	53.4(3)

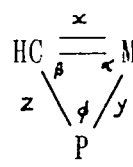

Table 4.17 *Comparison of Metallacycle Parameters between (12) and (1); †=distance (Å); ‡=degrees (°).*

Unfortunately, one of the neohexyl ligands shows disorder with

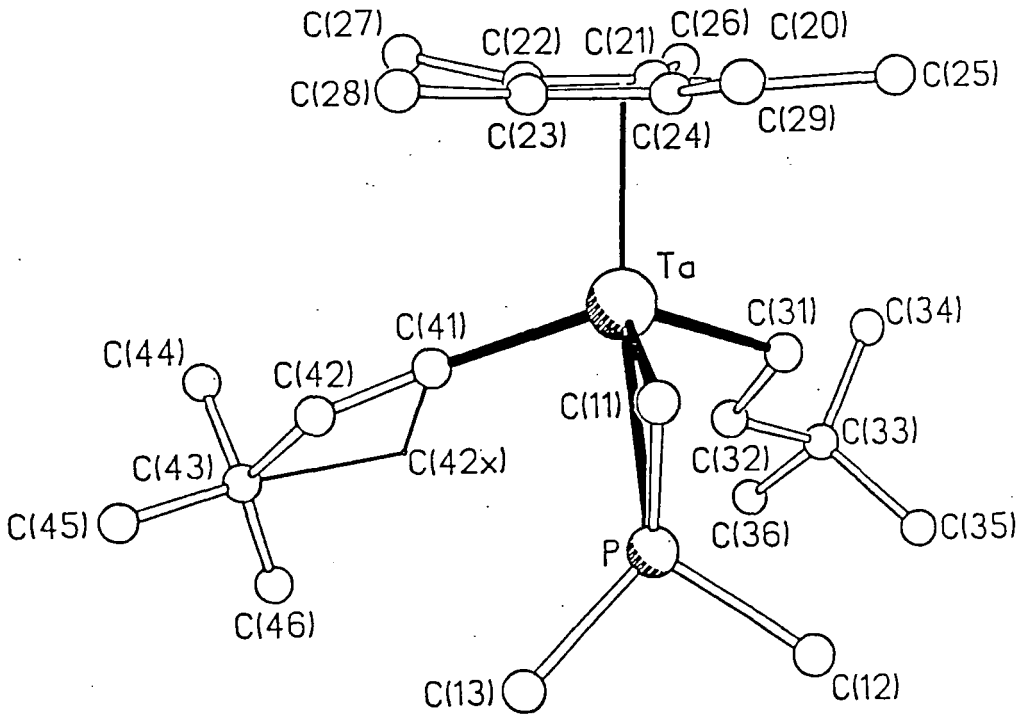

Figure 4.12 *The Molecular Structure of (12).*

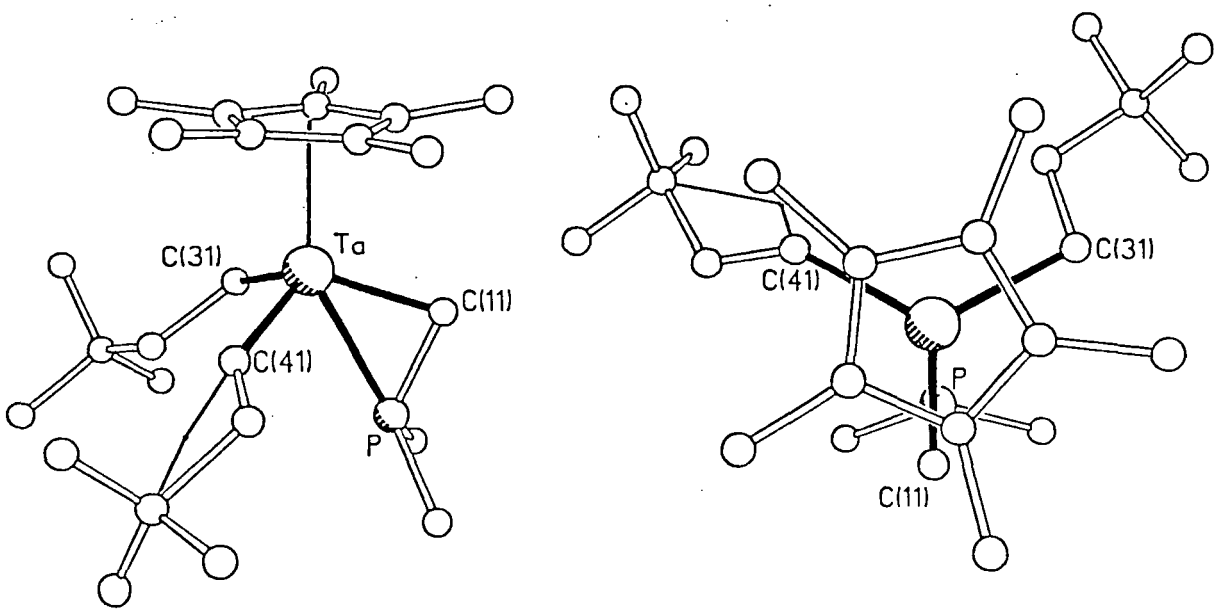

Figure 4.13 *View of (12) down the ring centroid-tantalum vector.*

Ta-P	2.501(2)	C(11)-Ta-C(22)	108.1(4)
		C(11)-Ta-C(41)	109.5(6)
Ta-C(11)	1.983(13)		
Ta-C(20)	2.448(10)	C(11)-P-C(12)	114.6(6)
Ta-C(21)	2.457(9)	C(11)-P-C(13)	113.6(7)
Ta-C(22)	2.467(11)	C(12)-P-C(13)	100.8(6)
Ta-C(23)	2.424(11)		
Ta-C(24)	2.449(12)	Ta-C(11)-P	84.8(6)
Ta-C(31)	2.242(11)	Ta-C(20)-C(25)	123.1(7)
Ta-C(41)	2.184(16)	Ta-C(31)-C(32)	111.2(7)
		Ta-C(21)-C(26)	122.8(9)
P-C(11)	1.715(13)	Ta-C(22)-C(27)	127.7(10)
P-C(12)	1.841(10)	Ta-C(23)-C(28)	123.1(9)
P-C(13)	1.838(11)	Ta-C(24)-C(29)	126.0(8)
		Ta-C(41)-C(42)	145.3(20)
C(20)-C(21)	1.409(16)	Ta-C(41)-C(42x)	133.2(16)
C(20)-C(24)	1.406(15)		
C(20)-C(25)	1.505(14)	C(31)-C(31)-C(33)	114.9(9)
C(21)-C(22)	1.412(14)	C(32)-C(33)-C(34)	110.8(10)
C(21)-C(26)	1.532(22)	C(34)-C(33)-C(35)	111.3(12)
C(22)-C(23)	1.404(19)	C(34)-C(33)-C(36)	107.4(13)
C(22)-C(27)	1.540(16)	C(32)-C(33)-C(35)	111.7(12)
C(23)-C(24)	1.406(15)	C(32)-C(33)-C(36)	105.1(11)
C(23)-C(28)	1.515(19)	C(35)-C(33)-C(36)	110.3(12)
C(24)-C(29)	1.511(21)	C(41)-C(42)-C(43)	119.9(28)
C(31)-C(32)	1.542(22)	C(41)-C(42x)-C(42)	59.1(21)
C(32)-C(33)	1.546(17)	C(41)-C(42)-C(42x)	53.6(20)
C(33)-C(34)	1.505(18)	C(41)-C(42x)-C(43)	117.5(23)
C(33)-C(35)	1.519(17)	C(42)-C(42x)-C(43)	62.1(18)
C(33)-C(36)	1.558(28)	C(42x)-C(42)-C(43)	70.1(22)
C(41)-C(42)	1.277(31)	C(42)-C(43)-C(44)	106.5(20)
C(41)-C(42x)	1.198(40)	C(42)-C(43)-C(45)	92.3(31)
C(42)-C(42x)	1.373(48)	C(42)-C(43)-C(42x)	47.8(17)
C(42)-C(43)	1.639(41)	C(42x)-C(43)-C(44)	106.4(16)
C(42x)-C(43)	1.743(30)	C(42x)-C(43)-C(45)	134.7(28)
C(43)-C(44)	1.431(26)	C(42x)-C(43)-C(46)	91.2(25)
C(43)-C(45)	1.499(53)	C(42)-C(43)-C(46)	130.5(25)
C(43)-C(46)	1.376(52)	C(42)-C(41)-C(42x)	67.3(24)
		C(44)-C(43)-C(45)	105.2(23)
P-Ta-C(11)	43.1(4)	C(44)-C(43)-C(46)	111.9(31)
P-Ta-C(22)	160.0(3)	C(45)-C(43)-C(46)	106.1(35)
P-Ta-C(24)	122.3(3)		
P-Ta-C(31)	84.3(3)		
P-Ta-C(41)	87.5(4)		
Ta-P-C(11)	52.1(4)		
Ta-P-C(12)	127.8(4)		
Ta-P-C(13)	131.3(4)		

Table 4.16 *Selected Distances (Å) and Angles (°) for Cp*Ta(CH$_2$CH$_2$CMe$_3$)$_2$(η^2-CHPMe$_2$) (12).*

carbon atom C(42) existing with approximately equal probability in sites C(42) and C(42x) (Figure 4.12) and rather erratic bond distances and angles with large e.s.d values. Therefore, we shall confine the discussion of the alkyl substituents to the non-disordered, neohexyl ligand.

The tantalum-carbon distance [Ta-C(31)] of 2.242(11)Å is within the range of tantalum-carbon single bonds in tantalum(V) complexes[23] (*ca.* 2.2-2.3Å) and is *ca.* 0.26Å longer than the [Ta-C(11)] bond which is formally a double bond. C(31)-C(32) and C(32)-C(33) distances of 1.542(22)Å and 1.546(17)Å respectively, agree well with the calculated covalent carbon-carbon distance of 1.54Å[24]. The distances within the t-butyl group are slightly shorter [1.527(16)Å average] but are comparable to those in other ^{t}butyl containing ligands[23d]. The angles within the ^{t}butyl group are tetrahedral (average 109.6^{o}) whilst ∠C(31)C(32)C(33) and ∠TaC(31)C(32) are slightly larger at 114.9(9)^{o} and 111.2(7)^{o} respectively. As formulated in Figure 4.10, the conformation about the C(31)-C(32) bond is staggered with the metal and ^{t}butyl ligands adopting mutually *trans* positions due undoubtedly to the bulk of these substituents. The dihedral angle between the planes defined by Ta-C(31)-C(32) and C(31)-C(32)-C(33) is only 3.8^{o}. The hydrogen atoms were not located in the crystal structure determination.

Of particular relevance to the solution behaviour of **(12)** is the degree of rotation that is sterically allowed about the Ta-C(31) and C(31)-C(32) bonds. Certainly there does not appear to be any hindrance to free rotation of the ^{t}butyl group as illustrated in Figure 4.13, but allowing all other parameters to remain fixed, complete rotation about the Ta-C(31) bond brings C(32) to within *ca.* 2.4Å of the ring methyl substituent C(26)[25]. Since the carbon-carbon Van der Waals distance is *ca.* 3.4Å, free rotation about the Ta-C(31) bond is clearly inhibited in

accordance with the solution ^{1}H NMR data. Similarly, rotation about the C(31)-C(32) bond brings the ^{t}butyl methyl carbons to within *ca.* 2.9Å of C(26), again implying a steric constraint to free rotation.

4.6.4 Reactions of $Cp^*Ta(PMe_3)HX(\eta^2\text{-}CHPMe_2)$ With Olefins: Selective, Catalytic Dimerisation of Ethylene to But-1-ene (X=Br,I)

The complexity of the reaction of (1) with ethylene involving the generation of new olefinic species prompted us to investigate the interactions of olefins with $Cp^*Ta(PMe_3)HX(\eta^2\text{-}CHPMe_2)$ [X = Br (3), I (4)] where the presence of only one hydride ligand was envisaged to lead to fewer side reactions and the potential for exploiting a chiral metal environment.

Both (3) and (4) cleanly reacted with a variety of olefins to afford an equilibrium mixture composed solely of either (3) or (4) and the corresponding alkyl complex formed from insertion of the olefin into the metal hydride bond (Equation 4.10).

$$Cp^*Ta(PMe_3)HX(\eta^2\text{-}CHPMe_2) + CH_2{=}CHR \underset{}{\overset{K_{ol}}{\rightleftharpoons}} Cp^*Ta(CH_2CH_2R)X(\eta^2\text{-}CHPMe_2) + PMe_3 \quad (4.10)$$

X=Br, I;
R=H, Me, tBu, Ph

In all cases, with the exception of ethylene, the equilibrium constants, K_{ol} were less than unity and no attempt was made to isolate the resulting alkyl complexes. Attempts to isolate the ethyl complexes were unsuccessful presumably due to the facility of the β-hydrogen elimination reaction. The equilibrium constants, K_{ol} in Equation 4.10 were measured at 296K by ^{1}H NMR spectroscopy, and are collected in Table 4.18.

OLEFIN	K_{ol}†	
	(3)	(4)
$CH_2=CH_2$	8.7(2)	2.1(1)
$CH_2=CHMe$	$3.5(2)\times10^{-2}$	$5.0(4)\times10^{-3}$
$CH_2=CH^tBu$	$1.1(1)\times10^{-1}$	$1.3(1)\times10^{-2}$
$CH_2=CHPh$	$5.2(2)\times10^{-3}$	$1.9(1)\times10^{-4}$
$CH_2=CMe_2$	‡	‡

Table 4.18 *K(ol) Values for the interaction of (3) and (4) with Olefins; †=average of three determinations; ‡=too small to measure.*

Analysis of the K_{ol} values reveals that for each olefin, K_{ol} (3) > K_{ol} (4) and that for both (3) and (4), the order of decreasing K_{ol} is:

$$CH_2=CH_2 > CH_2=CH^tBu > CH_2=CHMe > CH_2=CHPh > CH_2=CMe_2$$

A closer examination of Equation 4.10 reveals that K_{ol} is formally the product of three equilibrium constants as illustrated in Scheme 4.6.

$$\underset{(3)/(4)}{Cp^*Ta(PMe_3)HX(\eta^2\text{-}CHPMe_2)} + CH_2=CHR \overset{K_1}{\rightleftharpoons} \underset{+\ PMe_3}{Cp^*Ta(CH_2=CHR)HX(\eta^2\text{-}CHPMe_2)} \quad (I)$$

$$Cp^*Ta(CH_2=CHR)HX(\eta^2\text{-}CHPMe_2)\ (I) \overset{K_2,k_2}{\underset{k_{-2}}{\rightleftharpoons}} Cp^*Ta(CH_2CH_2R)X(\eta^2\text{-}CHPMe_2)\ (II)$$

$$Cp^*Ta(CH_2CH_2R)X(\eta^2\text{-}CHPMe_2)\ (II) + PMe_3 \overset{K_3}{\rightleftharpoons} Cp^*Ta(PMe_3)(CH_2CH_2R)X(\eta^2\text{-}CHPMe_2)\ (III)$$

Scheme 4.6

By ^1H NMR spectroscopy it appears that species (II) and (III) are in rapid equilibrium since only a single set of resonances is observed and the free PMe_3 signal is only slightly shifted from its usual position indicating that K_3 is very small. Therefore, K_{ol} may be approximated to $(K_1.K_2)$. The intermediate olefin complexes (I) are not

observable by ^{1}H NMR spectroscopy reflecting the low stability of d^0 olefin complexes.

The magnitude of K_1 will probably be most strongly affected by steric factors (cf. section 4.2.3), such that K_1 should decrease as:

$$\begin{matrix} & & & & (3) & > & (4) & \\ CH_2{=}CH_2 & > & CH_2{=}CHMe & > & CH_2{=}CHPh & > & CH_2{=}CH^tBu \end{matrix}$$

The above order is essentially that observed apart from an unusually high K_{o1} value for $CH_2{=}CH^tBu$. Presumably this results from a significantly large K_2 value.

Bercaw and co-workers have studied the mechanism of olefin insertion into a hydride ligand in early transition metal systems[26] (Equation 4.11).

$$Cp^*_2Nb(H)(CH_2{=}CHR) \underset{k_{-1}}{\overset{k_1}{\rightleftharpoons}} [Cp^*_2Nb(CH_2CH_2R)] \qquad (4.11)$$
$$R{=}H,\ Me,\ Ph$$

In these systems the alkyl tautomers were not observed by ^{1}H NMR which suggested that $k_{-1} \geq 100\ k_1$. Similarly, in Scheme 4.6, the fact that the olefin-hydride tautomers (I) are not observed establishes $k_2 \geq 100\ k_{-2}$ and consequently K_2 is large.

It was further demonstrated for Equation 4.11 that the rate of olefin insertion (k_1) increases as the steric bulk of R increases presumably due to destabilisation of the olefin complex. Electronic effects were shown to be dominant in the transition state such that the β-carbon atom (that atom to which the hydride ligand migrates) develops a partial positive charge and the hydride ligand migrates more nearly as H^- than as H^+. Consequently, the insertion reaction proceeds most rapidly with those substituents, R, best able to stabilise a developing positive charge at the β-carbon atom *viz.* k_1 decreases as Me > Ph > H.

Therefore, in Scheme 4.6 it is anticipated that k_2 will be largest

for the most bulky, electron releasing R substituent, ^{t}butyl, leading to a large equilibrium constant, K_2 capable of offsetting the low value of K_1 for this olefin. The equilibrium, K_{o1} is then seen to be sensitive to both steric and electronic effects.

Olefin (and acetylene) insertion into a metal hydride bond has been shown to proceed with net *cis* stereochemistry[27]. Consistently, *cis* addition to (3) and (4) has been specifically demonstrated by the insertion of phenylacetylene into the metal-hydride bond of (3) to afford the σ-vinyl complex (Scheme 4.7).

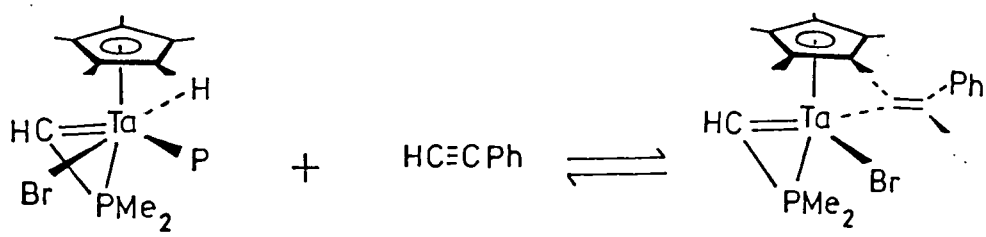

Scheme 4.7 *Reaction of (3) with PhC≡CH.*

The vicinial coupling $^{3}J(H_1H_2)$ of 18.8 Hz is indicative of a *trans* geometry for the vinyl ligand ($^{3}J(HH)_{cis}$ *ca.* 6-12 Hz)[21]. The ^{1}H NMR spectral data for this complex and the alkyl derivatives (II) in Scheme 4.6 are collected in Appendix 3.

Interestingly, each olefin gave a single insertion product, implying that when a choice of either Markovnikov or anti-Markovnikov addition is available, regioselective insertion occurs to afford the primary alkyl complex. This has been specifically demonstrated for neohexene by the isolation of $Cp^{*}Ta(CH_2CH_2CMe_3)_2(\eta^2\text{-}CHPMe_2)$ (section 4.6.2) and is inferred for propene by the observation of a triplet resonance for the propyl methyl substituent in $Cp^{*}Ta(Pr)Br(\eta^2\text{-}CHPMe_2)$ (Appendix 3) consistent with an n-propyl group. A doublet signal would

have been expected for the i-propyl product.

Presumably, the regioselective insertion reflects the mode of olefin coordination in the chiral hydrido-olefin precursor (Figure 4.14).

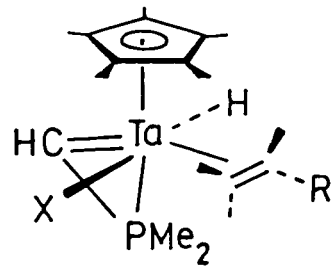

Figure 4.14 *Coordination of CH_2=CHR to [Cp*TaHX(η^2-CHPMe$_2$)].*

Steric interactions between the olefin substituent R, and both the ring methyl substituents and the halogen atom X, are expected to force the olefin to bind as shown above. Consequently, insertion *via* anti-Markovnikov addition leads to the sterically favoured primary alkyl product[28]. The prohibitive effect of steric interactions between olefin substituents and ring methyl substituents is clearly demonstrated by the lack of reactivity of methylpropene even upon prolonged thermolysis at 80°C, whereas propene reacts readily with both (3) and (4). Similar regioselective insertions in $Cp^*_2Nb(H)(CH_2=CHR)$ compounds were attributed to steric control of olefin coordination[26].

It has been shown that the ethyl complexes, $Cp^*Ta(CH_2CH_3)X(\eta^2$-$CHPMe_2)$ (X = Br, I) are stable only under an atmosphere of ethylene. However, heating the equilibrium mixture of (3) and excess ethylene (typically 5 equivalents) at 70°C for several hours resulted in the clean, selective dimerisation of ethylene to but-1-ene (^{1}H NMR). The reaction is catalytic in $Cp^*Ta(CH_2CH_3)Br(\eta^2$-$CHPMe_2)$ although catalysis

is slow, giving only 5.5 turnovers in 3.5h. using an initial 20 fold excess of ethylene. Destruction of the catalyst occurred only after the ethylene had been exhausted at which point, new olefinic resonances were seen in the ^{1}H NMR spectrum believed to be due to the isomerisation of but-1-ene to but-2-ene. The rate of dimerisation was reduced when the reaction was performed in a donor solvent (d^{8}-tetrahydrofuran). Scheme 4.8 presents a reasonable mechanism for the dimerisation reaction.

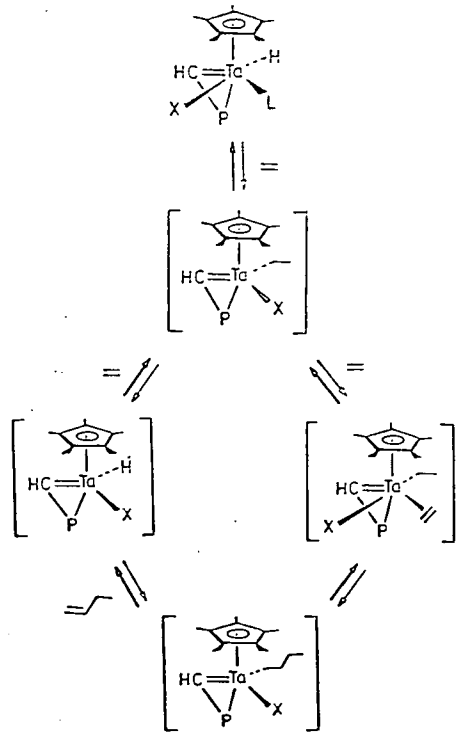

Scheme 4.8 *Proposed Mechanism for Dimerisation of Ethylene to But-1-ene.*

No intermediates could be detected by ^{1}H NMR spectroscopy, presumably they are too unstable under the conditions employed. The rate limiting step in Scheme 4.8 is probably olefin insertion into the metal-carbon bond of (a) to form the ^{n}butyl complex (b)[29]. Subsequently, β-hydrogen elimination from (b) produces but-1-ene specifically and the unsaturated hydride complex (c). Since ethylene is present in greater concentrations than but-1-ene, and substituted

olefins are sterically more hindered towards complexation[26], (c) will be trapped more effectively by ethylene than but-1-ene rendering the system inactive towards isomerisation until the ethylene has been exhausted. This mechanism is formally analogous to the Cossee mechanism[30] of Ziegler-Natta olefin polymerisation, the important carbon-carbon bond forming step of which has been specifically demonstrated[31]. There is no indication for olefin attack at the metallacycle which would result in destruction of this moiety.

4.7 SUMMARY

Various aspects of the chemistry of $Cp^*Ta(PMe_3)(H)_2(\eta^2\text{-}CHPMe_2)$ (1) have been investigated and are summarised in Scheme 4.9. Reversible hydrogen migrations cannot be observed on the NMR timescale but α-hydrogen migrations are promoted by the presence of the reagents dmpe and CO.

(1) reacts with MeX (X = Cl, Br, I) with elimination of methane to afford halogen derivatives in which the novel $Ta(\eta^2\text{-}CHPMe_2)$ metallacycle is retained. In contrast, unsaturated substrates (isocyanates, CO_2 and olefins) preferentially undergo insertion reactions with (1) as illustrated in Scheme 4.9. The product arising from insertion of neohexene is particularly noteworthy as being a rare example of a coordinatively unsaturated alkyl complex containing β-hydrogen atoms which is stable to decomposition up to 50°C. NMR and crystallographic studies provide no conclusive evidence for an "agostic" M-C-H interaction and suggest that this complex is sterically inhibited from assuming a conformation suitable to undergo β-hydrogen elimination.

The halo-derivative, $Cp^*Ta(PMe_3)HBr(\eta^2\text{-}CHPMe_2)$ has been shown to

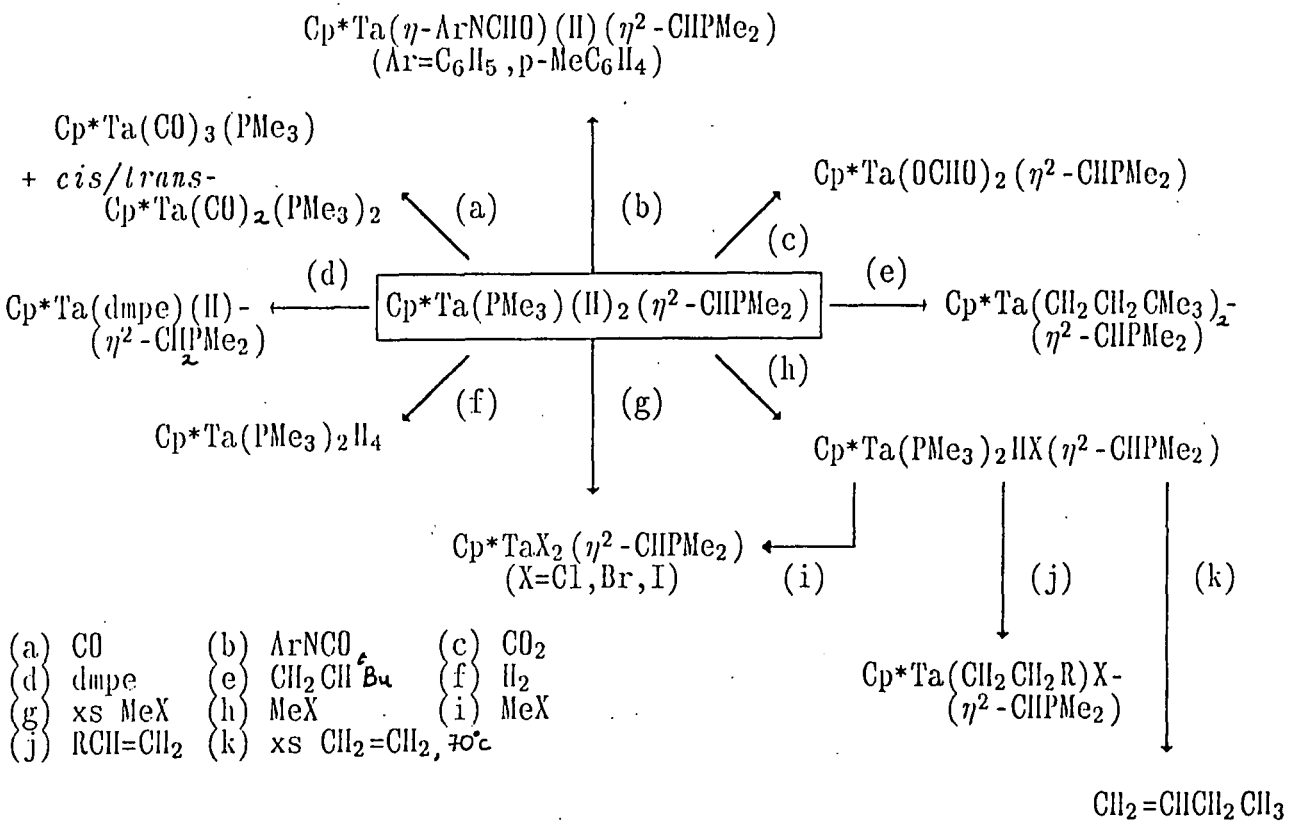

Scheme 4.9 *Some Reactions of Cp*Ta(PMe₃)(H)₂(η²-CHPMe₂).*

catalyse the dimerisation of ethylene to but-1-ene *via* a mechanism that is best formulated involving direct insertion of ethylene into a metal carbon bond (Cossee-type mechanism).

4.8 REFERENCES

1. J.W. Rathke and E.L. Muetterties, *J.Am.Chem.Soc.*, 1975, 97, 3272.
2. A. Van Assett, B.J. Burger, V.C. Gibson and J.E. Bercaw, *J.Am. Chem.Soc.*, 1986, 108, 5347.
3. H.W. Turner, R.R. Schrock, J.D. Fellman and S.J. Holmes, *J.Am. Chem.Soc.*, 1983, 105, 4942.
4. E.D. Becker, "*High Resolution NMR Theory and Chemical Applications*", 2nd Edition, Academic Press, New York (1980), Chapter 11.
5. M.L.H. Green, P.M. Hare and J.A. Bandy, *J.Organometallic Chem.*, 330, 61.
6. C.A. Tolman, *Chem.Rev.*, 1977, 77, 313.
7. R.G. Pearson, *Chem.Brit.*, 1967, 3, 103.
8. J.M. Mayer and J.E. Bercaw, *J.Am.Chem.Soc.*, 1982, 104, 2157.
9. V.C. Gibson, C.E. Graimann, P.M. Hare, M.L.H. Green, J.A. Bandy, P.D. Grebenik and K. Prout, *J.Chem.Soc.Dalton Trans.*, 1985, 2025.
10. (a) *trans*-$Cp^*Ta(CO)_2(PMe_3)_2$ - see reference 8.

    (b) *cis*-$Cp^*Ta(CO)_2(PMe_3)_2$ - see Chapter 2, section 2.4.8.

    (c) $Cp^*Ta(CO)_3(PMe_3)$ - see Chapter 2, section 2.4.10.
11. P.T. Wolczanski and J.E. Bercaw, *Acc.Chem.Res.*, 1980, 13, 121.
12. G. Smith, R.R. Schrock, M.R. Churchill and W.J. Youngs, *Inorg. Chem.*, 1981, 20, 387.
13. J.D. Wilkins, *J.Organometallic Chem.*, 1974, 67, 269.
14. D. Lyons, G. Wilkinson, M. Thorton-Pett and M.B. Hursthouse, *J.Chem.Soc.Dalton Trans.*, 1984, 695.
15. J.P. Collman, L.S. Hegedus, J.R. Norton and R.G. Finke, "*Principles and Applications of Organotransition Metal Chemistry*", University Science Books, California (1987).

16. B. Beguin, B. Denise and R.P.A. Sneedon, *J.Organometallic Chem.*, 1981, 208, C18.

17. C. Bianchini, C.A. Ghilardi, A. Meli, S. Midallini and A. Orlandini, *J.Organometallic Chem.*, 1983, 248, C13.

18. D.J. Darensbourg, M.B. Fischer, R.E. Schmidt Jr. and B.J. Baldwin, *J.Am.Chem.Soc.*, 1981, 103, 1297.

19. R.P.A. Sneedon, "*Comprehensive Organometallic Chemistry*", Edited by G. Wilkinson, F.G.A. Stone and E.W. Abel, Pergamon, New York (1982), Volume 8, Chapter 50.4.

20. H.W. Turner and R.R. Schrock, *J.Am.Chem.Soc.*, 1982, 104, 2331.

21. R.M. Silverstein, G.C. Bassler and T.C. Morrill, "*Spectrometric Identification of Organic Compounds*", John Wiley, New York (1981), page 208.

22. W. Kruse, *J.Organometallic Chem.*, 1972, 42, C39.

23. (a) L.J. Guggenberger and R.R. Schrock, *J.Am.Chem.Soc.*, 1975, 97, 6578.

    (b) R.R. Schrock, L.W. Messerle, C.D. Wood and L.J. Guggenberger, *J.Am.Chem.Soc.*, 1978, 100, 3793.

    (c) L.W. Messerle, P. Jennische, R.R. Schrock and G. Stucky, *J.Am.Chem.Soc.*, 1980, 102, 6744.

    (d) M.R. Churchill and H.J. Wasserman, *Inorg.Chem.*, 1981, 20, 2899.

24. J.E. Huheey, "*Inorganic Chemistry: Principles of Structure and Reactivity*", 3rd Edition, Harper, New York (1983).

25. Modelling studies performed by Mr. D.N. Williams using the COSMIC program.

26. N.M. Doherty and J.E. Bercaw, *J.Am.Chem.Soc.*, 1985, 107, 2670.

27. See for example: J.A. Labinger, D.W. Hart, W.E. Seibert (III) and J. Schwartz, *J.Am.Chem.Soc.*, 1975, 97, 3851.

28. J. Halpern, *Inorg.Chim.Acta*, 1985, 100, 41.

29. G.F. Schmidt and M. Brookhart, *J.Am.Chem.Soc.*, 1985, 107, 1443.

30. P. Cossee, *J.Catal.*, 1964, 3, 80.

31. P.L. Watson, *J.Am.Chem.Soc.*, 1982, 104, 337.

CHAPTER FIVE

STUDIES ON OXO. ALKOXO AND TERTIARY PHOSPHINE COMPOUNDS OF NIOBIUM AND TANTALUM.

5.1 INTRODUCTION

5.1.1 General

Oxo complexes play a central role in a variety of laboratory, industrial and biological oxidation processes[1]. Progress towards understanding the reactivity of the metal-oxo moiety in these systems is largely dependent upon the availability of convenient and generally applicable routes to complexes through which the properties of the oxo ligand can be addressed. However, useful starting materials such as metal oxyhalides have not been generally available *via* mild synthetic procedures.

In this chapter we describe the use of the commercially available compounds, Me_3SiOR (R = $SiMe_3$, Me, Et) as sources of the oxo and alkoxo functionalities for the convenient, high yield syntheses of oxyhalide and alkoxyhalide compounds of niobium and tantalum.

Subsequent derivatisation of $Nb(O)Cl_3$ by both tertiary phosphine and aryloxide ligands has allowed access to a range of complexes through which the structural and chemical properties of the [Nb=O] moiety may be addressed.

5.1.2 Me_3SiXR compounds as a source of 'X' and 'XR'

It was envisaged that Me_3SiOR (R = alkyl, $SiMe_3$) compounds would react with metal halides to form metal alkoxides or metal oxides according to Equations 5.1 and 5.2.

$$Me_3SiOR + [M]\text{-}Cl \rightleftharpoons Me_3SiCl + [M]\text{-}OR \qquad (5.1)$$

$$(Me_3Si)_2O + [M]\text{-}Cl_2 \rightleftharpoons 2Me_3SiCl + [M]{=}O \qquad (5.2)$$

This strategy receives considerable precedence from the chemistry of alkoxysilanes and disiloxanes. For example, tetraalkoxysilanes have been used to introduce an alkoxy moiety into the coordination sphere of boron (Equation 5.3)[2].

$$(^{n}BuO)_4Si + BCl_3 \xrightarrow{25^{o}C} (^{n}BuO)_3SiCl + {}^{n}BuOBCl_2 \qquad (5.3)$$

Further, Emeléus has demonstrated that $(R_3Si)_2O$ compounds react with BCl_3, presumably *via* an initial 1:1 adduct, to afford the corresponding trialkylsiloxyboron dichloride which subsequently decomposes at room temperature to afford B_2O_3 (Equation 5.4)[3].

$$(Me_3Si)_2O + BCl_3 \xrightarrow{-78^{o}C} [(Me_3Si)_2OBCl_3] \xrightarrow{-78^{o}C} Me_3SiOBCl_2 + Me_3SiCl$$

$$3Me_3SiOBCl_2 \xrightarrow{25^{o}C} 3Me_3SiCl + BCl_3 + B_2O_3 \qquad (5.4)$$

Although the trialkylsiloxyboron dihalides are not very stable under ambient conditions, the aluminium analogues (prepared by analogous procedures) are quite stable crystalline substances which may be distilled under vacuum[4].

In this laboratory, the use of $(Me_3Si)_2O$ for the convenient, high yield syntheses of transition metal oxo compounds has been demonstrated through the syntheses of Group 6 oxyhalides (Equations 5.5 - 5.7)[5].

$$WCl_6 + (Me_3Si)_2O \xrightarrow[25^{o}C]{CH_2Cl_2} \underset{99\%}{W(O)Cl_4} + 2Me_3SiCl \qquad (5.5)$$

$$W(O)Cl_4 + (Me_3Si)_2O \xrightarrow[ca.100^{o}C]{Pet.Ether} \underset{95\%}{W(O)_2Cl_2} + 2Me_3SiCl \qquad (5.6)$$

$$Mo(O)Cl_4 + (Me_3Si)_2O \xrightarrow[25^{o}C]{CH_2Cl_2} \underset{97\%}{Mo(O)_2Cl_2} + 2Me_3SiCl \qquad (5.7)$$

To our knowledge, the only previously reported use of silyl ethers for

the preparation of transition metal oxyhalides concerns the synthesis of $W(O)Cl_4$ by the reaction in Equation 5.8[6].

$$WCl_6 + Me_3SiOMe \xrightarrow[25^oC]{CH_2Cl_2} W(O)Cl_4 + Me_3SiCl + MeCl \qquad (5.8)$$

Furthermore, this synthetic strategy has recently been extended to hexamethyldisilthiane, $(Me_3Si)_2S$ and heptamethyldisilazane, $(Me_3Si)_2NMe$, facilitating the introduction of sulphido and methylimido moieties into the metal coordination sphere (Equations 5.9 - 5.11).

$$WCl_6 + (Me_3Si)_2S \xrightarrow[-78^oC]{CH_2Cl_2} W(S)Cl_4 + 2Me_3SiCl \ ^{7} \qquad (5.9)$$

$$TiCl_4 + (Me_3Si)_2S \longrightarrow Ti(S)Cl_2 + 2Me_3SiCl \ ^{8} \qquad (5.10)$$

$$SbCl_5 + (Me_3Si)_2NMe \xrightarrow[25^oC]{CH_2Cl_2} Sb(NMe)Cl_3 + 2Me_3SiCl \ ^{9} \qquad (5.11)$$

An important consideration in the synthetic strategy represented by Equations 5.1 and 5.2 concerns the reversibility of the process such that, for example, Me_3SiCl may react with a metal oxide to give a metal chloride and a disiloxane. Indeed, reactions of this nature have been used as synthetic routes to disiloxanes and to deoxygenate transition metal compounds (Equations 5.12 - 5.14).

$$2Et_3SiBr + ZnO \longrightarrow ZnBr_2 + (Et_3Si)_2O \ ^{10} \qquad (5.12)$$

$$Cp^*_2W(O) + 2Me_3SiCl \longrightarrow Cp^*_2WCl_2 + (Me_3Si)_2O \ ^{11} \qquad (5.13)$$

$$Cp^*Re(O)_3 + Me_3SiCl \xrightarrow{Ph_3P} Cp^*ReCl_4 + OPPh_3 + (Me_3Si)_2O \ ^{12} \qquad (5.14)$$

A consideration of bond dissociation energies[13] shows that the (Si-O) to (Si-Cl) conversion is endothermic by *ca.* 70 kJ mol^{-1}. In the absence of relevant values for the corresponding (M-Cl) and (M-O) fragments, this energy deficit is likely to be partly compensated by entropy (two

volatile Me_3SiCl molecules are generated in Equation 5.2) and the use of higher reaction temperatures. A further consideration is the low solubility of the product oxyhalide which may be deposited from solution and prevent appreciable back-reaction with Me_3SiCl.

Conversely, the (Si-S) to (Si-Cl) conversion is exothermic by *ca.* 90 kJ mol^{-1} and under similar conditions would be expected to proceed more readily than (Si-O) to (Si-Cl). This is supported by the observation that reactions of $(Me_3Si)_2S$ with metal halides are noticeably exothermic and proceed rapidly under ambient conditions[7] whereas the corresponding reactions with $(Me_3Si)_2O$ often require more forcing conditions.

5.2 SYNTHESIS OF ALKOXYHALIDES AND OXYHALIDES OF NIOBIUM AND TANTALUM

5.2.1 Reaction of $NbCl_5$ with Me_3SiOR (R=Me, Et, $SiMe_3$): Preparation and Characterisation of $[NbCl_4(OR)]_2$.

Niobium pentachloride reacted readily with equimolar amounts of Me_3SiOR (R = Me, Et, $SiMe_3$) in dichloromethane solvent at room temperature leading to dissolution of the starting halide and the formation of colourless or pale yellow solutions. White, crystalline, thermally sensitive solids of general formula $[NbCl_4(OR)]_2$ were isolated from these solutions for R = Me (1) and Et (2) (Equation 5.15).

$$2NbCl_5 + 2Me_3SiOR \longrightarrow [NbCl_4(OR)]_2 + 2Me_3SiCl \qquad (5.15)$$

R=Me (1), Et (2), $SiMe_3$ (3)

Unfortunately, it did not prove possible to isolate $[NbCl_4(OSiMe_3)]_2$ (3) under ambient conditions without partial decomposition due to its

thermal sensitivity. However the tantalum analogue of (3) is more stable and has been satisfactorily characterised (see section 5.2.2). Compounds (1) and (2) have been characterised by elemental analysis, infrared, NMR and mass spectroscopies. They are formulated as dimeric species on the basis of low resolution CI^+ mass spectrometry which locates ions at m/e 529 and m/e 531 for (1) and (2) respectively, which may be assigned to the fragments $[M_2+H]^+$ and $[M_2-C_2H]^+$. The solution instability of these compounds precluded accurate molecular weight measurements.

Presumably, both (1) and (2) possess edge-shared bioctahedral geometries by analogy to the crystallographically defined compounds $NbCl_5$[14] and $Nb(OMe)_5$[15]. However, the available data do not allow the unequivocal distinction between alkoxide and halide bridges. Although it has been suggested that phenoxy bridges prevail in $[NbCl_4.OPh]_2$[16], this does not appear to be the case for (1) and (2): infrared spectroscopy reveals bands assignable to ν(Nb-O) at 595 cm^{-1} and 580 cm^{-1} respectively which are consistent with terminal alkoxo groups[17]. The chloro ligands are then presumed to occupy the bridging sites. An X-ray structural analysis is presently in progress on (1) to resolve these details.

Compound (1) had been previously prepared according to Equation 5.16, and although postulated as being dimeric, no characterising data were provided[18].

$$NbCl_5 + SO(OMe)_2 \xrightarrow{CCl_4} 1/2[NbCl_4(OMe)]_2 + SO_2 + MeCl \qquad (5.16)$$

5.2.2 Reaction of $TaCl_5$ with Me_3SiOR (R=Me, Et, $SiMe_3$): Preparation and Characterisation of $[TaCl_4(OR)]_2$.

Tantalum pentachloride was found to react in an analogous manner to

niobium pentachloride with the alkoxysilanes, Me_3SiOR (R = Me, Et, $SiMe_3$) to afford the colourless, crystalline compounds $[TaCl_4(OR)]_2$ [R = Me (4), Et (5), $SiMe_3$ (6)] in high yields.

Characterisation was again provided by elemental analysis, infrared, NMR and mass spectroscopies (Chapter 7, section 7.5). In particular, the mass spectrum of (5) locates a highest mass ion at m/e 733 corresponding to $[M_2+H]$ and suggesting a dimeric formulation as established for $[NbCl_4(OR)]_2$ (*vide supra*). Although fragments assignable to dimeric species were not observed for (4) and (6), it is likely that they are dimeric by analogy to $[NbCl_4(OR)]_2$ and comparison of infrared data, which display terminal ν(Ta-O) absorptions[17] at 582 cm^{-1}, 569 cm^{-1} and 633 cm^{-1} for (4), (5) and (6) respectively. Presumably, as for the niobium analogue, the chloro ligands bridge the two metal centres.

Although $[NbCl_4(OSiMe_3)]_2$ is thermally unstable under ambient conditions the tantalum analogue is stable enough to isolate and characterise. Particularly characteristic of a metal coordinated siloxide is the resonance observed at 0.52 ppm [$^2J(SiH)$ = 6.4 Hz][19] in the 250 MHz ^1H NMR spectrum, which is displaced 0.41 ppm to higher frequency of the signal in $(Me_3Si)_2O$.

5.2.3 The Synthesis of $Nb(O)Cl_3$ (7)

It was reported in section 5.2.1 that the tetrachloroalkoxides $[NbCl_4(OR)]_2$ [R = Me (1), Et (2), $SiMe_3$ (3)] were insufficiently stable in solution for molecular weight determinations. The thermal instability of these compounds arises due to their facile decomposition to $Nb(O)Cl_3$ (7) with liberation of RCl (Equation 5.17).

$$[NbCl_4(OR)]_2 \xrightarrow[(CH_2Cl)_2]{80^oC} 2Nb(O)Cl_3 + 2RCl \qquad (5.17)$$

(R= Me, Et, $SiMe_3$)

The thermal instability of $[NbCl_4(OMe)]_2$ had been previously noted but was not investigated[20].

Of the compounds (1)-(3), (3) is the least stable, slowly releasing Me_3SiCl in solution (dichloromethane) at room temperature to give an off-white deposit of $Nb(O)Cl_3$. Similar, albeit slower decomposition occurs in the solid state.

Since the decomposition of (3) is cleaner at 80°C, $Nb(O)Cl_3$ may be synthesised directly in good yield (*ca.* 75%) by the treatment of $NbCl_5$ with $(Me_3Si)_2O$ in 1,2-dichloroethane solvent at 80°C according to equation 5.18.

$$NbCl_5 + (Me_3Si)_2O \xrightarrow[(CH_2Cl)_2]{80^oC} \underset{75\%}{Nb(O)Cl_3} + 2Me_3SiCl \qquad (5.18)$$

The $Nb(O)Cl_3$ produced by this method frequently contained minor organic contamination (see section 5.3) but this did not prove troublesome in subsequent transformations.

Previous syntheses of $Nb(O)Cl_3$ have been found to require either forcing or delicately balanced reaction conditions. A selection of such syntheses is presented in Equations 5.19-5.22.

$$3NbCl_5 + Nb_2O_5 \xrightarrow[Melt.]{250^oC} 5Nb(O)Cl_3 \ ^{21} \qquad (5.19)$$

$$Nb_2O_5 + 3CCl_4 \xrightarrow{200^oC} 2Nb(O)Cl_3 + 3C(O)Cl_2 \ ^{22} \qquad (5.20)$$

$$2NbCl_5 + O_2 \xrightarrow{150^oC} 2Nb(O)Cl_3 + 2Cl_2 \ ^{23} \qquad (5.21)$$

$$NbCl_5.OEt_2 \xrightarrow[3.5h]{90^oC} Nb(O)Cl_3 + 2EtCl \quad ^{23} \qquad (5.22)$$

The use of silyl ethers as a source of oxygen atoms affords a convenient synthetic route to $Nb(O)Cl_3$ which proceeds under more mild and controllable conditions than those mentioned above.

5.2.4 The Syntheses of $Nb(O)Cl_3L_2$ [L = CH_3CN (8), THF (9)]

Treatment of niobium pentachloride with $(Me_3Si)_2O$ in acetonitrile solvent at room temperature, afforded a colourless solution from which colourless crystals of $Nb(O)Cl_3(CH_3CN)_2$ (8) were isolated in 95% yield. Characterisation was provided by elemental analysis and infrared spectroscopy. In particular, a strong absorption at 960 cm^{-1} may be assigned to the ν(Nb=O) stretching vibration of a terminal niobium oxo double bond[24], which contrasts the bridging oxo ligands in polymeric $Nb(O)Cl_3$[22] which absorb at 780 cm^{-1}.

(8) is very sensitive to moisture. Thus exposure to air for *ca.* 30 sec. resulted in complete decomposition and the formation of bridging oxo ligands as evidenced by the presence of strong, broad absorptions between 600-900 cm^{-1} in the infrared spectrum.

The synthesis described here offers a direct route to the acetonitrile complex (8) which has been previously prepared only by dissolving $Nb(O)Cl_3$ (prepared by any of the methods described in sections 5.2.3) in acetonitrile[25]. The molecular structure of (8) showed it to be monomeric with a *cis*-meridional arrangement of acetonitrile and chloro ligands (Figure 5.1)[25]. The analogous treatment of $NbCl_5$ with $(Me_3Si)_2O$ in THF solvent did not afford $Nb(O)Cl_3(THF)_2$ (9) cleanly, possibly due to non-innocent participation of THF, which under certain circumstances is known to undergo oxygen abstraction[26].

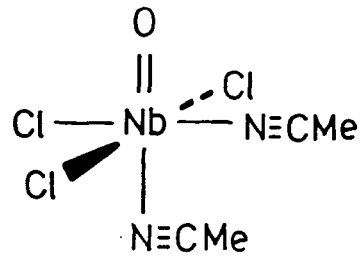

Figure 5.1 *Molecular Structure of* $Nb(O)Cl_3(CH_3CN)_2$.

Instead, (9) was obtained in 90% yield by the dissolution of (8) in THF. The product crystallised as colourless crystals upon addition of cold, light petroleum ether. Characterisation was provided by elemental analysis and infrared spectroscopy (Chapter 7, section 7.5). A strong band at 960 cm^{-1} in the infrared spectrum is consistent with a terminal (Nb=O) moiety[24], and the similarity of niobium-chlorine stretching frequencies below 400 cm^{-1} suggests that (8) and (9) are isostructural.

Complex (9) has not been previously reported, although the existence of $Nb(O)Cl_3(OEt_2)_2$ in solution was proposed on the basis of solution infrared measurements [965 cm^{-1}, ν(Nb=O)] and a shift in the ^1H NMR resonances of Et_2O upon complexation[27].

The preparations of (8) and (9) are summarised in Scheme 5.1.

$$NbCl_5 + (Me_3Si)_2O \xrightarrow[RT/2h.]{CH_3CN} Nb(O)Cl_3(CH_3CN)_2 \quad (8)$$

$$\Big\downarrow \text{THF/15 min.}$$

$$NbCl_5 + (Me_3Si)_2O \xrightarrow{THF} Nb(O)Cl_3(THF)_2 \quad (9)$$

Scheme 5.1 *Syntheses of (8) and (9)*

5.2.5 Attempted Synthesis of $Ta(O)Cl_3$

Of the Group 5 oxyhalides, $Ta(O)Cl_3$ has proved the most elusive; only two reports of a successful synthesis have been published

(Equations 5.23 and 5.24).

$$TaCl_5.OEt_2 \xrightarrow[17h.]{65^oC} Ta(O)Cl_3 + 2EtCl \quad ^{23} \qquad (5.23)$$

$$TaCl_5 + OCl_2 \xrightarrow[CCl_4]{-30^oC} Ta(O)Cl_3 + 2Cl_2 \quad ^{28} \qquad (5.24)$$

The successful preparation of $Nb(O)Cl_3$ described in section 5.2.3 prompted us to attempt the synthesis of $Ta(O)Cl_3$ using a similar strategy.

A variety of reactions were performed including the thermal decomposition of $[TaCl_4(OR)]_2$ (R = Me, Et, $SiMe_3$) in both chlorocarbons and aliphatic hydrocarbon solvents under various conditions of temperature and reaction time, and the direct reaction of $TaCl_5$ with $(Me_3Si)_2O$ at elevated temperatures in different solvents. In each case, an off-white powder was produced which contained strong broad infrared absorptions between 600-900 cm^{-1}, as expected for bridging (Ta-O-Ta) units but, unfortunately, consistent elemental analyses could not be obtained for these materials due to the incorporation of organic contaminants. Although similar observations were made in the synthesis of $Nb(O)Cl_3$, the degree of contamination is much greater in the tantalum system.

5.3 REACTION OF METAL HALIDES WITH Me_3SiOR (R=Me, Et, $SiMe_3$): MECHANISTIC ASPECTS.

5.3.1 General Aspects

The reaction of a metal halide with Me_3SiOR (R = Me, Et, $SiMe_3$) reagents is presumed to proceed according to Scheme 5.2.

$$MCl_n + Me_3SiOR \longrightarrow [Cl_nM.OR(SiMe_3)] \quad (a)$$

$$[Cl_nM.OR(SiMe_3)] \longrightarrow MCl_{n-1}OR \quad (b) + Me_3SiCl$$

$$MCl_{n-1}OR \longrightarrow M(O)Cl_{n-2} + RCl$$

Scheme 5.2 *Reaction of Metal Halides With Siloxanes*

The formation of an initial 1:1 adduct (a) in these reactions is assumed by analogy to the BCl_3 and $AlCl_3$ systems mentioned in section 5.1.2. However, in the reactions of niobium and tantalum pentachlorides with siloxanes these adducts did not prove isolable, presumably they are unstable towards condensation of Me_3SiCl and formation of metal alkoxides or siloxides (b). In the cases where M = Nb, Ta and R = Me, Et (Scheme 5.2), the corresponding alkoxides are the final products of reaction at room temperature. However, at elevated temperatures, they can be induced to undergo a second condensation reaction to afford the oxyhalide, $M(O)Cl_x$. The ease of this second condensation step follows the sequence: M=Nb; R=$SiMe_3$ > M=Ta; R=$SiMe_3$ > M=Nb; R=Me,Et > M=Ta; R=Me,Et.

5.3.2 Preparations of $M(O)Cl_3$ (M = Nb, Ta)

In section 5.2.3 it was noted that the thermal decomposition of $[NbCl_4(OR)]_2$ (R = Me, Et, $SiMe_3$) produced $Nb(O)Cl_3$. It was further observed that the product consistently contained traces of residual alkoxide or siloxide functionalities, although the degree of contamination was reduced by the use of a higher pyrolysis temperature.

It is presumed that this contamination results from the mode of decomposition of dimeric $[NbCl_4(OR)]_2$ (section 5.2.1) to polymeric $[Nb(O)Cl_3]_n$[22] illustrated in Scheme 5.3.

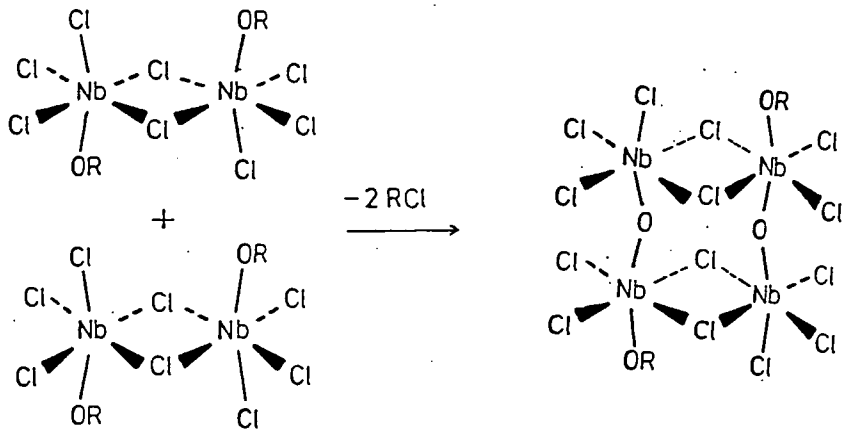

Scheme 5.3 *Schematic illustration of the Decomposition of* $[NbCl_4(OR)]_2$.

As condensation of RCl continues to augment the developing polymer chains so they become increasingly desolubilised and consequently precipitation may become competitive with condensation. The product obtained therefore retains a fraction of its alkoxide or siloxide "head-groups". At elevated temperatures, both the solubility and the rate of condensation are increased resulting in a product containing a relatively lower proportion of organic impurity.

An alternative explanation for the above observations, involving the back-reaction of $Nb(O)Cl_3$ with RCl may be rejected since heating a 1,2-dichloroethane suspension of the $Nb(O)Cl_3$ product with excess Me_3SiCl (*ca.* 5 equivalents) at 80^oC for 3h. gave no increase in the proportion of Me_3SiO groups incorporated into the product (infrared). Presumably this is a result of the low solubility of polymeric $[Nb(O)Cl_3]_n$. In the attempted synthesis of $Ta(O)Cl_3$, the degree of organic contamination was greater than for niobium, probably as a result of the somewhat higher thermal stability of the intermediate alkoxides and siloxide such that the rate of condensation of RCl is slower. Consequently, precipitation of the growing polymer chain of $Ta(O)Cl_3$ may

compete more effectively with condensation. Temperatures higher than 70°C were not employed due to the reported thermal instability of $Ta(O)Cl_3$[23].

5.3.3 Thermal Decomposition of $MCl_5.OEt_2$ (M=Nb,Ta)

In Scheme 5.2, an initial etherate complex was envisaged to decompose *via* a tetrachloroalkoxide or siloxide, to afford $M(O)Cl_3$ (M = Nb, Ta). Although the $MCl_5.OR(SiMe_3)$ adducts were not isolated, Fairbrother and Cowley have described the syntheses of $MCl_5.OEt_2$[29] (M = Nb, Ta) and demonstrated that they decompose to the oxytrichlorides with condensation of EtCl (Equation 5.25)[23].

$$MCl_5.OEt_2 \xrightarrow[\text{Reduced Pressure}]{\Delta} M(O)Cl_3 + 2EtCl \qquad (5.25)$$

M=Nb; 90°C; 3.5h.
M=Ta; 65°C; 17h.

In an attempt to observe the presumed intermediate alkoxides, the pyrolyses of $MCl_5.OEt_2$ were monitored by ^1H NMR spectroscopy in d-chloroform solvent.

Decomposition of $NbCl_5.OEt_2$ did not occur below 90°C, but after 35h. at 90°C *ca.* 70% of the etherate complex had decomposed to generate EtCl but no evidence of alkoxide species was obtained. This is due to the lower stability of the intermediate alkoxides with respect to the etherate, and is confirmed by the observation that $[NbCl_4(OEt)]_2$ undergoes complete decomposition to $Nb(O)Cl_3$ within 6h. at 70°C (*cf.* section 5.2.3).

Conversely, $TaCl_5.OEt_2$ decomposed at 60°C in d-chloroform again liberating EtCl but also producing broad, poorly resolved ^1H NMR signals at 5.56 ppm and 5.43 ppm assignable to the methylene hydrogens of tantalum ethoxide species. The broadness of these signals may indicate

the presence of fluxional, oligomeric compounds.

Therefore, whilst unambiguous identification of intermediate $[MCl_4(OEt)]_2$ was not obtained, the intermediacy of thermally unstable alkoxides has been demonstrated, thus highlighting the mechanistic similarities between $MCl_5.OEt_2$ and $MCl_5.OR(SiMe_3)$ decompositions.

5.4 PREPARATION OF $Nb(O)(OAr)_3$ [Ar=2,6-$Me_2C_6H_3$ (10) and 2,6-$^tBu_2C_6H_3$ (11)]

Despite the potential applications of oxyalkoxides to catalyse, for example, the polymerisation of cyclic esters[30] and the epoxidation of cyclic olefins[31], there is a paucity of data on the heavier Group 5 derivatives. Compounds of the form $Nb(O)Cl_n(OR)_{3-n}$ have been prepared by alcoholysis reactions of $Nb(O)Cl_3$[32], and the base stabilised complexes, $M(O)Cl_n(OR)_{3-n}(DMSO)_2$ (M = Nb, Ta) were obtained upon treatment of $MCl_2(OR)_3$ with DMSO[33].

In this laboratory it has been demonstrated that $W(O)Cl_4$ undergoes clean metathetical exchange with lithium aryloxide reagents according to Equation 5.26[34].

$$W(O)Cl_4 + 4LiOAr \xrightarrow[25^oC]{Toluene} W(O)(OAr)_4 + 4LiCl \qquad (5.26)$$

Ar = 2,6-$^iPr_2C_6H_3$
2,4,6-$Me_3C_6H_2$
2,6-$Me_2C_6H_3$

With minor modifications, this strategy has been found to be applicable to the syntheses of $Nb(O)(OAr)_3$; Ar = 2,6-$Me_2C_6H_3$ (10) and 2,6-$^tBu_2C_6H_3$ (11) [Equations 5.27 and 5.28].

$$Nb(O)Cl_3(CH_3CN)_2 + 3LiOAr \xrightarrow[65^oC/5h.]{Toluene} \underset{77\%}{Nb(O)(OAr)_3} + 3LiCl \qquad (5.27)$$

Ar = 2,6-$Me_2C_6H_3$ (10)

$$Nb(O)Cl_3(CH_3CN)_2 + 3LiOAr \xrightarrow[2.RT/16h]{1.Et_2O/-40^oC} \underset{72\%}{Nb(O)(OAr)_3} + 3LiCl \quad (5.28)$$

Ar = 2,6-$^tBu_2C_6H_3$ (11)

Both (10) and (11) are yellow, moisture sensitive, crystalline compounds. The t-butylphenoxide complex is more soluble in aromatic and aliphatic hydrocarbon solvents than the methylphenoxide derivative and is the less hygroscopic of the two. Elemental analysis (Chapter 7, section 7.5) confirmed the stoichiometry of (10) and (11).

Mass spectrometry (CI^+) reveals protonated parent ions for (10) and (11) at m/e 473 and m/e 725 respectively.

The 250 MHz, ^1H NMR spectra of (10) and (11) indicate the presence of coordinated aryloxide ligands which occupy equivalent solution environments at room temperature. In both cases, single resonances are obtained for the methyl or t-butyl substituents and an AB_2 [for (10)] or AX_2 [for (11)] pattern for the aromatic hydrogens. The $^{13}C\{^1H\}$ NMR data are consistent with these observations.

In the absence of crystallographic and molecular weight studies, the infrared spectra of (10) and (11) are quite informative. A strong, broad absorption at 895 cm^{-1} (that is not present in the parent phenol) may be assigned to a terminal ν(Nb=O) vibration[24] in (11). Unfortunately, several bands in in the region 915-874 cm^{-1} preclude the unambiguous assignment of the ν(Nb=O) vibration for (10), but the absence of strong, broad absorptions in the region[24] 800-600 cm^{-1} suggests that (10) also possesses a terminal oxo ligand. Furthermore, the presence of bands at 572 cm^{-1} and 565 cm^{-1} for (10) (again absent in the parent phenol) are consistent with terminal aryloxide ligands[16] (bridging phenoxide ligands absorb < 550 cm^{-1}). The more sterically encumbered t-butylphenoxide ligands in (11) are also assumed to be terminally coordinated although the infrared spectrum in the region of

ν(Nb-O) vibrations is more complex than for (10).

Therefore it is anticipated that both (10) and (11) will possess monomeric, trigonal pyramidal structures similar to that of the recently reported complex, $Nb(O)(N(SiMe_3)_2)_3$[26].

5.5 PREPARATION AND CHARACTERISATION OF TERTIARY PHOSPHINE ADDUCTS OF $Nb(O)Cl_3$

Simple adducts of $M(O)Cl_3$ (M = Nb, Ta) have been previously described containing a variety of donor ligands including NR_3[35], RCN[25], R_3PO[36], R_3AsO[36], DMSO[37], HMPA[38] and bipyridine[39]. To date however, no adducts with tertiary phosphine ligands have been reported.

It was envisaged that the molecular structure and the nature of the metal-oxo bond in adducts of the type, $M(O)Cl_3L_n$ would be sensitive to both the nature of L and the value of n.

This section describes the synthesis and characterisation of several tertiary phosphine complexes of $Nb(O)Cl_3$ in which the metal-oxo moiety is indeed found to be remarkably sensitive to its coordination environment.

5.5.1 Adducts of the type $Nb(O)Cl_3L_2$ (L = PMe_3, PEt_3, PPh_2Me, PPh_3)

Compounds of the type $Nb(O)Cl_3L_2$ were prepared by the two procedures outlined in Equations 5.29 and 5.30 (full preparative details are given in Chapter 7, section 7.5).

$$Nb(O)Cl_3 + 2PR_3 \xrightarrow[25^oC/12h]{CH_2Cl_2} Nb(O)Cl_3(PR_3)_2 \qquad (5.29)$$

R_3= Ph_3 (12), Ph_2Me (13), Et_3 (14)

$$Nb(O)Cl_3(THF)_2 + PR_3(xs) \xrightarrow[25^oC/12h]{CH_2Cl_2} Nb(O)Cl_3(PR_3)_2 \qquad (5.30)$$

$$R_3 = Me_3 \ (15)$$

The products (12)-(14) were isolated as moisture sensitive, yellow, crystalline solids upon removal of the volatile components and washing of the solid with a small quantity of light petroleum ether. Compound (15) was isolated as a white solid by filtration of the dichloromethane suspension. Characterisation was provided by elemental analysis, infrared, NMR and mass spectroscopies. Both (12) and (15) are not very hygroscopic indicating the tertiary phosphine ligands to be less labile than those of (13) and (14) which readily absorb moisture and decompose upon exposure (*ca.* 15-30 s) to moist air.

The infrared spectra of (12)-(15) were recorded over the range 4000-250 cm^{-1}. Apart from absorptions due to the tertiary phosphine ligands the spectra show bands assignable to metal-oxygen and metal-chlorine stretching modes. In particular, the strong absorptions at 939 cm^{-1} (12), 929 cm^{-1} (13), 930 cm^{-1} (14) and 923 cm^{-1} (15) are consistent with the presence of the terminal oxo ligand[24] and bands between *ca.* 310-380 cm^{-1} are assignable to (Nb-Cl) stretching vibrations[40].

The solubility properties of (15) are significantly different to those of (12)-(14). (15) is essentially insoluble in aromatic, aliphatic and chlorinated hydrocarbons. Also it is considerably more resistant to aerial hydrolysis than the others - the relative order of moisture sensitivity is (14) > (12) ≈ (13) > (15). These observations alone suggest that (15) is structurally dissimilar to the other derivatives, a hypothesis that is further supported by mass spectrometry. Specifically, the mass spectrum of (15) (CI^+,^{35}Cl) displays a fragment ion at m/e 604 attributable to a dimeric species whereas (12)-(14) show no peak to higher mass than the parent ion.

Thus, on the basis of the above data, and by analogy to the crystallographically defined complexes, $Nb(O)Cl_3L_2$ (L = CH_3CN[25], HMPA[38]) it is presumed that (12)-(14) are pseudo-octahedral monomers whereas (15) is a halogen-bridged dimer.

The 250 MHz ^1H NMR spectra (d-chloroform) of $Nb(O)Cl_3(PPh_3)_2$ (12) and $Nb(O)Cl_3(PPh_2Me)_2$ (13) consist of broadened resonances for the phenyl and methyl hydrogens suggesting the occurrence of ligand exchange on the NMR timescale. Similar observations were reported for the adduct $Nb(O)Cl_3(HMPA)_2$[38]. Consistently, the $^{31}P\{^1H\}$ NMR spectrum of (12) comprised a single broad band at 3.85 ppm ($\Delta\frac{1}{2}$ *ca.* 50 Hz) whilst (13) displayed no signal at all at room temperature. The low solubility of these complexes, however, precluded low temperature studies.

The complex $Nb(O)Cl_3(PEt_3)_2$ (14) displays unusual solution behaviour. The 250 MHz ^1H NMR data are collected in Table 5.1.

SHIFT (ppm)	REL.INT	MULT.	J (Hz)	ASSIGNMENT
4.01	1	m	J(PH)=18.6 J(HH)=6.0	$P_1CH\underline{H}H'$
3.02	1	m	J(PH)=7.2 J(HH)=6.0	$P_1CH\underline{H}H'$
2.46	4	dq	^{3}J(HH)=7.6 ^{2}J(PH)=12.8	$P_1\underline{CH_2}$
1.90	6	dq	^{3}J(HH)=7.7 ^{2}J(PH)=7.8	$P_2\underline{CH_2}$
1.33	9	dt	^{3}J(HH)=7.6 ^{3}J(PH)=18.7	$P_1CH_2\underline{CH_3}$
1.17	9	dt	^{3}J(HH)=7.8 ^{3}J(PH)=14.0	$P_2CH_2\underline{CH_3}$

Table 5.1 *^1H NMR Data for (14) (250 MHz, d-chloroform, 298K).*

One of the PEt_3 ligands appears to be normal, exhibiting a doublet of quartets signal at 1.90 ppm and a doublet of triplets resonance at 1.17

ppm assignable to the methylene and methyl hydrogens respectively. The second PEt_3 ligand is significantly different. The nine methyl hydrogens resonate at 1.33 ppm as a doublet of triplets whereas the six methylene hydrogens have become inequivalent. Four of these hydrogens (representing two equivalent Et groups) are found as a doublet of quartets at 2.46 ppm whilst two multiplets, each representing a single methylene hydrogen, are observed at 3.02 ppm and 4.01 ppm respectively, at considerably higher frequency than for normal PEt_3 methylene hydrogens (*ca.* < 2.0 ppm)[41].

These data are consistent with a solution state structure containing one normal coordinated PEt_3 ligand and a second PEt_3 ligand of which a single methylene group is held rigid, possibly by interactions either with the metal (agostic)[42] or the oxo ligand (hydrogen bond) as illustrated in Figure 5.2(a) and (b).

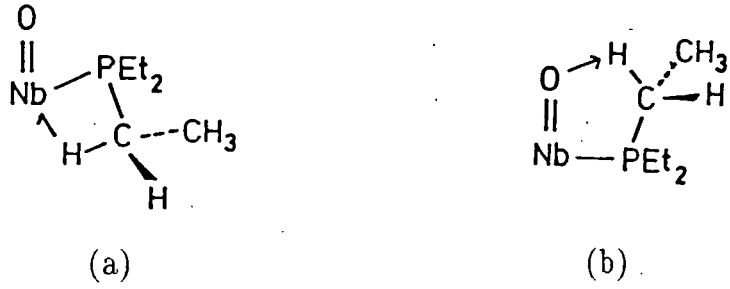

(a) (b)

Figure 5.2 *Possible Interactions in (14).*

Infrared spectroscopy provided no evidence for either of these interactions, but it is hoped that X-ray crystallographic studies will resolve these details.

Interestingly, the $^{31}P\{^1H\}$ NMR spectrum consists of a single, sharp resonance at 38.29 ppm implying that both phosphorus nuclei possess similar magnetic environments.

5.5.2 Adducts of the type $Nb(O)Cl_3(L\text{-}L)$ (L-L = dppe)

The complex $Nb(O)Cl_3(dppe)$ (16) was isolated in 97% yield, as a yellow crystalline solid from the reaction between $Nb(O)Cl_3$ and dppe in dichloromethane solvent at room temperature. Elemental analysis (Chapter 7, section 7.5.17) confirmed the stoichiometry and infrared spectroscopy indicated the presence of a terminal Nb=O ligand with $\nu(Nb{=}O) = 933\ cm^{-1}$. The complex is not as moisture sensitive as (12)-(14), no indication of hydrolysis or absorption of water was observed upon *ca.* 1 min. exposure to moist air.

The 250 MHz ^1H NMR spectrum (d-chloroform) reveals broad bands for the dppe hydrogens at 7.60 and 7.34 ppm (phenyl) and 2.72 ppm (methylene) possibly as a result of a fluxional process.

The mass spectrum (CI^+) did not reveal a parent ion. The highest mass at m/e 906 may be assigned to the ion $[Nb(OH)(dppe)_2]^+$ as no chlorine isotope pattern was observed for this peak.

Due to the similarity of the metal-chlorine stretching region in the infrared spectra of $Nb(O)Cl_3(CH_3CN)_2$ and (16), it is presumed that (16) has a similar octahedral geometry with a meridional arrangement of chloro ligands.

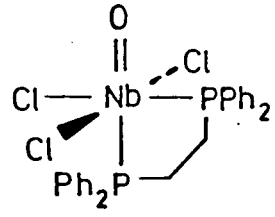

Figure 5.3 *Probable Geometry of (16).*

A closely related geometry is found in the chelate derivative $Nb(O)Cl_2(OEt)(bipy)$[39].

5.5.3 Adducts of the type $Nb(O)Cl_3L_3$ (L = PMe_3, PMe_2Ph)

The preparation of $Nb(O)Cl_3(PMe_3)_2$ (15) from the reaction of $Nb(O)Cl_3(THF)_2$ with PMe_3 was described in section 5.5.1. When the reaction is carried out using $Nb(O)Cl_3$, a trimethylphosphine complex of stoichiometry, $Nb(O)Cl_3(PMe_3)_3$ (17) is isolated in 79% yield.

This yellow, crystalline compound is moderately soluble in aromatic and chlorinated hydrocarbons and is highly moisture sensitive in contrast to (15). Exposure to moist air for *ca.* 15s. results in complete decomposition giving broad infrared absorptions between 600-900 cm^{-1} indicative of (M-O-M) bridging units[24] and a sharp band at 2410 cm^{-1} consistent with the generation of (P-H) bonds probably as $(HPMe_3)^+Cl^-$ [19]. The high moisture sensitivity of this complex reflects the lability of the PMe_3 ligands, which is also presumed to be the cause of the slightly low elemental analyses obtained for (17). Similar problems have been encountered with other PMe_3 complexes[43].

The infrared spectrum of (17) displays absorptions typical of coordinated PMe_3 at 1294 cm^{-1} [$\delta(CH_3)$], 953 cm^{-1} [$\rho(CH_3)$] and 743 cm^{-1} [$\nu_{as}(PC_3)$][44] respectively, and metal halide stretching vibrations are found in the region 270-350 cm^{-1}.

A most significant feature of the spectrum is the low value (882 cm^{-1}) observed for the ν(Nb=O) vibration. Previously characterised compounds containing terminal niobium oxo ligands invariably give absorptions > *ca.* 910 cm^{-1} [24]. The low value for (17) presumably reflects the high coordination number and the presence of three, sterically demanding, strongly basic PMe_3 ligands.

A single crystal, X-ray structural determination on (17) confirms that the complex is a seven coordinate monomer in which the coordination geometry may best be described as distorted, monocapped octahedral with

facial arrangements of chloro and trimethylphosphine ligands. The oxo ligand is in a site capping the P_3 face. A full description of the structure is presented in section 5.5.5.

The 250 MHz ^1H NMR spectrum of (17) (d-chloroform) locates the PMe_3 hydrogens as a slightly broadened doublet resonance at 1.43 ppm [$^2J(PH)$ = 8.6 Hz] suggesting equivalent solution environments for the phosphine ligands. The $^{31}P\{^1H\}$ NMR spectrum consists of a single, severely broadened band centred at -2.64 ppm ($\Delta\frac{1}{2}$ *ca.* 1000 Hz) possibly the result of ligand exchange.

The reaction between $Nb(O)Cl_3(CH_3CN)_2$ and PMe_3 in dichloromethane solvent proceeded differently to that observed for either $Nb(O)Cl_3$ or $Nb(O)Cl_3(THF)_2$. Thus, upon stirring the reactants at room temperature for 48h. a yellow-green solid was produced which was isolated by removal of the volatile components. Infrared spectroscopy of this crude material indicated it to be a mixture of two oxo complexes, one of which was (17). Dissolution of the crude mixture in toluene and cooling at -35°C for 2 days resulted in the selective crystallisation of the other component as green plates.

Elemental analysis confirmed the stoichiometry as $Nb(O)Cl_3(PMe_3)_3$ implicating an isomer of (17). Infrared spectroscopy revealed that this compound was essentially identical to (17) apart from a shift in the $\nu(Nb{=}O)$ stretching frequency of 11 cm^{-1} to lower wavenumber. The 250 MHz ^1H NMR spectrum consists of a single broad resonance at 1.24 ppm ($\Delta\frac{1}{2}$ *ca.* 30 Hz) while the $^{31}P\{^1H\}$ spectrum did not reveal any signal at room temperature.

Further, a single crystal X-ray diffraction study on the green isomer showed it to be isomorphous to the yellow isomer (17) with significant differences only in metal-oxygen and metal-chlorine parameters (see section 5.5.5). For discussion purposes, the yellow

isomer will be referred to as (17)-α and the green isomer (17)-β. It has been further demonstrated that pure (17)-α is converted to (17)-β slowly (days) at room temperature, upon stirring in either neat PMe_3 or dichloromethane. Extraction of the pale green residue with toluene followed by removal of the solvent and infrared analysis of the residue revealed the presence of (17)-β and a significant reduction in intensity of the signals due to (17)-α. The infrared spectrum also revealed broad bands at 840 cm^{-1} and 800 cm^{-1} assignable to (Nb-O-Nb) bridging units. Further, a broad resonance at 1080 cm^{-1} may be attributable to coordinated Me_3PO ligands (*cf.* $Nb(O)Cl_3(OPPh_3)_2$, 1070 cm^{-1})[45]. Similar bands are observed in the infrared spectrum of a sample of pure (17)-β after storage under argon for two months. The (17)-α to (17)-β conversion is presently the subject of further investigations.

The reaction between $Nb(O)Cl_3$ and PMe_2Ph in dichloromethane solvent at room temperature led to the isolation of a yellow, highly moisture sensitive crystalline compound. Due to the lability of the phosphine ligands, purification by recrystallisation from either dichloromethane or toluene solvents led to partial decomposition. Nevertheless, elemental analysis of freshly prepared samples indicated the complex to possess the stoichiometry, $Nb(O)Cl_3(PMe_2Ph)_3$ (18) (Chapter 7, section 7.5.20). The lower stability of (18) over (17) is consistent with the larger size and lower basicity of PMe_2Ph over PMe_3[46]. Repeated washing of a freshly prepared sample of (18) with petroleum ether (40-60^o) resulted in a residue whose composition was close to that of $Nb(O)Cl_3(PMe_2Ph)_2$.

The $^{31}P\{^1H\}$ NMR spectrum of (18) (d-chloroform) consists of a single broad resonance at -16.27 ppm ($\Delta\frac{1}{2}$ *ca.* 500 Hz; uncomplexed PMe_2Ph resonates at -47 ppm). Mass spectrometry reveals no fragment ions above m/e 215 (corresponding to $[Nb(OH)Cl_3]^+$). The presence of several bands

between 960-870 cm^{-1} in the infrared spectrum of (18) prevents an unambiguous assignment of the niobium oxygen stretching frequency, but the absence of broad bands between 870-750 cm^{-1} suggests that bridging oxo ligands[24] are not present. In the absence of further data therefore, we anticipate (18) to be monomeric, possibly of a similar geometry to (17).

5.5.4 Effect of Ligand, L on the ν(Nb=O) Vibrational Frequency in Complexes of the form, $Nb(O)Cl_3L_n$

Terminal ν(Nb=O) vibrational frequencies have been reported in the range 890-950 cm^{-1} [24], as strong, relatively sharp absorptions, whose frequency is sensitive to the metal coordination number and the nature of the ligand field[24]. The nature of the metal oxygen bonding may be rationalised qualitatively on the basis of the following canonical forms:

$$M{\rightarrow}O \text{ (a)} \leftrightarrow M{=}O \text{ (b)} \leftrightarrow M{\equiv}O \text{ (c)}$$

Here, the oxo ligand acts as a zero, two and four-electron donor respectively. Increasing the metal basicity would then be anticipated to lessen the contribution of canonical form (c) and result in a lowering of the ν(Nb=O) vibrational frequency. A similar rationale has been used to correlate ν(V=O) frequencies and consequently (V-O) force constants with the basicity of the ligand field in a range of oxo vanadium complexes[47]. Table 5.2 lists the ν(Nb=O) frequencies for a number of niobium complexes reported to contain terminal oxo ligands.

From the table it may be seen that, in general, the complexes with the higher coordination numbers have lower ν(Nb=O) frequencies. This is presumably the result of increased metal basicity and inter-ligand steric forces. Indeed the frequency of ν(Nb=O) for β-$Nb(O)Cl_3(PMe_3)_3$ at

871 cm^{-1} is the lowest such value reported for a terminal niobium-oxygen bond. All the pseudo octahedral complexes have ν(Nb=O) > *ca.* 920 cm^{-1} apart from $Nb(O)Cl_2(OPr^n)(bipy)$. It was presumed that in this complex significant pπ-dπ interactions between the metal and alkoxo groups reduced the contribution from canonical form (c). This hypothesis was further supported by the observation of a short (1.87Å) Nb-OEt distance and large ∠Nb-O-C (149°) for the crystallographically characterised analogue, $Nb(O)Cl_2(OEt)(bipy)$[39].

COMPOUND	ν(Nb=O)/cm^{-1}	CN	REF
$[Nb(O)Cl_3(PMe_3)_2]_2$	923	7,8	#
β-$Nb(O)Cl_3(PMe_3)_3$ [a]	871	7	#
α-$Nb(O)Cl_3(PMe_3)_3$ [a]	882	7	#
$Nb(O)Cl_2(OPr^n)(bipy)$	912	6 [b]	24
$Nb(O)Cl_3(PMePh_2)_2$	929	6 [c]	#
$Nb(O)Cl_3(PEt_3)_2$	930	6 [c]	#
$Nb(O)Cl_3$(dppe)	931	6 [c]	#
$Nb(O)Cl_3$(bipy)	934	6 [c]	24
$Nb(O)Cl_3(TPPO)_2$ [d]	935	6 [c]	45
$Nb(O)Cl_3(PPh_3)_2$	939	6 [c]	#
$Nb(O)Cl_3(HMPA)_2$ [a,e]	940	6	38,48
$Nb(O)Cl_3(CH_3CN)_2$ [a]	960	6	#,25
$Nb(O)Cl_3(THF)_2$	960	6 [c]	#

Table 5.2 *ν(Nb=O) Vibrational Frequencies for some Niobium Oxo complexes; CN=Coordination Number; a) X-ray; b) Assumed isostructural to -OEt analogue (X-ray); c) Assumed isostructural to $Nb(O)Cl_3(CH_3CN)_2$ and $Nb(O)Cl_3(HMPA)_2$; d) TPPO=triphenylphosphineoxide Ph_3PO; e) HMPA=hexamethyl phosphoramide $(Me_2N)_3PO$; #=This Work.*

Among the six coordinate complexes, the highest ν(Nb=O) frequencies, and presumably the strongest Nb=O bonds, are found with CH_3CN and THF, both of which are very labile in the complex and presumably do not engage in extensive pπ-dπ interactions with the metal. This appears reasonable since the ν(C≡N) vibration is little affected

upon CH_3CN coordination (*ie.* 2293, 2284 cm^{-1} in the complex *vs* 2295, 2253 cm^{-1} in the free ligand). The two other compounds containing oxygen donor ligands, $Nb(O)Cl_3(TPPO)_3$ and $Nb(O)Cl_3(HMPA)_2$, appear to be stronger bases towards $Nb(O)Cl_3$ than CH_3CN or THF. The higher ν(Nb=O) frequency for the HMPA complex presumably reflects the lower basicity of HMPA over TPPO resulting from the more electronegative NMe_2 substituents on phosphorus in the former.

With regard to the tertiary phosphine adducts, it was anticipated that sequential replacement of phenyl substituents for more electron releasing alkyl groups would result in a reduced ν(Nb=O) frequency and consequently a reduced niobium oxygen bond order. This general trend does appear to be corroborated by the data in Table 5.2 where the relative ability of the tertiary phosphine ligand to lower the ν(Nb=O) frequency follows the sequence:

$$PMe_3 > PMePh_2 \approx dppe > PPh_3$$

The PEt_3 complex however, appears to have a higher ν(Nb=O) vibrational frequency than expected on the basis of its electronic properties[46]. This may be the result of a different ligand field geometry for $Nb(O)Cl_3(PEt_3)_2$ compared with most other characterised $Nb(O)Cl_3L_n$ complexes. For example, the PEt_3 ligands may adopt a *trans* configuration in contrast to the normally observed *cis* geometry[25,38,39].

5.5.5 The Molecular Structures of α and β-$Nb(O)Cl_3(PMe_3)_3$. An Example of Bond-Stretch Isomerism ?

The isolation of two isomeric compounds with the formula, $Nb(O)Cl_3(PMe_3)_3$ was described in section 5.5.3. Both forms, yellow (17)-α and green (17)-β have been subjected to X-ray diffraction analysis by Dr. M. McPartlin and coworkers at the Polytechnic of North

London and the results of these studies are described below.

The Yellow Isomer, (17)-α

The crystal data are collected in Appendix 1F and the molecular structure is illustrated in Figures 5.4 and 5.5. Selected bond angles and distances are given in Table 5.3.

The complex is monomeric for which the coordination geometry may best be described as distorted, monocapped octahedral with facial arrangements of chloro and trimethylphosphine ligands giving the molecule virtual C_{3v} symmetry (Figure 5.5). The oxo group is in a site capping the face defined by the phosphine ligands and lies 1.16Å above the P(1), P(2), P(3) plane, with the niobium atom 0.62Å below this plane. This coordination is similar to that observed in $NbCl_4(PMe_3)_3$[49] yet very different to the seven coordinate complex $Nb(O)(S_2CNEt_2)_3$[50], in which the niobium atom is at the centre of a distorted pentagonal bipyramid.

The (Nb=O) bond length of 1.781(6)Å is significantly longer than the (Nb=O) distances usually observed in four to seven coordinate oxo-niobium complexes (average *ca.* 1.7Å). This presumably arises due to the presence of three, highly electron releasing PMe_3 ligands within the crowded coordination sphere of (17)-α. Consistently, as illustrated in section 5.5.4, the ν(Nb=O) vibrational frequency of (17)-α (882 cm^{-1}) is significantly lower than normally observed for both six coordinate (*ca.* 950 ± 20 cm^{-1})[50] and seven coordinate (900 cm^{-1} for $Nb(O)(S_2CNEt_2)_3$[50]) complexes.

The compounds (17)-α and $NbCl_4(PMe_3)_3$[49] are isomorphous (space group $P_{2_1/c}$). The average (Nb-Cl) distances in (17)-α [2.518(8)Å] are slightly longer than the average facial (Nb-Cl) distances in $NbCl_4(PMe_3)_3$ [2.453(13)Å] the opposite of the trend predicted on the

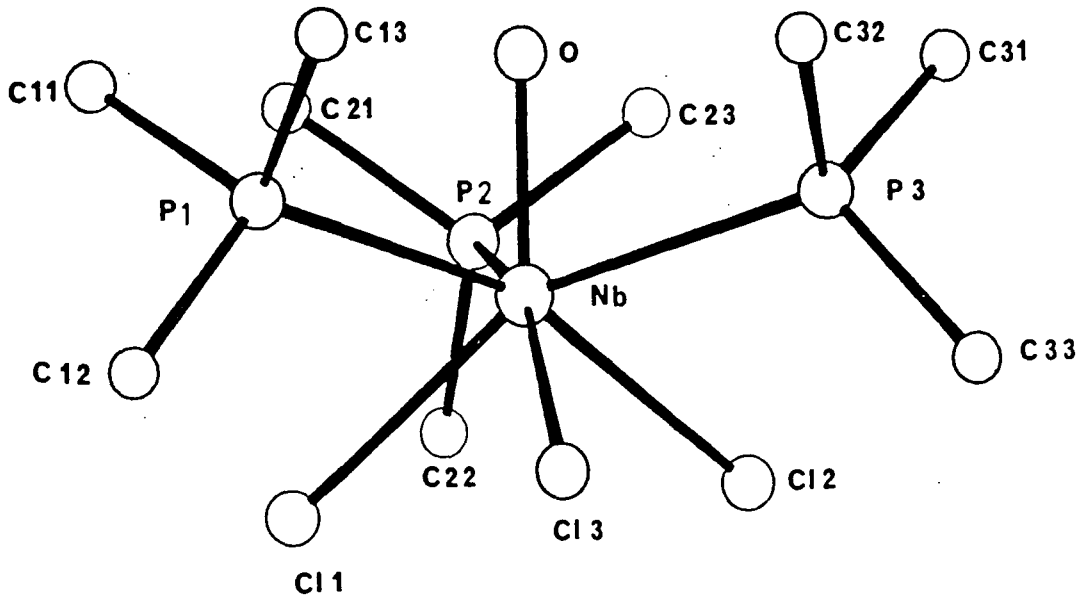

Figure 5.4 *Molecular Structure of α-Nb(O)Cl$_3$(PMe$_3$)$_3$.*

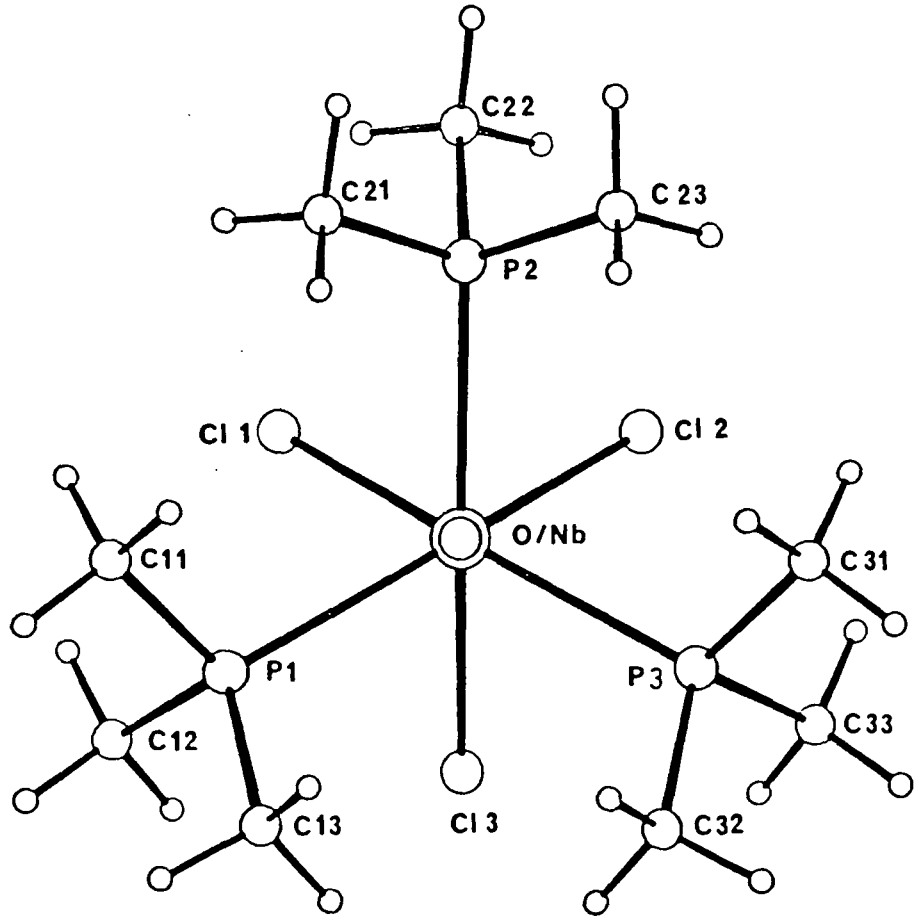

Figure 5.5 *View down the oxygen-niobium Vector of α-Nb(O)Cl$_3$(PMe$_3$)$_3$.*

Nb-Cl(1)	2.516(3)	Cl(1)-Nb-Cl(2)	90.9(1)
Nb-Cl(2)	2.533(3)	Cl(1)-Nb-Cl(3)	88.0(1)
Nb-Cl(3)	2.505(3)	Cl(2)-Nb-Cl(3)	92.3(1)
Nb-P(1)	2.642(3)	P(1)-Nb-Cl(1)	75.3(1)
Nb-P(2)	2.633(3)	P(1)-Nb-Cl(2)	161.9(1)
Nb-P(3)	2.645(3)	P(1)-Nb-Cl(3)	75.8(1)
		P(2)-Nb-Cl(1)	75.0(1)
Nb-O	1.781(6)	P(2)-Nb-Cl(2)	73.8(1)
		P(2)-Nb-Cl(3)	157.6(1)
P(1)-C(11)	1.799(9)	P(3)-Nb-Cl(1)	155.9(1)
P(1)-C(12)	1.812(9)	P(3)-Nb-Cl(2)	74.0(1)
P(1)-C(13)	1.817(10)	P(3)-Nb-Cl(3)	74.3(1)
P(2)-C(21)	1.785(11)		
P(2)-C(22)	1.790(11)	P(2)-Nb-P(1)	112.7(1)
P(2)-C(23)	1.807(11)	P(3)-Nb-P(1)	114.5(1)
P(3)-C(31)	1.808(9)	P(3)-Nb-P(2)	116.9(1)
P(3)-C(32)	1.805(10)		
P(3)-C(33)	1.791(10)	C(11)-P(1)-Nb	112.1(3)
		C(12)-P(1)-Nb	120.3(3)
		C(13)-P(1)-Nb	110.8(3)
O-Nb-Cl(1)	127.8(2)	C(21)-P(2)-Nb	112.7(4)
O-Nb-Cl(2)	121.2(2)	C(22)-P(2)-Nb	120.0(4)
O-Nb-Cl(3)	126.0(2)	C(23)-P(2)-Nb	110.8(4)
		C(31)-P(3)-Nb	110.9(3)
O-Nb-P(1)	76.9(2)	C(32)-P(3)-Nb	111.6(4)
O-Nb-P(2)	76.4(2)	C(33)-P(3)-Nb	119.9(4)
O-Nb-P(3)	76.3(2)		
		C(12)-P(1)-C(11)	103.5(5)
		C(13)-P(1)-C(11)	103.8(5)
		C(13)-P(1)-C(12)	104.8(4)
		C(22)-P(2)-C(21)	102.3(6)
		C(23)-P(2)-C(22)	105.0(5)
		C(23)-P(2)-C(21)	104.5(5)
		C(32)-P(3)-C(31)	103.5(5)
		C(33)-P(3)-C(31)	105.2(5)
		C(33)-P(3)-C(32)	104.3(5)

Table 5.3 *Bond Distances (Å) and Angles (°) for α-Nb(O)Cl_3(PMe_3)$_3$.*

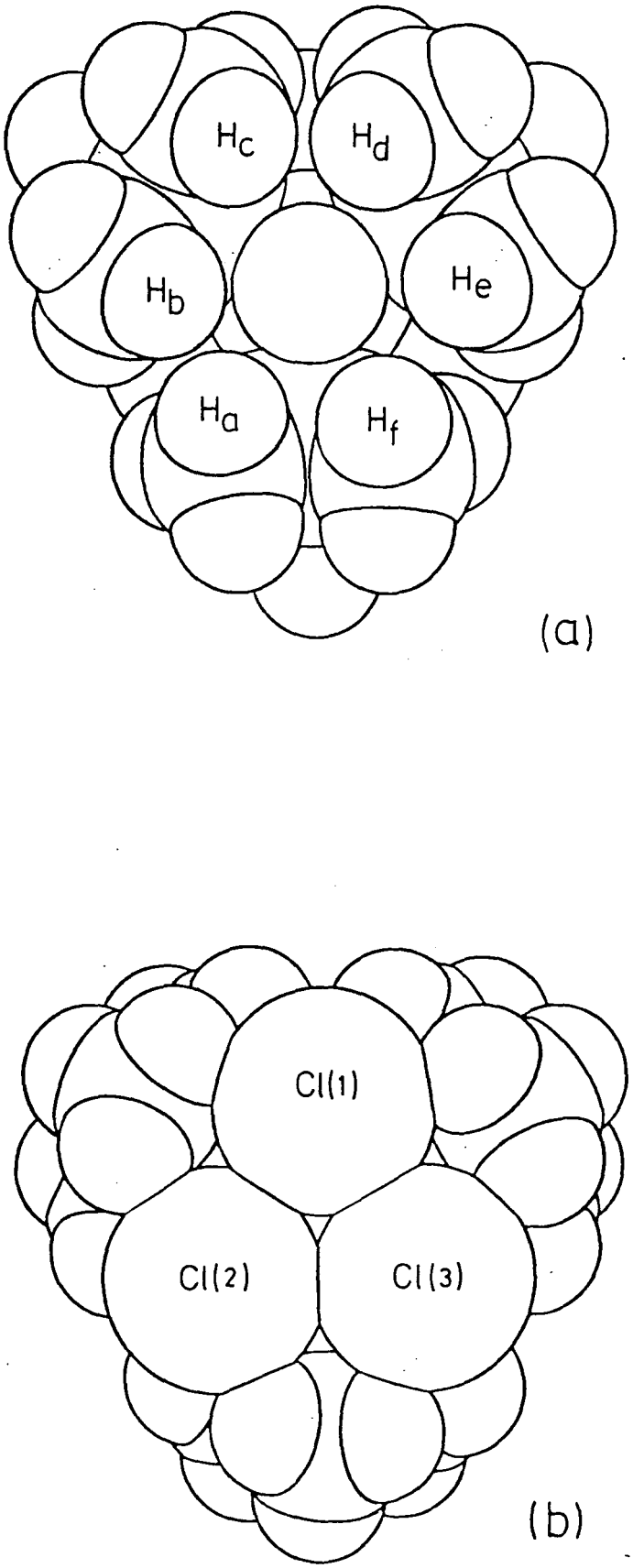

Figure 5.6 *Space Filling Diagrams of α-Nb(O)Cl$_3$(PMe$_3$)$_3$; (a) View down the oxygen-niobium Vector; (b) View down the chloro face.*

basis of oxidation state. Since both compounds possess average ∠P-Nb-Cl angles of *ca.* 159°, a similar average *trans* influence is anticipated due to the phosphine ligands. Therefore, the average lengthening observed in (17)-*α* may be attributed to the presence of the oxo ligand.

Interestingly, the Nb-Cl(2) bond is the longest [2.533(3)Å] whilst also having the most acute ∠O-Nb-Cl angle of 121.2°, an observation at variance with an oxo ligand *trans* influence. However, since the *trans* ∠P-Nb-Cl angle for Cl(2) is the largest (161.9°), this atom may experience a slightly larger PMe_3 *trans* influence.

The (Nb-P) bonds have an average length of 2.640(4)Å in (17)-*α* and 2.651(6)Å in $NbCl_4(PMe_3)_3$, the former having the slightly shorter distances as expected for niobium(V) over niobium(IV).

The acute ∠O-Nb-P angles [average 76.5(2)°] lead to a staggered arrangement of PMe_3 substituents with respect to the capping oxygen atom (as viewed along the P-Nb vector) in order to minimise interligand repulsions. A similar arrangement is found in $NbCl_4(PMe_3)_3$. Consequently, relatively close O··H contacts result, in the range 2.79-2.97Å. Figure 5.6(a) represents a space filling diagram of (17)-*α* viewed down the (O=Nb) vector illustrating the close contacts between the oxygen atom and six phosphine-methyl hydrogens (Ha-Hf). Figure 5.6(b) is a similar diagram viewed through the facial chlorine plane.

The Green Isomer, (17)-β

The green compound, (17)-*β* is isomorphous to (17)-*α* (space group $P_{2_1/c}$, Appendix 1G). Selected bond distances and angles are collected in Table 5.4.

Comparative values of selected parameters for (17)-*α* and (17)-*β* are displayed in Table 5.5. It can be seen that the average interatomic angles are essentially identical, although the *β*-isomer shows larger

Nb-Cl(1)	2.487(2)	Cl(1)-Nb-Cl(2)	90.7(1)
Nb-Cl(2)	2.509(2)	Cl(1)-Nb-Cl(3)	86.8(1)
Nb-Cl(3)	2.492(2)	Cl(2)-Nb-Cl(3)	93.0(1)
Nb-P(1)	2.646(2)	P(1)-Nb-Cl(1)	76.0(1)
Nb-P(2)	2.636(3)	P(1)-Nb-Cl(2)	163.1(1)
Nb-P(3)	2.644(2)	P(1)-Nb-Cl(3)	76.1(1)
		P(2)-Nb-Cl(1)	75.3(1)
Nb-O	2.087(5)	P(2)-Nb-Cl(2)	74.3(1)
		P(2)-Nb-Cl(3)	157.7(1)
P(1)-C(11)	1.814(8)	P(3)-Nb-Cl(1)	154.7(1)
P(1)-C(12)	1.807(8)	P(3)-Nb-Cl(2)	74.3(1)
P(1)-C(13)	1.801(10)	P(3)-Nb-Cl(3)	74.1(1)
P(2)-C(21)	1.815(9)		
P(2)-C(22)	1.807(10)	P(2)-Nb-P(1)	111.4(1)
P(2)-C(23)	1.795(10)	P(3)-Nb-P(1)	114.0(1)
P(3)-C(31)	1.805(8)	P(3)-Nb-P(2)	118.2(1)
P(3)-C(32)	1.821(9)		
P(3)-C(33)	1.804(8)	C(11)-P(1)-Nb	113.1(3)
		C(12)-P(1)-Nb	119.9(3)
		C(13)-P(1)-Nb	112.7(3)
O-Nb-Cl(1)	129.8(1)	C(21)-P(2)-Nb	113.5(3)
O-Nb-Cl(2)	119.3(1)	C(22)-P(2)-Nb	119.3(3)
O-Nb-Cl(3)	126.4(1)	C(23)-P(2)-Nb	112.4(4)
		C(31)-P(3)-Nb	112.0(3)
O-Nb-P(1)	77.6(1)	C(32)-P(3)-Nb	113.3(3)
O-Nb-P(2)	75.8(1)	C(33)-P(3)-Nb	119.5(3)
O-Nb-P(3)	75.5(1)		
		C(12)-P(1)-C(11)	103.2(4)
		C(13)-P(1)-C(11)	102.3(5)
		C(13)-P(1)-C(12)	103.5(4)
		C(22)-P(2)-C(21)	104.2(5)
		C(23)-P(2)-C(22)	102.3(5)
		C(23)-P(2)-C(21)	103.2(5)
		C(32)-P(3)-C(31)	103.1(4)
		C(33)-P(3)-C(31)	103.3(4)
		C(33)-P(3)-C(32)	103.9(4)

Table 5.4 *Bond Distances (Å) and Angles (°) for β-Nb(O)Cl_3(PMe_3)$_3$.*

individual deviations.

PARAMETER	(17)-α	(17)-β
(Nb=O)	1.781(6)	2.087(5)
(Nb-Cl) av.	2.518(8)	2.496(7)
(Nb-P) av.	2.640(4)	2.642(3)
∠O-Nb-Cl av.	125.0(20)	125.2(31)
∠O-Nb-P av.	76.5(2)	76.3(7)
∠P-Nb-P av.	114.7(12)	114.5(20)
∠Cl-Nb-Cl av.	90.4(13)	90.2(18)
∠P-Nb-Cl_{trans} av.	158.5(18)	158.5(25)

Table 5.5 *Comparative Values of some Parameters for (17)-α and (17)-β.*

The (Nb-Cl) distances are slightly shorter and the (Nb-P) distances marginally longer for the β-isomer.

Without doubt, the most marked difference between the isomers is the length of the niobium-oxygen bond. In (17)-β this bond has been lengthened by *ca.* 0.3Å over that in (17)-α and is *ca.* 0.4Å longer than the normal average niobium-oxygen distances (1.7Å) in niobium oxo compounds. Indeed this distance is comparable to the sum of the covalent radii of niobium and oxygen (2.1Å)[51] suggesting that the bond order is close to unity. Consistently the (Nb=O) bond length is between representative values of niobium-oxygen single bonds in μ_2-bridging oxo compounds (*ca.* 1.91Å)[52] and niobium-oxygen dative covalent bonds as, for example, in $[Cp'NbCl_3(H_2O)]_2(\mu\text{-}O)$ where $[Nb\text{-}O(H_2O)]$ is 2.19Å [$Cp' = C_5H_4Me$][52].

(17)-α and (17)-β. Bond-Stretch Isomers ?

Molecules in the solid state and also in solution which interconvert with varying degrees of ease, and whose only structural difference is a dramatic difference in the length of one or several

bonds have been termed bond-stretch isomers[53], or distortional isomers[54]. A number of systems have been studied which show this effect. For instance, compounds of the form $Mo(O)X_2L_3$ (X = halide or pseudohalide; L = tertiary phosphine) have been shown to exist in either blue or green forms[55]. Spectroscopically the only significant difference between the two is the ν(Mo=O) vibrational frequency which is commonly *ca.* 10 cm^{-1} lower for the green compounds. It was shown that blue-$Mo(O)Cl_2(PMe_2Ph)_3$[56] and green-$Mo(O)Cl_2(PEt_2Ph)_3$[55] (the green PMe_2Ph derivative has been reported but not structurally characterised), were isostructural with the only significant difference between the two being the lengths of the molybdenum-oxygen bonds [blue, 1.676(7)Å; green, 1.801(9)Å] and the bonds to the ligands *trans* to oxygen (Figure 5.7).

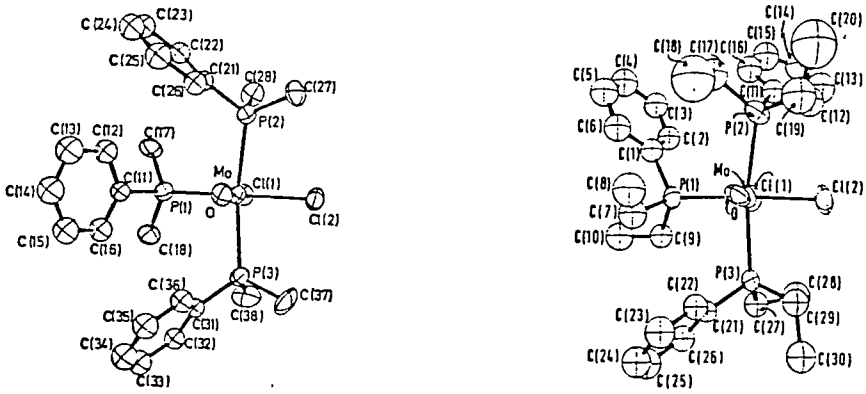

(a) (b)

Figure 5.7 *Molecular Structures of blue-$Mo(O)Cl_2(PMe_2Ph)_3$ (a) and green-$Mo(O)Cl_2(PEt_2Ph)_3$ (b).*

Similar effects have been observed in the complexes $[W(O)Cl_2L]\ PF_6$ (L = $MeN(CH_2CH_2NMe)_2CH_2CH_2$) for which both blue and green isomers were isolated and found to be stable in both the solid state and in solution[57].

The yellow and green isomers described here show several of the features expected for bond-stretch isomerism, the colour differences, presumably due to L → M charge transfer[57], the marked difference in the metal-oxygen distance and the concomitant difference in metal-oxygen stretching frequencies (Table 5.2, section 5.5.4). Hoffmann, Burdett and coworkers have forwarded explanations of bond-stretch isomerism in terms of a frontier orbital crossing of (M-L) and (M-O) antibonding molecular orbitals or a second order Jahn-Teller effect (SOJT)[53]. The former rationale appears to be valid only for d^n systems where $n>0$, whilst the latter is appropriate for d^n systems where $n\geq 0$ and is presumably more generally applicable.

The SOJT effect outlined by Hoffmann results in two energy minima as the (M-O) bond is lengthened and the equitorial bonds shortened and the effect has been demonstrated to be sensitive to the π-bonding capabilities of the ancillary ligands. π-donor ligands *trans* to the oxygen atom favour a double minimum and hence bond-stretch isomerism. Such an arrangement is indeed present in (17)-α and (17)-β although the symmetry difference between Hoffmanns idealised systems and that described here may warrant a more detailed molecular orbital analysis of $Nb(O)Cl_3(PMe_3)_3$. These studies have been initiated.

Although displaying behaviour typical of bond-stretch isomers, the magnitude of the effect shown by $Nb(O)Cl_3(PMe_3)_3$ [Δ(Nb=O) = *ca.* 0.3Å] is considerably larger that that shown in both d^2 and d^1 systems (typically 0.12-0.17Å)[54-57]. Crystal packing forces are unlikely to result in bond length changes > 0.1Å[54], and since both (17)-α and (17)-β are isomorphous with similar intramolecular ligand conformations the (Nb-O) bond difference undoubtedly results from factors other than packing or conformational differences.

The possibility that (17)-β contains a niobium hydroxide moiety as

opposed to an oxo group is not supported by infrared spectroscopy, which provides no evidence for a ν(OH) stretching vibration > 3000 cm^{-1} and the ν(Nb=O) vibration at 871 cm^{-1} is comparable in both shape and intensity to that in (17)-α and is *ca.* 300 cm^{-1} higher than is normally observed for metal-hydroxide (M-O) vibrations[40].

Studies are currently in progress to further delineate the factors involved in the niobium-oxygen bond lengthening as well as an investigation of the conversion of (17)-α to (17)-β.

5.6 SUMMARY

The convenient, mild syntheses of both base free and base stabilised $Nb(O)Cl_3$ have facilitated a study of simple substitution and addition reactions of this compound and a subsequent assessment of the sensitivity of the niobium-oxygen bonding to the nature of the ligand set. Some reactions of $Nb(O)Cl_3$ are summarised in Scheme 5.4.

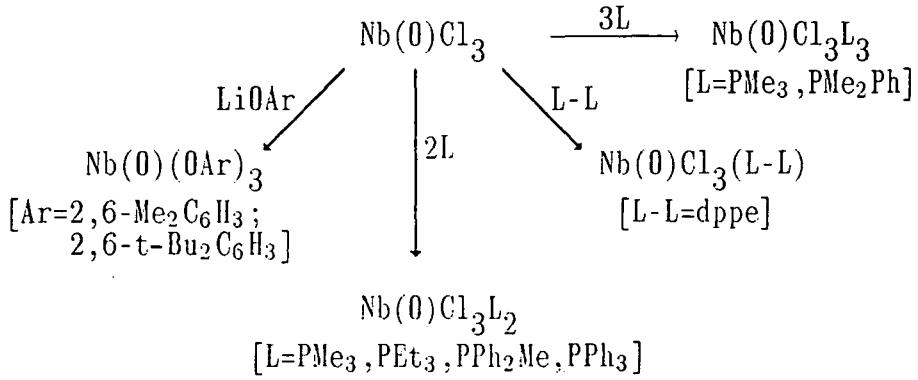

Scheme 5.4 *Some reactions of* $Nb(O)Cl_3$

A remarkable finding concerns the isolation of two isomers of $Nb(O)Cl_3(PMe_3)_3$ which differ significantly only in the length of the niobium-oxygen bond. Studies are being pursued to establish whether or

not this is a *bona fide* example of bond-stretch isomerism. Aspects of the work described here have been briefly communicated[58].

5.7 REFERENCES

1. R.A. Sheldon and J.K. Kochi, "*Metal Catalysed Oxidations of Organic Compounds*", Academic Press, New York (1981).
2. M.J. Frazer, W. Gerrard and J.A. Strickson, *J.Chem.Soc.*, 1960, 4701.
3. H.J. Emeléus and M. Onyszchuk, *J.Chem.Soc.*, 1958, 604.
4. M.F. Orlov, *Dokl.Acad.Nauk.SSSR.*, 1957, 114, 629.
5. V.C. Gibson, T.P. Kee and A. Shaw, *Polyhedron*, 1988, 7, 579.
6. R.R. Schrock, Personal Communication.
7. V.C. Gibson, A. Shaw and D.H. Williams, *Polyhedron*, in press.
8. U. Müller and V. Krug, *Angew.Chem. Int.Ed.Engl.*, 1988, 27, 293.
9. W. Neubert, H. Pritzkow and K.P. Latscha, *Angew.Chem. Int.Ed.Engl.*, 1988, 27, 287.
10. C. Eaborn, *J.Chem.Soc.*, 1950, 3077.
11. G. Parkin and J.E. Bercaw, *Polyhedron*, In press.
12. W.A. Herrmann, E. Herdtweck, M. Flöel, J. Kulpe, U. Küsthardt and J. Okuda, *Polyhedron*, 1987, 6, 1165.
13. J.E. Huheey, "*Inorganic Chemistry - Principles of Structure and Reactivity*", 3rd Edition, Harper, New York (1983).
14. A. Zalkin and D.E. Sands, *Acta Cryst.*, 1958, 11, 615.
15. A.A. Pinkerton, D. Schwarzenbach, L.G. Hubert-Pfalzgraf and J.G. Riess, *Inorg.Chem.*, 1976, 15, 1196.
16. K.C. Malhotra, U.K. Banerjee and S.C. Chaudhry, *J.Ind.Chem.Soc.*, 1980, 57, 868.
17. C.G. Barraclough, D.C. Bradley, J. Lewis and I.M. Thomas, *J.Chem. Soc.*, 1961, 2601.
18. M. Schoenherr and L. Kolditz, *Z.Chem.*, 1970, 10, 72.
19. R.M. Silverstein, G.C. Bassler and T.C. Morill, "*Spectrometric Identification of Organic Compounds*", 4th Edition, John Wiley, New York (1981).

20. (a) R.N. Kapoor, S. Prakash and P.N. Kapoor, *Ind.J.Chem.*, 1967, 5, 442.

(b) R.C. Mehrotra and P.N. Kapoor, *J.Less Common Metals*, 1966, 10, 348.

(c) S. Prakesh, P.N. Kapoor and R.N. Kapoor, *J.Prakt.Chem.*, 1967, 36, 24.

21. H. Schäfer and F. Kahlenberg, *Z.Anorg.Allg.Chem.*, 1960, 305, 327.

22. D.E. Sands, A. Zalkin and R.E. Elson, *Acta Cryst.*, 1959, 12, 21.

23. F. Fairbrother, A.H. Cowley and N. Scott, *J.Less Common Metals*, 1959, 1, 206.

24. V. Katovic and C. Djordjevic, *Inorg.Chem.*, 1970, 9, 1729.

25. C. Chavant, J.C. Daran, Y. Jeannin, G. Constant and R. Morancho, *Acta Cryst.*, 1975, B31, 1828.

26. L.G. Hubert-Pfalzgraf, M. Tsunoda and G. Le Borgne, *J.Chem.Soc. Dalton Trans.*, 1988, 533.

27. C. Santini-Scampucci and J.G. Riess, *J.Chem.Soc.Dalton Trans.*, 1974, 1433.

28. K. Dehnicke, *Angew.Chem. Int.Ed.Engl.*, 1961, 73, 535.

29. A. Cowley, F. Fairbrother and N. Scott, *J.Chem.Soc.*, 1958, 3133.

30. A. Hamitou, R. Jérôme, A.J. Hubert and Ph. Teyssié, *Macromolecules*, 1973, 651.

31. C.C. Su, J.W. Reed and E.S. Gould, *Inorg.Chem.*, 1973, 12, 337.

32. L.G. Hubert-Pfalzgraf and J.G. Riess, *Inorg.Chim.Acta.*, 1980, 41, 111.

33. L.G. Hubert-Pfalzgraf and J.G. Riess, *Inorg.Chim.Acta.*, 1980, 47, 7.

34. V.C. Gibson and A. Shaw, Unpublished results.

35. S.M. Sinitsyna, V.I. Sinyagin and Yu. A. Buslaev, *Izv.Akad.Nauk. SSSR, Meorg.Mater.*, 1969, 5, 514.

36. D.B. Copley, F. Fairbrother and A. Thompson, *J.Less Common Metals*, 1965, 5, 514.

37. D.B. Copley, F. Fairbrother, K.H. Grundy and A. Thompson, *J.Less Common Metals*, 1964, 6, 407.

38. L.G. Hubert-Pfalzgraf and A.A. Pinkerton, *Inorg.Chem.*, 1977, 16, 1895.

39. B. Kamenar and C.K. Prout, *J.Chem.Soc.*, (*A*)., 1970, 2379.

40. D.M. Adams, "*Metal-Ligand and Related Vibrations*", Edward Arnold, London (1967).

41. See for example: J.H. Wengrovius and R.R. Schrock, *Organometallics*, 1982, 1, 148.

42. M. Brookhart and M.L.H. Green, *J.Organometallic Chem.*, 1983, 250, 395.

43. S.M. Rocklage, H.W. Turner, J.D. Fellman and R.R. Schrock, *Organometallics*, 1982, 1, 703.

44. J. Nieman, J.H. Teuben, J.C. Huffman and K.G. Caulton, *J.Organometallic Chem.*, 1983, 255, 193.

45. W. Van der Veer and F. Jellinek, *Rec.Trv.Chim.Pays.Bas.*, 1966, 85, 842.

46. C.A. Tolman, *Chem.Rev.*, 1977, 77, 313.

47. J. Selkin, L.H. Halmas Jr. and S.P. McGlynn, *J.Inorg.Nucl.Chem.*, 1963, 25, 1359.

48. R.J. Dorschner, *J.Inorg.Nucl.Chem.*, 1972, 34, 2665.

49. F.A. Cotton, M.P. Diebold and W.J. Roth, *Polyhedron*, 1985, 4, 1103.

50. J.C. Dewan, D.L. Kepert, C.L. Raston, D. Taylor, A.H. White and E.N. Maslen, *J.Chem.Soc.Dalton Trans.*, 1973, 2082.

51. W.W. Porterfield, "*Inorganic Chemistry - A Unified Approach*", Addison-Wesley, New York (1984).

52. K. Prout and J.C. Daran, *Acta Cryst.*, 1979, B35, 2882.

53. (a) Y. Jean, A. Lledos, J.K. Burdett and R. Hoffmann, *J.C.S. Chem Commun.*, 1988, 140.

    (b) Y. Jean, A. Lledos, J.K. Burdett and R. Hoffmann, *J.Am.Chem. Soc.*, 1988, 110, 4506.

54. F.A. Cotton, M.P. Diebold and W.J. Roth, *Inorg.Chem.*, 1987, 26, 2848.

55. (a) J. Chatt, L. Manojlevic-Muir and K.W. Muir, *J.C.S. Chem Commun.*, 1971, 655.

    (b) L. Manojlevic-Muir and K.W. Muir, *J.C.S. Chem Commun.*, 1972, 686.

56. L. Manojlevic-Muir, *J.Chem.Soc (A).*, 1971, 2796.

57. K. Wieghardt, G. Backes-Dahmann, B. Nuker and J. Weiss, *Angew. Chem. Int.Ed.Engl.*, 1985, 24, 777.

58. (a) V.C. Gibson, T.P. Kee and A. Shaw, *Polyhedron*, 1988, 7, 2217.
    (b) V.C. Gibson, T.P. Kee, R.M. Sorrell, A.P. Bashall and M. McPartlin, *Polyhedron*, 1988, 7, 2221.

CHAPTER SIX

HALF-SANDWICH OXO, ALKOXO AND RELATED COMPOUNDS OF TANTALUM.

6.1 INTRODUCTION

The intermediacy of metal oxo and alkoxo species has often been proposed in homogeneous and heterogeneous transition metal mediated oxidations of organic substrates[1]. Consequently, the desire to model the active sites, potential intermediates and transformations, has led to much current interest in soluble, organometallic oxo and alkoxo compounds.

In this regard, the (η^5-C_5R_5) ligand (R = H, alkyl) has proved particularly suitable for the solubilisation and stabilisation of high oxidation state metal complexes containing hard ligands such as oxygen ('O' and 'OR')[2].

At Durham, a program of research is being directed towards the synthesis of organometallic complexes containing oxygen donor ligands and a study of their subsequent transformations of relevance to hydrocarbon oxidation. In this Chapter, several strategies for the synthesis of half-sandwich tantalum oxo and alkoxo complexes are described, which take advantage of various aspects of the chemistry described in Chapters 2-5.

6.2 REACTIONS OF $Cp^*Ta(PMe_3)(H)_2(\eta^2$-$CHPMe_2)$ (1) WITH ROH REAGENTS (R = H, ALKYL, ARYL)

6.2.1 Reaction of (1) with ROH (R = Me, ^iPr)

The reactivity of (1) described in Chapter 4 demonstrated that reversible hydrogen migrations could occur and that (1) could act as a synthetic precursor of the fragment, $[Cp^*Ta(PMe_3)_2]$. It was further

envisaged that phosphine lability would allow (1) to act as a source of the [Cp^*Ta] fragment and consequently may react with alcohols to form, ultimately, the tetraalkoxides, $Cp^*Ta(OR)_4$.

Only two such compounds have been reported[3] (Equations 6.1-6.2).

$$Cp^*TaL_2H_4 + 4MeOH \longrightarrow Cp^*Ta(OMe)_4 + 4H_2 + 2L \qquad (6.1)$$

[L = PMe_3, PMe_2Ph, $P(OMe)_3$]

$$Cp^*TaL_2H_4 + 4Me_2CO \longrightarrow Cp^*Ta(O^iPr)_4 + 2L \qquad (6.2)$$

[L = PMe_3, PMe_2Ph, $P(OMe)_3$]

It has been found that both the above compounds may also indeed be accessed by the reactions of (1) with four equivalents of MeOH and ^{i}PrOH respectively (Equation 6.3).

$$\underset{(1)}{Cp^*Ta(PMe_3)(H)_2(\eta^2\text{-}CHPMe_2)} + 4ROH \longrightarrow \underset{[R = Me\ (2),\ ^iPr\ (3)]}{Cp^*Ta(OR)_4} + 2H_2 + 2PMe_3 \qquad (6.3)$$

Both products were characterised by comparison of their ^{1}H NMR data with those of authentic samples[4]. When the reactions were monitored by ^{1}H NMR spectroscopy in d^6-benzene solvent, no intermediates were detected, indicating that any hydrido-alkoxide or tertiary phosphine alkoxide species are short-lived under the reaction conditions. Similar observations were reported for the reactions in Equations 6.1 and 6.2[3]. Two equivalents of PMe_3 were displaced (^{1}H NMR) and H_2 was observed (4.46 ppm). The use of more than four equivalents of the alcohol in Equation 6.3 led to further reaction involving the displacement of C_5Me_5H (^{1}H NMR) and the formation of unidentified alkoxide compounds.

It was observed that the presence of excess PMe_3 retarded the reaction, suggesting that rate determining initial PMe_3 displacement is followed by trapping of the incipient 16-electron fragment by ROH

(Equation 6.4). This type of exchange was discussed in Chapter 4.

$$Cp^*Ta(PMe_3)(H)_2(\eta^2\text{-}CHPMe_2) \underset{+\ PMe_3}{\overset{+\ ROH}{\rightleftharpoons}} Cp^*Ta(ROH)(H)_2(\eta^2\text{-}CHPMe_2) \quad (6.4)$$

Interestingly, the reactions in Equations 6.1 and 6.2 were also reported to proceed *via* initial PMe_3 displacement[3]. Reaction 6.3 with ^iPrOH was significantly slower than that with MeOH presumably reflecting the greater steric inhibition to ^iPrOH coordination.

6.2.2 Reaction of (1) with the diols, $HOCH_2CH_2OH$ and $1,2\text{-}(HO)_2C_6H_4$

In a similar manner to the reactions with alcohols, (1) reacted smoothly with the diols, $HOCH_2CH_2OH$ (ethan-1,2-diol) and $1,2\text{-}(HO)_2C_6H_4$ (catechol) under ambient conditions according to Equations 6.5 and 6.6.

$$\underset{(1)}{Cp^*Ta(PMe_3)(H)_2(\eta^2\text{-}CHPMe_2)} + 2HOCH_2CH_2OH \longrightarrow \underset{(4)}{1/n\ [Cp^*Ta(O_2C_2H_4)_2]_n} + 2PMe_3 + 2H_2 \quad (6.5)$$

$$\underset{(1)}{Cp^*Ta(PMe_3)(H)_2(\eta^2\text{-}CHPMe_2)} + 2(HO)_2C_6H_4 \longrightarrow \underset{(5)}{1/n\ [Cp^*Ta(O_2C_6H_4)_2(PMe_3)]_n} + PMe_3 + 2H_2 \quad (6.6)$$

The compounds precipitated from the reaction mixture as white (4) or yellow (5) solids in 60-90% yields. Characterisation was provided by elemental analysis, infrared and mass spectroscopy (Chapter 7, section 7.6). Both compounds possess low solubility in common organic solvents in contrast to $Cp^*Ta(OMe)_4$. This most probably arises due to marked structural differences. For example, it is highly likely that both (4) and (5) possess structures in which the metal atoms are linked by

bridging glycolate or catecholate ligands. In support of this hypothesis, the mass spectrum (CI^+) of (4) displays ions at m/e 873 and 829 which may be assigned to the dimeric fragments $[M_2+H]^+$ and $[M_2+H-OC_2H_4]^+$ respectively, as well as an ion at m/e 437 attributable to $[M+H]^+$. Thus, mass spectral data implicate a solid state structure involving at least dimeric units. Infrared spectroscopy reveals an absorption at 550 cm^{-1} assignable to ν(Ta-O) in the region expected for tantalum alkoxides[5], and compares favorably with that observed for $Ta(OEt)_5$ (556 cm^{-1})[5].

Unfortunately, (4) was not sufficiently soluble in suitable solvents for molecular weight study. Similarly, ^1H NMR spectroscopy did not prove informative. The 250 MHz ^1H NMR spectrum (d^6-benzene) displayed broad bands centred at 4.30 ppm and 4.11 ppm ($\Delta\frac{1}{2}$ *ca.* 200Hz) due to the diol methylene hydrogens and a broadened absorption at 2.09 ppm ($\Delta\frac{1}{2}$ *ca.* 8Hz) which may be attributed to the (η^5-C_5Me_5) hydrogens. A fluxional dimeric or oligomeric structure in solution is not inconsistent with these observations (Figure 6.1).

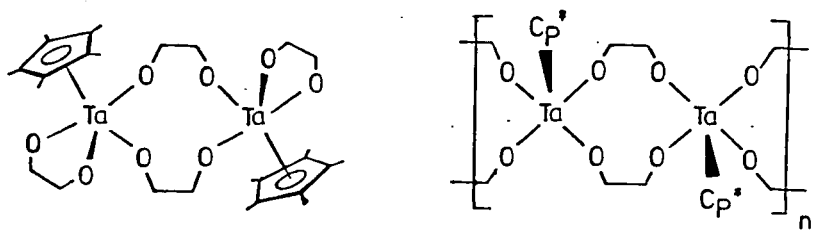

(a) (b)

Figure 6.1 *Possible dimeric (a) and oligomeric (b) Structures of (4).*

Compound (5) is unusual in that is has retained one molecule of PMe_3, as indicated by the elemental analysis (Chapter 7, section 7.6), infrared

spectrum (960 cm^{-1}, $\rho(CH_3)$)[6] and mass spectrum (m/e 76, $[PMe_3]^+$). Like (4), (5) is only sparingly soluble in common organic solvents, such that molecular weight studies were precluded. Mass spectrometry did display peaks at m/e 961 and m/e 837 which may be attributable to dimeric fragments. The base peak in the mass spectrum occurs at m/e 532 corresponding to $[M\text{-}PMe_3]^+$. Thus, as with (4), a dimeric or polymeric structure may be envisaged for (5). Bands at 529 cm^{-1} and 515 cm^{-1} in the infrared spectrum of (5) are consistent with ν(Ta-O) vibrations reported for the series of compounds[7] $[TaCl_n(OPh)_{5-n}]_m$ (*ca.* 520-550 cm^{-1}) which were reported to contain both bridging and terminal phenoxide ligands.

The 250 MHz ^1H NMR spectrum (d^8-tetrahydrofuran) of (5) displays at least seven Cp^* signals between 2.28-1.93 ppm. Associated PMe_3 signals resonate between 1.7-1.4 ppm. Thus, a complex mixture of species is produced in THF solution presumably indicating the presence of various oligomers.

Two half-sandwich niobium catecholate complexes have recently been reported, $CpNbCl_2(O_2C_6H_4)$ and $(CpNbCl)_2(\mu\text{-}O)(\mu\text{-}O_2C_6H_4)_2$[8]. The latter was shown to have a structure containing two bidentate, bridging catecholate ligands and a linear oxo bridge (Figure 6.2).

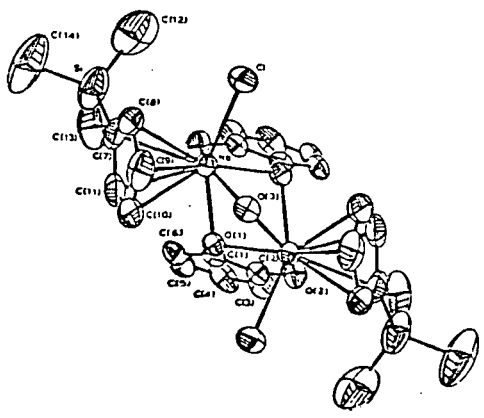

Figure 6.2 *Molecular Structure of* $(CpNbCl)_2(\mu\text{-}O)(\mu\text{-}O_2C_6H_4)_2$.

6.2.3 Reaction of (1) with phenols, ArOH (Ar = C_6H_5, 2,6-$Me_2C_6H_3$, 2,6-$^iPr_2C_6H_3$, 2,4,6-$Me_3C_6H_2$)

Complex (1) reacted smoothly with four equivalents of phenol to afford colourless crystals of $Cp^*Ta(OPh)_4$ (6) in *ca.* 80% yield (Equation 6.7).

$$\underset{(1)}{Cp^*Ta(PMe_3)(H)_2(\eta^2\text{-}CHPMe_2)} + 4PhOH \longrightarrow \underset{(6)}{Cp^*Ta(OPh)_4} + 2PMe_3 + 2H_2 \qquad (6.7)$$

(6) has been characterised by elemental analysis, infrared, ^1H, ^{13}C and mass spectroscopies. Unlike the catecholate complex (5), (6) is freely soluble in aromatic solvents and moderately soluble in aliphatic hydrocarbon solvents. Infrared spectroscopy locates the ν(Ta-O) vibrations at 515 cm^{-1}, within the range of other tantalum phenoxide complexes[7]. Mass spectrometry does not reveal ions above m/e 596, which corresponds to $[M\text{-}OPh+H]^+$. Further fragmentation entails loss of phenyl and phenoxide ligands.

The ^1H and ^{13}C NMR data show sharp, well resolved signals for both the (η^5-C_5Me_5) and Ph- ligands and are consistent with a single species in solution. When the reaction (6.7) was monitored by ^1H NMR spectroscopy it was observed that (1) and PhOH reacted immediately in the solid state with the evolution of a gas (presumably H_2). No intermediates could be detected by ^1H NMR. Since the phenyl group is more sterically demanding than Me and since the oxygen atom of PhOH would be expected to be a poorer electron donor than MeOH or ^iPrOH[9], the rapidity of reaction 6.7 suggests that PhOH reacts *via* a different mechanism to that involving MeOH and ^iPrOH, in Equations 6.3 and 6.4.

The greater acidity of PhOH (pK_a = 9.99) over MeOH (pK_a = 15.5) or

^{i}PrOH (pK_a = 16.5)[9] may result in preferential protonation of (1) at either the metal hydride or methine carbon sites rather than initial PMe_3 displacement. Indeed, hydrogen atoms coordinated to d^0 early transition metals are commonly hydridic in nature, and direct protonation is possible without prior coordination. A similar argument was used to explain the fact that $Cp^*TaL_2H_4$ (L = PMe_3, PMe_2Ph, $P(OMe)_3$) compounds reacted with anhydrous HCl gas at -80°C whereas the corresponding reactions with MeOH required several hours at 25°C[3].

Alternatively, since the α-carbon atom of high oxidation state alkylidene complexes is considered to be relatively nucleophilic, protonation at the methine carbon atom of (1) is also possible (*cf.* Equation 6.8).

$$Ta(CHCMe_3)(CH_2CMe_3)_3 \xrightarrow[-78^{o}C]{HCl} [Ta(CH_2CMe_3)_4Cl]\ ^{10} \qquad (6.8)$$

It was envisaged that the lower acidity of the ortho di-alkyl substituted phenols coupled with a greater steric demand would better facilitate the observation and isolation of intermediate species in the reaction of (1) with ROH reagents. Thus (1) reacted smoothly within minutes at room temperature with HO-2,6-$Me_2C_6H_3$ (2 equivalents) to afford a single product by ^{1}H NMR spectroscopy. The equivalent (η^5-C_5Me_5) hydrogens resonate at 2.08 ppm whilst the presence of two equivalent -O-2,6-$Me_2C_6H_3$ ligands is indicated by a singlet signal at 2.44 ppm (Me) and an AX_2 pattern assignable to the aryl hydrogens at 7.05 (d) and 6.76 (t) ppm with $^3J(HH)$ = 7.3 Hz.

Furthermore, a high frequency singlet resonance, integrating to two hydrogens, is observed at 11.54 ppm. This shift is supportive of metal hydride ligands coordinated to formally electron deficient, d^0 transition metal centres (*cf.* $TaHCl_2(CHCMe_3)(PMe_3)_3$, 10.00 ppm)[11]. The complex may then be formulated as $Cp^*Ta(H)_2(O\text{-}2,6\text{-}Me_2C_6H_3)_2$ (7) on the

basis of the above data (Equation 6.9). Two equivalents of PMe_3 are liberated in the reaction and are observable by ^1H NMR. No H_2 is observed in the reaction.

$$\underset{(1)}{Cp^*Ta(PMe_3)(H)_2(\eta^2\text{-}CHPMe_2)} + 2ArOH \longrightarrow Cp^*Ta(H)_2(OAr)_2 + 2PMe_3 \quad (6.9)$$

Ar = 2,6-$Me_2C_6H_3$ (7)
2,4,6-$Me_3C_6H_2$ (8)
2,6-$^iPr_2C_6H_3$ (9)

Similar rapid reactions occurred between (1) and HO-2,4,6-$Me_3C_6H_2$ and HO-2,6-$^iPr_2C_6H_3$ to produce the analogous compounds (8) and (9) respectively. Table 6.1 summarises the ^1H NMR data for (7)-(9).

COMPOUND	SHIFT (ppm)	REL.INT.	MULT.	J (Hz)	ASSIGNMENT
(7)	11.54	2	s	---	M-H
	7.05	4	d	$^3J(H_mH_p)$=7.3	Ar-H_m
	6.76	2	t	$^3J(H_mH_p)$=7.3	Ar-H_p
	2.44	12	s	---	Ar-Me
	2.08	15	s	---	C_5Me_5
(8)	11.54	2	s	---	M-H
	6.85	4	s	---	Ar-H_m
	2.46	12	s	---	Ar-Me(o)
	2.23	6	s	---	Ar-Me(p)
	2.12	15	s	---	C_5Me_5
(9)	16.09	2	s	---	M-H
	7.07	4	d	$^3J(H_mH_p)$=7.3	Ar-H_m
	6.90	2	t	$^3J(H_mH_p)$=7.3	Ar-H_p
	3.47	4	sp	$^3J(HH)$=6.8	CH$(CH_3)_2$
	2.04	15	s	---	C_5Me_5
	1.24	24	d	$^3J(HH)$=6.8	CH$(CH_3)_2$

Table 6.1 *250 MHz ^1H NMR for (7)-(9) (d^6-benzene).*

Attempts to isolate (7) led to decomposition to, as yet undefined products. Similarly (9) could be obtained only as an oil containing the uncomplexed phenol as indicated by both infrared and ^{1}H NMR spectroscopies. However, a broad infrared absorption at 1800 cm^{-1}, with a broad shoulder at 1780 cm^{-1} for this oil is consistent with the presence of two metal hydride ligands [*cf.* $Cp^*Ta(PMe_3)(H)_2(\eta^2\text{-}CHPMe_2)$, ν(M-H) = 1710(s), 1650(sh,br) cm^{-1}]. Although hydrido metal alkoxide complexes, such as $W(PMe_3)_4H_3(OMe)$[12] and $W_4(H)_2(O^iPr)_{14}$[13], have been previously reported, such combinations of hydride and alkoxide ligands remain unusual.

6.2.4 The Reaction of (1) with H_2O. The Molecular Structure of $(Cp^*Ta)_4(\mu_2\text{-}O)_4(\mu_3\text{-}O)_2(\mu_4\text{-}O)(OH)_2$ (10).

Complex (1) reacted with 5 equivalents of deoxygenated H_2O over the course of 24h. at 25°C to afford a white solid which appeared by ^{1}H NMR spectroscopy (d^6-benzene) to be a mixture of compounds. The infrared spectrum of this product displayed several strong absorptions between 580-860 cm^{-1} assignable to ν(Ta-O-Ta) vibrations[14], and a single sharp band at 3545 cm^{-1}, consistent with the presence of metal hydroxide ligands not engaged in hydrogen bonding[15]. No coordinated PMe_3 ligands were indicated. One of the components of this mixture crystallised as large colourless polyhedra from benzene solution and was subsequently studied by X-ray diffraction.

A crystal of dimensions 0.3 x 0.35 x 0.45 mm was sealed under argon in a pyrex capillary and the crystal structure determination was performed by Dr. W. Clegg at the University of Newcastle-upon-Tyne. The structural parameters are collected in Appendix 1H, the molecular structure is illustrated in Figures 6.3 and 6.4 and selected bond angles

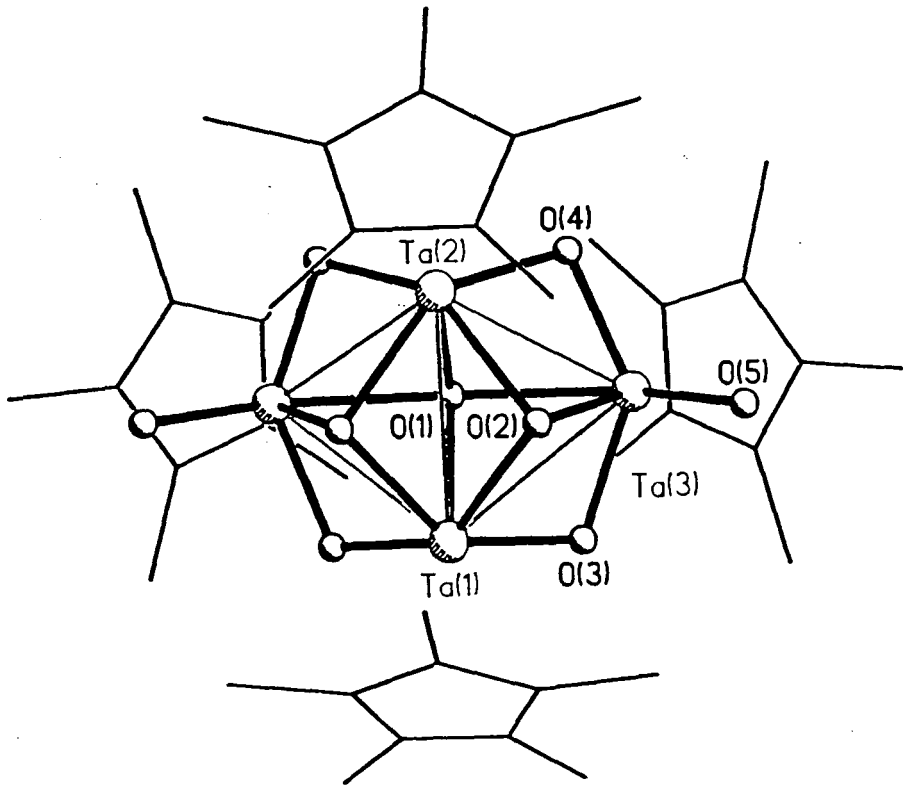

Figure 6.3 *Molecular Structure of* $Cp^*_4Ta_4(O)_7(OH)_2$ *(10).*

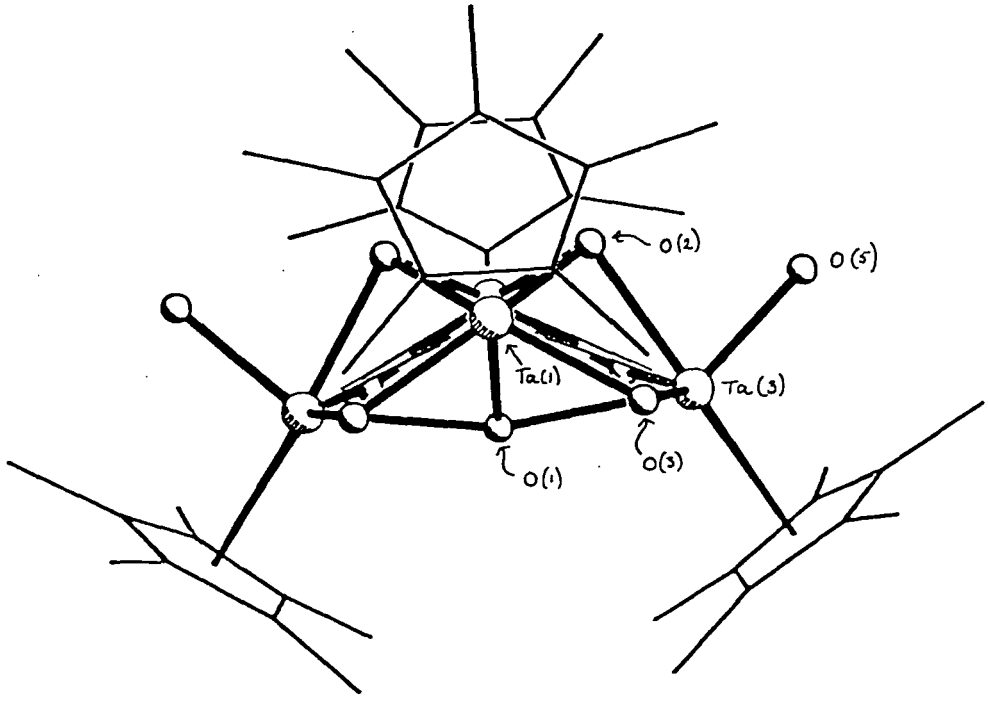

Figure 6.4 *Molecular Structure of* $Cp^*_4Ta_4(O)_7(OH)_2$ *(10) Profile.*

Ta(1)-Ta(2)	3.089(1)	Ta(1)-Ta(2)-Ta(3)	59.4(1)
Ta(1)-Ta(3)	3.022(1)	Ta(1)-Ta(2)-Ta(3')	59.3(1)
		Ta(1)-Ta(3)-Ta(2)	61.6(1)
Ta(2)-Ta(3)	3.013(1)	Ta(2)-Ta(1)-Ta(3)	59.1(1)
		Ta(2)-Ta(1)-Ta(3')	59.1(1)
Ta(1)-O(1)	2.103(5)	Ta(3)-Ta(1)-Ta(3')	101.2(1)
Ta(1)-O(2)	2.096(4)	Ta(3)-Ta(1)-Ta(3')	101.6(1)
Ta(1)-O(3)	1.951(4)		
Ta(2)-O(1)	2.128(7)	Ta(1)-Ta(3)-O(5)	108.5(1)
Ta(2)-O(2)	2.083(4)	Ta(2)-Ta(3)-O(5)	106.7(2)
Ta(2)-O(4)	1.940(4)		
Ta(3)-O(1)	2.358(1)	Ta(1)-O(1)-Ta(3)	85.1(1)
Ta(3)-O(2)	2.126(4)	Ta(1)-O(1)-Ta(3')	85.1(1)
Ta(3)-O(3)	1.957(5)	Ta(1)-O(1)-Ta(2)	93.8(2)
Ta(3)-O(4)	1.956(5)	Ta(1)-O(2)-Ta(3)	91.4(2)
Ta(3)-O(5)	1.950(5)	Ta(1)-O(3)-Ta(3)	101.3(2)
		Ta(1)-O(2)-Ta(2)	95.3(2)
		Ta(2)-O(1)-Ta(3)	84.2(2)
		Ta(2)-O(1)-Ta(3')	84.2(2)
		Ta(2)-O(2)-Ta(3)	91.4(1)
		Ta(2)-O(4)-Ta(3)	101.3(2)
		Ta(3)-O(1)-Ta(3')	164.3(3)
		O(1)-Ta(3)-O(5)	144.1(2)
		O(2)-Ta(3)-O(5)	77.7(2)
		O(3)-Ta(3)-O(5)	104.3(2)
		O(4)-Ta(3)-O(5)	102.3(2)

Table 6.2 *Selected Bond Distances (Å) and Angles (°) for $Cp^*_4Ta_4(O)_7(OH)_2$.*

and distances are collected in Table 6.2.

The compound has the stoichiometry $Cp^*_4Ta_4(O)_7(OH)_2$ (10) and consists of a butterfly core of four tantalum atoms with a plane of symmetry containing Ta(1) and Ta(2) (Figure 6.4). The polynuclear core is surrounded by seven bridging oxo ligands, four in doubly bridging environments [O(3), O(3'), O(4), O(4')], two in triply bridging environments [O(2), O(2')] and a unique quadruply bridging oxygen atom [O(1)]. The coordination sphere is completed by two terminal hydroxide ligands, one on each Ta(3) atom. Each metal atom is pentavalent and consequently, direct metal-metal bonds are not required to interpret the structure. Consistently, the metal-metal distances of 3.089(1)Å [Ta(1)-Ta(2)], 3.022(1)Å [Ta(1)-Ta(3)], and 3.013(1)Å [Ta(2)-Ta(3)] are significantly longer than those normally found in (Ta-Ta) bonded systems (typically *ca.* 2.6-2.8Å)[16].

A consideration of the two independent μ_2-O ligands [O(3) and O(4)] shows them to bridge in an angular manner with ∠Ta(1)O(3)Ta(3) = ∠Ta(2)O(4)Ta(3) = 101.3(2)°.

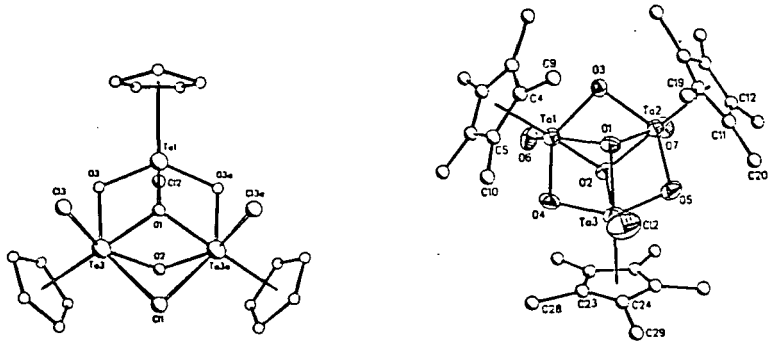

(a) (b)

Figure 6.5 *Molecular Structures of $Cp^*_3Ta_3O_4Cl_4$ (a) and $[Cp^*_3Ta_3O_5Cl(H_2O)_2]^+ Cl^-$ (b).*

Each bridge is slightly asymmetrical with Ta(2)-O(4) = 1.940(4)Å and Ta(3)-O(4) = 1.956(5)Å and the difference between Ta(1)-O(3) and Ta(3)-O(3) being statistically insignificant. These values are

comparable to the average (Ta-μ_2O) distances of 1.95Å in the recently reported compounds, $Cp^*_3Ta_3O_4Cl_4$ and $[Cp^*_3Ta_3O_5Cl(H_2O)_2]^+ Cl^-$ whose structures are illustrated in Figure 6.5[17].

However, the bonds are somewhat longer than those in linear (Ta-μ_2O) systems such as $[(Ta_2Cl_{10})(\mu\text{-}O)]^{2-}$; 1.880(1)Å [18] and $(Cp^*TaMe_3)_2(\mu\text{-}O)$; 1.909(7)Å [17] presumably due to more effective pπ-dπ interactions in the latter compounds[18].

The two triply bridging oxo ligands [O(2), O(2')] cap the trigonal faces defined by Ta(1)Ta(2)Ta(3) and Ta(1)Ta(2)Ta(3') respectively, in an asymmetrical manner, with an average (Ta-μ_3O) distance of 2.10(1)Å. This compares favorably to the analogous average distance of 2.13Å found in $[Cp^*_3Ta_3O_5Cl(H_2O)_2]^+Cl^-$ [17]. These parameters for the (M-μ_3O) moiety are also comparable to the corresponding average parameters for the half-sandwich cluster compounds in Table 6.3.

COMPOUND	Average d(M-O)/Å	Average ∠MOM (°)	Average d(M-M)/Å	REF
$Cp^*_4Ta_4O_7(OH)_2$	2.10(1)	92.7	3.04	#
$[Cp^*_3Ta_3O_5Cl(H_2O)_2]Cl$	2.13	92.7	----	17
$Cp_6Ti_6O_8$	1.97	94.2	2.89	19
$Cp_5V_5O_6$	1.86 *a*	91.1	2.75	20
	2.00 *e*	86.9		
$Cp_4Cr_4O_4$	1.94	92.8	2.81	20

Table 6.3 *Average d(M-μ_3O) and ∠M-μ_3O-M Parameters for some $[Cp_nM_nO_x]$ Compounds; #=This Work; a=Axial; e=Equitorial*

Although it is generally expected that larger ∠MOM angles accompany the shorter (M-O) distances, the presence of relatively short (M-M) contacts will tend to contract the angles at the bridging oxygen atom.

The oxygen atom O(1) occupies a μ_4-bridging position. However, the bridge is significantly asymmetrical with shorter distances to Ta(1) and

Ta(2) of 2.103(5)Å and 2.128(7)Å respectively and longer distances of 2.358(1)Å to symmetry related Ta(3) and Ta(3'). The shorter distances are comparable to the average (Ta-μ_3-O) distances of 2.10(1)Å in Table 6.3 whereas the longer distances are more consistent with dative covalent bonds (for comparison, known (Ta ← O) distances lie in the range *ca.* 2.22-2.31Å, *eg.* $Ta_2Cl_4(\mu_2\text{-}Cl)_2(^tBuC{\equiv}C^tBu)(THF)_2$, Ta-O(THF) = 2.282(8)Å[21] and $Ta_2Cl_4(\mu_2\text{-}Cl)_2(\mu_2\text{-}SMe_2)(THF)_2$, Ta-O(THF) = 2.239(6)Å[22].

The ∠Ta(1)O(1)Ta(2) angle of 93.8(2)^o is more acute than those for the μ_2-O ligands (101.3(2)^o) presumably reflecting the longer (Ta-O) distances in the μ_4-bridge. Conversely, the ∠Ta(3)O(1)Ta(3') angle of 164.3(3)Å reflects the larger separation of Ta(3) and Ta(3').

Several examples of μ_4-O coordination have been realised although generally the oxygen atom is at the centre of a regular tetrahedron of metal atoms as for example in $Be_4(O)(O_2CCH_3)_6$ [23], $Cu_4(O)Cl_6(OPPh_3)_4$ [24] and $Mg_4(O)Br_6(Et_2O)_4$ [25].

Finally, atoms Ta(3) and Ta(3') also possess terminal hydroxo ligands. Although the hydrogen atoms were not located on O(5) or O(5') their presence may be inferred from the infrared spectrum [ν(OH) = 3545 cm^{-1}] and by the absence of an absorption > 900 cm^{-1} assignable to terminal oxo ligands.

Moreover, the Ta(3)-O(5) distance of 1.950(5)Å is comparable to the average (Ta-μ_2O) values in the complex which formally represent single (Ta-O) bonds (and also compares favourably with the (Ta-O) single bond in $[TaCl_4(diars)_2]^+[TaCl_5.OEt]^-$ of 1.90(5)Å)[21].

Given the symmetry of the molecule and the bonding of the μ_4-O(1) ligand with dative bonds to Ta(3) and Ta(3') (Figure 6.6a) the μ_3-oxygens O(2), O(2') may be viewed as in Figure 6.6b.

Figure 6.6 *Representation of the Bonding in* $Cp^*_4Ta_4(O)_7(OH)_2$.

6.3 REACTIONS OF Cp^*TaCl_4 WITH Me_3SiOR reagents (R = Me, Et, C_3H_5, ReO_3, $SiMe_3$).

6.3.1 Preparations of $Cp^*TaCl_3.OR$ (R = Me (11), Et (12), C_3H_5 (13))

The use of Me_3SiOR reagents as sources of the alkoxide functionality was described in Chapter 5. Extension of this strategy to monocyclopentadienyl metal halides has allowed the isolation of compounds (11)-(13) according to Equation 6.10.

$$Cp^*TaCl_4 + Me_3SiOR \xrightarrow[70^oC]{CH_2Cl_2} Cp^*TaCl_3.OR + Me_3SiCl \qquad (6.10)$$

R = Me (11), 90%
Et (12), 80%
C_3H_5 (13), 67%

Compounds (11)-(13) were obtained as yellow crystalline solids by crystallisation from dichloromethane solvent. The reaction is presumed to proceed *via* initial coordination of Me_3SiOR to the tantalum complex forming a (1:1) adduct, as described in Chapter 5. Rapid condensation of Me_3SiCl will then afford the observed products. Attempts were not

made to isolate the adducts which are unstable at room temperature. Characterisation of the compounds (11)-(13) was provided by elemental analysis, infrared, ^{1}H, ^{13}C and mass spectroscopies (Chapter 7, section 7.6). Of particular interest is the ν(Ta-O) vibrational frequencies which are observed at 523 cm^{-1} (11), 563 cm^{-1} (12) and 560 cm^{-1} (13) respectively. The difference of *ca.* 40 cm^{-1} between (11) and (12) and (13) suggests that the -OMe ligand of (11) adopts a significantly different coordination mode to the -OEt and $-OC_3H_5$ ligands of (12) and (13), possibly indicating that the -OMe ligand bridges two metal centres, whilst both the -OEt and $-OC_3H_5$ ligands are terminally disposed. The recently reported complexes $(\eta^5\text{-}C_5H_4R)NbCl_3.OPh$ (R = H, $SiMe_3$) were anticipated to be dimeric but no supporting data were reported[8]. The above data are consistent with a dimeric formulation for (11) as in Figure 6.7.

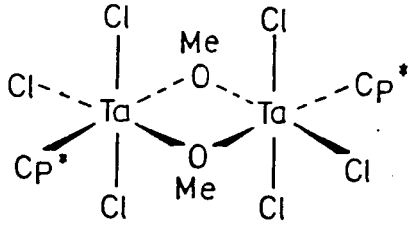

Figure 6.7 *Representation of the possible structure of (11).*

Consistently, the mass spectrum of (11) shows an envelope at m/e 819 which corresponds to the dimeric fragment $[M_2\text{-}2Cl\text{-}Me]^+$. Subsequent fragmentation results in the ions $[Cp^*TaCl_2.OMe]^+$ and $[TaCl_3.OMe]^+$ at m/e 417 and 317 respectively.

Conversely, (12) is best formulated with terminal -OEt ligands and the mass spectrum reveals no peaks above m/e 431 which corresponds to $[M\text{-}Cl]^+$.

Infrared spectroscopy indicates that (13) also possesses a terminal $-OC_3H_5$ group by analogy to (12). In addition, an absorption at 1645 cm^{-1} may be assigned to a ν(C=C) olefinic vibration indicating there to be no interaction between the vinyl group of the $-OC_3H_5$ ligand and the metal (ν(C=C) = 1648 cm^{-1} in $Me_3SiOC_3H_5$). This is further supported by the ^1H NMR spectrum which shows complex, second order multiplets between 4.9-5.7 ppm consistent with uncomplexed olefinic hydrogens.

The most prominent ions in the mass spectrum occur at m/e 443 and 421 corresponding to $[M-Cl]^+$ and $[M-OC_3H_5]^+$ respectively, with additional, very weak intensity envelopes attributable to dimeric fragments. On the basis of the above data, it is not possible to assign unambiguously, structures to (12) and (13). Interestingly, (12) could not be induced to react with a further equivalent of Me_3SiOEt even upon prolonged treatment with a large excess of the silane reagent at 80°C.

6.3.2 Preparation of $Cp^*TaCl_3.OReO_3$ (14)

Heterometallic oxides have been widely studied in connection with their ability to catalyse important processes such as hydrocarbon oxidation[1], olefin metathesis[27] and Fischer-Tropsch reactions[28] and with regard to their novel electrical conductivity properties[29].

Common synthetic routes to these oxides include pyrolysis of alkoxides[30] or hydrolysis of alkoxides or halides[17] and in most cases little control of product stoichiometry is achieved. A mild, controllable route to polymetallic oxides could exploit the ready condensation of Me_3SiCl between a metal chloride and a metal siloxide (Equation 6.11).

$$[M]\text{-}Cl + Me_3Si\text{-}O\text{-}[M'] \longrightarrow [M]\text{-}O\text{-}[M'] + Me_3SiCl \qquad (6.11)$$

The metals may be of the same or different elements. To test the validity of this approach for synthesising heterometallic oxides, the reaction between Cp^*TaCl_4 and $Me_3SiOReO_3$[31] has been investigated.

Cp^*TaCl_4 and $Me_3SiOReO_3$ reacted smoothly over 16h. at room temperature in dichloromethane solvent to afford yellow $Cp^*TaCl_3.OReO_3$ (14) in 57% yield. Compound (14) was found to be insufficiently soluble in solvents suitable for molecular weight or NMR study, but characterisation has been achieved by elemental analysis, infrared and mass spectroscopies (Chapter 7, section 7.6.7).

Specifically, the mass spectrum displays a band at m/e 670 assignable to $[M]^+$ (^{35}Cl, ^{185}Re) with daughter fragments at m/e 635 and 402 corresponding to $[M\text{-}Cl]^+$ and $[M\text{-}ReO_3Cl]^+$ respectively.

(14) is relative stable to moisture with no indication of hydrolysis or absorption of moisture upon *ca.* 5 min. exposure to air.

Infrared spectroscopy reveals a strong, broad band at 817 cm^{-1} indicative of bridging oxo ligands[14], and two strong, sharp bands at 987 cm^{-1} and 971 cm^{-1} (shoulder at 969 cm^{-1}) attributable to terminal ν(Re=O) vibrations. Previously reported complexes containing the (X-ReO_3) moiety have also been found to possess two ν(Re=O) bands due to symmetric and asymmetric $\nu(ReO_3)$ vibrations[32]. Figure 6.8 illustrates both unidentate and chelating perrhenate structures.

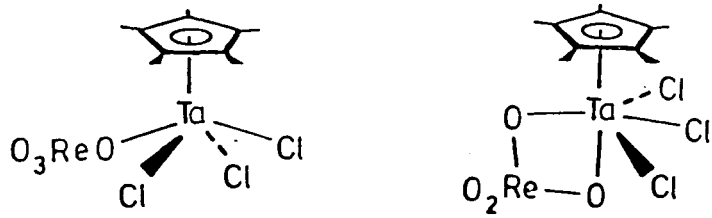

Figure 6.8 *Possible Structures for (14).*

An unambiguous assignment of the structure cannot be made on the basis of the the above data, however, the few other transition metal perrhenate complexes have been shown to possess a unidentate perrhenate ligand[32b,33]. Furthermore, the ν(Ta-Cl) vibrational region closely resembles that of $Cp^*TaCl_3.PMe_3$ and is quite different to that of Cp^*TaCl_3(dmpe) which disfavours the chelating structure shown in Figure 6.8(b). The possibility of ionic formulations such as $[Cp^*TaCl_3]^+[ReO_4]^-$ or $[Cp^*TaCl_2(\mu\text{-}Cl)_2TaCl_2Cp^*]^{2+}$ $[ReO_4]_2^-$ are inconsistent with the infrared data in that the perrhenate ion commonly displays two bands between 890-910 cm^{-1} which are not observed for (14)[34].

6.3.3 Reaction of Cp^*TaCl_4 With $(Me_3Si)_2O$: Preparation of $(Cp^*TaCl_3)_2(\mu\text{-}O)$ (15).

Following the synthesis of $Nb(O)Cl_3$ and $Nb(O)Cl_3L_2$ (L = THF, CH_3CN) *via* the reactions of $NbCl_5$ with $(Me_3Si)_2O$ described in Chapter 5, it was envisaged that $Cp^*Ta(O)Cl_2$ might prove accessible *via* the reaction of Cp^*TaCl_4 with $(Me_3Si)_2O$.

The reaction between Cp^*TaCl_4 and $(Me_3Si)_2O$ (one equivalent) was performed in 1,2-dichloroethane solvent at 75°C. The Me_3SiCl produced in the reaction was continuously removed by condensation onto a water-cooled trap. After 10h. the reaction mixture was allowed to cool to room temperature whereupon yellow crystals precipitated from solution. These were isolated and dried *in vacuo*. A further crop of yellow crystals were obtained by addition of petroleum ether to the supernatant solution.

The product was subsequently characterised as the oxo-bridged dimer $(Cp^*TaCl_3)_2(\mu\text{-}O)$ (15) recently obtained by Geoffroy and coworkers by hydrolysis of Cp^*TaCl_4[17]. The infrared spectrum of (15) gives a strong,

broad band centred at 690 cm^{-1} attributable to a ν(Ta-O-Ta) vibration[14] and mass spectrometry reveals peaks at m/e 402 and m/e 420 assignable to $[Cp^*Ta(O)Cl_2]^+$ and $[Cp^*TaCl_3\text{-}H]^+$ respectively.

The method described here allows the synthesis of pure (15) in *ca.* 49% yield which is a considerable improvement on the 8% yield afforded by the hydrolytic procedure. Geoffroy *et al.* proposed that the hydrolysis of Cp^*TaCl_4 proceeded according to Scheme 6.1[17].

$$Cp^*TaCl_4 + H_2O \longrightarrow [Cp^*TaCl_3(OH)] + HCl$$

$$[Cp^*TaCl_3(OH)] + Cp^*TaCl_4 \longrightarrow (Cp^*TaCl_3)_2(\mu\text{-}O)\ (15) + HCl$$

$$\Big\downarrow H_2O$$

$$(Cp^*TaCl_3(H_2O))_2(\mu\text{-}O)\ (16)$$

Scheme 6.1 *Proposed pathway of the reaction between Cp^*TaCl_4 and H_2O.*

An analogous reaction sequence may be proposed for the reaction of Cp^*TaCl_4 with $(Me_3Si)_2O$ (Scheme 6.2).

$$Cp^*TaCl_4 + (Me_3Si)_2O \longrightarrow [Cp^*TaCl_3.OSiMe_3] + Me_3SiCl$$

$$[Cp^*TaCl_3.OSiMe_3] + Cp^*TaCl_4 \longrightarrow (Cp^*TaCl_3)_2(\mu\text{-}O)\ (15) + Me_3SiCl$$

Scheme 6.2 *Possible pathway of the reaction between Cp^*TaCl_4 and $(Me_3Si)_2O$.*

The yield of (15) *via* the hydrolytic route was low because of the reaction of (15) with H_2O to form (16) which is the major product (*ca.* 85% yield)[17].

An alternative to Scheme 6.2 may be envisaged in which $Cp^*Ta(O)Cl_2$ is formed but is unstable towards reaction with Me_3SiCl under the reaction conditions (Scheme 6.3).

$$Cp^*TaCl_3.OSiMe_3 \rightleftharpoons Cp^*Ta(O)Cl_2 + Me_3SiCl$$

$$2Cp^*Ta(O)Cl_2 + 2Me_3SiCl \rightleftharpoons (Cp^*TaCl_3)_2(\mu\text{-}O)\ (15) + (Me_3Si)_2O$$

Scheme 6.3 *Alternative Pathway to (15).*

(15) was also formed, albeit more slowly, when the reaction between Cp^*TaCl_4 and $(Me_3Si)_2O$ was conducted at room temperature in dichloromethane solvent. The use of a coordinating solvent such as acetonitrile led to the isolation of (15) in 38% yield after 3.5h. at 80°C. There was no indication for the formation of $Cp^*Ta(O)Cl_2(CH_3CN)_x$ in this reaction.

6.4 SYNTHESIS, CHARACTERISATION AND PRELIMINARY REACTIVITY STUDIES OF $Cp^*Ta(O)Cl_2$ (17).

The failure to prepare $Cp^*Ta(O)Cl_2$ by reaction of Cp^*TaCl_4 with $(Me_3Si)_2O$, led us to investigate alternative routes to $Cp^*Ta(O)Cl_2$.

Transition metal centres have been reported to abstract oxygen atoms from a wide variety of oxygen containing molecules such as O_2[32a], N_2O[35], NO[36], CO_2[37], H_2O[17], H_2O_2[38], R_3NO[39], R_3PO[40] and R_2SO[41], some examples of which are given below (Equations 6.12-6.16).

$$Cp^*Re(CO)_2(THF) \xrightarrow[THF,\ 25^oC]{O_2\ (450\ psi)} Cp^*Re(O)_3 \quad [32a] \qquad (6.12)$$

$$(Cp_2TiCl)_2 + N_2O \xrightarrow[25^oC]{THF} (Cp_2TiCl)_2(\mu\text{-}O) + N_2 \quad [35] \qquad (6.13)$$

$$Cp^*_2VCl_2 + NO \xrightarrow[25^oC]{Toluene} Cp^*V(O)Cl_2 + (Cp^*V(O)Cl)_4 \quad [36] \qquad (6.14)$$

$$Cp_2Cr + Me_3NO \longrightarrow Cp_4Cr_4(O)_3(\eta^2\text{-}C_5H_4) \quad [39] \qquad (6.15)$$

$$NbCl_4Me + 3Ph_3PO \xrightarrow[25^oC]{CH_2Cl_2} Nb(O)Cl_2Me(Ph_3PO)_2 + Ph_3PCl_2 \quad ^{40} \quad (6.16)$$

Since it was envisaged that oxygen transfer from a suitable reagent to a Ta(III), d^2 complex would ultimately yield Ta(V) oxo compounds, the complex $Cp^*TaCl_2(PMe_3)_2$ described in Chapter 2, section 2.2.5 was anticipated to undergo the reaction described in Equation 6.17.

$$Cp^*TaCl_2(PMe_3)_2 \xrightarrow{[O]} Cp^*Ta(O)Cl_2 + 2PMe_3 \quad (6.17)$$

[O] = source of oxygen atoms.

It was shown in Chapter 2 that the PMe_3 ligands of this complex are labile and should be readily displaced by the oxygenating agent prior to oxygen atom transfer.

Indeed, $Cp^*TaCl_2(PMe_3)_2$ was found to react readily with the reagents, NO, Me_3NO, N_2O, DMSO and H_2O but no pure products could be isolated. With NO, Me_3NO and N_2O, oxygenation of PMe_3 occurred (infrared and ^1H NMR) and with H_2O, solvolysis of the (Ta-Cl) bonds resulted in the formation of $(Me_3PH)^+Cl^-$ [ν(PH) = 2470 cm^{-1}] [15].

However, a saturated toluene solution of $Cp^*TaCl_2(PMe_3)_2$ reacted cleanly with CO_2 (one atmosphere) at 25°C. Yellow crystals were deposited over a period of 16h; which were collected, washed with light petroleum ether and dried *in vacuo*. The crystalline compound was characterised as $Cp^*Ta(O)Cl_2$ (17) by elemental analysis, infrared, ^1H NMR and mass spectroscopies (Chapter 7, section 7.6.9). In particular, the stoichiometry of $C_{10}H_{15}Cl_2OTa$ was established by microanalysis:

Found (Required): %C, 29.61 (29.98); %H, 3.84 (3.76)

The 250 MHz ^1H NMR spectrum of (17) (d^6-benzene) gives a singlet resonance at 2.22 ppm attributable to the fifteen equivalent Cp^* hydrogens. The infrared spectrum reveals a characteristic Cp^* ring

breathing vibration at 1025 cm^{-1} and the ν(Ta-Cl) vibrations are found between 390-290 cm^{-1}. Significantly, a strong broad absorption at 675 cm^{-1} may be assigned to the stretching vibrations of bridging oxo ligands. No bands in the region 890-960 cm^{-1} attests to the absence of terminal oxo ligands.

Mass spectrometry $(CI)^+$ provides evidence for a dimeric structure, ions at m/e 805 and 769 correspond to $[M_2+H]^+$ and $[M_2-Cl]^+$ respectively. The only other tantalum containing ion in the spectrum is $[M+H]^+$ at m/e 403.

Unfortunately, (17) was not sufficiently soluble in hydrocarbon solvents or stable towards chlorocarbon solvents (*vide infra*) for molecular weight measurements, but on the basis of the above data we favour a dimeric structure for (17) containing two bridging oxo ligands, such that a more accurate representation for (17) is $(Cp^*TaCl_2)_2(\mu\text{-}O)_2$. This contrasts with the vanadium analogue, $Cp^*V(O)Cl_2$ which has been studied by X-ray diffraction and shown to be monomeric, possessing a distorted trigonal pyramidal geometry[42]. Interestingly, both monomeric and oxo bridged dimeric formulations of $Cp^*Re(O)Cl_2$ have been reported[43].

The synthesis of (17) reported here is unusual, formally involving the dissociation of CO_2 into 'O' and CO (Equation 6.18).

$$Cp^*TaCl_2(PMe_3)_2 + CO_2 \longrightarrow Cp^*Ta(O)Cl_2 + CO + 2PMe_3 \qquad (6.18)$$

The liberation of CO is confirmed by the observation of $Cp^*TaCl_2(PMe_3)(CO)_2$ (^1H NMR), formed as a byproduct *via* the reaction of $Cp^*TaCl_2(PMe_3)_2$ with CO according to Equation 6.19.

$$Cp^*TaCl_2(PMe_3)_2 + 2CO \longrightarrow Cp^*TaCl_2(PMe_3)(CO)_2 + PMe_3 \qquad (6.19)$$

The synthesis and characterisation of this compound were described in

The transition metal mediated deoxygenation of CO_2 giving CO and a metal oxide has been observed on previous occasions, such as those illustrated in Equations 6.20 and 6.21[37].

$$(Cp_2TiCl)_2 + CO_2 \xrightarrow[(10atm)]{90^oC} (Cp_2TiCl)_2(\mu\text{-}O) + CO \qquad (6.20)$$

$$3Cp_2Zr(CO)_2 + 3CO_2 \xrightarrow[(1atm)]{74^oC} (Cp_2Zr(O))_3 + 9CO \qquad (6.21)$$

Although the mechanism of formation of (17) has not been investigated, it is possible that the reaction proceeds *via* an intermediate (η^2-CO_2) complex similar to that proposed for the reaction in Equation 6.21 above[37].

Compound (17) is unstable to chlorocarbon solvents; being slowly converted to Cp^*TaCl_4 (^{1}H NMR) over several days at 25°C in chloroform. Of particular relevance to the failure of the reaction between Cp^*TaCl_4 and $(Me_3Si)_2O$ to produce (17), is the possibility of competitive reaction between (17) and Me_3SiCl highlighted in Scheme 6.3. (16) does indeed react with Me_3SiCl (2 equivalents) in d^6-benzene at 25°C to afford a major insoluble component and two soluble siloxide complexes which have not been fully identified. The insoluble compound was shown to be $(Cp^*TaCl_3)_2(\mu\text{-}O)$ (15) by infrared spectroscopy which may have resulted from the reactions of Scheme 6.4.

Consistently, $(Me_3Si)_2O$ is observed in the reaction mixture (^{1}H NMR). Studies are currently in progress to further delineate the course of these transformations and to investigate the wider reactivity of (17) towards organic substrates.

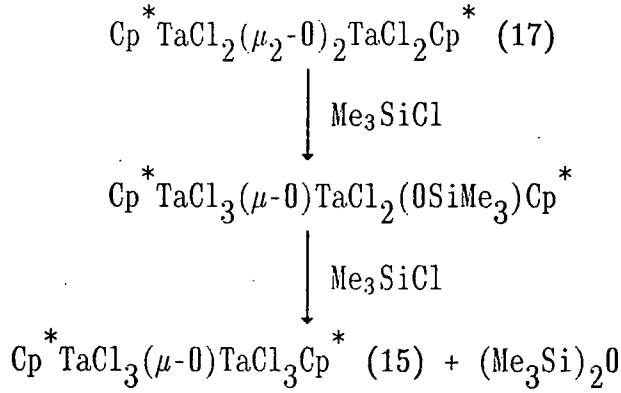

Scheme 6.4 *Potential Pathway for Conversion of (17) to (15)*

6.5 SUMMARY

A variety of oxo and alkoxo complexes of half-sandwich tantalum have been prepared *via* three general strategies.

(1) O-H bond cleavage reactions of alcohols and phenols.

(2) Condensation reactions of metal halides and siloxanes.

(3) Oxygen abstraction reactions of low valent tantalum complexes.

The compound $Cp^*Ta(PMe_3)(H)_2(\eta^2\text{-}CHPMe_2)$ has been shown to be a convenient source of the (Cp^*Ta) moiety facilitating the synthesis of compounds such as $Cp^*Ta(OR)_4$ (R = Me, ^iPr, Ph). With more sterically demanding phenols, products are obtained which may be formulated as $Cp^*Ta(H)_2(OAr)_2$ (Ar = 2,6-$Me_2C_6H_3$, 2,4,6-$Me_3C_6H_2$, 2,6-$^iPr_2C_6H_3$).

The use of Me_3SiOR reagents (R = alkyl, $SiMe_3$) has been extended to the synthesis of organometallic oxo and alkoxo compounds and the possibility for extending this methodology to the synthesis of heterobi- and polymetallic oxides has been demonstrated through the preparation of $[Cp^*TaCl_3.OReO_3]$.

The reaction between $Cp^*TaCl_2(PMe_3)_2$ and CO_2 has provided a useful

route to $Cp^*Ta(O)Cl_2$, the first heavy metal analogue of $CpV(O)Cl_2$, prepared by Fischer in 1958[44]. The remarkable reactivity of the metal-oxygen bonds in $Cp^*Ta(O)Cl_2$ towards chlorocarbons may explain why the heavier Group 5 $Cp'M(O)Cl_2$ compounds have remained elusive but nevertheless augers well for the reactivity of oxygen atoms in these environments[45].

6.6 REFERENCES

1. R.A. Sheldon and J.K. Kochi, "*Metal Catalysed Oxidations of Organic Compounds*", Academic Press, New York (1981).

2. W.A. Herrmann, E. Herdtweck, M. Flöel, J. Kulpe, U. Küsthardt and J. Okuda, *Polyhedron*, 1987, 6, 1165.

3. J.M. Mayer and J.E. Bercaw, *J.Am.Chem.Soc.*, 1982, 104, 2157.

4. 250 MHz ^1H NMR (d^6-benzene,298K), $Cp^*Ta(OMe)_4$ (2): 4.23(s,12H, -OMe), 1.98(s,15H,$C_5\underline{Me}_5$); $Cp^*Ta(O\text{-}iPr)_4$ (3): 4.67(sp,4H,$^3J(HH)$= 6Hz,$C\underline{H}(CH_3)_2$, 2.00(s,15H,$C_5\underline{Me}_5$), 1.25(d,24H,$^3J(HH)$= 6Hz,$CH(\underline{CH_3})_2$).

5. C.G. Barraclough, D.C. Bradley, J. Lewis and I.M. Thomas, *J.Chem. Soc.*, 1961, 2601.

6. J. Nieman, J.H. Teuben, J.C. Huffman and K.G. Caulton, *J.Organometallic Chem.*, 1983, 255, 193.

7. K.C. Malhotra, U.K. Banerjee and S.C. Chaudhry, *J.Ind.Chem.Soc.*, 1980, 57, 868.

8. F.A. Jalón, A. Otero, P. Royo, J.M. Fernández-G., M.J. Rosales and R.A. Toscano, *J.Organometallic Chem.*, 1987, 331, C1.

9. C.H. Rochester in "*The Chemistry of the Hydroxyl Group, Part 1*". Edited by S. Patai, Interscience, London (1971), Chapter 7.

10. R.R. Schrock and J.D. Fellman, *J.Am.Chem.Soc.*, 1978, 100, 3359.

11. J.D. Fellman, H.W. Turner and R.R. Schrock, *J.Am.Chem.Soc.*, 1980, 102, 6608.

12. K.W. Chiu, R.A. Jones, G. Wilkinson, A.M.R. Galas, M.B. Hursthouse and K.M.A. Malik, *J.Chem.Soc.Dalton Trans.*, 1981, 1204.

13. M. Akiyama, M.H. Chisholm, F.A. Cotton, M.W. Extine, D.A. Haitko, J. Leonelli and D. Little, *J.Am.Chem.Soc.*, 1981, 103, 779.

14. V. Katovic and C. Djordjevic, *Inorg.Chem.*, 1970, 9, 1720.

15. R.M. Silverstein, G.C. Bassler and T.C. Morill, "*Spectrometric Identification of Organic Compounds*", 4th Edition, John Wiley, New York (1981).

16. C.E. Holloway and M. Melník, *Rev.Inorg.Chem.*, 1985, 7, 1.

17. P. Jernakoff, C. De Meric De Bellefen, G.L. Geoffroy, A.L. Rheingold and S.J. Geib, *Organometallics*, 1987, 6, 1362.

18. F.A. Cotton and R.C. Najjar, *Inorg.Chem.*, 1981, 20, 1866.

19. J.C. Huffman, J.G. Stone, W.C. Krusell and K.G. Caulton, *J.Am.Chem.Soc.*, 1977, 99, 5829.

20. F. Bottomley, D.E. Paez and P.S. White, *J.Am.Chem.Soc.*, 1982, 104, 5651.

21. F.A. Cotton and W.T. Hall, *Inorg.Chem.*, 1980, 19, 2354.

22. F.A. Cotton, S.A. Duraj and W.J. Roth, *Acta Cryst.*, 1985, C41, 878.

23. W.H. Bragg, *Nature*, 1923, 111, 532.

24. J.A. Bertrand, *Inorg.Chem.*, 1967, 6, 495.

25. G. Stucky and R.E. Rundle, *J.Am.Chem.Soc.*, 1964, 86, 4821.

26. J.C. Dewan, D.L. Kepert, C.L. Raston and A.H. White, *J.Chem.Soc. Dalton Trans.*, 1975, 2031.

27. K.J. Ivin, "*Olefin Metathesis*", Academic Press, London (1983).

28. C.K. Rofer-De Poorter, *Chem.Rev.*, 1981, 81, 447.

29. P.P. Edwards, M.R. Harrison and R.Jones, *Chem.Brit.*, 1987, 23, 962.

30. D.C. Bradley and M.M. Faktor, *Trans.Faraday Soc.*, 1959, 55, 2117.

31. M. Schmidt and H. Schmidbaur, *Inorg.Synth.*, 1967, 9, 149.

32. (a) A.H. Klahn-Oliva and D. Sutton, *Organometallics*, 1984, 3, 1313.

(b) H.G. Mayfield Jr. and W.E. Bull, *Inorg.Chim.Acta.*, 1969, 3, 676.

33. W.A. Herrmann, R. Serrano, U. Küsthardt, M.L. Ziegler, E. Guggolz and T. Zahn, *Angew.Chem. Int.Ed.Engl.*, 1984, 23, 515.

34. R.H. Busey and O.L. Keller Jr., *J.Chem.Phys.*, 1964, 3, 676.

35. F. Bottomley, I.J.B. Lin and M. Mukaida, *J.Am.Chem.Soc.*, 1980, 102, 5238.

36. F. Bottomley, J. Darkwa, L. Sutin and P.S. White, *Organometallics*, 1986, 5, 2165.

37. G. Fachinetti, C. Floriani, A. Chiesi-Villa and C. Guastini, *J.Am. Chem.Soc.*, 1979, 101, 1767.

38. G. Parkin and J.E. Bercaw, *Polyhedron*, In press.

39. F. Bottomley, D.E. Paez, L. Sutin and P.S. White, *J.C.S. Chem Commun.*, 1985, 597.

40. C. Santini-Scampucci and J.G. Riess, *J.Chem.Soc.Dalton Trans.*, 1974, 1433.

41. D.B. Copley, F. Fairbrother, K.H. Grundy and A. Thompson, *J. Less Common Metals*, 1964, 6, 407.

42. W.A. Herrmann, G. Weichselbaumer and H.-J. Kneuper, *J.Organometallic Chem.*, 1987, 319, C21.

43. W.A. Herrmann, U. Küsthardt, M. Flöel, J. Kulpe, E. Herdtweck and E. Voss, *J.Organometallic Chem.*, 1986, 314, 151.

44. E.O. Fischer and S. Vigoureux, *Chem.Ber.*, 1958, 91, 1342.

45. V.C. Gibson and T.P. Kee, *J.C.S. Chem Commun.*, submitted for publication.

CHAPTER SEVEN

EXPERIMENTAL DETAILS

7.1 GENERAL

All manipulations of air and/or moisture sensitive materials were performed on a conventional vacuum/inert atmosphere (nitrogen or argon) line using standard Schlenk and cannula techniques, or in an inert atmosphere (nitrogen or argon) filled dry box.

The following solvents were dried by prolonged reflux over a suitable drying agent, being freshly distilled and deoxygenated before use (drying agent in parentheses): toluene (sodium metal), petroleum ether (40-60^{o}C and 100-120^{o}C, lithium aluminium hydride), tetrahydrofuran (sodium benzophenone ketyl), dichloromethane (calcium hydride), 1,2-dichloroethane (calcium hydride), acetonitrile (calcium hydride) and diethyl ether (lithium aluminium hydride).

The following NMR solvents were dried by vacuum distillation from a suitable drying agent (in parentheses) and stored over activated 4Å molecular sieves: d^{6}-benzene (phosphorus (V) oxide), d^{8}-toluene (phosphorus (V) oxide), d-chloroform (phosphorus (V) oxide), d^{8}-tetrahydrofuran (sodium benzophenone ketyl) and d^{3}-acetonitrile (4Å molecular sieves).

Elemental analyses were performed by the microanalytical services of this department.

Infrared spectra were recorded on Perkin-Elmer 577 and 457 grating spectrophotometers using either KBr or CsI windows. Absorptions abbreviated as: s (strong), m (medium), w (weak), br (broad), sp (sharp), sh (shoulder). *Mass spectra* were recorded on a VG 7070E Organic Mass Spectrometer.

NMR spectra were recorded on the following instruments, at the frequencies listed, unless stated otherwise: Brucker AC 250, ^{1}H (250.13 MHz), ^{13}C (62.90 MHz), ^{31}P (101.26 MHz); Varian EM 360L, ^{1}H (60 MHz);

Hitachi Perkin-Elmer R-24(B), ^{1}H (60 MHz). The following abbreviations have been used for band multiplicities: s (singlet), d (doublet), t (triplet), q (quartet), qnt (quintet), vct (virtually coupled triplet), m (multiplet). Chemical shifts are quoted as δ in ppm with respect to the following references, unless stated otherwise: ^{31}P (dilute aq. H_3PO_4, 0 ppm); ^{13}C (C_6D_6, 128.0 ppm); ^{1}H (C_6D_6, 7.15 ppm and $CDCl_3$, 7.24 ppm).

The following chemicals were prepared by previously published procedures: NaCp[1], $^{n}Bu_3SnCp$[2], Me_3SiCp^*[3], $CpTaCl_4$[4] and Cp^*TaCl_4[5]. Modified preparative procedures for the following are described below: PMe_3[6], KCp^*, Cp^*H[7] and $^{n}Bu_3SnCp^*$[8]. All other chemicals were obtained commercially and used as received unless stated otherwise.

7.1.1 Preparation of Trimethylphosphine (PMe_3)

A 5ℓ round bottomed flask, fitted with a pressure equalizing dropping funnel, efficient mechanical stir bar and a dry-ice condenser, was charged with magnesium turnings (180g, 7.5 mol.) and di-n-butylether (2 litres, sodium dried). The apparatus was then purged with nitrogen. A nitrogen atmosphere was maintained throughout the experiment. Methyl iodide (1000g, 7.05 mol.) was added dropwise to the stirred suspension over a period of *ca.* 2 h., at such a rate as to maintain a reaction temperature of *ca.* 30°C. Upon completion of the addition, the mixture was allowed to cool to room temperature whilst stirring for a further 2 h. Subsequently the mixture was cooled to 0°C and a degassed solution of triphenylphosphite (660g, 2.13 mol.) in di-n-butylether (*ca.* 500 cm^3) was added dropwise with stirring, over a period of 3 h. After approximately half of the phosphite/ether solution had been added, the reaction mixture became viscous due to the precipitation of magnesium

salts. Consequently a further 500 cm^3 of di-n-butylether was added. After the addition, the mixture was allowed to reach room temperature and was stirred for a further 2 h. The dropping funnel was then replaced with a distillation take-off device connected *via* a condenser to a 500 cm^3 round bottomed flask cooled in dry-ice/acetone. The reaction mixture was then heated to *ca.* 140°C and the fraction boiling between 35°-80°C was collected (*ca.* 400 cm^3). Further distillation through a 15cm, glass helix-packed column, collecting the fraction boiling between 39-41°C, provided pure PMe_3. Yield, 104g (64%).

7.1.2 Preparation of Potassium Pentamethylcyclopentadienide (KCp^*)

Pentamethylcyclopentadiene (8.0g, 58.8 mmol.) was added *via* syringe, under a counterflow of nitrogen, to a stirred suspension of potassium hydride (2.35g, 58.8 mmol.) in THF (300 cm^3) cooled to -78°C. The mixture was then allowed to warm to room temperature and was stirred for 16h under a constant, slow purge of nitrogen. Subsequently, the mixture was allowed to stand for several hours whereupon the product separated as a flocculent white solid. The supernatant solution was decanted from the solid, which was collected, washed with petroleum ether (2 x 100 cm^3, 40-60°C) and dried *in vacuo*. Yield, 8.8g (86%).

7.1.3 Preparation of Pentamethylcyclopentadiene (Cp^*H)

The synthetic transformations involved are outlined in Scheme 7.1. 1,2 Dibromobutane was prepared by the dropwise addition of bromine (512g, 3.2 mol.) to a cooled (-20°C) mixture of *cis* and *trans* but-2-ene (180g, 3.2 mol.) in a 500 cm^3 twin-necked, round bottomed flask. The product was distilled from the reaction mixture at 18-20°C (1.0 Torr).

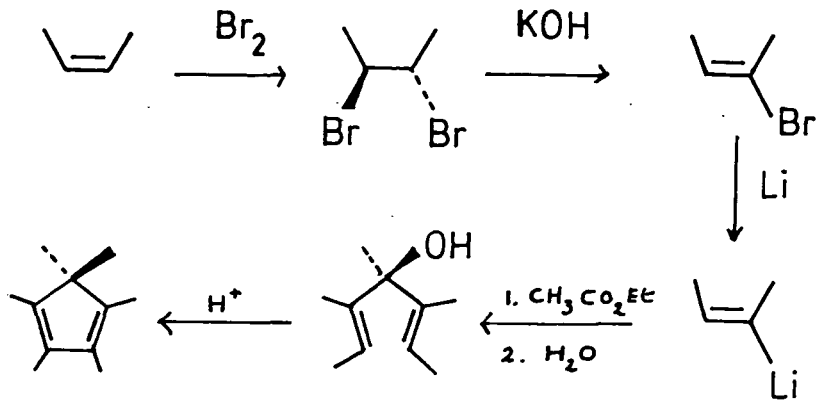

Scheme 7.1

A 2ℓ round bottomed flask, fitted with a pressure equalizing dropping funnel, efficient mechanical stir bar, thermometer and reflux take-off device was charged with the dibromobutane above and ethan-1,2-diol (300 cm^3). With the flask contents heated to 115°C, an ethan-1,2-diol solution of KOH (230g in 500 cm^3) was added dropwise over a period of 3h, so that the 2-bromobutene formed distilled directly from the reaction vessel (at 83-85°C). Once isolated, the 2-bromobutene was purified by passage down a column containing activated alumina (*ca.* 25cm length, 6cm diam.), dried over molecular sieves (4Å) and deoxygenated.

A 3ℓ round bottomed flask, fitted with a pressure equalizing dropping funnel, reflux condenser and mechanical stir bar was charged with lithium wire (28g, 4 mol., cut to 5mm pieces) and diethyl ether (500 cm^3, sodium dried). The mixture was deoxygenated and purged with nitrogen. A nitrogen atmosphere was maintained throughout the reaction. The dropping funnel was charged with 2-bromobutene (45 cm^3, 0.44 mol.), which was added dropwise to the stirred lithium/ether mixture at a rate

sufficient to maintain gentle reflux. The dropping funnel was then charged with ethyl acetate (92 cm^3, 0.94 mol.) and 2-bromobutene (162 cm^3, 1.59 mol.), and this mixture was added dropwise over a period of *ca.* 5h, again at a rate sufficient to maintain gentle reflux. Once the addition was complete, the mixture was stirred at room temperature overnight.

A saturated aqueous solution of ammonium chloride (120g in 600 cm^3) was then added dropwise with stirring to neutralise the remaining lithium, and the resulting mixture was transferred to a 2ℓ separating funnel where the aqueous layer was washed with diethyl ether (3 x 100 cm^3), the combined ether extracts were then concentrated to *ca.* 300 cm^3 on a rotary evaporator.

This diethyl ether concentrate was added dropwise to a slurry of p-toluenesulphonic acid monohydrate (18g, 94.6 mmol.) in diethyl ether (250 cm^3) in a 1ℓ round bottomed flask, fitted with a reflux condenser. The rate of addition was such as to maintain gentle reflux. After the addition was complete, the mixture was stirred for a further 30 mins. at room temperature and was then poured into 600 cm^3 of a saturated, aqueous solution of sodium hydrogen carbonate (42g, 0.5 mol.) containing sodium carbonate (9.5g, 89.6 mmol.). The yellow aqueous phase was removed and extracted with diethyl ether (3 x 100 cm^3). The ether extracts were then combined, dried over sodium sulphate, and concentrated to *ca.* 200 cm^3 on a rotary evaporator.

This crude product was distilled through a 15cm glass helix-packed column. Two fractions were collected: the first at 28-29°C (1.5 Torr) as a colourless liquid (44.9g) and a pale yellow fraction (6.74g) at 40-44°C (1.5 Torr). Yield, 40% (based on ethyl acetate). Both fractions were found to be sufficiently pure for further use.

7.1.4 Preparation of Tri-n-butyltinpentamethylcyclopentadienide ($^{n}Bu_3SnCp^*$)

Tri-n-butyltin chloride (16.5g, 50.6 mmol.) was added, by syringe, to a suspension of potassium pentamethylcyclopentadienide (8.8g, 50.6 mmol.) in toluene (350 cm^3) maintained at room temperature. After stirring for 2 days, the gelatinous precipitate of potassium chloride was allowed to settle and the supernatant solution filtered. The residue was washed with petroleum ether (2 x 50 cm^3, 40-60°C) and all washings were combined. The volatiles were removed under reduced pressure to leave $^{n}Bu_3SnCp^*$ as a viscous yellow liquid. Yield 19g (89%). This material was found to be of sufficient purity for use in subsequent reactions.

7.2 EXPERIMENTAL DETAILS TO CHAPTER 2

7.2.1 Reaction of $CpTaCl_4$ with PMe_3: Preparation of $CpTaCl_4.PMe_3$

Trimethylphosphine (0.11 cm^3, 1.04 mmol.) was condensed onto a mixture of $CpTaCl_4$ (0.4g, 1.04 mmol.) and dichloromethane (25 cm^3) at -196°C. Upon warming to room temperature, the mixture was stirred under nitrogen (one atmosphere) for 16h. to afford an orange solution and a beige coloured suspension. Filtration, followed by removal of the volatile components under reduced pressure afforded a yellow-orange solid, which was washed with petroleum ether (10 cm^3, 40-60°C) and dried *in vacuo*. Recrystallisation from toluene (*ca.* 20 cm^3) at -35°C gave yellow crystals of $CpTaCl_4.PMe_3$. Yield, 0.15g (31%). Elemental Analysis for $C_8H_{14}Cl_4PTa$, Found (Required): %C, 21.18 (20.71); %H, 3.03

(3.05); IR (Nujol,KBr,cm^{-1}): 3120(w), 3100(w), 1443(s), 1415(m), 1300(w), 1285(m), 1075(m,sp), 1030(m,sp), 1020(m,sp), 960(s,br), 885(m), 855(s), 740(m), 735(m,sh); ^{1}H NMR (250MHz,d^{6}-benzene,298K): 6.16(s,5H, $C_5\underline{H}_5$), 1.50(d,9H,$^{2}J(PH)$=10.9Hz,$P\underline{Me}_3$); ^{31}P NMR (d^{6}-benzene,298K,broad band decoupled): 11.83(s,$\underline{P}Me_3$); ^{13}C NMR (d^{6}-benzene,298K,broad band decoupled): 124.20(s,$\underline{C}_5H_5$), 14.13(d,$^{1}J(PC)$=29.4Hz,PMe_3); Mass Spectrum m/e (CI,isobutane carrier gas,^{35}Cl): 427 $[M-Cl]^+$, 351 $[M-Cl-PMe_3]^+$.

Performing the above reaction in toluene solvent instead of dichloromethane afforded $CpTaCl_4.PMe_3$ in 37% yield, along with a toluene insoluble blue-grey solid.

7.2.2 Reaction of $CpTaCl_4$ With Magnesium in the Presence of PMe_3 (I): Preparation of $CpTaCl_3.PMe_3$

Trimethylphosphine (0.16g, 2.1 mmol.) was vacuum condensed from a graduated cold finger onto a mixture of $CpTaCl_4$ (0.4g, 1.04 mmol.), magnesium turnings (12.48mg, 0.52 mmol.) and THF (25 cm^3) cooled to -196°C in a "Rotoflo" glass ampoule (150 cm^3 capacity). The mixture was allowed to warm to room temperature, whereupon one atmosphere of nitrogen was introduced into the vessel. Stirring was maintained at this temperature until all the magnesium had been consumed (4h). The volatiles were removed under reduced pressure and the residue was extracted into toluene (50 cm^3) containing a little trimethylphosphine (0.1 cm^3) to afford a purple solution. Filtration followed by concentration (*ca.* 8 cm^3) and cooling (-78°C) afforded purple crystals of $CpTaCl_3.PMe_3$. Yield, 0.30g (68%). Elemental Analysis for $C_8H_{14}Cl_3PTa$, Found (Required): %C, 21.90 (22.42); %H, 3.62 (3.30); IR (Nujol,KBr,cm^{-1}): 3090(w), 1428(m), 1414(m), 1300(m), 1283(m), 1029(w), 1010(w), 955(s,br), 870(sh), 850(sh), 840(m), 832(m), 819(s), 737(m),

670(w); ^{1}H NMR (250MHz,d^{6}-benzene,298K): No signals between +200 and -200 ppm; Mass Spectrum m/e (EI,70 eV,^{35}Cl): 351 $[M-PMe_3]^+$, 316$[M-PMe_3-Cl]^+$.

7.2.3 Reaction of Cp^*TaCl_4 With Magnesium in the Presence of dmpe: Preparation of Cp^*TaCl_3(dmpe)

Dmpe (0.20g, 1.33 mmol.) was added, *via* syringe against a counterflow of nitrogen, to a suspension of Cp^*TaCl_4 (0.4g, 0.87 mmol.) and magnesium turnings (0.01g, 0.44 mmol.) in THF (30 cm^3) at room temperature. Stirring at room temperature produced first a yellow solution which darkened through orange to a deep purple-brown after all the magnesium had been consumed (6h). The volatiles were removed and the purple residue extracted with toluene (60 cm^3) to afford a purple solution. Filtration, followed by concentration to 5 cm^3 and cooling to -60°C, afforded purple crystals, which were collected, washed with petroleum ether (2 x 4 cm^3, 40-60°C) and dried *in vacuo*. Yield, 0.3g (60%). Elemental Analysis for $C_{16}H_{31}Cl_3P_2Ta$, Found (Required): %C, 33.26 (33.55); %H, 5.54 (5.47); IR (Nujol,CsI,cm^{-1}): 1430(m), 1420(m), 1300(m), 1290(s), 1148(m), 1095(w), 1075(w), 1030(m), 1010(w), 970(s), 955(s), 945(s), 880(w), 870(w), 850(w), 805(w), 750(m), 740(m), 730(m), 710(m), 660(m), 353(m), 290(s,sh), 280(s), 265(s); ^{1}H NMR (250MHz,d^{6}-benzene,298K): No signals between +200 and -200 ppm; Mass Spectrum m/e (EI,70 eV,^{35}Cl): 420 $[M-dmpe-H]^+$, 386$[M-dmpe-Cl]^+$; Magnetic moment (d^{6}-benzene,298K): μ_{eff}= 1.5 BM (Evans).

7.2.4 Reaction of $CpTaCl_4$ With Magnesium in the Presence of PMe_3 (II): Preparation of $CpTaCl_2(PMe_3)_3$

Trimethylphosphine (2.74g, 36 mmol.) was vacuum condensed onto a mixture of $CpTaCl_4$ (3.5g, 9.0 mmol.), magnesium turnings (0.22g, 9.0 mmol.) and THF (50 cm^3) frozen at -196°C in a thick-walled "Rotoflo" glass ampoule (150 cm^3 capacity). The mixture was allowed to warm to room temperature, whereupon one atmosphere of nitrogen was admitted. Stirring was maintained at room temperature until all the magnesium had been consumed (12h). The volatiles were removed under reduced pressure and the residue was extracted with toluene (100 cm^3). After filtration, the red solution was concentrated to 20 cm^3 and cooled to -78°C to afford red crystals, which were collected, washed with petroleum ether (2 x 5 cm^3) and dried *in vacuo*. Two further toluene extractions (2 x 50 cm^3) of the crude residue afforded a combined yield of 1.44g (30%). Elemental Analysis for $C_{14}H_{32}Cl_2P_3Ta$, Found (Required): %C, 30.90 (30.84); %H, 5.40 (5.93); IR (Nujol,CsI,cm^{-1}): 3090(w), 1440(m,br), 1416(s), 1308(m), 1300(m,sh), 1289(m), 1278(m), 1270(m), 1107(w), 1068(w), 993(m), 945(s,br), 866(m), 839(m,br), 831(m), 806(m), 775(m), 759(m), 720(s), 710(s), 703(s), 660(m), 379(w), 352(m), 295(m), 260(s); ^1H NMR (250MHz,d^6-benzene,296K): 4.13(m,5H,$^3J(PH)$=3.5,2.7Hz,$C_5\underline{H}_5$†), 1.20(vct,18H,J(PH)=3.3Hz,2*trans*-$P\underline{Me}_3$,); 1.11(d,9H,$^2J(PH)$=6.7Hz,$P\underline{Me}_3$); ^{31}P NMR (d^6-benzene,296K,broad band decoupled): -26.46(s,$\underline{P}Me_3$), -29.79(s,2*trans*-$P\underline{Me}_3$); ^{13}C NMR (d^6-benzene,296K,broad band decoupled): 88.65(s,$\underline{C}_5H_5$), 24.01(d,$^1J(PC)$=21.9Hz,$P\underline{Me}_3$), 16.83(vct,J(PC)=10.3Hz, 2*trans*-$P\underline{Me}_3$).

†Coupling pattern is a poorly resolved dt and the quoted J-values are approximate; values obtained in d^8-toluene.

7.2.5 Reaction of Cp^*TaCl_4 With Magnesium in the Presence of PMe_3: Preparation of $Cp^*TaCl_2(PMe_3)_2$

Trimethylphosphine (2.03g, 26.7 mmol.) was condensed onto Cp^*TaCl_4 (3.5g, 7.63 mmol.), magnesium turnings (0.18g, 7.63 mmol.) and THF (40 cm^3) frozen at -196°C. Upon warming to room temperature, one atmosphere of argon was introduced. After stirring for 1h. at ambient temperature, a red colouration developed in the THF solution. A further 9h. stirring was required to consume all the magnesium. Removal of the volatile components under reduced pressure and extraction of the brown residue into petroleum ether (80 cm^3, 40-60°C) afforded a deep cherry-red solution. Filtration, followed by concentration under reduced pressure (20 cm^3) and cooling to -78°C afforded red crystals. Repeated extractions of the crude residue, followed by crystallisation as above, gave a combined yield of 2.7g (66%). Elemental Analysis for $C_{16}H_{33}Cl_2P_2Ta$, Found (Required): %C, 35.00 (35.63); %H, 6.04 (6.18); IR (Nujol,CsI,cm^{-1}): 1425(m), 1300(m), 1286(m), 1280(m,sh), 1028(m), 951(s,br), 844(m), 731(s), 667(m), 415(w), 355(m), 336(m,sh), 277(m); ^1H NMR (250MHz,d^6-benzene,0.037M,298K): 91.45(s,15H,$C_5\underline{Me}_5$), 20.56(s,18H, $2P\underline{Me}_3$,); Magnetic moment (d^6-benzene,298K): μ_{eff}= 2.1 BM (Evans).

7.2.6 Preparation of Cp^*NbCl_4

A solution of Me_3SiCp^* (0.38g, 1.85 mmol.) in toluene (20 cm^3) was added dropwise with stirring over a period of 20 min. to a suspension of finely ground $NbCl_5$ (0.5g, 1.85 mmol.) in toluene (40 cm^3) cooled at 0°C. An immediate reaction ensued to give a clear red solution, from which a brown solid was precipitated during the subsequent 12h. period at room temperature. After 24 h. at room temperature, the volatiles

were removed under reduced pressure and the residue was extracted into dichloromethane (60 cm^3) and filtered to afford a deep red solution. Concentration (20 cm^3) and cooling to -78°C produced red crystals which were collected, washed with petroleum ether (2 x 10 cm^3, 40-60°C) and dried *in vacuo*. Yield 0.46g (67%). Recrystallisation from dichloromethane afforded pure Cp^*NbCl_4. Elemental Analysis for $C_{10}H_{15}Cl_4Nb$, Found (Required): %Nb, 24.64 (25.11); %Cl, 38.14 (38.33); %C, 32.91 (32.46); %H, 4.07 (4.10); IR (Nujol,CsI,cm^{-1}): 1480(m,br), 1430(m), 1070(w), 1018(m), 905(w), 805(w), 735(w), 655(m), 436(m), 411(m), 350(s,br); ^1H NMR (250MHz,d-chloroform,298K): 2.49(s,$C_5\underline{Me}_5$); Mass Spectrum m/e (EI,70 eV,^{35}Cl): 333 $[M-Cl]^+$, 297 $[M-2Cl-H]^+$, 214 $[NbOCl_3]^+$, 179 $[NbOCl_2]^+$.

7.2.7 Reaction of $Cp^*TaCl_2(PMe_3)_2$ With Diphenylacetylene: Preparation of $Cp^*TaCl_2(\eta^2$-PhC≡CPh)

Toluene (30 cm^3) was added to a solid mixture of $Cp^*TaCl_2(PMe_3)_2$ (0.4g, 0.74 mmol.) and diphenylacetylene (0.13g, 0.74 mmol.) at room temperature. The mixture was stirred for 2 weeks to give an orange solution which was filtered, concentrated (10 cm^3) and cooled to -78°C to afford the product as orange crystals. Yield, 0.27g (65%). Elemental Analysis for $C_{24}H_{25}Cl_2Ta$, Found (Required): %C, 50.98 (50.99); %H, 4.58 (4.47); IR (Nujol,CsI,cm^{-1}): 3080(w), 3050(w), 1644(w), 1593(w), 1570(w), 1442(s), 1270(w,br), 1176(m), 1160(m), 1073(m), 1030(m), 940(m), 925(m), 840(w), 788(m). 769(s), 717(m), 710(m), 692(s), 608(w), 553(w), 520(w), 390(m), 345(s), 330(s); ^1H NMR (250MHz,d^6-benzene,298K): 7.78(d,4H,$^3J(H_oH_m)$=7.7Hz,ArH_o), 7.23(dd,4H,$^3J(H_oH_m)$= 7.7Hz,$^3J(H_mH_p)$=7.14Hz,ArH_m), 7.04(t,2H,$^3J(H_mH_p)$=7.14Hz,ArH_p), 1.82(s,15H,$C_5\underline{Me}_5$); ^{13}C NMR (d^6-benzene,298K, broad band decoupled):

222.00(s,Ph$\underline{C}\equiv\underline{C}$Ph), 141.60(s,Ph-$C_{ipso}$), 130.29(s,Ph-C), 128.84(s,Ph-C), 128.60(s,Ph-C), 120.95(s,$\underline{C}_5Me_5$), 11.78(s,$C_5\underline{Me}_5$); Mass Spectrum m/e (EI,70 eV,^{35}Cl): 564 $[M]^+$, 528 $[M-Cl-H]^+$, 386 $[M-Ph_2C_2]^+$.

7.2.8 Reaction of $CpTaCl_2(PMe_3)_3$ With Carbon Monoxide: Preparation of $CpTaCl_2(PMe_3)_2(CO)$

A thick-walled glass "Rotoflo" ampoule containing $CpTaCl_2(PMe_3)_3$ (0.2g, 0.37 mmol.) in toluene (30 cm^3) was evacuated and cooled to -78^{o}C. One atmosphere of carbon monoxide was introduced into the vessel at this temperature. The mixture was allowed to warm to room temperature and was stirred for 1h. The excess carbon monoxide was carefully vented and the mixture was filtered. Removal of the solvent under reduced pressure afforded pure $CpTaCl_2(PMe_3)_2(CO)$ as pink crystals, which were washed with petroleum ether (5 cm^3, 40-60^{o}C) and dried *in vacuo*. Yield, 0.16g (87%). Elemental Analysis for $C_{12}H_{23}Cl_2OP_2Ta$, Found (Required): %C, 29.00 (28.99); %H, 4.49 (4.67); IR (Nujol,CsI,cm^{-1}): 3080(w), 1890(s,br), 1432(m), 1420(m), 1303(m), 1280(m), 1117(w), 1070(w), 1006(m), 950(s,br), 861(m), 846(m), 838(m), 829(m), 820(m), 810(m), 737(m), 729(s), 670(m), 600(w), 523(m), 500(m), 356(m), 273(s); ^{1}H NMR (250MHz,d^6-benzene,298K): 4.44(t,5H,^{3}J(PH)=2.5Hz,$C_5\underline{H}_5$), 1.19(vct,18H, J(PH)=8.2Hz,2P$\underline{Me}_3$); ^{31}P NMR (d^6-benzene,298K,broad band decoupled): -28.10(s,2$\underline{P}Me_3$); ^{13}C NMR (d^6-benzene,298K,broad band decoupled): 247.76(s,$\underline{C}O$,^{2}J(PC) unresolved), 89.75(s,$\underline{C}_5H_5$), 16.41(vct,J(PC)=10.1 Hz,2P$\underline{Me}_3$); Mass Spectrum m/e (EI,70 eV,^{35}Cl): 381 $[Cp_2TaCl_2]^+$, 351 $[CpTaCl_3]^+$, 332 $[CpTaOCl_2]^+$, 316 $[CpTaCl_2]^+$.

7.2.9 Reaction of $Cp^*TaCl_2(PMe_3)_2$ With Carbon Monoxide: Preparation of $Cp^*TaCl_2(PMe_3)(CO)_2$

A thick-walled glass "Rotoflo" ampoule was charged with $Cp^*TaCl_2(PMe_3)_2$ (0.2g, 0.37 mmol.) and toluene (30 cm^3). The red solution was evacuated whilst being cooled to -78°C. At this temperature, one atmosphere of carbon monoxide was introduced into the vessel. Warming to ambient temperature with stirring produced a purple coloured solution. After 3h. the solution was filtered, concentrated to 5 cm^3 and cooled (-78°C) to afford purple crystals. These were collected, washed with cold petroleum ether (2 x 5 cm^3, 40-60°C) and dried *in vacuo*. Yield, 0.18g (94%). Elemental Analysis for $C_{15}H_{24}Cl_2O_2PTa$, Found (Required): %C, 34.63 (34.70); %H, 4.65 (4.67); IR (Nujol,KBr,cm^{-1}): 1988(s), 1900(s), 1880(s), 1428(w), 1305(w), 1290(m, sp), 1283(m,sp), 975(s), 960(m), 745(m), 483(m), 465(m); ^1H NMR (250MHz,d^6-benzene,298K): 1.75(s,15H,$C_5\underline{Me}_5$), 1.26(d,9H,$^2J(PH)$=9.8Hz, $P\underline{Me}_3$); ^{31}P NMR (d^6-benzene,298K,broad band decoupled): -26.60(s,$\underline{P}Me_3$); ^{13}C NMR (d^6-benzene,298K,broad band decoupled): 238.10(d,$^2J(PC)$=25.2Hz, $2\underline{C}O$), 104.83(s,$\underline{C}_5Me_5$), 14.99(d,$^1J(PC)$=27.0Hz,$P\underline{Me}_3$), 11.28(s,$C_5\underline{Me}_5$)

7.2.10 Preparation of *cis*-$Cp^*Ta(CO)_2(PMe_3)_2$

Trimethylphosphine (0.15g, 1.9 mmol.) and THF (30 cm^3) were condensed onto a mixture of $Cp^*TaCl_2(PMe_3)(CO)_2$ (0.5g, 0.96 mmol.) and sodium amalgam (11.1g amalgam, 0.5% w/w, 2.4 mmol.) cooled to -196°C in a 150 cm^3 "Rotoflo" glass ampoule. Upon warming to *ca.* 0°C, one atmosphere of argon was introduced and the mixture was stirred at room temperature for 24h. to give an orange-brown solution. Removal of the volatiles under reduced pressure, followed by extraction into toluene

($50cm^3$) and filtration afforded an orange-red solution. Concentration ($10\ cm^3$) and cooling of this solution to -78°C gave orange crystals. Yield, 0.3g (61%). Elemental Analysis for $C_{18}H_{33}O_2P_2Ta$, Found (Required): %C, 41.00 (41.22); %H, 6.78 (6.36); IR (Nujol,KBr,cm^{-1}): 1822(s), 1732(s), 1440(m), 1306(w), 1298(w), 1287(m), 1280(m), 1025(w), 960(s), 941(s), 855(w), 843(w), 715(w), 665(m); ^1H NMR (250MHz,d^6-benzene,298K): 1.93(s,15H,$C_5\underline{Me}_5$), 1.13(vct,18H,J(PH)=6.4Hz,$2P\underline{Me}_3$); ^{31}P NMR (d^6-benzene,298K,broad band decoupled): -15.97(s,$2\underline{P}Me_3$); ^{13}C NMR (d^6-benzene,298K,broad band decoupled): 278.11(d,^{2}J(PC)=22.9Hz,$2\underline{C}O$), 104.47(s,$\underline{C}_5Me_5$), 22.96(m,$2P\underline{Me}_3$), 12.40(s,$C_5\underline{Me}_5$); Mass Spectrum m/e (CI,isobutane carrier gas): 525 $[M+H]^+$, 497 $[M-CO+H]^+$, 468 $[M-2CO]^+$, 449 $[M-PMe_3+H]^+$, 421 $[M-PMe_3-CO+H]^+$, 391 $[M-2CO-PMe_3-H]^+$, 373 $[M-2PMe_3+H]^+$.

7.2.11 Preparation of $Cp^*Ta(CO)_4$

(a) From $Cp^*TaCl_2(PMe_3)(CO)_2$

THF ($40\ cm^3$) was vacuum transferred onto a mixture of $Cp^*TaCl_2(PMe_3)(CO)_2$ (0.5g, 0.96 mmol.) and sodium amalgam (11.1g, 0.5% w/w, 2.4 mmol.) in a $150\ cm^3$ "Rotoflo" glass ampoule cooled to -78°C. One atmosphere of carbon monoxide was then introduced. Upon warming to room temperature the mixture was stirred for 24h., changing from purple to brown and finally to orange-brown. The volatile components were removed under reduced pressure and the residue was extracted into toluene ($80\ cm^3$). Filtration of the resulting orange solution, followed by concentration to $10\ cm^3$ and cooling to -78°C, afforded $Cp^*Ta(CO)_4$ as orange crystals. Yield, 0.26g (65%).

(b) From Cp^*TaCl_4

Trimethylphosphine (0.084g, 1.1 mmol.) was condensed onto a mixture

of Cp^*TaCl_4 (0.5g, 1.1 mmol.), sodium amalgam (22.5g amalgam, 0.5% w/w, 4.95 mmol.) and THF (40 cm^3) cooled in a methanol slush bath (-94°C) in a 150 cm^3 "Rotoflo" glass ampoule. One atmosphere of carbon monoxide was then introduced into the vessel. Upon warming to room temperature and stirring for 1h., a red-brown colouration developed, at which point the atmosphere was replenished at -94°C. Continued stirring at room temperature for a further 20h. resulted in colour changes from purple to brown and finally orange-brown. Work-up as described for (a) afforded $Cp^*Ta(CO)_4$. Yield, 0.22g (47%). The filtrate from this crystallisation contained a second complex, formulated as $Cp^*Ta(CO)_3(PMe_3)$ in *ca.* 7% yield (^1H NMR) (see Chapter 2, section 2.4.10). Elemental Analysis for $C_{14}H_{15}O_4Ta$, Found (Required): %C, 39.70 (39.26); %H, 3.67 (3.54); IR (THF Solution,CsI,cm^{-1}): 2020(s,sp), 1905(s,br); ^1H NMR (250MHz,d-chloroform,298K): 2.14(s,$C_5\underline{Me}_5$); Mass Spectrum m/e (EI,70 eV): 428 $[M]^+$, 400 $[M-CO]^+$, 370 $[M-2CO-2H]^+$, 342 $[M-3CO-2H]^+$, 314 $[M-4CO-2H]^+$.

7.3 EXPERIMENTAL DETAILS TO CHAPTER 3

All NMR data for compounds described in this section are presented and discussed in Chapter 3.

7.3.1 Preparation of $Cp^*Ta(PMe_3)(H)_2(\eta^2\text{-}CHPMe_2)$

Trimethylphosphine (25 cm^3) was condensed onto a mixture of Cp^*TaCl_4 (3.0g, 6.6 mmol.) and sodium sand (1.0g, 43.5 mmol.) in a 150 cm^3, thick-walled "Rotoflo" glass ampoule, cooled at -78°C. Upon warming to room temperature, one atmosphere of argon was introduced and stirring was continued. The PMe_3 solvent adopted a yellow colouration

within 15 min. and gradually darkened over a period of 4 days to give a deep brown PMe_3 solution. The ampoule was carefully degassed and the excess PMe_3 was condensed into a receiving vessel to leave a brown residue. Extraction with petroleum ether (80 cm^3, 40-60°C) followed by filtration afforded a light-orange solution which was concentrated (20 cm^3) and cooled to -78°C to give off-white crystals of $Cp^*Ta(PMe_3)(H)_2(\eta^2\text{-}CHPMe_2)$. Yield, 1.4g (46%). Further purification was achieved by vacuum sublimation at 75-80°C (5 x 10^{-3} Torr). Elemental Analysis for $C_{16}H_{33}P_2Ta$, Found (Required): %C, 40.94 (41.03); %H, 7.15 (7.12); IR (Nujol,CsI,cm^{-1}): 3030(m), 1710(s), 1650(s,br), 1485(m), 1420(m), 1300(m,sp), 1280(s,sp), 1033(m), 962(s,br), 925(s,br), 870(m), 860(m), 845(m), 830(m), 783(w), 730(m), 722(s), 686(s), 670(m), 655(m), 586(w), 375(m), 347(m), 330(w); Mass Spectrum m/e (EI, 70eV): 468 $[M]^+$, 466 $[M\text{-}H_2]^+$, 390 $[M\text{-}H_2\text{-}PMe_3]^+$, 374 $[M\text{-}H_2\text{-}PMe_3\text{-}CH_4]^+$.

7.3.2 Preparation of $(\eta^7\text{-}C_5Me_3(CH_2)_2)Ta(H)_2(PMe_3)_2$

Trimethylphosphine (0.43g, 5.7 mmol.) and THF (25 cm^3) were condensed into a 150 cm^3 "Rotoflo" glass ampoule containing Cp^*TaCl_4 (0.5g, 1.09 mmol.) and sodium amalgam (20g, 0.5% w/w, 4.35 mmol.) cooled to -196°C. Upon warming to room temperature, one atmosphere of argon was introduced and the mixture was stirred for 24h., during which the THF solution changed colour from yellow to deep red-brown. The volatile components were removed under reduced pressure and the residue was extracted with petroleum ether (25 cm^3, 40-60°C) to afford an orange-brown solution. Concentration of this solution (*ca.* 10 cm^3) and cooling to -78°C for 24h. produced off-white crystals which were collected and dried *in vacuo*. Yield, 0.27g (53%). Further purification was achieved by slow vacuum sublimation at 75-80°C (5 x 10^{-3} Torr). Elemental

Analysis for $C_{16}H_{33}P_2Ta$, Found (Required): %C, 40.99 (41.03); %H, 7.16 (7.12); IR (Nujol,CsI,cm^{-1}): 3050(m), 1635(s,br), 1430(s), 1413(s), 1342(s), 1303(m), 1297(m), 1287(s), 1278(s), 1270(m), 1092(m), 1077(w), 1024(m), 948(s,br), 930(sh), 872(m), 855(m), 845(m), 837(s), 782(w), 733(s), 720(s), 703(m), 675(m), 668(m), 650(m,br), 610(m), 420(m), 363(m), 345(m), 310(w), 277(w); Mass Spectrum m/e (CI,isobutane carrier gas): 468 $[M]^+$ (weak), 466 $[M-2H]^+$, 407 $[M-PMe_2]^+$, 390 $[M-2H-PMe_3]^+$.

7.4 EXPERIMENTAL DETAILS TO CHAPTER 4

For compounds described in sections 7.4.1, 7.4.6, 7.4.7 and 7.4.9 below, NMR data are presented and discussed in Chapter 4.

7.4.1 Preparation of $Cp^*Ta(dmpe)(H)(\eta^2\text{-}CH_2PMe_2)$

Dmpe (0.19g, 1.28 mmol.) was added, *via* syringe to a toluene (30 cm^3) solution of $Cp^*Ta(PMe_3)(H)_2(\eta^2\text{-}CHPMe_2)$ (0.6g, 1.28 mmol.) in an argon-filled dry box. The mixture was heated at 70°C for 3h. to afford an orange solution. The volatile components were then removed under reduced pressure and the residue was extracted into petroleum ether (50 cm^3, 40-60°C). Filtration followed by concentration (*ca.* 8-10 cm^3) and cooling to -78°C afforded orange crystals which were collected and dried *in vacuo*. Yield, 0.47g (68%). Elemental Analysis for $C_{19}H_{40}P_3Ta$, Found (Required): %C, 42.02 (42.06); %H, 7.51 (7.45); IR (Nujol,CsI,cm^{-1}): 1650(m,br), 1422(m), 1292(m), 1275(m), 1265(m), 1100(w,br), 1030(m), 938(s,br), 918(m,sh), 893(m), 825(m), 800(m), 715(m), 705(m), 680(m), 667(m), 615(m), 460(w), 425(w), 396(m), 350(m,br); Mass Spectrum m/e (EI,70 eV): 542 $[M]^+$, 464 $[M-PMe_3-2H]^+$.

7.4.2 Preparation of $Cp^*Ta(PMe_3)HBr(\eta^2\text{-}CHPMe_2)$

Methyl bromide (0.81g, 8.55 mmol.) was condensed from a graduated "cold finger" onto a frozen solution of $Cp^*Ta(PMe_3)(H)_2(\eta^2\text{-}CHPMe_2)$ (0.8g, 1.71 mmol.) in toluene (40 cm^3) in a 150 cm^3 "Rotoflo" glass ampoule. Upon warming to *ca.* -20°C, nitrogen was admitted and stirring was maintained at room temperature for 3h. The solution was then filtered and the volatiles were removed under reduced pressure. The off-white crystalline product was recrystallised from petroleum ether (35 cm^3, 40-60°C) at -78°C to afford white crystals which were dried *in vacuo*. Yield, 0.82g (88%). Elemental Analysis for $C_{16}H_{32}BrP_2Ta$, Found (Required): %C, 35.47 (35.08); %H, 6.02 (5.91); IR (Nujol,KBr,cm^{-1}): 3100(w), 1710(m,br), 1420(m), 1300(m,sp), 1280(m,sp), 1270(m,sp), 1030(w), 970(s), 950(s), 930(m), 895(w), 890(w), 885(w), 860(w), 730(m), 725(m), 690(m), 670(w), 650(w), 625(w), 600(m); ^1H NMR (250MHz,d^6-benzene,298K): 9.22(s,1H,M=C<u>H</u>), 5.66(dd,1H,$^2J(PH)$=47.5,25.0Hz,M-<u>H</u>), 2.09(s,15H,C_5<u>Me_5</u>), 1.52(d,3H,$^2J(PH)$=11.0Hz,P<u>Me_2</u>), 1.46(d,3H,$^2J(PH)$=10.6Hz,P<u>Me_2</u>), 1.32(d,9H,$^2J(PH)$=7.0Hz,P<u>Me_3</u>); ^{31}P NMR (d^6-benzene,298K, broad band decoupled): -33.23(d,1P,$^2J(PP)$=47.7Hz,<u>P</u>Me_3), -104.20(d,1P, $^2J(PP)$=47.7Hz,<u>P</u>Me_2); ^{13}C NMR (d^6-benzene,298K,broad band decoupled): 196.69(d,$^1J(PC)$=48.7Hz,M=<u>C</u>H), 111.15(s,<u>C_5</u>Me_5), 18.94(d,$^1J(PC)$=14.7Hz, P<u>Me_3</u>), 12.56(s,C_5<u>Me_5</u>), 11.30‡(d,$^1J(PC)$=24.2Hz,P<u>Me_2</u>); Mass Spectrum m/e (EI,70eV): 470 $[M\text{-}PMe_3\text{-}H]^+$, 394 $[M\text{-}2PMe_3\text{-}H]^+$.

7.4.3 Preparation of $Cp^*Ta(PMe_3)HI(\eta^2\text{-}CHPMe_2)$

Methyl iodide (0.12g, 0.85 mmol.) was added *via* syringe to a

‡Only one P<u>Me_2</u> carbon is resolved, the other is obscured by the signal at 18.94 ppm.

solution of $Cp^*Ta(PMe_3)(H)_2(\eta^2\text{-}CHPMe_2)$ (0.4g, 0.85 mmol.) in toluene (25 cm^3) at room temperature in a nitrogen filled dry box. The resulting solution was stirred for 24h. at room temperature, filtered, concentrated (*ca.* 5 cm^3) and cooled (-78°C) to afford colourless crystals which were collected, washed with petroleum ether (5 cm^3, 40-60°C) and dried *in vacuo*. Yield, 0.35g (69%). Elemental Analysis for $C_{16}H_{32}IP_2Ta$, Found (Required): %C, 32.21 (32.33); %H, 5.48 (5.44); IR (Nujol,KBr,cm^{-1}): 1755(m,br), 1730(m,br), 1415(m), 1300(m,sp), 1280(s,sp), 1273(m,sh), 1160(w), 1072(w), 1030(m), 969(s), 955(s), 929(s), 865(w), 850(w), 835(w), 730(s), 690(m), 670(w), 654(w), 630(m), 600(m); ^1H NMR (250MHz,d^6-benzene,298K): 9.53(s,1H,M=C<u>H</u>), 4.08(dd,1H, $^2J(PH)$=51.4,28.0Hz,M-<u>H</u>), 2.07(s,15H,C_5<u>Me_5</u>), 1.68(d,3H,$^2J(PH)$=10.8Hz, P<u>Me_2</u>), 1.42(d,9H,$^2J(PH)$=6.8Hz,P<u>Me_3</u>), 1.40(d,3H,$^2J(PH)$=10.2Hz,P<u>Me_2</u>); ^{31}P NMR (d^6-benzene,298K,broad band decoupled): -40.96(d,1P,$^2J(PP)$=46.1Hz, <u>P</u>Me_3), -107.83(d,1P,$^2J(PP)$=46.1Hz,<u>P</u>Me_2); ^{13}C NMR (d^6-benzene,298K,broad band decoupled): 202.11(d,$^1J(PC)$=50.1Hz,M=<u>C</u>H), 110.71(s,<u>C_5</u>Me_5), 20.63(d, $^1J(PC)$=19.9Hz,P<u>Me_3</u>), 19.49(d,$^1J(PC)$=28.7Hz,P<u>Me_2</u>), 13.63(d,$^1J(PC)$=24.3Hz, P<u>Me_2</u>), 13.20(s,C_5<u>Me_5</u>); Mass Spectrum m/e (CI,isobutane carrier gas): 518 $[M\text{-}PMe_3]^+$, 442 $[M\text{-}2PMe_3]^+$.

7.4.4 Preparation of $Cp^*TaBr_2(\eta^2\text{-}CHPMe_2)$

Methyl bromide (0.5g, 5.3 mmol.) was condensed onto a frozen solution of $Cp^*Ta(PMe_3)(H)_2(\eta^2\text{-}CHPMe_2)$ (0.25g, 0.53 mmol.) in toluene (25 cm^3). Upon warming to room temperature, nitrogen was admitted and the reaction mixture was heated to 70°C for 4h. to give a dark red-brown solution over a pale precipitate. The supernatant solution was removed by filtration and the residue washed with toluene (2 x 10 cm^3). The combined toluene extracts were concentrated (10 cm^3) and layered with

petroleum ether (20 cm^3, 40-60°C). The resultant orange crystals were collected, washed with petroleum ether (2 x 5 cm^3, 40-60°C) and dried *in vacuo*. Yield, 0.19g (65%). Elemental Analysis for $C_{13}H_{22}Br_2PTa$, Found (Required): %C, 28.54 (28.38); %H, 4.12 (4.04); IR (Nujol,KBr,cm^{-1}): 1420(m), 1282(m), 1075(w), 1030(m), 955(s,br), 869(m), 840(w), 740(m), 703(m), 665(m); ^1H NMR (250MHz,d^6-benzene,298K): 10.49(s,1H,M=C<u>H</u>), 1.90(s,15H,C_5<u>Me</u>$_5$), 1.62(d,6H,^2J(PH)=11.3Hz,P<u>Me</u>$_2$); ^{31}P NMR (d^6-benzene, 298K,broad band decoupled): -28.40(s,P<u>Me</u>$_2$); ^{13}C NMR (d^6-benzene,298K, broad band decoupled): 207.14(d,^1J(PC)=48.1Hz,M=<u>C</u>H), 118.37(s,<u>C</u>$_5$Me$_5$), 12.14(s,C_5<u>Me</u>$_5$), 12.4‡†(d,J(PC)~20Hz,P<u>Me</u>$_2$); Mass Spectrum m/e (CI, isobutane carrier gas): 551 $[M+H]^+$, 471 $[M-Br+H]^+$.

7.4.5 Preparation of $Cp^*TaI_2(\eta^2$-$CHPMe_2)$

Methyl iodide (0.61g, 4.3 mmol.) was added *via* syringe to a stirred solution of $Cp^*Ta(PMe_3)(H)_2(\eta^2$-$CHPMe_2)$ (0.4g, 0.85 mmol.) in toluene (30 cm^3) at room temperature. After stirring for 4 days the dark solution was filtered, and the remaining pale residue was washed with toluene (2 x 10 cm^3). The combined toluene extracts were concentrated to 10 cm^3 and layered with petroleum ether (20 cm^3) to give orange-brown micro-crystals which were washed with petroleum ether (*ca.* 10 cm^3, 40-60°C) and dried *in vacuo*. Yield, 0.43g (78%). Elemental Analysis for $C_{13}H_{22}I_2PTa$, Found (Required): %C, 23.76 (24.24); %H, 3.37 (3.45); IR (Nujol,CsI,cm^{-1}): 1415(m,br), 1295(m), 1287(m), 1075(m), 1064(m), 1021(m), 962(s,br), 881(m), 865(m), 783(w), 762(m), 754(m), 730(m), 693(w), 580(w), 365(s), 312(w); ^1H NMR (250MHz,d^6-benzene,298K): 11.28 (s,1H,M=C<u>H</u>), 1.99(s,15H,C_5<u>Me</u>$_5$), 1.80(d,6H,^2J(PH)=11.3Hz,P<u>Me</u>$_2$); ^{31}P NMR

‡†The P<u>Me</u>$_2$ carbon signal is partially obscured by the C_5<u>Me</u>$_5$ signal, only one half of doublet being observed. Accurate shift and J-values are thus unavailable.

(d^6-benzene,298K,broad band decoupled): -37.60(s,$\underline{P}Me_2$); ^{13}C NMR (d^6-benzene,298K,broad band decoupled): 97.83(s,$\underline{C}_5Me_5$), 16.18(d,$^1J(PC)$= 30.0Hz,$P\underline{Me}_2$), 13.87(s,$C_5\underline{Me}_5$) (Methylidyne carbon not found); Mass Spectrum m/e (CI,isobutane carrier gas): 645 $[M-H]^+$, 517 $[M-I]^+$.

7.4.6 Synthesis of $Cp^*Ta(\eta$-PhNCHO)(H)(η^2-$CHPMe_2$)

Phenylisocyanate (0.038g, 0.32 mmol.) was added *via* syringe to a solution of $Cp^*Ta(PMe_3)(H)_2(\eta^2$-$CHPMe_2)$ (0.15g, 0.32 mmol.) in toluene (20 cm^3). After stirring at room temperature for 1h., the solution was filtered, concentrated to 5 cm^3, and layered with cold petroleum ether (10 cm^3, 40-60°C). Immediately a white solid formed which was isolated by filtration and dried *in vacuo*. Yield, 0.1g (61%). This solid was recrystallised from toluene:petroleum ether [1:2 v/v]. Elemental Analysis for $C_{20}H_{29}NOPTa$, Found (Required): %C, 46.12 (46.97); %H, 5.55 (5.73); %N, 2.42 (2.74); IR (Nujol,KBr,cm^{-1}): 3050(w), 3025(w), 1738(m), 1560(s), 1390(m), 1270(s), 1222(m), 1029(w), 956(m), 938(m), 929(m), 835(w), 761(s), 719(m), 693(m), 685(m), 645(w), 615(w); Mass Spectrum m/e (EI,70eV): 511 $[M]^+$, 451 $[M-Me_2NO]^+$, 435 $[M-PMe_3]^+$, 392 $[M-PhNCO]^+$.

7.4.7 Synthesis of $Cp^*Ta(\eta$-p-$CH_3C_6H_4NCHO)(H)(\eta^2$-$CHPMe_2)$

A procedure analogous to that described for the phenylisocyanate derivative was employed, using the following reagents: $Cp^*Ta(PMe_3)(H)_2$-(η^2-$CHPMe_2$) (0.5g, 1.07 mmol.), p-$CH_3C_6H_4NCO$ (0.14g, 1.07 mmol.) in toluene (30 cm^3). Yield, 0.24g (43%). The product was obtained as colourless crystals by recrystallisation from petroleum ether (40-60°C). Elemental Analysis for $C_{21}H_{31}NOPTa$, Found (Required): %C, 48.53 (48.00);

%H, 6.23 (5.96); %N, 2.42 (2.67); IR (Nujol,CsI,cm^{-1}): 3050(w), 3015(m), 2720(w), 1905(w), 1738(s), 1550(s,br), 1512(s), 1420(m), 1318(s), 1295(s), 1270(s), 1225(s), 1110(m), 1069(w), 1030(m), 1019(m), 960(s), 935(s,br), 857(m), 825(s), 812(s), 715(s), 683(s), 645(m), 630(m,br), 549(m), 524(m), 425(w), 415(w), 378(s), 347(m), 300(m,br); Mass Spectrum m/e (EI,70eV): 525 $[M]^+$, 465 $[M-PMe_2+H]^+$, 449 $[M-PMe_3+H]^+$, 406 $[M-C_6H_5NCO]^+$, 348 $[Cp^*TaO_2]^+$, 332 $[Cp^*TaO]^+$, 119 $[PhNCO]^+$.

7.4.8 Reaction of $Cp^*Ta(PMe_3)(H)_2(\eta^2\text{-}CHPMe_2)$ With CO_2

A petroleum ether solution of $Cp^*Ta(PMe_3)(H)_2(\eta^2\text{-}CHPMe_2)$ (0.29g, 0.62 mmol. in 20 cm^3, 40-60°C) was treated with one atmosphere of CO_2 at room temperature. Precipitation of a white solid occurred instantaneously, and after 24h. the product was isolated by filtration, washed with petroleum ether (2 x 5 cm^3, 40-60°C) and dried *in vacuo*. Yield, 0.23g. Elemental Analysis for $C_{15}H_{24}O_4PTa$, Found (Required): %C, 37.70 (37.51); %H, 5.14 (5.05); IR (Nujol,KBr,cm^{-1}): 2720(w), 2220(w), 1650(s,br), 1565(s,br), 1420(m,br), 1290(m,br), 1265(m,br), 1095(s,br), 1030(m), 955(s,br), 786(m), 773(m), 710(s,br), 545(s,br); ^1H NMR (250MHz,d-chloroform,298K): 2.0(s,br,$\Delta\frac{1}{2}$=40Hz,$C_5\underline{Me}_5$); Mass Spectrum m/e (CI,isobutane carrier gas): 448 $[M-O_2]^+$, 370 $[M-H_2O_2-PMe_3]^+$, 333 $[Cp^*Ta(OH)]^+$, 316 $[Cp^*Ta]^+$, 301 $[TaCO_2(PMe_3)]^+$.

7.4.9 Synthesis of $Cp^*Ta(CH_2CH_2CMe_3)_2(\eta^2\text{-}CHPMe_2)$

3,3-Dimethyl-1-butene (neohexene) (0.45g, 5.3 mmol.) was added *via* syringe to a stirred solution of $Cp^*Ta(PMe_3)(H)_2(\eta^2\text{-}CHPMe_2)$ (0.5g, 1.06 mmol.) in petroleum ether (30 cm^3, 40-60°C) in a nitrogen filled dry box. After stirring for 4 days, the mixture was filtered and the

volatiles were removed under reduced pressure. The resulting off-white gelatinous solid was redissolved in a minimum of petroleum ether (3 cm^3), and cooled to -78°C for 24h. to give colourless crystals. Yield, 0.39g (66%). Elemental Analysis for $C_{25}H_{48}PTa$, Found (Required): %C, 53.30 (53.55); %H, 8.85 (8.65); IR (Nujol,KBr,cm^{-1}): 1420(w), 1385(m), 1360(s), 1267(m), 1232(m), 1203(w), 1020(w), 962(w), 940(s), 850(w), 823(w), 705(m), 684(m), 641(m), 613(w); Mass Spectrum m/e (EI,70eV): 561 $[M+H]^+$, 477 $[M-CH_2=CHBu^t+H]^+$, 473 $[M-CH_3CH_2Bu^t-H]^+$, 416 $[M-CH_3CH_2Bu^t-Bu^t-H]^+$, 390 $[Cp^*Ta(\eta\text{-}CHPMe_2)]^+$.

7.5 EXPERIMENTAL DETAILS TO CHAPTER 5

7.5.1 Synthesis of $[NbCl_4(OMe)]_2$

A dichloromethane solution of Me_3SiOMe (1.15g, 11.1 mmol. in 15 cm^3 CH_2Cl_2) was added dropwise to a suspension of $NbCl_5$ (3.0g, 11.1 mmol.) in dichloromethane (20 cm^3) at room temperature. The $NbCl_5$ suspension reacted during stirring over 2h. to give a colourless solution. Filtration, followed by concentration to half volume and cooling to -78°C, afforded colourless crystals of $[NbCl_4(OMe)]_2$. Yield, 2.60g (88%). Elemental Analysis for CH_3Cl_4NbO, Found (Required): %Nb, 34.80 (34.96); %Cl, 53.24 (53.36); %C, 4.36 (4.52); %H, 0.99 (1.14); IR (Nujol,KBr,cm^{-1}): 1425(m), 1140(w), 1059(s,br), 600(m), 595(w), 390(s,br), 354(s); ^1H NMR (250MHz,d-chloroform,298K): 5.17(s,OMe); Mass Spectrum m/e (CI,isobutane carrier gas,^{35}Cl): 529 $[M_2+H]^+$, 215 $[Nb(OH)Cl_3]^+$.

7.5.2 Synthesis of $[NbCl_4(OEt)]_2$

Me_3SiOEt (2.19g, 18.5 mmol.) was reacted with $NbCl_5$ (5.0g, 18.5 mmol.) in dichloromethane (40 cm^3) using a similar procedure to that described for $[NbCl_4(OMe)]_2$. Yield, 4.66g (90%). Elemental Analysis for $C_2H_5Cl_4NbO$, Found (Required): %Nb, 33.06 (33.21); %Cl, 50.17 (50.68); %C, 8.75 (8.59); %H, 1.89 (1.80); IR (Nujol,CsI,cm^{-1}): 1442(m), 1350(m), 1260(w), 1086(m), 1030(s,br), 743(m), 580(m), 388(s,br), 258(s); ^1H NMR (250MHz,d-chloroform,298K): 5.46(q,2H,$^3J(HH)$=7.0Hz, -C<u>H</u>$_2$-), 1.76(t,3H,$^3J(HH)$=7.0Hz,-C<u>H</u>$_3$); Mass Spectrum m/e (CI,isobutane carrier gas,^{35}Cl): 531 $[M_2-C_2H]^+$, 260 $[M-H_2O]^+$, 253 $[M-C_2H]^+$, 243 $[M-Cl]^+$, 215 $[Nb(OH)Cl_3]^+$.

7.5.3 Synthesis of $[TaCl_4(OMe)]_2$

An analogous procedure to that described for $[NbCl_4(OMe)]_2$ was used in the reaction between Me_3SiOMe (0.58g, 5.58 mmol.) and $TaCl_5$ (2.0g, 5.58 mmol.) in dichloromethane solvent (40 cm^3). The product was isolated as colourless crystals. Yield, 1.8g (91%). Elemental Analysis for CH_3Cl_4OTa, Found (Required): %Ta, 51.53 (51.15); %Cl, 40.47 (40.08); %C, 3.64 (3.39); %H, 0.91 (0.86); IR (Nujol,KBr,cm^{-1}): 1160(m), 1094(s, br), 582(m), 388(s), 350(s); ^1H NMR (250MHz,d-chloroform,298K): 5.28(s, O<u>Me</u>); Mass Spectrum m/e (EI,70eV,^{35}Cl): 322 $[TaCl_4+H]^+$, 316 $[TaCl_3OCH_3-H]^+$, 287 $[TaCl_3+H]^+$, 251 $[TaCl_2]^+$, 216 $[TaCl]^+$, 181 $[Ta]^+$.

7.5.4 Synthesis of $[TaCl_4(OEt)]_2$

$[TaCl_4(OEt)]_2$ was isolated as colourless crystals from the reaction of $TaCl_5$ (2.0g, 5.58 mmol.) and Me_3SiOEt (0.66g, 5.58 mmol.) in

dichloromethane solvent (40 cm^3) as described for $[NbCl_4(OMe)]_2$. Yield, 1.7g (83%). Elemental Analysis for $C_2H_5Cl_4OTa$, Found (Required): %Ta, 49.00 (49.20); %C, 6.51 (6.53); %H, 1.43 (1.37); IR (Nujol, KBr,cm^{-1}): 1446(m,sh), 1260(w), 1095(s), 1070(s,br), 948(s), 569(w), 393(s), 357(s); ^1H NMR (250MHz,d-chloroform,298K): 5.57(q,2H,$^3J(HH)$=7.0Hz, -C<u>H</u>$_2$-), 1.70(t,3H,$^3J(HH)$=7.0Hz,-C<u>H</u>$_3$); Mass Spectrum m/e (CI, isobutane carrier gas,^{35}Cl): 733 $[M_2+H]^+$, 716 $[M_2-OH]^+$, 701 $[M_2-OH-Me]^+$, 350 $[TaCl_4Et]^+$, 331 $[TaCl_3OEt]^+$.

7.5.5 Synthesis of $[TaCl_4(OSiMe_3)]_2$

A dichloromethane solution of $(Me_3Si)_2O$ (1.36g, 8.37 mmol. in 20 cm^3 CH_2Cl_2) was added dropwise to a stirred suspension of $TaCl_5$ (3.0g, 8.37 mmol.) in dichloromethane (30 cm^3). Dissolution of the $TaCl_5$ occurred over the course of 2h. at room temperature to afford a clear, pale yellow solution. Filtration, followed by concentration to *ca.* 10 cm^3 and cooling at -78°C for 1h. afforded the product as colourless crystals, which were collected and dried *in vacuo*. Yield, 3.1g (90%). Elemental Analysis for $C_3H_9Cl_4OSiTa$, Found (Required): %C, 8.84 (8.75); %H, 1.98 (2.21); IR (Nujol,KBr,cm^{-1}): 1410(w), 1258(s), 950(s,br), 855(s,br), 832(s,br), 760(s), 633(m), 522(w), 380(s), 360(s), 340(s); ^1H NMR (250MHz,d-chloroform,298K): 0.52(s,$^2J(SiH)$=6.4Hz,Si<u>Me</u>$_3$).

7.5.6 Synthesis of $Nb(O)Cl_3$

A 1,2-dichloroethane solution of $(Me_3Si)_2O$ (1.8g, 11.1 mmol. in 15 cm^3 $C_2H_4Cl_2$) was added to a suspension of $NbCl_5$ (3.0g, 11.1 mmol.) in 1,2-dichloroethane (20 cm^3) at room temperature. The mixture was swiftly warmed to 80°C with stirring, and maintained at this temperature

for 4.5h. Dissolution of the yellow $NbCl_5$ was accompanied by formation of a white, granular precipitate. After cooling to room temperature, the supernatant solution was decanted from the white solid, which was collected, washed with petroleum ether (2 x 10 cm^3, 40-60°C) and dried *in vacuo*. Yield, 2.03g (75%). Elemental Analysis for Cl_3NbO, Found (Required): %Nb, 43.30 (43.16); %Cl, 49.62 (49.41); IR (Nujol,CsI,cm^{-1}): 1257(m), 940(m,sh), 780(s,br), 414(s,br), 295(s); Mass Spectrum m/e (EI,70eV,^{35}Cl): 393 $[Nb_2O_2Cl_5]^+$, 214 $[NbOCl_3]^+$, 179 $[NbOCl_2]^+$, 163 $[NbCl_2]^+$, 144 $[NbOCl]^+$, 128 $[NbCl]^+$, 109 $[NbO]^+$.

7.5.7 Synthesis of $Nb(O)Cl_3(CH_3CN)_2$

An acetonitrile solution of $(Me_3Si)_2O$ (1.8g, 11.1 mmol. in 15 cm^3 CH_3CN) was added dropwise at room temperature to a suspension of $NbCl_5$ (3.0g, 11.1 mmol.) in acetonitrile (20 cm^3). The mixture was stirred at room temperature for 2h. to give a colourless solution which was filtered, concentrated to *ca.* 5 cm^3 and cooled to -78°C. The resultant colourless, crystalline product was collected and dried *in vacuo*. Yield, 3.1g (95%). Elemental Analysis for $C_4H_6Cl_3N_2NbO$, Found (Required): %C, 15.94 (16.15); %H, 2.11 (2.02); %N, 9.41 (9.42); IR (Nujol,CsI,cm^{-1}): 2322(s), 2310(s), 2293(s), 2284(s), 1368(m), 1355(m), 1026(m), 960(s, br), 947(s), 935(s), 370(s,br), 333(s), 250(m).

7.5.8 Synthesis of $Nb(O)Cl_3(THF)_2$

Tetrahydrofuran (30 cm^3) was added to $Nb(O)Cl_3(CH_3CN)_2$ (0.53, 1.78 mmol.) at -30°C. The mixture was warmed to room temperature with stirring to afford a colourless solution. After 15 min. the mixture was filtered, concentrated to 5 cm^3 and cooled to -78°C. Addition of cold

petroleum ether (10 cm^3, 40-60°C, *ca.* -30°C) gave colourless crystals of $Nb(O)Cl_3(THF)_2$. Yield, 0.57g (90%). Elemental Analysis for $C_8H_{16}Cl_3NbO_3$, Found (Required): %C, 26.13 (26.70); %H, 4.42 (4.45); IR (Nujol,CsI, cm^{-1}): 1366(m), 1347(s), 1301(m), 1250(m), 1180(m), 1138(w), 1060(s), 1048(m), 1029(m), 1018(m), 1016(s), 996(m), 960(s), 861(s,br), 833(s,br), 676(m), 578(w), 365(s,br), 327(s), 250(m).

7.5.9 Synthesis of $NbCl_5(OEt_2)$

Diethyl ether (50 cm^3) was added *via* cannula to finely ground $NbCl_5$ (2.0g, 7.4 mmol.) at room temperature. Within 10 min. a white, flocculent solid appeared, which slowly dissolved over 12h. at room temperature to afford a yellow-green solution. Filtration, concentration (25 cm^3) and cooling at -35°C for 24h. gave yellow-green crystals which were collected and dried *in vacuo*. Yield, 2.21g (87%). Elemental Analysis for $C_4H_{10}Cl_5NbO$, Found (Required): %Nb, 26.86 (26.99); %Cl, 51.80 (51.48); %C, 14.26 (13.95); %H, 3.04 (2.93); IR (Nujol,KBr,cm^{-1}): 1374(m,sp), 1320(m), 1279(m), 1190(m), 1146(m), 1089(m), 992(s,br), 877(s), 828(m), 760(s,br), 511(m), 467(m), 375(s,br); ^1H NMR (250MHz,d-chloroform,298K): 4.57(q,4H,$^3J(HH)$=6.9Hz, $OC\underline{H}_2$-), 1.44(t,6H,$^3J(HH)$=6.9Hz,-$C\underline{H}_3$).

7.5.10 Synthesis of $TaCl_5(OEt_2)$

This complex was isolated as colourless crystals using a procedure analogous to that described for $NbCl_5(OEt_2)$. Yield 86%. Elemental Analysis for $C_4H_{10}Cl_5OTa$, Found (Required): %Ta, 41.74 (41.85); %Cl, 40.35 (41.00); %C, 11.67 (11.11); %H, 2.57 (2.34); IR (Nujol,KBr,cm^{-1}): 1317(m), 1275(m), 1188(s), 1146(m), 1090(s), 990(s,br), 868(s), 823(m),

785(m), 754(s,br), 513(m), 464(m),396(s), 335(s,br); ^{1}H NMR (250MHz,d-chloroform,298K): 4.73(q,4H,$^{3}J(HH)$=6.9Hz,$OC\underline{H}_2$-), 1.47(t,6H,$^{3}J(HH)$=6.9Hz, -$C\underline{H}_3$).

7.5.11 Reaction of $Nb(O)Cl_3(CH_3CN)_2$ With LiO-2,6-$Me_2C_6H_3$: Preparation of $Nb(O)(O\text{-}2,6\text{-}Me_2C_6H_3)_3$

Toluene (40 cm^3) was added *via* cannula to a mixture of $Nb(O)Cl_3(CH_3CN)_2$ (0.5g, 1.68 mmol.) and LiO-2,6-$Me_2C_6H_3$ (0.65g, 5.04 mmol.) under an argon atmosphere at room temperature. The solution immediately adopted a yellow colouration. The mixture was stirred at room temperature for 30 min. and then heated to 65^{o}C for 5h. The resulting yellow solution was filtered, concentrated to 15 cm^3 and layered with an equal volume of petroleum ether (40-60^{o}C). The product precipitated as a yellow, microcrystalline solid which was collected, washed with petroleum ether (2 x 5 cm^3, 40-60^{o}C) and dried *in vacuo*. Yield, 0.61g (77%). Elemental Analysis for $C_{24}H_{36}O_4Nb$, Found (Required): %C, 60.87 (61.01); %H, 6.32 (5.77); IR (Nujol,KBr,cm^{-1}): 3040(m,br), 1588(m), 1421(m), 1265(s), 1210(s,br), 1190(s,br), 1163(m,sh), 1090(m), 1030(w), 980(w), 915(m,sh), 892(s), 874(s,br), 810(m,br), 765(s), 730(s,br), 572(m), 565(m,sh), 490(w), 413(m), 365(s,br); ^{1}H NMR (250MHz,d^6-benzene, 298K): 6.74(d,6H,$^{3}J(HH)$=7.5Hz, Ar$\underline{H}_m$), 6.61(t,3H,$^{3}J(HH)$=7.5Hz,Ar$\underline{H}_p$), 2.31(s,18H,Ar$\underline{Me}$); ^{13}C NMR (d^6-benzene,298K,broad band decoupled): 161.44(s,C_{ipso}), 128.74(s,C_m), 127.34(s,C_o), 122.70(s,C_p), 17.31(s,$\underline{Me}$); Mass Spectrum m/e (CI, isobutane carrier gas): 578 $[Nb(OAr)_4+H]^+$, 473 $[Nb(OAr)_3OH]^+$, 123 $[ArOH_2]^+$.

7.5.12 Reaction of $Nb(O)Cl_3(CH_3CN)_2$ With LiO-2,6-$^tBu_2C_6H_3$: Preparation of $Nb(O)(O\text{-}2,6\text{-}^tBu_2C_6H_3)_3$

A stirred suspension of LiO-2,6-$^tBu_2C_6H_3$ (1.07g, 5.04 mmol.) in diethyl ether (20 cm^3) was added dropwise to a suspension of $Nb(O)Cl_3(CH_3CN)_2$ (0.5g, 1.68 mmol.) in diethyl ether (30 cm^3) maintained at *ca.* -40°C. The ether rapidly developed a yellow colouration. After the addition was complete (20 min) the mixture was allowed to warm to room temperature and stirred for 16h. Subsequently the volatile components were removed under reduced pressure and the residue was extracted into toluene (50 cm^3) to afford a yellow-orange solution. Filtration of this solution, followed by concentration (10 cm^3) and cooling (-78°C) produced yellow crystals, which were collected, washed with cold petroleum ether (5 cm^3, 40-60°C at *ca.* -30°C) and dried *in vacuo*. Yield, 0.88g (72%). Elemental Analysis for $C_{42}H_{63}O_4Nb$, Found (Required): %Nb, 12.51 (12.83); %C, 68.54 (69.61); %H, 8.79 (8.70); IR (Nujol,CsI,cm^{-1}): 3065(w), 3010(s), 1405(s), 1395(s), 1265(m), 1210(s), 1190(s), 1128(s), 1113(s), 1023(w), 963(s), 895(s,br), 828(m), 800(m), 755(m), 750(m), 697(m), 583(w), 565(w), 550(w), 525(w), 465(m), 373(m); ^1H NMR (250MHz,d-chloroform, 298K): 7.25(d,6H,$^3J(HH)$=7.8Hz,Ar$\underline{H}_m$), 6.90(t,3H,$^3J(HH)$=7.8Hz,Ar$\underline{H}_p$), 1.43(s,54H,($C\underline{H}_3$)$_3$C); ^{13}C NMR (d-chloroform,298K,broad band decoupled): 162.08(s,C_{ipso}), 139.53(s,C_o), 125.67(s,C_m), 122.24 (s,C_p), 35.49(s,(CH_3)$_3\underline{C}$), 31.97(s,($\underline{C}H_3$)$_3$C); Mass Spectrum m/e (CI,isobutane carrier gas): 725 $[M+H]^+$, 667 $[M-^tBu]^+$, 655 $[M-^tBu-Me+3H]^+$, 613 $[M-2^tBu+3H]^+$, 206 $[ArOH]^+$.

7.5.13 Reaction of $Nb(O)Cl_3$ With PPh_3: Preparation of $Nb(O)Cl_3(PPh_3)_2$

Dichloromethane (40 cm^3) was added, *via* cannula, to a mixture of

$Nb(O)Cl_3$ (0.5g, 2.32 mmol.) and PPh_3 (1.21g, 4.64 mmol.) at room temperature. An immediate reaction resulted in the mixture adopting a yellow colouration. After all the $Nb(O)Cl_3$ had reacted (*ca.* 12h) the resulting yellow-orange solution was filtered and the volatiles removed under reduced pressure to afford a yellow solid, which was washed with petroleum ether (2 x 10 cm^3, 40-60°C) and dried *in vacuo*. Yield, 1.27g (74%). Elemental Analysis for $C_{36}H_{30}Cl_3NbOP_2$, Found (Required): %C, 57.96 (58.44); %H, 4.10 (4.10); %Cl, 14.77 (14.37); IR (Nujol,CsI,cm^{-1}): 3054(w,br), 1586(w), 1484(m), 1438(s), 1331(w), 1311(w), 1186(w), 1164(w), 1100(s), 1029(m), 999(m), 939(s), 750(s), 701(s), 696(s), 523(s), 509(s), 500(s), 454(m), 445(m), 379(s), 332(m), 316(s); ^1H NMR (250MHz,d-chloroform,298K): 7.47(s,br,12H,Ph$\underline{H}_o$), 7.40(s,br,18H,Ph$\underline{H}_{m/p}$); ^{31}P NMR (d-chloroform,298K,broad band decoupled): 3.85(s,br,$\Delta\frac{1}{2}$=50Hz, 2$\underline{P}Ph_3$); Mass Spectrum m/e (CI,isobutane carrier gas,^{35}Cl): 735 $[M-3H]^+$, 557 $[Nb(OH)(PPh_3)_2-Ph]^+$, 279 $[Ph_3PO+H]^+$, 263 $[Ph_3P+H]^+$.

7.5.14 Reaction of $Nb(O)Cl_3$ With $PMePh_2$: Preparation of $Nb(O)Cl_3(PMePh_2)_2$

Methyldiphenylphosphine (0.93g, 4.64 mmol.) was added, *via* syringe, to a stirred suspension of $Nb(O)Cl_3$ (0.5g, 2.32 mmol.) in dichloromethane solvent (40 cm^3) at room temperature. The $Nb(O)Cl_3$ reacted over 12h. to afford a yellow-orange solution. The solution was then filtered and the volatiles were removed under reduced pressure to leave a microcrystalline yellow solid, which was washed with petroleum ether (*ca.* 10 cm^3, 40-60°C) and dried *in vacuo*. Yield, 1.2g (84%). Elemental Analysis for $C_{26}H_{26}Cl_3NbOP_2$, Found (Required): %C, 50.39 (50.71); %H, 4.53 (4.26); IR (Nujol,CsI,cm^{-1}): 3047(w,br), 1587(w), 1574(w), 1486(m), 1437(s), 1336(m), 1311(m), 1287(m), 1190(m), 1161(w), 1101(s), 1072(w),

1029(m), 1001(m), 929(s,br), 889(s,br), 742(s), 697(s), 512(s), 480(m), 443(m), 371(s), 327(s), 312(s); ^{1}H NMR (250MHz,d-chloroform,298K): 7.46(s,br,8H,Ph-H_o), 7.33(s,br,12H,Ph-$H_{m/p}$), 1.77(s,br,6H,P<u>Me</u>PH_2); Mass Spectrum m/e (CI,isobutane carrier gas,^{35}Cl): 615 $[M+H]^+$, 595 $[M-H_2O]^+$, 383 $[NbCl_3PPh_2]^+$, 217 $[Ph_2MePO+H]^+$, 215 $[Nb(OH)Cl_3]^+$, 201 $[Ph_2MeP+H]^+$.

7.5.15 Reaction of $Nb(O)Cl_3$ With PEt_3: Preparation of $Nb(O)Cl_3(PEt_3)_2$

Triethylphosphine (0.96g, 8.12 mmol.) was added, *via* syringe, to a stirred suspension of $Nb(O)Cl_3$ (0.5g, 2.32 mmol.) in dichloromethane (40 cm^3) at room temperature. An immediate reaction led to complete dissolution of the $Nb(O)Cl_3$ within *ca.* 30s. to afford a yellow solution. After stirring for 2h., the solution was filtered and the volatiles removed under reduced pressure to give a yellow solid, which was washed with cold (*ca.* -30°C) petroleum ether (10 cm^3, 40-60°C) and dried *in vacuo*. Yield, 0.95g (91%). Elemental Analysis for $C_{12}H_{30}Cl_3NbOP_2$, Found (Required): %C, 30.45 (31.91); %H, 6.36 (6.71); IR (Nujol,CsI, cm^{-1}): 1412(m), 1320(w), 1143(w), 1050(m), 1042(m), 930(s,br), 842(m), 810(m), 786(m), 776(m), 738(m), 726(m), 330(s,br); ^{1}H NMR (250MHz,d-chloroform,298K): Data discussed in Chapter 5; Mass Spectrum m/e (CI,isobutane carrier gas,^{35}Cl): 449 $[M-H]^+$, 313 $[M-PEt_3-H_3O]^+$, 135 $[Et_3PO+H]^+$, 119 $[Et_3P+H]^+$.

7.5.16 Preparation of $[Nb(O)Cl_3(PMe_3)_2]_2$

Trimethylphosphine (0.34g, 4.45 mmol.) was condensed onto a frozen solution of $Nb(O)Cl_3(THF)_2$ (0.4g, 1.11 mmol.) in dichloromethane (25 cm^3) at -196°C. Upon warming to room temperature, one atmosphere of argon was admitted. The mixture was stirred for 12h. to afford a

yellow-orange solution and a pale solid. The solution was filtered and the residue washed with dichloromethane (2 x 5 cm^3) and dried *in vacuo*. Yield, 0.18g (44%). Elemental Analysis for $C_6H_{18}Cl_3NbOP_2$, Found (Required): %C, 19.66 (19.61); %H, 4.44 (4.95); IR (Nujol,CsI,cm^{-1}): 1425(m), 1309(m), 1304(s), 1227(w), 1145(w), 1037(w), 981(s), 964(s), 923(s), 882(w), 844(w), 776(w), 738(w), 650(w), 318(s,br); Mass Spectrum m/e (CI,isobutane carrier gas,^{35}Cl): 604 $[M_2\text{-}PMe_3\text{-}O\text{-}Cl\text{-}H]^+$, 590 $[M_2\text{-}PMe_3\text{-}O\text{-}Cl\text{-}CH_3]^+$, 575 $[M_2\text{-}PMe_3\text{-}O\text{-}Cl\text{-}2CH_3]^+$, 561 $[M_2\text{-}PMe_3\text{-}O\text{-}Cl\text{-}2CH_3\text{-}CH_2]^+$, 549 $[M_2\text{-}PMe_3\text{-}O\text{-}Cl\text{-}2C_2H_4]^+$, 535 $[M_2\text{-}PMe_3\text{-}O\text{-}Cl\text{-}5CH_2]^+$, 521 $[M_2\text{-}PMe_3\text{-}O\text{-}Cl\text{-}6CH_2]^+$, 507 $[M_2\text{-}PMe_3\text{-}O\text{-}Cl\text{-}7CH_2]^+$, 495 $[M_2\text{-}PMe_3\text{-}O\text{-}Cl\text{-}C_8H_{14}]^+$, 369 $[M+3H]^+$, 77 $[PMe_3+H]^+$.

7.5.17 Reaction of $Nb(O)Cl_3$ With Dppe: Preparation of $Nb(O)Cl_3(dppe)$

Dichloromethane (40 cm^3) was added, *via* cannula, to a solid mixture of $Nb(O)Cl_3$ (0.5g, 2.32 mmol.) and dppe (0.92g, 2.32 mmol.) at room temperature. An immediate reaction occurred to give a yellow solution. Within 2h. the solid had dissolved completely to afford a yellow-orange solution, which was filtered and the volatile components removed under reduced pressure to afford a yellow solid, which was washed with petroleum ether (2 x 10 cm^3, 40-60^oC) and dried *in vacuo*. Yield, 1.38g (97%). Elemental Analysis for $C_{26}H_{24}Cl_3NbOP_2$, Found (Required): %C, 50.88 (50.88); %H, 4.12 (3.95); %Cl, 17.59 (17.33); IR (Nujol,CsI,cm^{-1}): 3047(w,br), 1584(w), 1571(w), 1484(m), 1435(s), 1414(m), 1333(w), 1189(w), 1097(m), 1070(w), 1027(m), 1000(m), 933(m), 892(m), 863(m), 827(m), 742(s), 693(s), 518(s), 395(m,br), 415(w), 357(s,br), 327(m,br); ^1H NMR (250MHz,d-chloroform,298K): 7.60(s,br,8H,$Ph\underline{H}_o$), 7.34(s,br,12H, $Ph\underline{H}_{m/p}$), 2.72(s,br,4H,$P\underline{CH_2}\underline{CH_2}P$); Mass Spectrum m/e (CI,isobutane carrier gas,^{35}Cl): 906 $[Nb(OH)(dppe)_2]^+$, 583 $[M\text{-}C_2H_5]^+$, 399 $[dppe+H]^+$.

7.5.18 Reaction of $Nb(O)Cl_3$ With PMe_3: Preparation of α-$Nb(O)Cl_3(PMe_3)_3$

Trimethylphosphine (0.62g, 8.12 mmol.) was condensed onto a frozen mixture of $Nb(O)Cl_3$ (0.5g, 2.32 mmol.) and dichloromethane (50 cm^3). The mixture was allowed to warm to room temperature and was stirred for 12h. to afford a clear yellow solution. Filtration followed by concentration (10 cm^3) and cooling to -35°C afforded yellow crystals, which were collected and dried *in vacuo*. Yield, 0.81g (79%). Elemental Analysis for $C_9H_{27}Cl_3NbOP_3$, Found (Required): %C, 23.64 (24.37); %H, 6.09 (6.15); IR (Nujol,CsI,cm^{-1}): 1419(m), 1294(m), 1280(s), 953(s,br), 882(s), 844(w), 743(s), 669(m), 351(m), 299(s), 277(s); ^1H NMR (250MHz, d-chloroform,298K): 1.43(d,$^2J(PH)$=8.6Hz,P$\underline{Me}_3$); ^{31}P NMR (d-chloroform, 298K,broad band decoupled): -2.64(s,br,$\Delta\frac{1}{2}$ *ca.*1000Hz,$\underline{P}Me_3$); Mass Spectrum m/e (CI, isobutane carrier gas,^{35}Cl): 366 $[M-PMe_3]^+$, 347 $[M-PMe_3-H_3O]^+$, 331 $[M-PMe_3-Cl]^+$, 296 $[M-PMe_3-2Cl]^+$.

7.5.19 Reaction of $Nb(O)Cl_3(CH_3CN)_2$ With PMe_3: Preparation of β-$Nb(O)Cl_3(PMe_3)_3$

A procedure analogous to that described for α-$Nb(O)Cl_3(PMe_3)_3$ was used but with $Nb(O)Cl_3(CH_3CN)_2$ starting material. Stirring at room temperature for 2 days afforded a yellow-green suspension. Filtration followed by removal of the volatiles under reduced pressure afforded a yellow-green solid mixture of α- and β- isomers. Recrystallisation from a saturated toluene solution at -35°C afforded the β-product as green plates. Elemental Analysis for $C_9H_{27}Cl_3NbOP_3$, Found (Required): %C, 23.77 (24.37); %H, 6.20 (6.15); IR (Nujol,CsI,cm^{-1}): 1428(m), 1298(m), 1282(s), 954(s,br), 871(s), 849(w), 742(s), 669(w), 352(m), 336(m), 302(s), 277(m,br); ^1H NMR (250MHz,d-chloroform,298K): 1.24(s,br,

$\Delta\frac{1}{2}$=30Hz,P<u>Me</u>$_3$).

7.5.20 Reaction of Nb(O)Cl_3 With PMe_2Ph: Preparation of Nb(O)$Cl_3(PMe_2Ph)_3$

Dimethylphenylphosphine (1.12g, 8.12 mmol.) was added, *via* syringe, to a suspension of $NbOCl_3$ (0.5g, 2.32 mmol.) in dichloromethane (35 cm^3) at room temperature in a nitrogen filled dry box. An immediate reaction ensued leading to complete dissolution of the Nb(O)Cl_3 over a period of *ca.* 15 min. to afford a yellow-orange solution. After stirring for a further 3h., the solution was filtered and the volatiles removed under reduced pressure to give a slightly oily yellow crystalline solid. This solid was washed with cold (-78^{o}C) petroleum ether (*ca.* 8 cm^3, 40-60^{o}C) and dried *in vacuo*. Yield, 1.24g (85%). Elemental Analysis for $C_{24}H_{33}Cl_3NbOP_3$, Found (Required): %C, 44.31 (45.77); %H, 5.02 (5.29); %Cl, 19.78 (16.89); IR (Nujol,CsI, cm^{-1}): 3075(w), 3045(w), 1584(w), 1571(w), 1489(m), 1439(m), 1420(m), 1407(w), 1298(m), 1283(s), 1111(m), 965(m), 960(s), 926(s), 911(s), 904(m,sh), 899(m,sh), 882(m), 871(s), 758(m), 747(s), 725(m), 690(s), 491(s), 410(m), 359(w), 339(s), 297(s,br), 250(m); ^{31}P NMR (d-chloroform,298K,broad band decoupled): -16.27(s,br,$\Delta\frac{1}{2}$=500Hz,P<u>Me</u>$_2$Ph); Mass Spectrum m/e (CI,isobutane carrier gas,^{35}Cl): 215 $[Nb(OH)Cl_3]^+$, 139 $[PhMe_2P+H]^+$.

7.6 EXPERIMENTAL DETAILS TO CHAPTER 6

7.6.1 Reaction of $Cp^*Ta(PMe_3)(H)_2(\eta^2\text{-}CHPMe_2)$ With Ethan-1,2-diol: Synthesis of $Cp^*Ta(O_2C_2H_4)_2$

Ethan-1,2-diol (0.07g, 1.07 mmol.) was added *via* syringe to a vigorously stirred solution of $Cp^*Ta(PMe_3)(H)_2(\eta^2\text{-}CHPMe_2)$ (0.25g, 0.53 mmol.) in petroleum ether (30 cm^3) at room temperature. A white, flocculent precipitate was observable after *ca.* 1h. After 24h. the product was isolated by filtration, washed with petroleum ether (2 x 10 cm^3, 40-60°C) and dried *in vacuo*. Yield, 0.14g (60%). Elemental Analysis for $C_{14}H_{23}O_4Ta$, Found (Required): %C, 38.16 (38.54); %H, 5.48 (5.32); IR (Nujol,KBr,cm^{-1}): 1278(m), 1235(w), 1162(s), 1142(s), 1120(m), 1100(m), 1082(m), 1040(m), 925(m), 895(m), 630(w), 580(w), 550(m), 473(m), 460(m,br); Mass Spectrum m/e (CI,isobutane carrier gas): 873 $[M_2+H]^+$, 829 $[M_2-OC_2H_4+H]^+$, 437 $[M+H]^+$, 348 $[Cp^*TaO_2]^+$.

7.6.2 Reaction of $Cp^*Ta(PMe_3)(H)_2(\eta^2\text{-}CHPMe_2)$ With Catechol [1,2-$(HO)_2C_6H_4$]: Synthesis of $Cp^*Ta(O_2C_6H_4)_2(PMe_3)$

Petroleum ether (40 cm^3) was added to a solid mixture of $Cp^*Ta(PMe_3)(H)_2(\eta^2\text{-}CHPMe_2)$ (0.25g, 0.53 mmol.) and catechol (0.12g, 1.07 mmol.) at room temperature. Stirring for 30 min. resulted in the dissolution of the catechol and precipitation of a yellow solid. After 24h. the product was isolated by filtration, washed with petroleum ether (2 x 10 cm^3, 40-60°C) and dried *in vacuo*. Yield, 0.28g (86%). Elemental Analysis for $C_{25}H_{32}O_4PTa$, Found (Required): %C, 49.37 (49.34); %H, 5.72 (5.31); IR (Nujol,KBr,cm^{-1}): 3045(w), 1587(w), 1345(m), 1339(w), 1291(m), 1277(s), 1264(s), 1255(s), 1215(m), 1100(m), 1095(m), 1040(m),

1020(m), 1013(m), 985(w), 960(m), 820(m), 809(s), 756(s), 732(s), 650(m), 629(s), 600(m), 529(m), 515(m), 489(w); Mass Spectrum m/e (EI,70eV): 961 $[M_2\text{-}(HO)_2C_6H_4\text{-}PMe_3\text{-}C_4H_4(OH)]^+$, 837 $[961\text{-}(HO)_2C_6H_4\text{-}CH_2]^+$, 532 $[Cp^*Ta(O_2C_6H_4)_2]^+$.

7.6.3 Synthesis of $Cp^*Ta(OPh)_4$

Phenol (0.12g, 1.3 mmol.) was added to a toluene solution (20 cm^3) of $Cp^*Ta(PMe_3)(H)_2(\eta^2\text{-}CHPMe_2)$ (0.15g, 0.32 mmol.) in a nitrogen filled dry box. After stirring for 2h. at room temperature, the volatiles were removed under reduced pressure to give a pale yellow oil which was washed with cold (*ca.* -60°C) petroleum ether (2 x 5 cm^3, 40-60°C) to afford a white solid. This was then recrystallised from petroleum ether (40 cm^3, 40-60°C) to afford colourless crystals. Yield, 0.18g (82%). Elemental Analysis for $C_{34}H_{35}O_4Ta$, Found (Required): %C, 58.98 (59.30); %H, 5.22 (5.13); IR (Nujol,KBr,cm^{-1}): 3055(w), 3015(w), 1588(s), 1288(s), 1250(s,br), 1161(m), 1153(m), 1069(m), 1022(m), 1000(m,sp), 881(s,br), 860(s), 852(s), 827(m), 757(s), 734(m), 692(s), 630(s), 600(m), 585(m), 515(m), 435(m); ^1H NMR (250MHz,d^6-benzene,298K): 7.04 (dd,8H,$J(H_oH_m)$=8Hz,$J(H_oH_p)$=7Hz,$\underline{H}_m$), 6.83(d,8H,$J(H_oH_m)$=8Hz,$\underline{H}_o$), 6.69(t, 4H,$J(H_oH_p)$=7Hz,$\underline{H}_p$), 2.12(s,15H,$C_5\underline{Me}_5$); ^{13}C NMR (d^6-benzene,298K,broad band decoupled): 163.84(s,C_{ipso}), 129.29(s,C_m), 124.64(s,$\underline{C}_5Me_5$), 120.94 (s,C_p), 119.94(s,C_o), 11.54(s,$C_5\underline{Me}_5$): Mass Spectrum m/e (CI,isobutane carrier gas): 596 $[M\text{-}OPh+H]^+$, 519 $[M\text{-}OPh\text{-}Ph+H]^+$, 426 $[M\text{-}2OPh\text{-}Ph+H]^+$.

7.6.4 Reaction of Cp^*TaCl_4 With Me_3SiOCH_3: Preparation of $Cp^*TaCl_3.OCH_3$

Me_3SiOCH_3 (0.23g, 2.18 mmol.) was added, *via* syringe, to a suspension of Cp^*TaCl_4 (1.0g, 2.18 mmol.) in 1,2-dichloroethane (40 cm^3)

in a nitrogen filled dry box. The mixture was heated to 70°C for 12h. to give a yellow solution. Filtration followed by concentration (*ca.* 10 cm^3) and layering of this solution with petroleum ether (*ca.* 20 cm^3, 40-60°C) resulted in precipitation of the product as yellow crystals, which were collected and dried *in vacuo*. Yield, 0.89g (90%). Elemental Analysis for $C_{11}H_{18}Cl_3OTa$, Found (Required): %C, 28.85 (29.13); %H, 3.82 (4.01); %Cl, 23.60 (23.45); IR (Nujol,CsI,cm^{-1}): 1483(m), 1435(m), 1127(s,br), 1041(m), 1025(m), 963(w), 805(w), 683(w), 523(m), 381(m), 335(s), 290(s); ^1H NMR (250MHz,d-chloroform,298K): 4.57(s,3H,$OC\underline{H}_3$), 2.44(s,15H,$C_5\underline{Me}_5$); ^{13}C NMR (d-chloroform,298K,broad band decoupled): 128.53(s,$\underline{C}_5Me_5$), 67.17(s,$O\underline{Me}$), 12.84(s,$C_5\underline{Me}_5$); Mass Spectrum m/e (EI, 70eV,^{35}Cl): 819 $[M_2\text{-}2Cl\text{-}Me]^+$, 417 $[M\text{-}Cl]^+$, 317 $[M\text{-}C_5Me_5]^+$.

7.6.5 Reaction of Cp^*TaCl_4 With $Me_3SiOC_2H_5$: Preparation of $Cp^*TaCl_3.OC_2H_5$

This complex was prepared by an analogous procedure to that described for $Cp^*TaCl_3.OCH_3$. Recrystallisation of the crude product from toluene afforded yellow crystals of $Cp^*TaCl_3.OC_2H_5$. Yield 80%. Elemental Analysis for $C_{12}H_{20}Cl_3OTa$, Found (Required): %C, 30.72 (30.82); %H, 4.52 (4.32); %Cl, 22.44 (22.74); IR (Nujol,CsI,cm^{-1}): 1115(s,br), 1082(s), 1030(m), 1020(m), 940(m), 807(w), 800(w), 720(w), 563(m), 376(m), 340(s), 300(m), 286(m,sh); ^1H NMR (250MHz,d-chloroform, 298K): 4.84(q,2H,$^2J(HH)$=7.0Hz,$OC\underline{H}_2CH_3$), 2.44(s,15H,$C_5\underline{Me}_5$), 1.37(t,3H, $^2J(HH)$=7.0Hz,$OCH_2C\underline{H}_3$); ^{13}C NMR (d-chloroform,298K): 128.32(s,$\underline{C}_5Me_5$), 76.20(t,$^1J(CH)$=149.6Hz,-$O\underline{C}H_2$-), 17.27(q,$^1J(CH)$=127.2Hz, -$OCH_2\underline{C}H_3$), 12.96(q,$^1J(CH)$=128.1Hz,$C_5\underline{Me}_5$); Mass Spectrum m/e (EI,70eV, ^{35}Cl): 431 $[M\text{-}Cl]^+$, 421 $[M\text{-}OEt]^+$, 403 $[M\text{-}Cl\text{-}C_2H_4]^+$, 396 $[M\text{-}2Cl]^+$, 386 $[M\text{-}Cl\text{-}OEt]^+$, 351 $[M\text{-}2Cl\text{-}OEt]^+$, 331 $[M\text{-}C_5Me_5]^+$, 303 $[M\text{-}C_5Me_5\text{-}C_2H_4]^+$.

7.6.6 Reaction of Cp^*TaCl_4 With $Me_3SiOC_3H_5$: Preparation of $Cp^*TaCl_3.OC_3H_5$

A procedure analogous to that described for $Cp^*TaCl_3.OCH_3$ was used. The reaction mixture, however, was heated at 70°C for 1h. only. Recrystallisation of the crude product from dichloromethane:petroleum ether (40-60°C) [1:1 v/v] afforded the product as yellow crystals. Yield 67%. Elemental Analysis for $C_{13}H_{20}Cl_3OTa$, Found (Required): %C, 32.26 (32.55); %H, 4.19 (4.21); IR (Nujol,CsI,cm^{-1}): 1645(m), 1486(m), 1430(m), 1409(w), 1348(w), 1288(m), 1136(s,br), 1032(s,br), 927(s,sp), 910(w), 692(m), 560(w), 447(w), 379(m), 339(m), 307(s); ^1H NMR (250MHz, d-chloroform,298K)‡‡: 4.9(m,3H,$C\underline{H}_2CH=C\underline{H}_2$), 5.2(m,1H,$CH_2CH=C\underline{H}_2$,cis to methylene), 5.7(m,1H,$CH_2C\underline{H}=CH_2$), 2.07(s,15H,$C_5\underline{Me}_5$); Mass Spectrum m/e (CI,isobutane carrier gas,^{35}Cl): 821 $[M_2-C_5Me_5]^+$ (weak), 769 $[M_2-C_5Me_5-Cl-OH]^+$ (weak), 669 $[M_2-2C_5Me_5-OH]^+$ (weak), 479 $[M+H]^+$ (weak), 443 $[M-Cl]^+$, 421 $[M-OC_3H_5]^+$, 403 $[Cp^*Ta(OH)Cl_2]^+$.

7.6.7 Reaction of Cp^*TaCl_4 With $ReO_3(OSiMe_3)$: Preparation of $Cp^*TaCl_3.OReO_3$

Dichloromethane (30 cm^3) was added, *via* cannula, onto a mixture of $ReO_3(OSiMe_3)$ (0.14g, 0.44 mmol.) and Cp^*TaCl_4 (0.2g, 0.44 mmol.) maintained at *ca.* -40°C. Upon warming to ambient temperature and stirring for 16h., a brown-orange CH_2Cl_2 solution was obtained over a yellow solid. The solution was decanted off and the yellow solid washed with petroleum ether (2 x 5 cm^3, 40-60°C) and dried *in vacuo*. Yield of $Cp^*TaCl_3.OReO_3$, 0.17g (57%). Elemental Analysis for $C_{10}H_{15}Cl_3O_4ReTa$,

‡‡Spectrum is complicated by second order couplings and simple analysis is not possible. Decoupling 4.9 ppm peak allows assignment of the other two as coupled by J(HH)=17 Hz, *ie. trans* hydrogens.

Found (Required): %C, 17.30 (17.84); %H, 2.26 (2.23); IR (Nujol,CsI, cm^{-1}): 1483(m), 1432(m), 1268(w), 1069(w), 1019(m), 987(s), 971(s), 969(s,sh), 817(s,br), 737(m), 700(w), 600(w), 467(w), 443(w), 429(w), 370(m), 361(m), 336(s), 316(s); Mass Spectrum m/e (CI,isobutane carrier gas, ^{185}Re, ^{35}Cl): 670 $[M]^+$, 635 $[M-Cl]^+$, 402 $[M-ReO_3Cl]^+$.

7.6.8 Reaction of Cp^*TaCl_4 With $(Me_3Si)_2O$: Synthesis of $(Cp^*TaCl_3)_2(\mu\text{-}O)$

(a) An acetonitrile solution of $(Me_3Si)_2O$ (0.34g, 2.09 mmol. in 20 cm^3 CH_3CN) was added dropwise to a stirred suspension of Cp^*TaCl_4 in acetonitrile (0.5g, 1.09 mmol. in 30 cm^3 CH_3CN) at room temperature. The mixture was then heated to 80°C for 3.5h., producing a flocculent yellow suspension. The supernatant solution was filtered and the yellow, crystalline residue was washed with petroleum ether (2 x 10 cm^3, 40-60°C) and dried *in vacuo*. Yield, 0.18g (38%). The filtrate contains further quantities of $(Cp^*TaCl_3)_2(\mu\text{-}O)$ (by IR), but purification of this crude product was not attempted.

(b) A solution of $(Me_3Si)_2O$ in 1,2-dichloroethane (0.88g, 5.45 mmol. in 20 cm^3 CH_2ClCH_2Cl) was added *via* cannula to a suspension of Cp^*TaCl_4 in 1,2-dichloroethane (1.0g, 2.18 mmol. in 40 cm^3 CH_2ClCH_2Cl). The mixture was then heated to 75°C for 10h., the resultant Me_3SiCl being removed by distillation. The mixture was then allowed to cool to room temperature whereupon yellow crystals precipitated from the solution. These were collected and washed with petroleum ether (2 x 10 cm^3, 40-60°C) and dried *in vacuo*. A further crop of yellow crystals was obtained by treatment of the filtrate with petroleum ether (20 cm^3, 40-60°C). Yield, 0.46g (49%). Elemental Analysis for $C_{20}H_{30}Cl_6OTa_2$, Found

(Required): %C, 27.80 (27.89); %H, 3.54 (3.52); %Cl, 24.27 (24.70); IR (Nujol,CsI, cm^{-1}): 1485(m), 1436(m), 1073(w), 1023(m), 690(s,br), 610(w), 600(m), 429(w), 377(s), 337(s), 328(s), 314(s,sh), 296(s), 278(m); ^{1}H NMR (250MHz,d^{6}-benzene,298K): 2.07(s,$C_5\underline{Me}_5$); Mass Spectrum m/e (EI,70eV,^{35}Cl): 420 $[Cp^{*}TaCl_3\text{-}H]^{+}$, 402 $[Cp^{*}Ta(0)Cl_2]^{+}$.

7.6.9 Reaction of $Cp^{*}TaCl_2(PMe_3)_2$ With Carbon Dioxide: Preparation of $Cp^{*}Ta(0)Cl_2$.

A thick-walled, 150 cm^3 glass "Rotoflo" ampoule, containing a saturated toluene solution of $Cp^{*}TaCl_2(PMe_3)_2$ (0.5g, 0.93 mmol. in 25 cm^3 toluene) was cooled to -78°C and evacuated. One atmosphere of carbon dioxide was introduced into the vessel and the reaction mixture was stirred for 16h. at room temperature. The mixture was then allowed to stand for 2h., whereupon yellow crystals separated from the toluene solution. These were collected and dried *in vacuo*. Recrystallisation from toluene (30 cm^3) afforded $Cp^{*}Ta(0)Cl_2$ as yellow crystals. Yield, 0.12g (32%). Further purification was achieved by vacuum sublimation at 170°C (5 x 10^{-3} Torr). Elemental Analysis for $C_{10}H_{15}Cl_2OTa$, Found (Required): %C, 29.61 (29.98); %H, 3.84 (3.76); IR (Nujol,CsI,cm^{-1}): 1430(m), 1070(w), 1025(m), 803(w), 675(s,br), 610(w), 598(m), 550(m), 436(w), 387(s), 330(s), 310(s), 291(s); ^{1}H NMR (250MHz,d^{6}-benzene, 298K): 2.22(s,$C_5\underline{Me}_5$); Mass Spectrum m/e (CI,isobutane carrier gas, ^{35}Cl): 805 $[M_2+H]^{+}$, 769 $[M_2\text{-}Cl]^{+}$, 403 $[M+H]^{+}$.

7.7 REFERENCES

1. R.B. King and F.G.A. Stone, *Inorg.Synth.*, 1963, 7, 99.

2. H.P. Fritz and C.G. Kreiter, *J.Organometallic Chem.*, 1964, 1, 323.

3. G.H. Llinás, M. Mena, F. Palacios, P. Royo and R. Serrano, *J.Organometallic Chem.*, 1988, 340, 37.

4. M.J. Bunker, A. De Cian, M.L.H. Green, J.J.E. Moreau and N. Siganporia, *J.Chem.Soc.Dalton Trans.*, 1980, 2155.

5. V.C. Gibson, J.E. Bercaw, W.J. Bruton Jr. and R.D. Sanner, *Organometallics*, 1986, 5, 976.

6. W. Wolfsberger and H. Schmidbaur, *Synth.React.Inorg.Metal.-Org. Chem.*, 1974, 4, 149.

7. J.M. Manriquez, P.J. Fagan, L.D. Schertz and T.J. Marks, *Inorg. Synth.*, 1982, 21, 181.

8. R.D. Sanner, S.T. Carter and W.J. Bruton, Jr., *J.Organometallic Chem.*, 1982, 240, 157.

APPENDICES

CRYSTAL DATA. COLLOQUIA AND LECTURES.

APPENDIX 1A: CRYSTAL DATA FOR $Cp^*TaCl_3(PMe_3)$

$C_{13}H_{24}Cl_3PTa$:	498.6
Crystal System:	Orthorhombic
Space Group:	$P2_12_12_1$
Cell Dimensions:	a = 8.3306(4) Å
	b = 14.289(1) Å
	c = 15.145(1) Å
	U = 1802.8 $Å^3$
	Z = 4
	D_c = 1.837 g cm^{-3}.
Final R-value:	0.0330 (wR = 0.0386)

APPENDIX 1B: CRYSTAL DATA FOR $Cp^*TaCl_2(PMe_3)(CO)_2$

$C_{15}H_{24}Cl_2O_2PTa$:	519.18
Crystal System:	Orthorhombic
Space Group:	$P2_12_12_1$
Cell Dimensions:	a = 9.876(1) Å
	b = 12.122(1) Å
	c = 15.567(1) Å
	U = 1863.6 $Å^3$
	Z = 4
	D_c = 1.850 g cm^{-3}.
Final R-value:	0.0330 (wR = 0.024)

APPENDIX 1C: CRYSTAL DATA FOR $Cp^*Ta(PMe_3)(H)_2(\eta^2\text{-}CHPMe_2)$

$C_{16}H_{33}P_2Ta$:	468.33
Crystal System:	Orthorhombic
Space Group:	$P2_12_12_1$
Cell Dimensions:	a = 9.131(1) Å
	b = 13.399(1) Å
	c = 16.518(2) Å
	U = 2020.9 $Å^3$
	Z = 4
	D_c = 1.539 g cm^{-3}.
Final R-value:	0.0331 (wR = 0.0382)

APPENDIX 1D: CRYSTAL DATA FOR $(\eta^7\text{-}C_5Me_3(CH_2)_2)Ta(H)_2(PMe_3)$

$C_{16}H_{33}P_2Ta$:	468.33
Crystal System:	Orthorhombic
Space Group:	P_{nma}
Cell Dimensions:	a = 11.2309(6) Å
	b = 11.9809(5) Å
	c = 14.4881(7) Å
	U = 1949.5 $Å^3$
	Z = 4
	D_c = 1.595 g cm^{-3}.
Final R-value:	0.0196 (wR = 0.0193)

APPENDIX 1E: CRYSTAL DATA FOR $Cp^*Ta(CH_2CH_2CMe_3)_2(\eta^2\text{-}CHPMe_2)$

$C_{25}H_{48}PTa$:	560.6
Crystal System:	Monoclinic
Space Group:	$P2_1/c$
Cell Dimensions:	a = 17.663(2) Å
	b = 10.401(2) Å
	c = 16.776(3) Å
	β = 115.73(1) ^{o}
	U = 2776.4 $Å^3$
	Z = 4
	D_c = 1.341 g cm^{-3}.
Final R-value:	0.0361 (wR = 0.0406)

APPENDIX 1F: CRYSTAL DATA FOR α-$Nb(O)Cl_3(PMe_3)_3$

$C_9H_{27}Cl_3NbOP_3$:	443.41
Crystal System:	Monoclinic
Space Group:	$P2_1/c$
Cell Dimensions:	a = 15.250(3) Å
	b = 11.131(2) Å
	c = 11.673(3) Å
	β = 93.61(2) ^{o}
	U = 1977.54 $Å^3$
	Z = 4
	D_c = 1.490 g cm^{-3}.
Final R-value:	0.0418 (wR = 0.0410)

APPENDIX 1G: CRYSTAL DATA FOR β-$Nb(O)Cl_3(PMe_3)_3$

$C_9H_{27}Cl_3NbOP_3$:	443.41
Crystal System:	Monoclinic
Space Group:	$P2_1/c$
Cell Dimensions:	a = 15.149 Å
	b = 11.334 Å
	c = 11.652 Å
	β = 95.532 ^{o}
	U = 1982.6 $Å^3$
	Z = 4
	D_c = 1.486 g cm^{-3}.
Final R-value:	0.0469 (wR = 0.0482)

APPENDIX 1H: CRYSTAL DATA FOR $Cp^*_4Ta_4(O)_7(OH)_2.1/2C_6H_6$

$C_{40}H_{65}O_9Ta_4$:	1449.8
Crystal System:	Monoclinic
Space Group:	C2/m
Cell Dimensions:	a = 18.809(4) Å
	b = 16.066(3) Å
	c = 14.884(3) Å
	β = 100.50(2) ^{o}
	U = 4422.4 $Å^3$
	Z = 4
	D_c = 2.178 g cm^{-3}.
Final R-value:	0.0301 (wR = 0.0329)

APPENDIX 2

^{1}H NMR DATA FOR $Cp^*Ta(PR_3)(H)_2(\eta^2\text{-}CHPMe_2)$ COMPLEXES.

Notes: †*Signals for the coordinated PR_3 ligands cannot be unambiguously assigned due to signal overlap;* ‡*No hydride signal found; (250 MHz, d^6-benzene, 298K).*

PR_3	SHIFT (ppm)	REL. INT.	MULT.	J (Hz)	ASSIGNMENT
PMe_2Ph	9.23	1	t	J(PH)= 2.7	M=C<u>H</u>
	7.1-7.5	5	m	---	Ph
	4.14	2	dd	J(PH)=53.0 J(PH)=18.0	M-<u>H</u>
	2.06	15	s	---	C_5<u>Me_5</u>
	1.75	6	d	^{2}J(PH)= 6.4	P<u>Me_2</u>Ph
	1.33	6	d	^{2}J(PH)=10.4	P<u>Me_2</u>
$PMePh_2$†	9.39	1	t	J(PH)= 2.4	M=C<u>H</u>
	4.48	2	dd	J(PH)=56.3 J(PH)=18.3	M-<u>H</u>
	2.07	15	s	---	C_5<u>Me_5</u>
	1.15	6	d	^{2}J(PH)=10.0	P<u>Me_2</u>
PEt_3†	9.22	1	t	J(PH)= 2.9	M=C<u>H</u>
	3.75	2	dd	J(PH)=51.8 J(PH)=18.0	M-<u>H</u>
	2.18	15	s	---	C_5<u>Me_5</u>
	1.39	6	d	^{2}J(PH)=11.8	P<u>Me_2</u>
$P(OMe)_3$‡	9.08	1	t	J(PH)=2.9	M=C<u>H</u>
	3.42	9	d	^{3}J(PH)=9.6	P(O<u>Me</u>)$_3$
	2.27	15	s	---	C_5<u>Me_5</u>
	1.43	6	d	^{2}J(PH)=11.7	P<u>Me_2</u>

APPENDIX 3

^{1}H NMR DATA FOR Cp*TaRX(η^2-CHPMe$_2$) COMPOUNDS.

Notes: †Methylene hydrogen signals not resolved; ‡Only assignable resonances; (250 MHz, d^6-benzene, 298K).

COMPLEX	SHIFT (ppm)	REL. INT.	MULT.	J (Hz)	ASSIGNMENT
Cp*Ta(CH_2CH_3)Br-(η^2-CHPMe$_2$)	9.59	1	s	---	M=C<u>H</u>
	1.83	15	s	---	C_5<u>Me$_5$</u>
	1.72	3	d	^{2}J(PH)=10.4	P<u>Me$_2$</u>
	1.53	3	d	^{2}J(PH)= 9.8	P<u>Me$_2$</u>
	1.22	3	t	^{3}J(HH)= 8.0	CH_2<u>CH_3</u>
	0.70	2	m	---	<u>CH_2</u>CH_3†
Cp*Ta(CH_2CH_3)I-(η^2-CHPMe$_2$)	9.85	1	s	---	M=C<u>H</u>
	1.85	3	d	^{2}J(PH)=10.2	P<u>Me$_2$</u>
	1.85	15	s	---	C_5<u>Me$_5$</u>
	1.49	3	d	^{2}J(PH)= 9.9	P<u>Me$_2$</u>
	0.87	3	t	^{3}J(HH)= 8.0	CH_2<u>CH_3</u>
	0.60	2	m	---	<u>CH_2</u>CH_3†
Cp*Ta($CH_2CH_2CH_3$)Br-(η^2-CHPMe$_2$)	9.65	1	s	---	M=C<u>H</u>
	1.83	15	s	---	C_5<u>Me$_5$</u>
	1.71	3	d	^{2}J(PH)=10.8	P<u>Me$_2$</u>
	1.18	3	t	^{3}J(HH)= 8.0	CH_2CH_2<u>CH_3</u>†
Cp*Ta($CH_2CH_2CH_3$)I-(η^2-CHPMe$_2$)‡	9.93	1	s	---	M=C<u>H</u>
	1.86	15	s	---	C_5<u>Me$_5$</u>
	1.86	3	d	^{2}J(PH)=10.2	P<u>Me$_2$</u>
Cp*Ta($CH_2CH_2CMe_3$)Br-(η^2-CHPMe$_2$)	9.63	1	s	---	M=C<u>H</u>
	1.85	15	s	---	C_5<u>Me$_5$</u>
	1.71	3	d	^{2}J(PH)=10.3	P<u>Me$_2$</u>
	1.59	3	d	^{2}J(PH)= 9.7	P<u>Me$_2$</u>
	0.10	9	s	---	CH_2CH_2C<u>Me$_3$</u>†
Cp*Ta($CH_2CH_2CMe_3$)I-(η^2-CHPMe$_2$)	9.91	1	s	---	M=C<u>H</u>
	1.88	15	s	---	C_5<u>Me$_5$</u>
	1.82	3	d	^{2}J(PH)=11.7	P<u>Me$_2$</u>
	1.58	3	d	^{2}J(PH)=10.2	P<u>Me$_2$</u>
	0.98	9	s	---	CH_2CH_2C<u>Me$_3$</u>†

APPENDIX 3

^{1}H NMR DATA FOR Cp*TaRX(η^2-CHPMe$_2$) COMPOUNDS (CONT'D).

COMPLEX	SHIFT (ppm)	REL. INT.	MULT.	J (Hz)	ASSIGNMENT
Cp*Ta(CH_2CH_2Ph)Br-(η^2-CHPMe$_2$)‡	9.74	1	s	---	M=C<u>H</u>
	1.81	15	s	---	C_5<u>Me$_5$</u>
	1.71	3	d	^{2}J(PH)=10.6	P<u>Me$_2$</u>
	1.63	3	d	^{2}J(PH)=	P<u>Me$_2$</u>
Cp*Ta(CH_2CH_2Ph)I-(η^2-CHPMe$_2$)‡	10.04	1	s	---	M=C<u>H</u>
	1.85	15	s	---	C_5<u>Me$_5$</u>
Cp*Ta(CH=CHPh)Br-(η^2-CHPMe$_2$)	9.87	1	s	---	M=C<u>H</u>
	7.56	1	dd	^{3}J(HH)=18.8 J(PH)= 3.7	(CH=C<u>H</u>Ph)
	7.29	2	d	^{3}J(H_oH_m)=7.5	Ph-<u>H$_o$</u>
	7.18	2	dd	^{3}J(H_oH_m)=7.5 ^{3}J(H_mH_p)=7.1	Ph-<u>H$_m$</u>
	7.04	1	t	^{3}J(H_mH_p)=7.1	Ph-<u>H$_p$</u>
	6.54	1	dd	^{3}J(HH)=18.8 J(PH)= 3.6	(C<u>H</u>=CHPh)
	1.88	15	s	---	C_5<u>Me$_5$</u>
	1.67	3	d	^{2}J(PH)=10.9	P<u>Me$_2$</u>
	1.45	3	d	^{2}J(PH)=10.5	P<u>Me$_2$</u>

APPENDIX 4

FIRST YEAR INDUCTION COURSES: OCTOBER 1985

The course consists of a series of one hour lectures on the services available in the department.

1. Departmental Organisation.
2. Safety Matters.
3. Electrical appliances and infrared spectroscopy.
4. Chromatography and Microanalysis.
5. Atomic absorption and inorganic analysis.
6. Library facilities.
7. Mass spectroscopy.
8. Nuclear Magnetic Resonance.
9. Glass blowing techniques.

RESEARCH COLLOQUIA, SEMINARS AND LECTURES ORGANISED BY THE DEPARTMENT OF CHEMISTRY

* - Indicates Colloquia attended by the author.

DURING THE PERIOD: 1985-1986

* BARNARD, Dr. C.J.F. (Johnson Matthey Group) "Platinum Anti-Cancer Drug Development"	20th February 1986
BROWN, Dr. J.M. (University of Oxford) "Chelate Control in Homogeneous Catalysis"	12th March 1986
CLARK, Dr. B.A.J. (Kodak Ltd.) "Chemistry & Principles of Colour Photography"	28th November 1985

	CLARK, Dr. J.H. (University of York) "Novel Fluoride Ion Reagents"	29th January 1986
	DAVIES, Dr. S.G. (University of Oxford) "Chirality Control and Molecular Recognition"	14th November 1985
*	DEWING, Dr. J. (U.M.I.S.T.) "Zeolites - Small Holes, Big Opportunities"	24th October 1985
	ERTL, Prof. G. (University of Munich) "Heterogeneous Catalysis"	7th November 1985
	GRIGG, Prof. R. (Queen"s University, Belfast) "Thermal Generation of 1,3-Dipoles"	13th February 1986
*	HARRIS, Prof. R.K. (University of Durham) "The Magic of Solid State NMR"	27th February 1986
	HATHWAY, Dr. D. (University of Durham) "Herbicide Selectivity"	5th March 1986
*	IDDON, Dr. B. (University of Salford) "The Magic of Chemistry"	6th March 1986
	JACK, Prof. K.H. (University of Newcastle) "Chemistry of Si-Al-O-N Engineering Ceramics"	21st November 1985
	LANGRIDGE-SMITH, Dr.P.R.R. (Edinburgh University) "Naked Metal Clusters - Synthesis, Characterisation and Chemistry"	14th May 1986
*	LEWIS, Prof. Sir Jack (University of Cambridge) "Some more Recent Aspects in the Cluster Chemistry of Ruthenium and Osmium Carbonyls"	23rd January 1986
*	LUDMAN, Dr. C.J. (University of Durham) "Some Thermochemical Aspects of Explosions"	17th October 1985
	MACBRIDE, Dr. J.A.H. (Sunderland Polytechnic) "A Heterocyclic Tour on a Distorted Tricycle - Biphenylene"	20th November 1985
	O'DONNELL, Prof. M.J. (Indiana-Purdue University) "New Methodology for the Synthesis of Amino Acids"	5th November 1985
	PARMAR, Dr. V.S. (University of Delhi) "Enzyme Assisted ERC Synthesis"	13th September 1985
	PHILLIPS, Dr. N.J. (Loughborough Univ.Technology) "Laser Holography"	30th January 1986
	PROCTOR, Prof. G. (University of Salford) "Approaches to the Synthesis of some Natural Products"	19th February 1986
*	SCHMUTZLER, Prof. R. (University of Braunschweig) "Mixed Valence Diphosphorus Compounds"	9th June 1986

*	SCHRODER, Dr. M. (University of Edinburgh) "Studies on Macrocyclic Complexes"	5th March 1986
	SHEPPARD, Prof. N. (University of East Anglia) "Vibrational and Spectroscopic Determinations of the Structures of Molecules Chemisorbed on Metal Surfaces"	15th January 1986
	TEE, Prof. O.S. (Concordia University, Montreal) "Bromination of Phenols"	12th February 1986
	TILL, Miss C. (University of Durham) "ESCA and Optical Emission Studies of the Plasma Polymerisation of Perfluoroaromatics"	26th February 1986
	TIMMS, Dr. P. (University of Bristol) "Some Chemistry of Fireworks"	31st October 1985
	WADDINGTON, Prof. D.J. (University of York) "Resources for the Chemistry Teacher"	28th November 1985
	WHITTLETON, Dr. S.N. (University of Durham) "An Investigation of a Reaction Window"	30th October 1985
	WILDE, Prof. R.E. (Texas Technical University) "Molecule Dynamic Processes from Vibrational Bandshapes"	23rd June 1986
	YARWOOD, Dr. J. (University of Durham) "The Structure of Water in Liquid Crystals"	12th February 1986

DURING THE PERIOD: 1986-1987

	ALLEN, Prof. Sir G. (Unilever Research) "Biotechnology and the Future of the Chemical Industry"	13th November 1986
*	BARTSCH, Dr. R. (University of Sussex) "Low Co-ordinated Phosphorus Compounds"	6th May 1987
	BLACKBURN, Dr. M. (University of Sheffield) "Phosphonates as Analogues of Biological Phosphate Esters"	27th May 1987
	BORDWELL, Prof. F.G.(Northeastern University,USA) "Carbon Anions, Radicals, Radical Anions and Radical Cations"	9th March 1987
*	CANNING, Dr. N.D.S. (University of Durham) "Surface Adsorption Studies of Relevance to Heterogeneous Ammonia Synthesis"	26th November 1986
*	CANNON, Dr. R.D. (University of East Anglia) "Electron Transfer in Polynuclear Complexes"	11th March 1987

*	CLEGG, Dr. W. (University of Newcastle-upon-Tyne) "Carboxylate Complexes of Zinc; Charting a Structural Jungle"	28th January 1987
	DÖPP, Prof. D. (University of Duisburg) "Cyclo-additions and Cyclo-reversions Involving Captodative Alkenes"	5th November 1986
	DORFMÜLLER, Prof. T. (University of Bielefeld) "Rotational Dynamics in Liquids and Polymers"	8th December 1986
	GOODGER, Dr. E.M. (Cranfield Inst.Technology) "Alternative Fuels for Transport"	12th March 1987
	GREENWOOD, Prof. N.N. (University of Leeds) "Glorious Gaffes in Chemistry"	16th October 1986
	HARMER, Dr. M. (I.C.I. Chemicals & Polymer Group) "The Role of Organometallics in Advanced Materials"	7th May 1987
	HUBBERSTEY, Dr. P. (University of Nottingham) "Demonstration Lecture on Various Aspects of Alkali Metal Chemistry"	5th February 1987
	HUDSON, Prof. R.F. (University of Kent) "Aspects of Organophosphorus Chemistry"	17th March 1987
	HUDSON, Prof. R.F. (University of Kent) "Homolytic Rearrangements of Free Radical Stability"	18th March 1987
	JARMAN, Dr. M. (Institute of Cancer Research) "The Design of Anti Cancer Drugs"	19th February 1987
	KRESPAN, Dr. C. (E.I. Dupont de Nemours) "Nickel(0) and Iron(0) as Reagents in Organofluorine Chemistry"	26th June 1987
*	KROTO, Prof. H.W. (University of Sussex) "Chemistry in Stars, between Stars and in the Laboratory"	23rd October 1986
*	LEY, Prof. S.V. (Imperial College) "Fact and Fantasy in Organic Synthesis"	5th March 1987
*	MILLER, Dr. J. (Dupont Central Research, USA) "Molecular Ferromagnets; Chemistry and Physical Properties"	3rd December 1986
*	MILNE/CHRISTIE, Dr.A./Mr.S.(International Paints) "Chemical Serendipity: A Real Life Case Study"	20th November 1986
	NEWMAN, Dr. R. (University of Oxford) "Change and Decay: A Carbon-13 CP/MAS NMR Study of humification and Coalification Processes"	4th March 1987

OTTEWILL, Prof. R.H. (University of Bristol) 22nd January 1987
"Colloid Science a Challenging Subject"

* PASYNKIEWICZ, Prof. S. (Technical Univ.,Warsaw) 11th May 1987
"Thermal Decomposition of Methyl Copper and its Reactions with Trialkylaluminium"

ROBERTS, Prof. S.M. (University of Exeter) 24th June 1987
"Synthesis of Novel Antiviral Agents"

RODGERS, Dr. P.J. (I.C.I. Billingham) 12th February 1987
"Industrial Polymers from Bacteria"

* SCROWSTON, Dr. R.M. (University of Hull) 6th November 1986
"From Myth and Magic to Modern Medicine"

SHEPHERD, Dr. T. (University of Durham) 11th February 1987
"Pteridine Natural Products; Synthesis and Use in Chemotherapy"

THOMSON, Prof. A. (University of East Anglia) 4th February 1987
"Metalloproteins and Magneto-optics"

* WILLIAMS, Prof. R.L. (Metropolitan Police Forensic Science) 27th November 1987
"Science and Crime"

WONG, Prof.E.H. (University of New Hampshire,USA) 29th October 1986
"Coordination Chemistry of P-O-P Ligands"

* WONG, Prof.E.H. (University of New Hampshire,USA) 17th February 1987
"Symmetrical Shapes from Molecules to Art and Nature"

DURING THE PERIOD: 1987-1988

BIRCHALL, Prof. D. (I.C.I. Advanced Materials) 25th April 1988
"Environment Chemistry of Aluminium"

BORER, Dr. K. (University of Durham Industrial Research Laboratories) 18th February 1988
"The Brighton Bomb - (A Forensic Science View)"

BOSSONS, L. (Durham Chemistry Teachers' Centre) 16th March 1988
"GCSE Practical Assessment"

BUTLER, Dr. A.R. (University of St.Andrews) 5th November 1987
"Chinese Alchemy"

CAIRNS-SMITH, Dr. A. (Glasgow University) 28th January 1988
"Clay Minerals and the Origin of Life"

* DAVIDSON, Dr. J. (Herriot-Watt University) November 1987
"Metal Promoted Oligomerisation Reactions of Alkynes"

* GRAHAM, Prof. W.A.G. (University of Alberta, Canada) "Rhodium and Iridium Complexes in the Activation of Carbon-Hydrogen Bonds"	3rd March 1988
GRAY, Prof. G.W. (University of Hull) "Liquid Crystals and their Applications"	22nd October 1987
HARTSHORN, Prof. M.P. (University of Canterbury, New Zealand) "Aspects of Ipso-Nitration"	7th April 1988
HOWARD, Dr. J. (I.C.I. Wilton) "Chemistry of Non-Equilibrium Processes"	3rd December 1987
JONES, Dr. M.E. (Durham Chemistry Teachers' Centre) "GCSE Chemistry Post-mortem"	29th June 1988
JONES, Dr. M.E. (Durham Chemistry Teachers' Centre) "GCE Chemistry A-Level Post-mortem"	6th July 1988
KOCH, Prof. H.F. (Ithaca College, U.S.A.) "Does the E2 Mechanism Occur in Solution"	7th March 1988
LACEY, Mr. (Durham Chemistry Teacher's Centre) "Double Award Science"	9th February 1988
LUDMAN, Dr. C.J. (Durham University) "Explosives"	10th December 1987
McDONALD, Dr. W.A. (I.C.I. Wilton) "Liquid Crystal Polymers"	11th May 1988
MAJORAL, Prof. J.-P. (Université Paul Sabatier) "Stabilisation by Complexation of Short-Lived Phosphorus Species"	8th June 1988
MAPLETOFT, Mrs. M. (Durham Chemistry Teachers' Centre) "Salters' Chemistry"	4th November 1987
NIETO DE CASTRO, Prof. C.A. (University of Lisbon and Imperial College) "Transport Properties of Non-Polar Fluids"	18th April 1988
OLAH, Prof. G.A. (University of Southern California) "New Aspects of Hydrocarbon Chemistry"	29th June 1988
PALMER, Dr. F. (University of Nottingham) "Luminescence (Demonstration Lecture)"	21st January 1988
* PINES, Prof. A. (University of California, Berkeley, U.S.A.) "Some Magnetic Moments"	28th April 1988

RICHARDSON, Dr. R. (University of Bristol) — 27th April 1988
"X-Ray Diffraction from Spread Monolayers"

ROBERTS, Mrs. E. (SATRO Officer for Sunderland) — 13th April 1988
Talk - Durham Chemistry Teachers' Centre
"Links between Industry and Schools"

ROBINSON, Dr. J.A. (University of Southampton) — 27th April 1988
"Aspects of Antibiotic Biosynthesis"

ROSE, van Mrs. S. (Geological Museum) — 29th October 1987
"Chemistry of Volcanoes"

SAMMES, Prof. P.G. (Smith, Kline and French) — 19th December 1987
"Chemical Aspects of Drug Development"

SEEBACH, Prof. D. (E.T.H. Zurich) — 12th November 1987
"From Synthetic Methods to Mechanistic Insight"

SODEAU, Dr. J. (University of East Anglia) — 11th May 1988
Durham Chemistry Teachers's Centre: "Spray Cans, Smog and Society"

SWART, Mr. R.M. (I.C.I.) — 16th December 1987
"The Interaction of Chemicals with Lipid Bilayers"

* TURNER, Prof. J.J. (University of Nottingham) — 11th February 1988
"Catching Organometallic Intermediates"

UNDERHILL, Prof. A. (University of Bangor) — 25th February 1988
"Molecular Electronics"

WILLIAMS, Dr. D.H. (University of Cambridge) — 26th November 1987
"Molecular Recognition"

* WINTER, Dr. M.J. (University of Sheffield) — 15th October 1987
"Pyrotechnics (Demonstration Lecture)"

CONFERENCES AND SYMPOSIA ATTENDED

(* denotes paper presentation)

1. International Conference "*Molecules, Clusters and Networks in the Solid State*", University of Birmingham, 8th-11th July, 1986.

2. "*Third International Conference on the Chemistry of the Platinum Group Metals*", University of Sheffield, 13th-17th July, 1987.

3. * "*Durham University Graduate Symposium*", University of Durham, 30th March, 1988.

4. * "*Twenty-third University of Strathclyde Inorganic Chemistry Conference*", University of Strathclyde, 27th-28th June, 1988.

APPENDIX 5 SYNTHESIS AND CHARACTERISATION OF Cp^*NbCl_4

Since most previous studies on half-sandwich niobium compounds have focused on the $[(\eta^5\text{-}C_5H_5)Nb]$ system[1], an extension to $[(\eta^5\text{-}C_5Me_5)Nb]$ derivatives was considered desirable.

However, hitherto, a convenient synthesis of Cp^*NbCl_4 has proved elusive. The reaction of $^nBu_3SnCp^*$ with $NbCl_5$ was found to result in the formation of an intractable brown-black material[2] and although Herrmann and co-workers[3] used this material to successfully prepare $Cp^*Nb(CO)_4$, no characterising data was provided for their precursor.

We have found that Cp^*NbCl_4 can be prepared cleanly from the reaction between Me_3SiCp^* and $NbCl_5$ in toluene solvent at 0^oC.

$$Me_3SiCp^* + NbCl_5 \xrightarrow[0^oC]{\text{Toluene}} Cp^*NbCl_4 + Me_3SiCl$$

The product was isolated as red crystals in 67% yield by removal of the volatile materials under reduced pressure and crystallisation of the residue from dichloromethane solvent. Elemental analysis was consistent with the required stoichiometry (Chapter 7, section 7.2.6). The mass spectrum does not reveal a parent ion. The highest mass fragment is found at m/e 333, which corresponds to $[Cp^*NbCl_3]^+$ (^{35}Cl). Infrared spectroscopy confirms the presence of $(\eta^5\text{-}C_5Me_5)$, an absorption at 1018 cm^{-1} being due to a characteristic ring breathing mode (*cf.* Cp^*TaCl_4, 1023 cm^{-1}). Further, the 250 MHz ^1H NMR-spectrum (d-chloroform) locates the equivalent Cp^* methyl hydrogens as a singlet at 2.49 ppm (*cf.* Cp^*TaCl_4, 2.73 ppm, $CDCl_3$).

REFERENCES

1. See for example: M.J. Bunker and M.L.H. Green, *J.Chem.Soc.Dalton Trans.*, 1981, 85.

2. V.C. Gibson - Unpublished observations.

3. W.A. Herrmann, W. Kalcher, H. Biersack, I. Bernal and M. Creswick, *Chem. Ber.*, 1981, 114, 3558.